THE

LONDON, EDINBURGH, AND DUBLIN

PHILOSOPHICAL MAGAZINE

AND

JOURNAL OF SCIENCE.

[SEVENTH SERIES.]

FEBRUARY 1936.

XIII. *On the Notion of Generalized Plane Stress.* By R. V. Southwell, F.R.S.*

The Problem.

1. THIS paper deals with a flat plate of isotropic material, having uniform thickness $2h$, which is stretched or bent by tractions applied to its edge. Taking the middle-surface as the x–y plane, we have the boundary conditions

$$X_z = Y_z = Z_z = 0, \text{ when } z = \pm h, \quad . \quad . \quad . \quad (1)$$

as an expression of the circumstance that the flat faces are unstressed. Our problem is to examine the configurations of equilibrium which these conditions permit.

When h is small, it is clear that X_z, Y_z, Z_z will in general be small throughout the plate. In the theory of Plane Stress † we assume that they are, in fact, zero everywhere, and we examine the stress-distributions which are consistent with this simplifying assumption. The stress-equations of equilibrium are satisfied if we express the remaining stress-components X_x, Y_y, X_y in terms of a single function χ, as follows :

$$X_x = \frac{\partial^2 \chi}{\partial y^2}, \quad Y_y = \frac{\partial^2 \chi}{\partial x^2}, \quad X_y = -\frac{\partial^2 \chi}{\partial x \partial y}. \quad . \quad . \quad (2)$$

* Communicated by the Author.

† *Cf.* A. E. H. Love, ' Mathematical Theory of Elasticity,' § 145.

The " stress-function " * χ is found to have the form

$$\left.\begin{aligned} &\chi=\chi_0+z\chi_1-\frac{1}{2}\frac{\sigma}{1+\sigma}z^2\Theta_0, \\ &\chi_0,\ \chi_1 \text{ being functions independent of } z, \text{ such that} \\ &\nabla_1{}^2\chi_0=\Theta_0, \quad \nabla_1{}^2\chi_1=\beta, \end{aligned}\right\} \quad (3)$$

where Θ_0 is a plane-harmonic function of x and y, β is a constant, and $\nabla_1{}^2$ stands for the operator

$$\partial^2/\partial x^2+\partial^2/\partial y^2.$$

2. Filon † has remarked that practically useful (though not exact) information regarding the stresses can be obtained without imposing all of the restrictions postulated in the theory of Plane Stress. If we assume that

$$\left.\begin{aligned} &Z_z=0 \textit{ everywhere}, \text{ but that} \\ &X_z=Y_z=0 \textit{ only when } z=\pm h, \end{aligned}\right\} \quad . \quad . \quad . \quad (4)$$

then the first two of the stress-equations of equilibrium can be integrated to give two relations between the *average* values of X_x, Y_y, X_y, namely,

$$\left.\begin{aligned} &\frac{\partial}{\partial x}\bar{X}_x+\frac{\partial}{\partial y}\bar{X}_y=0, \\ &\frac{\partial}{\partial x}\bar{X}_y+\frac{\partial}{\partial y}\bar{Y}_y=0, \\ &\text{where (for example) } \bar{X}_x \text{ stands for } \frac{1}{2h}\int_{-h}^{h} X_x\,dz. \end{aligned}\right\} \quad (5)$$

Also (Z_z being zero) the stress-strain relations can be integrated to give

$$\left.\begin{aligned} &\bar{X}_x=\lambda'\left(\frac{\partial\bar{u}}{\partial x}+\frac{\partial\bar{v}}{\partial y}\right)+2\mu\frac{\partial\bar{u}}{\partial x}, \\ &\bar{Y}_y=\lambda'\left(\frac{\partial\bar{u}}{\partial x}+\frac{\partial\bar{v}}{\partial y}\right)+2\mu\frac{\partial\bar{v}}{\partial y}, \\ &\bar{X}_y=\mu\left(\frac{\partial\bar{u}}{\partial y}+\frac{\partial\bar{v}}{\partial x}\right), \end{aligned}\right\} \quad . \quad . \quad . \quad (6)$$

* Commonly known as " Airy's stress-function " (G. B. Airy, Brit. Ass. Rep. 1862).

† L. N. G. Filon, " On an Approximate Solution for the Bending of a Beam of Rectangular Cross-Section under any System of Load," Phil. Trans. R. S. (A) cci., pp. 63–155 (1903).

in which the bars have the significance explained in the third of (5), and

$$\lambda' = 2\lambda\mu/(\lambda+2\mu), \quad . \quad . \quad . \quad . \quad . \quad . \quad (7)$$

λ and μ being Lamé's elastic constants. Equations (5) show that $\overline{X}_x$, $\overline{Y}_y$, X_y can be expressed in terms of an "average stress-function" $\overline{\chi}$, and equations (6), which determine the average values of $\bar{u}$, $\bar{v}$, are exactly similar in form to the equations governing u, v in the theory of Plane Strain * (the only difference being that λ is replaced by λ'). Accordingly χ (like the stress-function which appears in that theory) will satisfy the equation

$$\nabla_1^4 \chi = 0, \quad . \quad . \quad . \quad . \quad . \quad . \quad . \quad (8)$$

and we deduce that a given distribution of tractions applied to the edge will produce the same (average) distribution of internal stresses, whether the plate is infinitely thick (plane strain), infinitely thin (plane stress), or moderately thin (generalized plane stress) †.

3. States of stress which are conditioned by the assumptions (4) have been termed states of "*Generalized Plane Stress*" ‡: evidently Plane Stress is a particular example, and it can be seen at once that (8) is satisfied by the average value of χ as determined from (3). Provided that we are content with a knowledge of *average* stresses, it would seem that there is no necessity for the assumption that X_z, Y_z are zero except at the plane surfaces of the plate, and in this way the theory of Plane Stress can be given a wider application.

But while it is clear that the less stringent assumptions (4), as compared with those which govern a state of plane stress, go some way in the direction of greater generality, equally it is clear that in requiring Z_z to vanish everywhere § they must impose some restriction.

* Love, *op. cit.* § 144. In a state of plane strain w vanishes, and u, v are functions of x and y only.

† *Cf.* Filon, *loc. cit.* p. 67.

‡ Love, *op. cit.* § 94. Coker and Filon, 'Photo-Elasticity,' § 2.23.

§ We can, in fact, deduce (5) and (6) provided that $\int_{-h}^{h} Z_z dz = 0$, so that only the average value of Z_z, strictly speaking, is required to vanish in order that (8) may hold (*cf.* Filon, *loc. cit.* p. 68). But both Love (*op. cit.*) and Coker and Filon (*op. cit.*) do in fact state as an assumption of "generalized plane stress" that Z_z is zero everywhere, and Filon in his original paper (*loc. cit.* p 66) argues that this assumption is plausible when the thickness is small. See p. 204.

Moreover, while the assumption made in the theory of Plane Stress, that X_z, Y_z, Z_z vanish identically, can be defended as plausible on physical grounds (*cf.* § 1), it is difficult to see reasons why Z_z should vanish *identically* in circumstances such that X_z, Y_z have finite values within the plate. Coker and Filon * give some attention to this question, but I confess that I do not find their argument convincing. They remark †, "... It is important to show that the assumption .... that $Z_z=0$ (or at any rate that Z_z is so small that we can reasonably neglect it) does not contradict the fundamental equations. The most direct way of proving this is by showing that an exact solution does actually exist, which makes Z_z zero throughout. ....", and they proceed to discuss one exact solution of this kind. But in their particular example X_z and Y_z vanish identically, showing that it relates to a state of (ordinary) plane stress, and for this reason it seems to me to be hardly relevant. They remark, "... this is only one of many solutions which make Z_z zero throughout: the others do not make X_z and Y_z vanish identically": as it seems to me, the generality of those other solutions is the real question at issue, and this I have sought to examine in the present paper.

Summary and Conclusions.

4. Imposing the restrictions (4), I have sought the most general solution, subject to those restrictions, of the equations of equilibrium and of compatibility of strains. The analysis leads to expressions for the stress-components involving the usual differentials of a stress-function χ and also differentials of a new function here denoted by Φ; the new function enters into the expressions for all five of the (non-zero) stress-components, whereas χ (as in the theory of Plane Stress) affects only the expressions for X_x, Y_y, X_y. Apart from the introduction of Φ, the solution has greater generality on account of new terms which enter into the expression for χ: what has to be decided is the increase of generality which in consequence can be permitted in the boundary conditions—*i. e.*, in the specified distribution of the applied (edge) tractions.

* *Op. cit.* § 2.26.

† In the original, X_z, Y_z, Z_z are written as $\widehat{xz}$, $\widehat{yz}$, $\widehat{zz}$.

This part of the problem is difficult, and rigorous treatment has not been attempted here. The applied tractions (assumed to have specified values at all points in the edge) may be resolved into components X_ν, Y_ν, Z_ν (ν denoting the outward normal to the edge): thus we have three boundary conditions to be satisfied, and two functions (of restricted forms) available for that purpose. In § 9 it is assumed (as seems justifiable in relation to a thin plate) that every one of the stress-components can be expressed in a *finite* series of integral powers of z; and on this understanding it is shown that the occurrence in our solution of the function Φ does not permit a more general distribution of stresses than is obtained in the ordinary theory of Plane Stress, *unless the applied tractions* X_ν, Y_ν, Z_ν *are suitably related.*

The more general form for χ, on the other hand, does give our solution a somewhat wider application. In a state of Plane Stress χ is given by (3) of § 1, whereas the less stringent assumptions (4) of Generalized Plane Stress lead to the expression

$$\left.\begin{aligned} \chi=\chi_0+z\chi_1-\frac{1}{2}\frac{\sigma}{1+\sigma}z^2F_0+\frac{1}{6}\frac{2-\sigma}{1+\sigma}z^3F_1, \\ \text{with the relations} \\ \nabla_1^2\chi_0=F_0, \quad \nabla_1^2\chi_1=F_1, \quad \nabla_1^2F_0=\nabla_1^2F_1=0, \end{aligned}\right\} \tag{9}$$

which show that χ_1 is now an *unrestricted* plane bi-harmonic function. In consequence no restriction has to be imposed upon the terms of order z in X_ν, Y_ν; but (since χ_1 determines F_1) those terms must be associated with suitable terms of order z^3 in X_ν, Y_ν—just as, in the theory of Plane Stress, the form of the function χ_0 imposes no restriction on the terms independent of z in X_ν, Y_ν, but (by determining Θ_0) requires that they be associated with suitable terms of order z^2. In addition, by determining F_1, χ_1 affects the form of Φ and thereby calls for an appropriate distribution of edge tractions of type Z_ν.

The general conclusion to be drawn from our examination (leaving out of account special types of stress-distribution, introduced by the function Φ, which demand relations between X_ν, Y_ν, Z_ν not likely to be satisfied in practice) is that the less stringent assumptions of

Generalized Plane Stress give its solution for *flexural* actions (contributed by the odd powers of z in the expression for X) the same degree of generality as is possessed, for actions which leave the middle-surface plane, by the ordinary theory of Plane Stress. *No wider application is forthcoming in respect of actions of this latter (extensional) kind.*

Analysis of the Problem.

5. In any configuration of equilibrium the stress-components are related * by three stress-equations of equilibrium, of the type

$$\frac{\partial X_x}{\partial x}+\frac{\partial X_y}{\partial y}+\frac{\partial X_z}{\partial z}=0, \quad . \quad . \quad . \quad . \quad (10)$$

and by six "equations of compatibility," expressible in the forms

$$\left.\begin{aligned}&(1+\sigma)\nabla^2(X_x, Y_y, Z_z, Y_z, Z_x, X_y)\\&+\left[\frac{\partial^2}{\partial x^2}, \frac{\partial^2}{\partial y^2}, \frac{\partial^2}{\partial z^2}, \frac{\partial^2}{\partial y\partial z}, \frac{\partial^2}{\partial z\partial x}, \frac{\partial^2}{\partial x\partial y}\right]\Theta=0,\\&\text{where}\\&\Theta=X_x+Y_y+Z_z.\end{aligned}\right\} \quad (11)$$

The third equation of equilibrium, when $Z_z=0$, shows that we may write

$$Z_x=\frac{\partial\phi_1}{\partial y}, \quad Z_y=-\frac{\partial\phi_1}{\partial x}, \quad . \quad . \quad . \quad . \quad (i.)$$

and the first and second equations, when these substitutions are made, show that we may write

$$\left.\begin{aligned}X_x&=\frac{\partial\phi_2}{\partial y}, \quad X_y+\frac{\partial\phi_1}{\partial z}=-\frac{\partial\phi_2}{\partial x},\\Y_y&=\frac{\partial\phi_3}{\partial x}, \quad X_y-\frac{\partial\phi_1}{\partial z}=-\frac{\partial\phi_3}{\partial y}.\end{aligned}\right\} \quad . \quad . \quad (ii.)$$

Then (since $Z_z=0$) we have

$$\frac{\partial\phi_2}{\partial y}+\frac{\partial\phi_3}{\partial x}=X_x+Y_y=\Theta,$$

* *Cf.* Love, *op. cit.* § 145.

and it follows that we may write

$$\left.\begin{aligned} \phi_2 &= \frac{\partial \chi}{\partial y} + 2\frac{\partial \phi_4}{\partial x}, \\ \phi_3 &= \frac{\partial \chi}{\partial x} - 2\frac{\partial \phi_4}{\partial y}, \end{aligned}\right\} \quad \ldots \quad \text{(iii.)}$$

where χ is *any* solution of the equation

$$\nabla_1^2 \chi = \Theta.$$

We can now replace (ii.) by the expressions

$$\left.\begin{aligned} X_x &= \frac{\partial^2 \chi}{\partial y^2} + 2\frac{\partial^2 \phi_4}{\partial x \partial y}, \\ Y_y &= \frac{\partial^2 \chi}{\partial x^2} - 2\frac{\partial^2 \phi_4}{\partial x \partial y}, \\ X_y &= -\frac{1}{2}\left(\frac{\partial \phi_2}{\partial x} + \frac{\partial \phi_3}{\partial y}\right) = -\frac{\partial^2 \chi}{\partial x \partial y} + \left[\frac{\partial^2}{\partial y^2} \quad \frac{\partial^2}{\partial x^2}\right]\phi_4, \\ \frac{\partial \phi_1}{\partial z} &= \frac{1}{2}\left(\frac{\partial \phi_3}{\partial y} - \frac{\partial \phi_2}{\partial x}\right) = -\nabla_1^2 \phi_4, \end{aligned}\right\} \quad (12)$$

which are to be combined with

$$Z_x = \frac{\partial \phi_1}{\partial y}, \quad Z_y = -\frac{\partial \phi_1}{\partial x}, \quad \ldots \quad \text{(i.) } bis$$

and with the relation

$$\Theta = \nabla_1^2 \chi. \quad \ldots \quad \text{(iii.) } bis.$$

6. These expressions constitute a complete solution of the stress equations of equilibrium, but we have still to satisfy the relations (11). From the first three, since $Z_z = 0$, we deduce that

$$\nabla_1^2 \Theta = \frac{\partial^2 \Theta}{\partial z^2} = 0, \quad \ldots \quad \text{(i)}$$

and it follows that we may write

$$\nabla_1^2 \chi = \Theta = F_0 + zF_1, \quad \ldots \quad (13)$$

where F_0, F_1 are plane-harmonic functions of x and y. It has been said (§ 5) that χ may be *any* solution of this

equation: accordingly we replace (13), for the present, by

$$\left.\begin{aligned} &\chi=\chi_0+z\chi_1, \\ &\text{where } \chi_0,\ \chi_1 \text{ are functions of } x \text{ and } y \text{ only, such that} \\ &\nabla_1^2\chi_0=F_0,\quad \nabla_1^2\chi_1=F_1,\quad \nabla_1^2F_0=\nabla_1^2F_1=0. \end{aligned}\right\} \quad (14)$$

We now substitute for the stress-components, in (11), from (12) and (14). Since F_0, F_1 are plane-harmonic, they are related with other plane-harmonic functions G_0, G_1 by the equations

$$\left.\begin{aligned} \frac{\partial}{\partial x}(G_0, G_1)+\frac{\partial}{\partial y}(F_0, F_1)=0, \\ \frac{\partial}{\partial y}(G_0, G_1,)-\frac{\partial}{\partial x}(F_0, F_1)=0, \end{aligned}\right\} \quad . \quad . \quad . \quad (15)$$

and these can be used to simplify the resulting equations. We thus obtain

$$\left.\begin{aligned} \frac{\partial^2}{\partial x\partial y}\{\sigma(G_0+zG_1)-2(1+\sigma)\nabla^2\phi_4\}=0, \\ \left[\frac{\partial^2}{\partial y^2}-\frac{\partial^2}{\partial x^2}\right]\{\sigma(G_1+zG_1)-2(1+\sigma)\nabla^2\phi_4\}=0, \\ (1+\sigma)\nabla^2\phi_1+G_1=Z, \end{aligned}\right\} \quad (16)$$

where Z is a function of z only. These relations replace (11), and are to be combined with the relation

$$\frac{\partial\phi_1}{\partial z}+\nabla_1^2\phi_4=0, \quad . \quad . \quad . \quad . \quad (12)\ bis$$

which was obtained in § 5.

7. We shall satisfy this last equation if we write

$$(1+\sigma)\phi_1=-\nabla_1^2\phi, \quad (1+\sigma)\phi_4=\frac{\partial\phi}{\partial z}, \quad . \quad . \quad (17)$$

and then, substituting for ϕ_4 in the first and second of (16), we obtain after integration with respect to z

$$\sigma(zG_0+\tfrac{1}{2}z^2G_1)-2\nabla^2\phi$$
$$=f(x, y)+\tfrac{1}{2}(x^2+y^2)Z_1''+xZ_2''+yZ_3''+Z_4'', \quad (i.)$$

where Z_1, Z_2, Z_3, Z_4 are undetermined functions of z only, dashes denote differentiations with respect to z, and $f(x, y)$ is independent of z. The third of (16), when we substitute for ϕ_1 from (17), requires that

$$\nabla_1^2\nabla^2\phi=G_1-Z, \quad . \quad . \quad . \quad . \quad . \quad . \quad \text{(ii.)}$$

and eliminating ϕ between (i.) and (ii.) we have the relations

$$Z_1''=Z, \quad \nabla_1^2 f=-2G_1. \quad . \quad . \quad . \quad . \quad . \quad (18)$$

Making use of (18), we can express the general solution of (i.) in the form

$$2\phi=H-\tfrac{1}{2}z^2f(x, y)+\sigma\left(\frac{1}{6}z^3G_0+\frac{1}{24}z^4G_1\right)-\frac{1}{12}z^4G_1$$
$$-\tfrac{1}{2}(x^2+y^2)Z_1-xZ_2-yZ_3-Z_5, \quad \text{(iii.)}$$

where H is an unrestricted harmonic function and Z_5 is a function of z only, related with Z_1, Z_4 by the equation

$$Z_5''+2Z_1=Z_4''. \quad . \quad . \quad . \quad . \quad . \quad . \quad \text{(iv.)}$$

Then, making use of (18) again, we have from (17),

$$\left.\begin{aligned} 2(1+\sigma)\phi_1&=-\nabla_1^2\{H-\tfrac{1}{2}z^2f(x, y)\}+2Z_1,\\ 2(1+\sigma)\phi_4&=\frac{\partial}{\partial z}\{H-\tfrac{1}{2}z^2f(x, y)\}+\sigma(\tfrac{1}{2}z^2G_0+\tfrac{1}{6}z^3G_1)\\ &\quad -\tfrac{1}{3}z^3G_1-\tfrac{1}{2}(x^2+y^2)Z_1'-xZ_2'-yZ_3'-Z_5', \end{aligned}\right\} \quad \text{(v.)}$$

and the expressions (12) for the stress-components become

$$\left.\begin{aligned} X_x&=\frac{\partial^2\chi}{\partial y^2}+\frac{1}{1+\sigma}\frac{\partial^2}{\partial x\partial y}\left\{\frac{\partial\Phi}{\partial z}+\sigma(\tfrac{1}{2}z^2G_0+\tfrac{1}{6}z^3G_1)-\tfrac{1}{3}z^3G_1\right\},\\ Y_y&=\frac{\partial^2\chi}{\partial x^2}-\frac{1}{1+\sigma}\frac{\partial^2}{\partial x\partial y}\left\{\frac{\partial\Phi}{\partial z}+\sigma(\tfrac{1}{2}z^2G_0+\tfrac{1}{6}z^3G_1)-\tfrac{1}{3}z^3G_1\right\},\\ X_y&=-\frac{\partial^2\chi}{\partial x\partial y}+\frac{1}{2(1+\sigma)}\left[\frac{\partial^2}{\partial y^2}-\frac{\partial^2}{\partial x^2}\right]\\ &\qquad\left\{\frac{\partial\Phi}{\partial z}+\sigma(\tfrac{1}{2}z^2G_0+\tfrac{1}{6}z^3G_1)-\tfrac{1}{3}z^3G_1\right\},\\ Z_x&=-\frac{1}{2(1+\sigma)}\frac{\partial}{\partial y}\nabla_1^2\Phi,\\ Z_y&=\frac{1}{2(1+\sigma)}\frac{\partial}{\partial x}\nabla_1^2\Phi, \end{aligned}\right\}$$

. . . (19)

where

$$\Phi = H - \tfrac{1}{2}z^2 f(x, y). \quad . \quad . \quad . \quad . \quad . \quad (20)$$

We observe that the functions Z_1, Z_2, ... etc., in the expression for ϕ, do not affect the stress-components.

8. Again making use of the relations (15), which require that

$$\left.\begin{aligned} \frac{\partial^2}{\partial x\,\partial y}(G_0, G_1) &= \frac{\partial^2}{\partial x^2}(F_0, F_1) = -\frac{\partial^2}{\partial y^2}(F_0, F_1), \\ \tfrac{1}{2}\left[\frac{\partial^2}{\partial y^2} - \frac{\partial^2}{\partial x^2}\right](G_0, G_1) &= \frac{\partial^2}{\partial x\,\partial y}(F_0, F_1), \end{aligned}\right\} \quad \text{(i.)}$$

we can further simplify the form of our solution. For in virtue of these relations we may omit from (19) the terms involving G_0, G_1, provided that we now take the stress-function to be given by

$$\chi = \chi_0 + z\chi_1 + \frac{1}{1+\sigma}\{\tfrac{1}{3}z^3F_1 - \sigma(\tfrac{1}{2}z^2F_0 + \tfrac{1}{6}z^3F_1)\},$$

$$= \chi_0 + z\chi_1 - \frac{1}{2}\frac{\sigma}{1+\sigma}z^2F_0 + \frac{1}{6}\frac{2-\sigma}{1+\sigma}z^3F_1, \quad . \quad . \quad (9)\ bis$$

where F_0, F_1 are plane-harmonic functions of x and y, and

$$\nabla_1^2\chi_0 = F_0, \quad \nabla_1^2\chi_1 = F_1. \quad . \quad . \quad . \quad (14)\ bis$$

On this understanding the less stringent assumptions (4), as compared with those which govern a state of Plane Stress, have been shown to increase the generality of our solution in two respects: (1) by giving a less restricted form to the stress-function χ, and (2) by introducing additional terms in the expressions for the stress-components—namely, partial differentials of a new function Φ. The function Φ is defined by (20), H being harmonic and (so far) unrestricted, and $f(x, y)$ a function governed by the second of (18).

9. It remains to examine the boundary conditions and to decide what restriction must be imposed upon the applied tractions (at the edge of the plate) in order that our solution may be exact. This question is difficult, and rigorous discussion must be left to mathematicians: here it seems justifiable to simplify the problem by assuming that the applied tractions (and

therefore H) can be expressed in finite series of integral powers of z. We write

$$H=H_0+zH_1+\tfrac{1}{2}z^2H_2+\ldots\frac{1}{n!}z^nH_n, \quad . \quad . \quad (21)$$

where H_0, H_1, . . . , H_n are functions of x and y only. Then (since H is harmonic) it is clear that H_n and H_{n-1} must be plane-harmonic functions, and that in general $(p+2 \not> n)$

$$\nabla_1^2H_p+H_{p+2}=0. \quad . \quad . \quad . \quad . \quad . \quad (22)$$

Provided that $n>4$, the highest power of z which occurs in the expressions for X_x, Y_y, X_y will be z^{n-1}, and the highest power of z which occurs in the expressions for Z_x, Z_y will be z^{n-2}; in both instances the term of highest order will come wholly from H. Using the symbol D to denote differentiation with respect to z, we may write

$$\left.\begin{aligned}
(1+\sigma)D^{n-1}X_x&=\frac{\partial^2}{\partial x\partial y}H_n,\\
(1+\sigma)D^{n-1}Y_y&=-\frac{\partial^2}{\partial x\partial y}H_n,\\
2(1+\sigma)D^{n-1}X_y&=\left[\frac{\partial^2}{\partial y^2}-\frac{\partial^2}{\partial x^2}\right]H_n,\\
2(1+\sigma)D^{n-2}Z_x&=-\frac{\partial}{\partial y}\nabla_1^2(\tfrac{1}{2}z^2H_n+H_{n-2})=\frac{\partial}{\partial y}H^n,\\
2(1+\sigma)D^{n-2}Z_y&=\frac{\partial}{\partial x}\nabla_1^2(\tfrac{1}{2}z^2H_n+H_{n-2})=-\frac{\partial}{\partial x}H_n,
\end{aligned}\right\} \quad (23)$$

and then it is clear that three boundary conditions are imposed on H_n, whereas a single condition would serve to determine its value at every point. For example, from the last two of (23) we deduce that

$$2(1+\sigma)D^{n-2}Z_v=2(1+\sigma)D^{n-2}(lZ_x+mZ_y)=\frac{\partial}{\partial s}H_n, \quad (24)$$

where Z_v is the component of the applied traction in the direction of z: this equation serves to determine the boundary values of H_n, except for a constant term which involves a like constant in H_n and so does not affect the stress-components; accordingly H_n, since it must be plane-harmonic, is known at all points within the area

of the plate, and hence, by the first three of (23), the edge values of $D^{n-1}(X_x, Y_y, X_y)$ are determinate. This means that the values of $D^{n-1}(X_\nu, Y_\nu)$ are no longer at our disposal to fix as we like, once we have specified $D^{n-2}Z_\nu$ at all points on the edge.

Alternatively we might have determined H_n from the edge values of either X_ν or Y_ν. The conclusion to be drawn from this examination is that complete freedom of choice for the edge tractions does not extend to terms of the order z^{n-1} in X_x, Y_y, X_y or to terms of the order z^{n-2} in Z_x, Z_y, if $n>4$: in other words, relations are imposed by our initial assumptions between the terms of order higher than z^3 in X_ν, Y_ν and the terms of order higher than z^2 in Z_ν. Therefore, in looking for terms which are not related in this way, we may assume that the series (21) for H contains no term of higher order than z^4.

10. On this understanding H_4 and H_3, in (21), are plane-harmonic, and terms of order z^3 are contributed to the expressions for X_x, Y_y, X_y both by H_4 and by χ as given in (9). Corresponding with (23) we have

$$\left.\begin{aligned}
(1+\sigma)D^3X_x &= (2-\sigma)\frac{\partial^2 F_1}{\partial y^2} + \frac{\partial^2}{\partial x \partial y}H_4, \ \dots \\
(1+\sigma)D^3Y_y &= (2-\sigma)\frac{\partial^2 F_1}{\partial x^2} - \frac{\partial^2}{\partial x \partial y}H_4, \ \dots \\
(1+\sigma)D^3X_y &= -(2-\sigma)\frac{\partial^2 F_1}{\partial x \partial y} + \frac{1}{2}\left[\frac{\partial^2}{\partial y^2} - \frac{\partial^2}{\partial x^2}\right]H_4, \dots \\
2(1+\sigma)D^2Z_x &= -\frac{\partial}{\partial y}\nabla_1^2\{\tfrac{1}{2}z^2H_4 + H_2 - f(x,y)\} \\
&\qquad = \frac{\partial}{\partial y}(H_4 - 2G_1), \ \dots \\
2(1+\sigma)D^2Z_y &= \frac{\partial}{\partial x}\nabla_1^2\{\tfrac{1}{2}z^2H_4 + H_2 - f(x,y)\} \\
&\qquad = -\frac{\partial}{\partial x}(H_4 - 2G_1), \ \dots
\end{aligned}\right\} \quad \text{(i.)}$$

and from these we deduce the relation

$$2(1+\sigma)D^2Z_\nu = \frac{\partial}{\partial s}(H_4 - 2G_1), \quad \dots \quad \text{(ii.)}$$

which corresponds with (24) of § 9. Since H_4 and G_1 are plane-harmonic, the boundary values of D^2Z_ν serve to determine (H_4-2G_1) at all points within the area of the middle-surface.

Again using (15), we may write the first three of (i.) in the forms

$$\left.\begin{aligned}(1+\sigma)D^3X_x &= \frac{\partial^2}{\partial x\partial y}\{H_4-(2-\sigma)G_1\} = -(1+\sigma)D^3Y_y,\\ (1+\sigma)D^3X_y &= \frac{1}{2}\left[\frac{\partial^2}{\partial y^2}-\frac{\partial^2}{\partial x^2}\right]\{H_4-(2-\sigma)G_1\},\end{aligned}\right\} \quad \text{(iii.)}$$

which, since (H_4-2G_1) is known everywhere, show that two boundary conditions (specified values of X_ν, Y_ν) are imposed on G_1. But G_1 is plane-harmonic, and therefore completely determined by either one of these two boundary conditions: therefore some relation is imposed by our solution between the terms of order z^3 in X_ν, Y_ν and the term of order z^2 in Z_ν.

11. Corresponding with (i.) of § 10 we have

$$\left.\begin{aligned}(1+\sigma)D^2X_y &= -\sigma\frac{\partial^2F_0}{\partial y^2}+\frac{\partial^2}{\partial x\partial y}H_3, \text{ ... etc.},\\ 2(1+\sigma)DZ_x &= \frac{\partial}{\partial y}H_3,\\ 2(1+\sigma)DZ_y &= -\frac{\partial}{\partial x}H_3,\end{aligned}\right\} \quad \text{(i.)}$$

showing that H_3 is determined by the boundary values of Z_ν, leaving only a plane-harmonic function (F_0) for satisfying specified values of X_ν, Y_ν. We deduce, as before, that relations are imposed by our assumptions between the terms of order z^2 in X_ν, Y_ν and the term of order z in Z_ν.

12. It thus appears that any additional generality which our solution may possess will come from the first three terms in (21), and we may conclude by examining the boundary conditions on the assumption that

$$\left.\begin{aligned}H &= H_0+zH_1+\tfrac{1}{2}z^2H_2,\\ \text{where } H_1, H_2 &\text{ are plane-harmonic and}\\ \nabla_1^2H_0+H_2 &= 0.\end{aligned}\right\} \quad \ldots \quad (25)$$

The last two of (19) now give

$$\left.\begin{aligned} 2(1+\sigma)Z_x &= \frac{\partial}{\partial y}(H_2 - z^2 G_1), \\ 2(1+\sigma)Z_y &= -\frac{\partial}{\partial x}(H_2 - z^2 G_1), \end{aligned}\right\} \quad . \quad . \quad . \quad (i.)$$

whence, since Z_x, Z_y must vanish on the flat faces of the plate, we deduce that on those faces

$$H_2 = h^2 G_1 + \text{const.} \quad . \quad . \quad . \quad . \quad . \quad (26)$$

Then we have

$$2(1+\sigma)Z_\nu = (h^2 - z^2)\frac{\partial G_1}{\partial s}, \quad . \quad . \quad . \quad . \quad (27)$$

showing that Z_ν must have a parabolic distribution with respect to z. Its value at the middle-surface ($z=0$) will serve to determine G_1 and its associated plane-harmonic function F_1.

The expressions for X_x, Y_y, X_y, when we substitute from (25) and (26), take the forms

$$\left.\begin{aligned} X_x &= \frac{\partial^2 \chi}{\partial y^2} + \frac{1}{1+\sigma}\frac{\partial^2}{\partial x \partial y}[H_1 + z\{h^2 G_1 - f(x, y)\}], \\ Y_y &= \frac{\partial^2 \chi}{\partial x^2} - \frac{1}{1+\sigma}\frac{\partial^2}{\partial x \partial y}[H_1 + z\{h^2 G_1 - f(x, y)\}], \\ X_y &= -\frac{\partial^2 \chi}{\partial x \partial y} + \frac{1}{2(1+\sigma)}\left[\frac{\partial^2}{\partial y^2} - \frac{\partial^2}{\partial x^2}\right] \\ &\qquad [H_1 + z\{h^2 G_1 - f(x, y)\}], \end{aligned}\right\} \quad . \quad (28)$$

and in them G_1 has been completely determined by (27), so that, from the second of (18), $f(x, y)$ is known except as regards a plane-harmonic component. Thus, as regards the satisfaction of further boundary conditions, the only terms provided by the function

$$[H_1 + z\{h^2 G_1 - f(x, y)\}]$$

in (28) are plane-harmonic, and as such they can be merged in χ, in the manner adopted in § 8. No additional generality is thereby given to χ as compared with the form (9) found previously: the functions χ_0, χ_1 are still governed by (14), and in those equations F_1 has been determined by Z_ν.

13. As stated in § 4, the final conclusion of this investigation is that, under the simplified assumptions (4) of Generalized Plane Stress, χ_1 (like χ_0 in the ordinary theory of Plane Stress) is an unrestricted plane-harmonic function which permits any values to be specified for the terms of order z in X_ν, Y_ν; but (since χ_1 determines F_1) these terms must be associated with suitable terms of order z^3 in X_ν, Y_ν, and (since F_1 determines G_1 and so Z_ν) with suitable quadratic terms in Z_ν. In the general case it would be difficult to formulate precisely the nature of the restrictions which are imposed; but from a practical point of view it is sufficient to know that the restrictions exist, since in any event we could not ensure their satisfaction in any particular instance.

XIV. *The Use of Factorial Moments in the Treatment of the Hypergeometric Distribution and in Tests for Regression.* *By* H. T. Gonin, *M.Sc.* (*Stellenbosch*), *Ph.D.* (*Edin.*) *.

UP to the present most writers in dealing with the hypergeometric series and other distributions in which we have to do with summations over integer values of the variate have employed ordinary power moments. In the present paper it is shown that factorial moments are the appropriate ones to be used for these distributions, and some well-known results are proved by this method.

J. Neyman's condition that the regression should be a parabola of the nth degree is modified to suit cases where we are dealing with discrete values of the variate.

We shall first find the factorial moments of the hypergeometric distribution.

The rth factorial moment of $\phi(x)$ is defined by

$$m_{(r)}=\Sigma x^{(r)}\phi(x),$$

where $$x^{(r)}=x(x-1)\ldots(x-r+1).$$

Consider the following problem :—

In a population of N, $Np=m$ possess the character A; samples of n are now drawn *en bloc*, repeating the operation

* Communicated by the Author.

after replacing the sample each time. Find the factorial moments of the sampling distribution and the frequency function.

The characters are A and not A ($\bar{A}$), and the categories sample and not sample.

Following the work of H. E. Soper (' Frequency Arrays,' 1922) we have at once that the frequency generating function is the coefficient of s^n in

$$(1+As)^{Np}(1+s)^{Nq}/{}^{N}C_n,$$

i. e., in

$$(1+As)^{m}(1+s)^{N-m}/{}^{N}C_n.$$

The frequency function is the coefficient of A^x in the coefficient of s^n in $(1+As)^m(1+s)^{N-m}/{}^{N}C_n$,

i. e.,

$$\frac{n!\,m!\,(N-m)^{(n-x)}}{(n-x)!\,x!\,(m-x)!\,N^{(n)}} \equiv \psi(x, N, m, n).$$

The factorial moment generating function (f.m.g.f.) is the coefficient of s^n in

$$(1+\overline{s}+\alpha s)^m(1+s)^{N-m}/{}^{N}C_n, \quad [A=1+\alpha],$$

i. e., the coefficient of s^n in

$$\left\{(1+s)^N+m\alpha s(1+s)^{N-1} + \frac{m(m-1)}{2!}\alpha^2 s^2(1+s)^{N-2}+\ldots\right\}/{}^{N}C_n.$$

Now this is

$$G(\alpha)= 1+\frac{mn}{N}\alpha+\frac{m^{(2)}n^{(2)}}{N^{(2)}}\frac{\alpha^2}{2!}+\ldots$$

$$= F(-m, -n; -N; -\alpha),$$

a terminating hypergeometric series.

The rth factorial moment is therefore $\dfrac{m^{(r)}n^{(r)}}{N^{(r)}}$.

Consider again the double hypergeometric series of Isserlis. Suppose a limited population of size N to contain m marked and $N-m$ unmarked characters; a sample of n is drawn and not replaced, a second sample of n' is drawn. The chance of s marked characters in the first sample and s' in the second is

$$\phi(s, s') = \frac{n!\, n'!\, (\mathrm{N}-n-n')!\, m!\, (\mathrm{N}-m)!}{s!\, s'!\, (n-s)!\, (n'-s')!\, \mathrm{N}!\, (m-s-s')!\, (\mathrm{N}-n-n'-m+s+s')!}$$

$$= \frac{n!\, n'!\, (\mathrm{N}-n-n')^{(m-s-s')}}{s!\, s'!\, (n-s)!\, (n'-s')!\, (m-s-s')!\, \mathrm{N}^{(m)}}.$$

The regression, scedastic, clitic, and kurtic curves of this discontinuum have been examined by Karl Pearson (Biom. vol. xvi. 1924, pp. 172–204) and S. J. Pretorius (Biom. vol. xxii. 1930–31, pp. 140–143).

We shall obtain these very easily by the use of factorial moments.

Consider $\psi(x, \mathrm{N}, m, n)$ earlier defined. The f.m.g.f. of this frequency function is

$$\mathrm{F}(-m, -n\,;\ -\mathrm{N}\,;\ -\alpha).$$

Now

$$\phi(s, s') \equiv \psi(s, \mathrm{N}, m, n)\ \psi(s', \mathrm{N}-n, m-s, n').$$

If we keep s *fixed* we find the mean of the s' array to be $n'\dfrac{m-s}{\mathrm{N}-n}$, *i. e.*, simply the coefficient of α in

$$\mathrm{F}(-m+s\,;\ -n'\,;\ -\mathrm{N}+n\,;\ -\alpha).$$

Hence the regression lines are

$$\tilde{s}' = n'\frac{m-s}{\mathrm{N}-n} \quad \text{and} \quad \tilde{s} = n\frac{m-s'}{\mathrm{N}-n'},$$

as found by K. Pearson.

Second Moment Array.

Let $\nu_r(s')$ be the rth moment around the mean for the array when s is fixed, $\nu_r'(s')$ be the rth moment round an arbitrary origin when s is fixed; also $\nu_{[r]}(s')$ the rth factorial moment round an arbitrary origin of the array.

Pearson finds that

$$\nu_2(s') = n'\frac{\mathrm{N}-n-n'}{\mathrm{N}-n-1}\left[\frac{1}{4} - \left(\frac{m-s}{\mathrm{N}-n} - \frac{1}{2}\right)^2\right]. \quad . \quad (1)$$

We find, since

$$\nu_2(s') = \nu_2'(s') - [\nu_1'(s')]^2,$$

and

$$\nu_2'(s') = \nu_{[2]}(s') + \nu_1'(s'),$$

$$\nu_2(s')=\frac{n'^{(2)}(m-s)^{(2)}}{(N-n)^{(2)}}+\frac{n'(m-s)}{N-n}-\frac{n'^2(m-s)^2}{(N-n)^2},$$

which corresponds to (1). Here $\nu_{[2]}(s')$ is the coefficient of $\frac{\alpha^2}{2!}$ in $F(-m+s,\ -n';\ -N+n;\ -\alpha)$.

Third Moment Array.

S. J. Pretorius gives :

$$\nu_3(s')$$
$$=n'\frac{N-n-n'}{N-n-1}\frac{N-n-2n'}{N-n-2}\frac{m-s}{N-n}\left(1-\frac{m-s}{N-n}\right)\left(1-2\frac{m-s}{N-n}\right).$$

We use the relations

$$\nu_3(s')=\nu_3'(s')+3\nu_1'(s')\nu_2'(s')+2\nu_1^{3'}(s') \quad . \quad . \quad (A)$$
$$\left(\mu_r=m_r-r\bar{x}m_{r-1}+\binom{r}{2}\bar{x}^2m_{r-2}+\ldots(-1)^r\bar{x}^r\right);$$

and
$$\begin{cases}\nu_3'=\nu_{[3]}+3\nu_{[2]}+\nu_{[1]},\\ \nu_1'=\nu_{[1]},\\ \nu_2'=\nu_{[2]}+\nu_{[1]}.\end{cases}$$

Also
$$\nu_{[r]}=\frac{n'^{(r)}(m-s)^{(r)}}{(N-n)^{(r)}}.$$

In General.

Use

$$\nu_r(s')=\nu_r'-r\nu_1'\nu_{r-1}'+\binom{r}{2}\nu_1'^2\nu_{r-2}'+\ldots+(-1)^r\nu_1'^r, \quad (A)$$

and
$$\nu_r'=\nu_{[r]}+C_1\nu_{[r-1]}+C_2\nu_{[r-2]}+\ldots,$$

where the C's are Stirling's numbers of the second kind.

Also
$$\nu_{[r]}=\frac{n'^{(r)}(m-s)^{(r)}}{(N-n)^{(r)}}.$$

Hence we get $\nu_r(s')$ at once.

The Product Moments of Isserlis's Discontinuum.

H. E. Soper, in his 'Frequency Arrays,' gives the following generating function of $\phi(s, s')$:—

The G.F. of $\phi(s, s')$ is given by the coefficient of $s_1^n s_2^{n'}$ in

$$(1+s_1+s_2)^{N-m}(1+A_1s_1+A_2s_2)^m/{}^NC_{n,n'}.$$

Putting $A_1=1+\alpha,$

$A_2=1+\beta,$

we have the f.m.g.f. of $\phi(s, s')$ as the coefficient of $s_1^n s_2^{n'}$ in

$$(1+s_1+s_2)^{N-m}(1+s_1+s_2+\alpha s_1+\beta s_2)^m/{}^N C_{n,n'}.$$

And this is

$$1+\frac{m}{N}\{n\alpha+n'\beta\}+\frac{m^{(2)}}{N^{(2)}}\left\{n^{(2)}\frac{\alpha^2}{2!}+nn'\alpha\beta+\frac{n'^{(2)}\beta^2}{2!}\right\}$$

$$+\frac{m^{(3)}}{N^{(3)}}\left\{\frac{n^{(3)}\alpha^3}{3!}+\frac{n^{(2)}n'\alpha^2\beta}{2!\,1!}+\frac{n^{(1)}n'^{(2)}\alpha\beta^2}{1!\,2!}+\frac{n'^{(3)}\beta^3}{3!}\right\}$$

$$+\ldots;$$

therefore the (r_1, r_2)th factorial moment is the coefficient of $\frac{\alpha^{r_1}\beta^{r_2}}{r_1!\,r_2!}$,

i. e. $$\Sigma\Sigma\phi(s, s')s^{(r_1)}s'^{(r_2)}=\frac{m^{(r_1+r_2)}n^{(r_1)}n'^{(r_2)}}{N^{(r_1+r_2)}}.$$

Criteria for various Types of Regression.

Tschuprow, in his ' Grundbegriffe und Grundprobleme der Korrelationstheorie,' has given us the condition which the moments of the correlation function must fulfil in order that the regression should be (1) linear, (2) parabolic. Karl Pearson has given the conditions that the regression should be a parabola of the third and fourth degrees, and J. Neyman (Biom. vol. xviii. 1926, pp. 257) has generalized the formulæ of Pearson and A. A. Tschuprow to a regression curve which is a parabola of the nth degree.

We shall modify the theory of the respective writers, using factorial moments throughout so as to suit discrete frequency distributions.

We shall adopt Tschuprow's notation; given two fortuitous (" zufälligen ") variables X and Y.

Let $p_{i/}$ be the probability that X takes on one of its k possible values, namely the value X_i;

$p_{/j}$ the probability that Y takes on one of its l possible values, namely the value Y_j;

$p_{i/}^{(j)}$ the probability that X takes on the value X_i, Y having taken on the value Y_j.

Also $$m_{f/g}=\mathrm{E}x^f y^g=\sum_i\sum_j p_{ij}x_i^f y_j^g,$$

$$\mu_{f/g}=\sum_i\sum_j p_{ij}[x_i-m_{1/0}]^f[y_j-m_{0/1}]^g.$$

Also $$m_{/1}^{(i)}=\sum_j p_{ij}^{(i)}y_j.$$

Neyman's general condition is :

$$m_{h/1}=-\frac{1}{\mathrm{P}^{(n)}}\begin{vmatrix} 0 & m_{h/0} & m_{h+1/0}\cdots & m_{h+n/0} \\ m_{0/1} & m_{0/0} & m_{1/0} & m_{n/0} \\ m_{1/1} & m_{1/0} & m_{2/0} & m_{n+1/0} \\ \cdot\ \cdot & \cdot\ \cdot & \cdot\ \cdot & \cdot\ \cdot \\ m_{n/1} & m_{n/0} & m_{n+1/0} & m_{2n/0} \end{vmatrix}.$$

In Neyman's notation

$$\left.\begin{aligned} m_{h/0}&=\mu_h, \\ m_{k/1}&=\lambda_k, \end{aligned}\right\}$$

where $$\mathrm{P}^{(n)}=|\,p_{ik}\,|,$$

and $$p_{ik}=m_{i+k/0}\qquad \begin{pmatrix} i=0,\ 1,\ 2\ \ldots\ n \\ k=0,\ 1,\ 2\ \ldots\ n \end{pmatrix}.$$

This is easily obtained, since

$$m_{/1}^{(i)}=a_{/0}+a_{/1}x_i+\ \ldots\ +a_{/n}x_i^n.$$

Multiplying both sides by $p_{i/}x_i^h$, and summing for i, we get

$$\text{(I.)}\quad m_{h/1}=a_{/0}m_{h/0}+a_{/1}m_{h+1/0}+\ \ldots\ +a_{/n}m_{h+n/0}$$

for $h=0,\ 1,\ 2\ \ldots\ n$.

This therefore gives $n+1$ equations out of which the $n+1$ constants a can be determined. Inserting these values of a back in (I.) we get Neyman's condition as Tschuprow indicated.

If, however, we add equation (I.) to the $n+1$ equations we have $n+2$ consistent equations in $n+1$ unknowns.

Hence the augmented determinant of the system must vanish.

Using a variant of Schweins's Theorem due to

A. C. Aitken (see Edin. Math. Notes, March 1935) we obtain at once

$$m_{h/1}=\frac{m_{0/1}}{\mathrm{P}^{(0)}}+\frac{\sum_i \mathrm{P}_{1i}^{(r)} m_{1i}\ \sum_i \mathrm{P}_{1i}^{(r)} m_{h+1/0}}{\mathrm{P}^{(0)}\mathrm{P}^{(1)}}$$

$$+\ \ldots \frac{\sum_i \mathrm{P}_{ri}^{(r)} m_{i/1}\ \sum_i \mathrm{P}_{ri}^{(r)} m_{h+i,0}}{\mathrm{P}^{(r-1)}\mathrm{P}^{(r)}},$$

where $\mathrm{P}^{(r)}$ has already been defined, and $\mathrm{P}_{ri}^{(i)}$ denotes the determinant which is the cofactor of p_{ik} in $\mathrm{P}^{(r)}$.

This is the expansion of Neyman's condition.

Again, if we add to the $n+1$ equations the equation

$$m_{/1}^{(i)}=a_{/0}+a_{/1}x_i+\ \ldots\ +a_{/n}x_i^n,$$

we get at once, applying Aitken's variant, an expression for $m_1^{(i)}$ in terms of a set of orthogonal polynomials.

For linear regression the condition to be fulfilled is given by

$$\frac{m_{h/1}-m_{h/0}m_{0/1}}{m_{h+1/0}-m_{h/0}m_{1/0}}=\frac{m_{1/1}-m_{1/0}m_{0/1}}{m_{2/0}-m_{1/0}^2}$$

for all positive integral h.

Discrete Case.

Let
$$m_{h/1}=\sum_i\sum_j p_{i/j}x_i^{(h)}y_j,$$

$$m_{h,f/0}=\sum_i p_{i/}x_i^{(h)}x_i^{(f)}.$$

Starting with

$$\text{(I.)}\ m_{/1}^{(i)}=a_{/0}+a_{/1}x_i+\ \ldots\ +a_{/n}x_i^{(n)}$$

as the regression curve of Y on X, multiplying both sides by $p_{i/}x_i^{(h)}$, and summing for i, (I.) becomes

$$m^{h/1}=a_{/0}m_{h/0}+a_{/1}m_{h,\,1/0}+\ \ldots\ +a_{/n}m_{h,\,n/0}.$$

This gives us, in the same way as before, the following modified condition :—

$$m_{h/1}=-\frac{1}{\mathrm{P}^{(n)}}\begin{vmatrix} 0 & m_{h/0} & m_{h,\,1/0} & \ldots & m_{h,\,n/0} \\ m_{0/1} & m_{0/0} & m_{1/0} & & m_{n/0} \\ m_{1/1} & m_{0,\,1/0} & m_{1,\,1/0} & & m_{n,\,1/0} \\ \cdot & \cdot & \cdot & & \cdot \\ m_{n/1} & m_{0,\,n/0} & m_{1,\,n/0} & & m_{n,\,n/0} \end{vmatrix},$$

where $$P^{(n)}=|p_{ik}| \quad \begin{pmatrix} i=0,\ 1,\ 2,\ \ldots\ n \\ k=0,\ 1,\ 2,\ \ldots\ n \end{pmatrix}$$

and $$p_{ik}=m_{i,\,k/0} \qquad (m_{0,\,k/0}\equiv m_{k/0}).$$

(I.) can be expanded by Schweins's Theorem as in Neyman's case.

Linear Case.

The condition that the parameters m must fulfil becomes

$$\frac{m_{h/1}-m_{h/0}m_{0/1}}{m_{h,\,1/0}-m_{h/0}m_{1/0}}=\frac{m_{1/}\ -m_{1/0}m_{0/1}}{m_{1,\,1/0}-m_{1/0}^{2}} \quad . \quad . \quad . \quad (A)$$

for all positive integral h.

Example I.

We consider S. D. Wicksell's statement "all surfaces derived from the multinomial, binomial, and hypergeometric series must necessarily have linear regression."

If we sample from a fourfold table n times with replacement each time we obtain the frequency generating function

$$\{1+p_1(t-1)+p_{,}'(u-1)+p_{11}(t-1)(u-1)\}^{n}$$

in the usual notation.

This gives as f.m.g.f.

$$(1+p_1\,\alpha+p_1'\beta+p_{11}\alpha\beta)^{n}.$$

Now $m_{h/1}$ is given by the coefficient of $\dfrac{\alpha^{h}\beta}{h\,!}$ in this.

Therefore

$$\begin{aligned} m_{h/1}&=n^{(h)}p_1{}^{h}np_1'+n\delta(n-1)^{(h-1)}hp_1{}^{n-1} \\ &=n^{(h)}p_1{}^{h}np_1'+n^{(h)}\delta p_1{}^{h-1}, \end{aligned}$$

where $\delta=p_{11}-p_1p_1'$.

Again $$\begin{aligned} m_{h,f/0}&=\Sigma p_{i}x_i{}^{(h)}x_i{}^{(f)} \\ &=\Sigma p_{i}x_i{}^{(f+h)}+fh\Sigma p_{i}x_i{}^{(f+h-1)} \\ &\quad+\frac{f^{(2)}h^{(2)}}{2\,!}\Sigma p_{i}x_i{}^{(f+h-2)}+\ldots, \end{aligned}$$

applying Vandermonde's identity.

Also $$\begin{aligned} m_{1/1}&=n^{(2)}p_1{}^{2}+np, \\ m_{h/0}&=n^{(h)}p_1{}^{h}, \\ m_{1/0}&=np_1m_{0/1}=np_1'. \end{aligned}$$

Therefore $$\text{L.H.S. of (A)} = \frac{\delta}{p_1 q_1},$$

$$\text{R.H.S. of (A)} = \frac{\delta}{p_1 q_1}.$$

Therefore the regression is linear, and

$$r^2 = \frac{\delta^2}{p_1 q_1 p_1' q_1'}.$$

Example II.

Consider the double hypergeometric frequency function of Isserlis :

$$\phi(s, s') = \frac{m!\, n!\, n'!\, (\mathrm{N}-n-n')!\, (\mathrm{N}-m)!}{s!\, s'!\, (n-s)!\, (n'-s')!\, (m-s-s')!\, (\mathrm{N}-n-n'+s+s')!}.$$

We have shown that

$$\Sigma\Sigma\phi(s_1 s')s^{(r_1)}s'^{(r_2)} = \frac{m^{(r_1+r_2)}n^{(r_1)}n'^{(r_2)}}{\mathrm{N}^{(r_1+r_2)}}.$$

Hence $$m_{h/0} = \frac{m^{(h)}n^{(h)}}{\mathrm{N}^{(h)}},$$

$$m_{1/0} = \frac{mn}{\mathrm{N}},$$

$$m_{0/1} = \frac{mn'}{\mathrm{N}},$$

$$m_{h,1/0} = \frac{m^{(h+1)}n^{(h+1)}}{\mathrm{N}^{(h+1)}} + h\frac{m^{(h)}n^{(h)}}{\mathrm{N}^{(h)}}.$$

(This last result follows from the expansion of $\Sigma p_i x_i^{(h)} x_i^{(f)}$ given earlier.)

Also $$m_{h/1} = \frac{m^{(h+1)}}{\mathrm{N}^{(h+1)}} n^{(h)} n'.$$

Inserting in (A) we get

$$\text{L.H.S.} = -\frac{n'}{\mathrm{N}-n},$$

$$\text{R.H.S.} = -\frac{n'}{\mathrm{N}-n}.$$

Hence the regression is linear and negative and

$$r^2=\frac{nn'}{(\mathrm{N}-n)(\mathrm{N}-n')}.$$

Example III.

Consider next the problem of sampling from a fourfold table n times *en bloc* from a limited population N, replacing the sample each time.

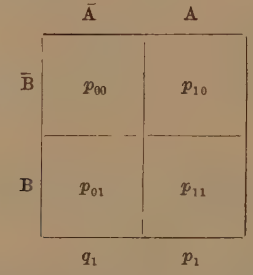

The generating function of the distribution of the characters A and B is given by the coefficient of s^n in

$$(1+s)^{\mathrm{N}p_{00}}(1+s\mathrm{A})^{\mathrm{N}p_{10}}(1+s\mathrm{B})^{\mathrm{N}p_{01}}(1+s\mathrm{AB})^{\mathrm{N}p_{11}}/{}^{\mathrm{N}}\mathrm{C}_n.$$

The f.m.g.f. is the coefficient of s^n in

$$(1+s)^{\mathrm{N}p_{00}}(1+s+\alpha s)^{\mathrm{N}p_{10}}(1+s+\beta s)^{\mathrm{N}p_{01}}$$
$$\times(1+s+\alpha+\beta+\alpha\beta s)^{\mathrm{N}p_{11}}/{}^{\mathrm{N}}\mathrm{C}_n. \quad \text{(B)}$$

Let
$$\mathrm{N}p_1=m,$$
$$\mathrm{N}p_1'=m'.$$

Then we have, putting $\beta=0$,

$$m_{h/0}=\frac{m^{(h)}n^{(h)}}{\mathrm{N}^{(h)}}.$$

Also
$$m_{1/0}=\frac{mn}{\mathrm{N}},$$

and
$$m_{h,\,1/0}=m_{h+1/0}+hm_{h/0}$$
$$=\frac{m^{(h+1)}n^{(h+1)}}{\mathrm{N}^{(h+1)}}+h\frac{m^{(h)}n^{(h)}}{\mathrm{N}^{(h)}},$$

$$m_{1,\,1/0}=\frac{m^{(2)}n^{(2)}}{\mathrm{N}^{(2)}}+\frac{mn}{\mathrm{N}}.$$

Hence all we need to apply our test for linearity of regression is the coefficients of $\alpha\beta$ and $\frac{\alpha^h\beta}{h!\,1!}$ in the expression (B).

We obtain quite easily that the coefficient of $\frac{\alpha^h\beta}{h!}$ is

$$[Np_{01}m^{(h)}+Np_{11}(m-1)^{(h)}]\frac{n^{(h+1)}}{N^{(h+1)}}$$

$$+Np_{11}h(m-1)^{(h-1)}\frac{n^{(h)}}{N^{(h)}};$$

therefore $m_{h/1}-m_{h/0}m_{0/1}$

$$=\left[\left(m'-\frac{mm'}{N}-N\delta\right)m^{(h)}+\left(\frac{mm'}{N}+N\delta\right)(m-h)^{(h)}\right]\frac{n^{(h+1)}}{N^{(h+1)}}$$

$$+h\left(\frac{mm'}{N}+N\delta\right)(m-1)^{(h-1)}\frac{n^{(h)}}{N^{(h)}}-\frac{m'nm^{(h)}n^{(h)}}{N.\,N^{(h)}}$$

(where as before $\delta=p_{11}-p_1p_1'$)

$$=ch(-N^2\delta n+N^3\delta)$$

$$=c\delta hN^2(N-n),$$

where $$c=\frac{(m-1)^{(h-1)}n^{(h)}}{N^{(h)}N(N-h)}.$$

Now $m_{h,1/0}-m_{h/0}m_{1/0}$

$$=\frac{m^{(h)}n^{(h)}}{N^{(h)}}-\left[\frac{(m-h)(n-h)}{N-h}+h-\frac{mn}{N}\right]$$

$$=\frac{m^{(h)}n^{(h)}}{N^{(h)}N.\,(N-h)}h[(N-m)(N-n)];$$

therefore L.H.S. of (A)$=\frac{N^2\delta}{(N-m)m}$,

also R.H.S. of (B)$=\frac{N^2\delta}{(N-m)m}$.

Therefore the regression is linear;

also $$r^2=\frac{N^4\delta^2}{(N-m)(N-m')mm'}=\frac{\delta^2}{p_1p_1'a_1a_1'}.$$

This completes the proof of the result indicated by Wicksell.

References.

K. Pearson. (1) "On a certain Double Hypergeometric Series and its Representation by Continuous Frequency Surfaces." Biom. vol. xvi. pp. 172–204 (1924).
——. (2) "On a General Method of Determining the Successive Terms in a Skew Regression Line." Biom. vol. xiii. pp. 296–300.
S. J. Pretorius. "Skew Bivariate Frequency Surfaces examined in the Light of Numerical Illustrations." Biom. vol. xxii. pp. 140–143 (1930–31).
A. A. Tschuprow. 'Grundbegriffe und Grundprobleme der Korrelationstheorie.' Teubner, 1927.
S. D. Wicksell. "The Application of Solid Hypergeometric Series to Frequency Distributions in Space." Phil. Mag. vol. xxxiii. ser. 6, pp. 389–394 (1917).
A. C. Aitken. "Variant of Schweins's Theorem." Edin. Math. Notes, March 1935.
H. E. Soper. 'Frequency Arrays.' Cambridge, 1922.

XV. *On the Rotation of Dipoles in Elastic and Viscous Media.* *By* N. L. Yates-Fish, *M.A., D.Phil., University College of Swansea* *.

1. *Introduction.*

THE variation of the dielectric constant with frequency and temperature, which is observed in the case of many liquids (and gases), is explained by the theory of Debye. According to this theory the molecules of these liquids possess a permanent electric dipole moment. The polarization of the medium under the action of an external field is due, therefore, not only to the distortion of the electronic and atomic structure of the molecules, but also to their orientation. The amount of this orientation is limited by the tendency of thermal agitation to set up a random distribution. Where steady or slowly varying electric fields are concerned it is only necessary to consider the distribution corresponding to a state of statistical equilibrium. In dealing with high frequency oscillating fields, however, the time taken to attain equilibrium also becomes important; this time is specified by a "time of relaxation" τ. Debye's theory is able to account for the observed variation of the dielectric constant with frequency if the value of τ is suitably chosen in each case.

* Communicated by the Author.

In order to determine the value of τ theoretically, it is necessary to know the magnitude of the couple acting on a dipole as it rotates in the liquid. To calculate this Debye assumes that the molecule can be regarded as a rigid sphere rotating in a viscous medium, and he then makes use of the formula deduced by Stokes for such a case. Satisfactory agreement with experiment is obtained by taking a reasonable value for the radius of the molecule, together with the value of the coefficient of viscosity determined in the ordinary way.

An attempt has recently been made by A. Gemant * to extend the dipole theory to amorphous solids. To represent the behaviour of such bodies Gemant makes use of the conception of "relaxing" or "fugitive" elasticity, which was first put forward by Maxwell. According to this conception, any deformation produced in the medium is considered to be opposed momentarily by an elastic restoring force, which, however, decays exponentially with time, the rate of decay being specified by a time of relaxation τ_0.

Following the lines of the Debye theory, Gemant assumes that the molecule can be regarded as a rigid sphere. It is then necessary to know the value of the couple acting on a rigid sphere when rotated through a small angle in an elastic medium. Gemant states that he is unable to find a calculation of this quantity in the literature.

It is the object of this paper to show that the value of the couple in this case can be deduced from the result obtained by Stokes for the analogous case of rotation in a viscous fluid.

2. *Statement of the Problem.*

When a rigid body embedded in a viscous fluid rotates about an axis with a small angular velocity ω it experiences a couple of magnitude $-C_1\eta\omega$, where η is the coefficient of viscosity of the fluid and C_1 a constant depending on the size and shape of the body.

When a rigid body embedded in a perfectly elastic medium is displaced through a small angle θ it experiences a couple of magnitude $-C_2E\theta$, where E is the modulus

* A. Gemant, Phil. Mag. xix. p. 746 (1935).

rigidity of the medium and C_2 another constant also depending on the size and shape of the body.

It is proposed to show that for a body of a given size and shape the constants C_1 and C_2 are equal.

The proof to be put forward depends upon the possibility of postulating a medium in which the relation between stress and strain is of such a general nature that the cases of true viscosity and true elasticity can be obtained from it as special cases. Now this property is, in fact, exhibited by a medium possessing the relaxing or fugitive type of elasticity already referred to as having been postulated by Maxwell and used by Gemant in his theory. The particular method of attacking the problem which is adopted below has the advantage of bringing out very clearly the properties of this kind of medium.

Throughout this paper we shall consider only deformations of a shearing nature, *i. e.*, it is assumed that there is no compression of the medium. It would therefore appear that the proof is only strictly applicable to solids of revolution rotating about their axes.

We shall also assume that the amount of the displacement at any given moment can be completely specified by a single co-ordinate, x, to which the strain at every point in the medium is proportional. This will be true if the changes of form are not so rapid that the finite time of propagation of a disturbance through the medium has to be taken into account.

These limitations also apply to the alternative proof given later. Fortunately they are not important in the application of the result to the theory of dipole rotation.

3. *The Proof.*

Let x be any quantity which suffices to determine the strain at all points in the medium. Corresponding to x there will be a force (using the word in a generalized sense) which we will call p.

Then in a perfectly elastic medium we would have for small displacements

$$p = -\mathrm{K}x,$$

where K is an elastic constant whose value depends on the geometry of the deformation.

The fundamental assumption in the conception of relaxing elasticity is that the stress at every point in the

medium decays exponentially with the time. This leads to the first postulate which is required in order to define the medium :—

(1) If a deformation dx is set up at a time t, the resulting force dp at a later time T is given by

$$dp = -\mathrm{K} e^{-\frac{\mathrm{T}-t}{\tau_0}} dx. \quad . \quad . \quad . \quad . \quad . \quad . \quad (1)$$

This property in itself, however, does not provide an adequate definition. It needs to be supplemented by a second postulate :—

(2) When the displacement x is varied with time, the force p at any time T is equal to the sum of the elementary forces dp (determined by equation (1)) due to all the elementary deformations dx set up at all times, t, in the past.

Taking T as the zero of time (so that t is always negative), we accordingly write the complete equation relating the force to the displacement as follows :—

$$p = -\mathrm{K} \int_{-\infty}^{0} e^{\frac{t}{\tau_0}} \frac{dx}{dt} dt. \quad . \quad . \quad . \quad . \quad . \quad (2)$$

It should be noticed that the time of relaxation τ_0 is a characteristic of the medium alone, and is independent of the geometry of the distortion.

Suppose a particular series of deformations is to be set up in such a medium. Then, owing to the existence of the time of relaxation τ_0, the nature of the opposing forces exerted by the medium will depend on the order of magnitude of the period of time over which the series of deformations is spread. This can be seen by considering two limiting cases, as follows :—

Case A.—If we make the period of time referred to sufficiently great, we can regard $\frac{dx}{dt}$ as a constant over the range of time during which the integrand in (2) is appreciable. Then

$$p = -\mathrm{K} \frac{dx}{dt} \int_{-\infty}^{0} e^{\frac{t}{\tau_0}} dt = -\mathrm{K}\tau_0 \frac{dx}{dt}. \quad . \quad . \quad . \quad (3)$$

In this case, therefore, the force is proportional to the rate of change of the displacement, so that the medium behaves as a viscous fluid.

Case B.—If the whole of the (small) displacement x occurs in a period of time small compared with τ_0, we can regard $e^{\frac{t}{\tau_0}}$ as sensibly unity over the whole range of integration. Then

$$p=-\mathrm{K}\int\frac{dx}{dt}dt=-\mathrm{K}x. \quad . \quad . \quad . \quad . \quad (4)$$

In this case, therefore, the force is proportional to the total displacement, so that the medium behaves as a perfectly elastic solid.

A medium having the properties postulated above will therefore behave as a viscous fluid when the changes of form are sufficiently slow, and as an elastic solid when they are sufficiently rapid.

Moreover, it follows immediately that the coefficient of viscosity in the first case is equal to the coefficient of rigidity in the second case multiplied by the time of relaxation. This can easily be seen by applying equations (3) and (4) to the relative displacement, in a direction parallel to their surfaces, of two parallel planes of unit area separated by unit distance. Let K′ be the particular value of K for this kind of deformation. From the definitions of viscosity and rigidity we have

$$p=\eta\frac{dx}{dt} \quad \text{and} \quad p=\mathrm{E}x$$

respectively, and comparing these with (3) and (4) we see that

$$\mathrm{K}'\tau_0=\eta \quad \text{and} \quad \mathrm{K}'=\mathrm{E},$$

so that

$$\eta=\mathrm{E}\tau_0.$$

Let us now apply our results to the problem of the rotation of a rigid body embedded in the medium. We accordingly put

$$x=\theta \quad \text{and} \quad \frac{dx}{dt}=\omega$$

in equations (3) and (4). If K″ is the value of K appropriate to any particular example of this problem, we have

$$\mathrm{K}''\tau_0=\mathrm{C}_1\eta \quad \text{and} \quad \mathrm{K}''=\mathrm{C}_2\mathrm{E},$$

where C_1 and C_2 are the constants defined in § 2. It

follows that $C_1/C_2 = E\tau_0/\eta = 1$. The constants are therefore equal, which is what we set out to prove.

In the particular example of the rotation of a rigid sphere of radius a embedded in a medium of infinite extent, the value of the couple calculated by Stokes for the viscous case is $-8\pi a^3\eta\omega$. The corresponding couple for the elastic case will therefore be $-8\pi a^3 E\theta$.

4. *Alternative Proof.*

As we have already said, the above method of attacking the problem has the advantage of bringing out very clearly the properties of a medium possessing relaxing elasticity. It must be emphasized that the validity of the proof does not in any way depend on whether such a medium actually exists in nature. An alternative proof in which the subject is treated from a different standpoint will now be given. For what follows I am indebted to Dr. P. M. Davidson.

We consider the rigid body, a solid of revolution, surrounded by a medium whose outer boundary, held fixed, we will assume for the moment to be a surface of revolution having the same axis as the body. We take two cases: in case A the medium is a viscous fluid and the body is kept rotating with a constant angular velocity ω about its axis; in case B the medium is a true solid, and by means of forces applied to the body the system is held, at rest everywhere, with the body rotated about its axis through a small angle θ from the position of equilibrium. The two media, neither of which need be incompressible, we define by the well-known differential equations of a solid * and a viscous fluid †. We wish to show that the solution for case B, which we understand from Mr. Gemant has never been given, is immediately derivable from the solution specified in standard calculations ‡ for case A.

We begin by reminding the reader that if $\mathbf{k}$ is a unit vector in the direction of the axis, and $\mathbf{r}$ the vectorial

* See almost any text-book which treats elasticity; for example, Webster's 'Partial Differential Equations of Mathematical Physics' (Teubner, 1927), p. 37, eqn. (136).

† For this Lamb's 'Hydrodynamics' (1916), p. 573, eqn. (2), is suggested. The corresponding equation in Webster is profoundly misprinted.

‡ Lamb, *loc. cit.*, in Art. 334, quotes the calculation for a sphere in a viscous fluid with a concentric spherical boundary, and gives a reference for the more general shapes.

distance from a fixed point on the axis to a point in the space occupied by the medium, we fix the value of a vector **F** at every point in that space if we demand that on the inner boundary (the surface of the body) its value shall be the vector product [**kr**], that it shall vanish on the outer boundary, and that everywhere between them the divergence of the gradient of its (scalar) component along each and every spatial direction shall vanish. Of this vector **F**, determined uniquely by the geometry of the system, we may remark that its direction at any **r** is that of [**kr**], and that the divergence of **F** is zero.

Let the angular displacement θ, and the angular velocity ω, defined above, appear clockwise when we look along the direction of **k**. Then the solution specified (*loc. cit.*) for case A is obtained by setting the vectorial velocity, say **v**, in the fluid, equal to $\omega\mathbf{F}$, a vector which satisfies the boundary conditions for case A, and satisfies also, for small ω, the differential equation of the fluid. In our case B, on the other hand, a glance at the boundary conditions and the differential equation of the solid tells us that the vectorial displacement, say **d**, in the solid, will be $\theta\mathbf{F}$, provided, of course, that the displacements are not large enough to make the equation of the solid inaccurate. (To be more precise about the limitations here imposed on ω and θ, let us suppose, by way of example, that the rigid body is a sphere of radius a, and that the distance between a point on the body and a point on the outer boundary is always at least of the same order as a. Then ω must be small compared with $\eta/\rho a^2$ (η being the viscosity and ρ the density of the fluid) in order that the equation of the fluid shall reduce to the form satisfied by **F**, and θ must be small compared with unity in order that the equation of the solid shall not become inaccurate.)

We now fix our attention on an element of area in the surface of the body (or more generally on any element of area in the medium) and call to mind the expressions for the tangential forces in a solid * and in a fluid †. Remembering that **d** and **v** have the values $\theta\mathbf{F}$ and $\omega\mathbf{F}$, we see that in case B if the rigidity is E the tangential force is $\mathrm{E}\theta$ times a simple vector function determined entirely by the (vectorial) element of area and the vector field **F**, while the tangential force in case A differs

* See, for example, Webster, p. 37, eqn. (135).
† Webster, p. 38, eqn. (135′).

only in having $\eta\omega$ instead of $E\theta$. It follows, of course, that the couples about the axis exerted by the media on the body are $CE\theta$ and $C\eta\omega$, with the same C in both.

Before concluding that the states thus specified could exist in reality, we must ask, as in all such calculations, whether they are stable. And we may count ourselves fortunate that in the case with which we are concerned—the solid—the stability of the state which we have specified is obvious. We need not pause to ask about the fluid, for even if the motion specified for it in the standard calculation were altogether unstable *, so that even if set up it would break down on the slightest vibration, instability arising even at microscopic ω's and vitiating its practical applicablity, there can be no doubt that our corresponding solution for case B is a stable and possible state, and is the only one satisfying the definition of case B.

If the medium extends in all directions to distances very large compared with the dimensions of the body, the value of C is practically independent of the actual shape of the outer boundary ; we thought of it as a surface of revolution coaxial with the body, but in such cases the limitation is unnecessary.

XVI. *On the Pressure Dependence of Unimolecular Reactions.* *By* E. A. Stewardson, *M.Sc., Ph.D., Department of Physics, National Central University, Nanking* †.

1. *Introduction.*

THE development of theories of homogeneous unimolecular gas reactions during recent years has been largely influenced by the discovery by Hinshelwood and his co-workers [1] in England, and by Ramsperger and others [2] in America, of the so-called quasiunimolecular reactions, *i. e.*, dissociation of which the rate is unimolecular at sufficiently high concentrations, but of which the rate falls off at lower concentrations and

* For many years it was believed, on experimental grounds, that this was actually the case ; but now it is generally accepted that the motion is stable at sufficiently small w's.

† Communicated by Prof. L. R. Wilberforce, M.A.

ultimately becomes bimolecular. Such reactions are most naturally described in terms of Lindemann's time-lag theory [3], according to which a finite interval of time elapses between activation and dissociation of a given molecule, so that at concentrations so high that the time between collisions is very short compared with the time lag a given molecule, activated by one collision, stands a much greater chance of being de-activated by a second collision than of dissociating, while at very low concentrations, when the period between collisions is very long compared with the lag period, all activated molecules stand a high chance of dissociating. If the activations are produced by collisions, so that the activation rate is proportional to the square of the concentration, then Lindemann's hypothesis is easily seen to lead to the general result that at high concentrations the rate of dissociation will be proportional to the concentration, *i. e.*, is unimolecular, and at very low concentrations it will be proportional to the square of the concentration, *i. e.*, it is bimolecular. Theories of unimolecular reactions based on this conception have been developed by Hinshelwood [4], Rice [5], Rice and Ramsperger [6], and more recently by Kassel [7] and others, who have placed the theory on a quantum mechanical basis. In the hands of Kassel particularly the theory has received very full development, and most known reactions of the unimolecular type have received fairly adequate description in terms of it.

Although these theories are all effectively time-lag theories, the time-lag itself is employed implicitly rather than explicitly. It is not without interest, therefore, to assume the time-lag explicitly and to use the classical kinetic theory expressions for the free path to calculate directly the chance that a given activated molecule will dissociate, and deduce therefrom the dependence of the dissociation rate on the pressure. Such treatment of the matter is given in the present paper. The resulting expressions for the rate are rather complicated, and although some measure of quantitative agreement with experiment is attained, it is doubtful whether they are of much practical utility. However, a number of interesting points emerge from this mode of treatment. In particular it is possible to estimate the order of magnitude of the time lag for known reactions, and also,

as is shown, it is easily possible to extend the analysis to cover the case of admixture with a foreign non-reacting gas, giving results in qualitative agreement with experiment.

2. *Calculation of the Pressure Effect.*

The activation is assumed to be produced by collisions of a special type, namely, those of sufficient energy resources, so that the rate of activation will be a collision frequency, and as we are not concerned with the absolute rate of dissociation, but only with its variation with the pressure, we may write the activation rate in the form $\gamma\nu^2$, where ν is the number of reactant molecules per unit volume and γ is independent of ν.

It is also assumed that if τ be the average time between activation and subsequent dissociation of a molecule, then the actual time-lags for a large number of molecules are distributed about this average according to the normal probability law, *i. e.*, the chance that an activated molecule will exist for time t without dissociating is $e^{-\frac{t}{\tau}}$. This is equivalent to assuming that the specific reaction rate is the same for all activated molecules (or, alternatively, that an activated molecule is a unique type so far as energy content is concerned). In practice this will not be true (indeed, Kassel [7] has shown that the best agreement with experiment is obtained by assuming that the probability of dissociation increases with the difference between actual energy content and the minimum activation energy). A more exact theory would distinguish a number of activated states, i, j, . . . with corresponding probabilities, $e^{-\frac{t}{\tau_i}}$, $e^{-\frac{t}{\tau_j}}$, ... For the present, however, the simpler model will be assumed. Effectively this will restrict the application of the theory to molecules of simple type, the approximation becoming less valid the more complex the molecule to which it is applied. For simplicity it is assumed also that the collision radius σ is independent of the energy content of the molecule, and is, therefore, the same for all participating molecules.

Finally, it is assumed that an activated molecule which suffers a collision before it can dissociate will be deactivated. This is reasonable, since an activated

molecule is one of exceptionably high energy content, and is much more likely to lose rather than gain energy by such encounters; and even if its energy does not fall below the minimum activation value it will most likely undergo redistribution, and the molecule may be regarded as a newly activated one about to start on a fresh career.

The number of activated molecules produced per unit volume in time dt will be $\gamma\nu^2\,dt$. Assuming the velocity distribution to be Maxwellian, the number of them possessing velocities in the range $(c,\ c+dc)$ will be

$$4\pi\sqrt{\frac{h^3m^3}{\pi^3}}\,.\,c^2e^{-hmc^2}\,dc\,.\,\gamma\nu^2\,dt, \quad . \quad . \quad . \quad (1)$$

where $h=1/2k\mathrm{T}$, k being the universal gas constant $(1{\cdot}36\times10^{-16}$ erg per molecule), T the absolute temperature, and m is the mass of a molecule.

Now the chance that a molecule survives for time t after activation is $e^{-\frac{t}{\tau}}$, and the chance that it dissociates in that time is $1-e^{-\frac{t}{\tau}}$. Also the chance that it goes a distance x without collision is $e^{-\frac{x}{\lambda_c}}$, where λ_c is the mean free path of a molecule of velocity c. Hence the chance that it does not suffer a collision in time t is $e^{-\frac{ct}{\lambda_c}}$.

Now suppose the $\gamma\nu^2\,dt$ molecules to be activated at the end of the interval dt. Then the number of them having velocities in the range $(c,\ c+dc)$ which are free from collision for time t is

$$4\sqrt{\frac{h^3m^3}{\pi^3}}\,.\,c^2e^{-hmc^2}e^{-\frac{ct}{\lambda_c}}dc\,.\,\gamma\nu^2\,dt. \quad . \quad . \quad . \quad (2)$$

Call this quantity N. Then of these the number that survive for a time t without undergoing dissociation is $\mathrm{N}e^{-\frac{t}{\tau}}$. The number that survive for $t-\delta t$ (where δt is small compared with τ) is $\mathrm{N}e^{-\frac{t-\delta t}{\tau}}$. Hence the number which dissociate during the interval δt is

$$\mathrm{N}\left\{e^{-\frac{t-\delta t}{\tau}}-e^{-\frac{t}{\tau}}\right\}=\mathrm{N}e^{-\frac{\delta t}{\tau}}\,.\,\frac{\delta t}{\tau}, \quad . \quad . \quad . \quad (3)$$

since $\delta t/\tau$ is small. This will be less than the actual number which, possessing the specified velocities, dissociate during δt, as there will be some which are collision-free for a time between t and $t-\delta t$, and which will dissociate just before collision. Hence (3) is a lower limit. We may assign an upper limit by taking all those free for a time greater than $t-\delta t$, and assuming that they all survive the interval δt without collision. It is easily seen that this number differs from (3) by a small quantity of the second order, and hence (3) is a sufficiently good approximation.

Similarly, if we consider the activation to be produced at the beginning of the interval dt, we again obtain a quantity differing only in a second order term from (3). Hence, as the number of dissociations will lie between these values, we may take (3) as giving the number of molecules which, possessing the specified velocities and being activated during the interval dt, dissociate during the interval δt. Written in full this is

$$\frac{4\pi}{\tau}\sqrt{\frac{h^3m^3}{\pi^3}}\,.c^2e^{-hmc^2}e^{-\frac{ct}{\lambda_c}}e^{-\frac{t}{\tau}}\gamma\nu^2\,dc\,dt\,\delta t. \quad . \quad . \quad (4)$$

Summing up for all velocities, and for activations derived from all intervals dt anterior to δt, the number of dissociations during the interval δt is

$$\frac{4\pi}{\tau}\sqrt{\frac{h^3m^3}{\pi^3}}\,\delta t\int_{c=0}^{\infty}\int_{t=0}^{\infty}c^2e^{-hmc^2}e^{-\frac{ct}{\lambda_c}-\frac{t}{\tau}}\gamma\nu^2\,dc\,dt. \quad (5)$$

Hence the rate of dissociation ξ is given by

$$\xi=\frac{4\pi}{\tau}\sqrt{\frac{h^3m^3}{\pi^3}}\int_{c=0}^{\infty}\int_{t=0}^{\infty}c^2e^{-hmc^2}e^{-\frac{ct}{\lambda_c}-\frac{t}{\tau}}\gamma\nu^2\,dc\,dt. \quad (6)$$

If we assume that the rate of dissociation is sufficiently slow to consider ν constant during the time in which effective contributions are made to the integral in (6) (and in general this approximation will be valid), we may write (6) in the form

$$\xi=\frac{4\pi}{\tau}\sqrt{\frac{h^3m^3}{\pi^3}}\gamma\nu^2\int_{c=0}^{\infty}\int_{t=0}^{\infty}c^2e^{-hmc^2}e^{-\frac{ct}{\lambda_c}-\frac{t}{\tau}}dc\,dt$$

or, carrying out the integration with respect to the time,

$$\xi=\frac{4\pi}{\tau}\sqrt{\frac{h^3m^3}{\pi^3}}\gamma\nu^2\int_0^\infty\frac{c^2e^{-hmc^2}\,dc}{\frac{c}{\lambda_c}+\frac{1}{\tau}}. \quad . \quad . \quad . \quad . \quad (7)$$

Now the mean free path of a molecule of velocity c in a gas composed of molecules of one type only is

$$\lambda_c=\frac{hmc^2}{\sqrt{\pi}.\nu\sigma^2\psi(c\sqrt{hm})},$$

where ψ is a function such that

$$\psi(x)=xe^{-x^2}+(2x^2+1)\int_0^x e^{-x^2}\,dx.$$

Hence

$$\xi=\frac{4\pi}{\tau}\sqrt{\frac{h^3m^3}{\pi^3}}\gamma\nu^2\int_0^\infty\frac{c^2e^{-hmc^2}\,dc}{\frac{1}{\tau}+\frac{\sqrt{\pi}.\nu\sigma^2\psi(c\sqrt{hm})}{hmc}}.$$

Writing $x^2=hmc^2$ and $\beta=\tau\sigma^2\sqrt{\frac{\pi}{hm}}$, this reduces to

$$\xi=\frac{4\gamma\nu^2}{\sqrt{\pi}}\int_0^\infty\frac{x^2e^{-x^2}dx}{1+\beta\nu\frac{\psi(x)}{x}}, \quad . \quad . \quad . \quad . \quad (8)$$

and the unimolecular constant K is given by

$$\mathrm{K}=\frac{4\gamma\nu}{\sqrt{\pi}}\int_0^\infty\frac{x^2e^{-x^2}\,dx}{1+\beta\nu\frac{\psi(x)}{x}}. \quad . \quad . \quad . \quad . \quad (9)$$

This gives the variation of K with ν. Owing to the complex nature of $\psi(x)$, the direct evaluation of the integral appears to be impossible, but its behaviour for extreme values of ν, representing great concentration and great dilution, however, is easily deducible.

Let

$$\mathrm{I}(\beta\nu)=\int_0^\infty\frac{x^2e^{-x^2}\,dx}{1+\beta\nu\frac{\psi(x)}{x}},$$

and let $R(\beta\nu)=\beta\nu I(\beta\nu)$. Then K is given by

$$K=\frac{4\gamma}{\beta\sqrt{\pi}}.R(\beta\nu). \quad . \quad . \quad . \quad . \quad . \quad (10)$$

Now the quantity under the integral in $I(\beta\nu)$ involves two functions of x, namely, $x^2e^{-x^2}$ and $\psi(x)/x$. The first of these has the value zero for $x=0$ and for $x=\infty$, and attains a maximum of e^{-1} for $x=1$. The second has the value 2 at $x=0$, and is always greater than this for all positive values of x*. From the known properties of $x^2e^{-x^2}$ it is obvious that the effective contributions to $I(\beta\nu)$ are derived from values from zero to the neighbourhood of 4, by which time $\psi(x)/x$ has increased from 2 to about 7. The actual value of $I(\beta\nu)$ depends on the parameter $\beta\nu$, which is proportional to the concentration ν, and, therefore, to the partial pressure of the dissociating gas. If ν is large enough to make $\beta\nu$ large compared with unity, then we may write

$$I(\beta\nu)=\int_0^\infty \frac{x^2e^{-x}}{\beta\nu\dfrac{\psi(x)}{x}}\,dx$$

and

$$K=\frac{4\gamma}{\beta\sqrt{\pi}}R(\beta\nu)$$

$$=\frac{4\gamma}{\beta\sqrt{\pi}}\int_0^\infty \frac{x^2e^{-x^2}}{\dfrac{\psi(x)}{x}}\,dx, \quad . \quad . \quad . \quad (11)$$

i. e., K is independent of ν, and the reaction is rigorously unimolecular. The integral in (11) has been evaluated by quadrature. Its value is 0·1626 approx. Hence K_∞, the unimolecular constant for infinite concentration, is

$$K_\infty=\frac{4\gamma}{\beta\sqrt{\pi}}(0{\cdot}163)=\frac{{\cdot}65\,\gamma}{\beta\sqrt{\pi}}. \quad . \quad . \quad . \quad (12)$$

* Direct expansion of $\psi(x)$ gives the following series for $\psi(x)/x$:

$$\psi(x)/x=2+\frac{2}{3}x^2-\frac{1}{15}x^4+\frac{1}{105}x^6\ldots.$$

For large values of x the well known asymptotic expansion for the error function leads to

$$\psi(x)/x\doteqdot\frac{\sqrt{\pi}}{2x}(2x^2+1)-\frac{e^{-x^2}}{2x^4},$$

while for very large values of x, $\psi(x)/x=x\sqrt{\pi}$. As a matter of fact the positive part of the hyperbola $y=\sqrt{(4+\pi x^2)}$ approximates remarkably closely to $\psi(x)/x$ for all values of x.

If ν is small enough to make $\beta\nu$ small compared with unity, then for those values of x which appreciably affect the integral the quantity $\beta\nu\psi(x)/x$ is also small, and we may write

$$I(\beta\nu)=\int_0^\infty x^2e^{-x^2}dx=\tfrac{1}{4}\sqrt{\pi}.$$

In this case, from (8), the rate of dissociation is

$$\xi=\frac{4\gamma\nu^2}{\sqrt{\pi}}I(\beta\nu)=\gamma\nu^2,$$

i. e., the reaction is now bimolecular, the bimolecular constant being equal to the activation constant γ, so that

Table I.

$\beta\nu$.	$I(\beta\nu)$.	$R(\beta\nu)$.	k/k_∞.
∞	·0	·1626	1·000
10^3.....	·0001622	·1622	·998
10^2.....	·001615	·1615	·993
10	·01567	·1567	·964
1	·11789	·1179	·725
10^{-1}.....	·34603	·0346	·213
10^{-2}.....	·43096	·0043	·026
0	·4431	·0000	·000

the activation and dissociation rates are now identical, as is to be expected on general grounds.

In order to compare with known reactions, values of $I(\beta\nu)$ and $R(\beta\nu)$ have been obtained by quadrature for various values of $\beta\nu$. This enables the ratio K/K_∞ to be calculated, for from (10) and (12)

$$\frac{K}{K_\infty}=6{\cdot}15\ R(\beta\nu). \quad . \quad . \quad . \quad . \quad . \quad (13)$$

Table I. gives the values of the various quantities involved.

It will be seen that appreciable departure from a unimolecular rate occurs when $\beta\nu$ is of the order of 10. The value of β depends, among other things, on τ and σ, both of which are determined by the structure of the

dissociating body. Hence the value of ν at which the rate begins to depart appreciably from a strict unimolecular form is a function of the reacting body. On the other hand, the theory is certainly too restrictive, since from (10) the dependence of K on ν is identical in form for all substances, differing only in scale.

A point of interest is the consideration of the temperature coefficients. From (12)

$$K_\infty = \frac{\cdot 65\gamma\sqrt{hm}}{\pi\tau\sigma^2} = \frac{\cdot 65\gamma}{\pi\tau\sigma^2}\sqrt{\frac{m}{2k\overline{T}}},$$

and, therefore,

$$\log K_\infty = \log \gamma - \tfrac{1}{2}\log T + \log (\text{const.})$$

and

$$\frac{d(\log K_\infty)}{dT} = \frac{d(\log \gamma)}{dT} - \frac{1}{2T}.$$

Also, since the bimolecular constant K_2 for low concentration is equal to γ, we have

$$\frac{d(\log K_2)}{dT} = \frac{d(\log \gamma)}{dT}.$$

Hence the value of E/RT^2 deduced experimentally when the reaction is in the unimolecular state should differ from that obtained in the bimolecular state by an amount of the order of $1/2T$. In actual practice $1/2T$ is of the order of 10^{-3} of E/RT^2, so that with existing technique the values of E deduced experimentally from the unimolecular and bimolecular rates would probably be indistinguishable.

Finally, it is important to consider the effect of temperature on the pressure dependence of K. From (13) we have

$$\frac{K}{K_\infty} = 6{\cdot}15R(\beta\nu) = 6{\cdot}15\beta\nu\int_0^\infty \frac{x^2e^{-x^2}\,dx}{1+\beta\nu\dfrac{\psi(x)}{x}},$$

$$= 6{\cdot}15\int_0^\infty \frac{x^2e^{-x^2}\,dx}{\dfrac{1}{\beta\nu}+\dfrac{\psi(x)}{x}}.$$

If p be the pressure, then $p=\nu k\mathrm{T}$; also

$$\beta=\tau\sigma^2\sqrt{\frac{\pi}{hm}}=\tau\sigma^2\sqrt{\frac{2k\mathrm{T}.\pi}{m}},$$

and, therefore,

$$\frac{1}{\beta\nu}=\frac{1}{\tau\sigma^2}\sqrt{\frac{mk}{2\pi}}\cdot\frac{\sqrt{\mathrm{T}}}{p},$$

and

$$=6{\cdot}15\int_0^\infty\frac{x^2e^{-x^2}\,dx}{\frac{1}{\tau\sigma^2}\sqrt{\frac{mk}{2\pi}}\cdot\frac{\sqrt{\mathrm{T}}}{p}+\frac{\psi(x)}{x}}.$$

The pressure and temperature occur in this expression as the single factor $\sqrt{\mathrm{T}}/p$, and it follows that an increase in temperature will produce a change in $\mathrm{K}/\mathrm{K}_\infty$ in the opposite direction to that due to an increase in the pressure, *i. e.*, if the temperature is increased a higher pressure will be required to maintain $\mathrm{K}/\mathrm{K}_\infty$ at a given value, this being in qualitative agreement with experiment.

3. *Comparison with Experiment.*

The quantities given in Table I. may be used to effect a comparison with experiment.

From (10)

$$\log_{10}\mathrm{K}=\log_{10}\mathrm{R}(\beta\nu)+\log_{10}(\text{const.}).$$

At a given temperature ν is proportional to the pressure; hence we may write

$$\log_{10}p_{mm}=\log_{10}\beta\nu+\log_{10}(\text{const.}),$$

so that, in making comparison with experimental values of $\log_{10}\mathrm{K}$ and $\log_{10}p$, there are two adjustable constants available.

The simplest body known to decompose according to a unimolecular law is nitrous oxide. Extensive data by Nagasako and Volmer, and by Volmer and Kummerow, are given in Kassel's book, 'Kinetics of Homogeneous Gas Reactions.' Fig. 1 shows the result of taking

$$\log_{10}\mathrm{K}=\log_{10}\mathrm{R}(\beta\nu)-1{\cdot}94,$$
$$\log_{10}p_{mm}=\log_{10}\beta\nu+3{\cdot}65.$$

The curve is drawn from the values of $R(\beta\nu)$ and $\beta\nu$ given in Table I., the points in circles being the experimental values for N_2O at 938° K. The agreement is quite good, and although the curve falls slightly below the experimental values at low pressures, the discrepancy is approximately the same as that due to the formula

Fig. 1.

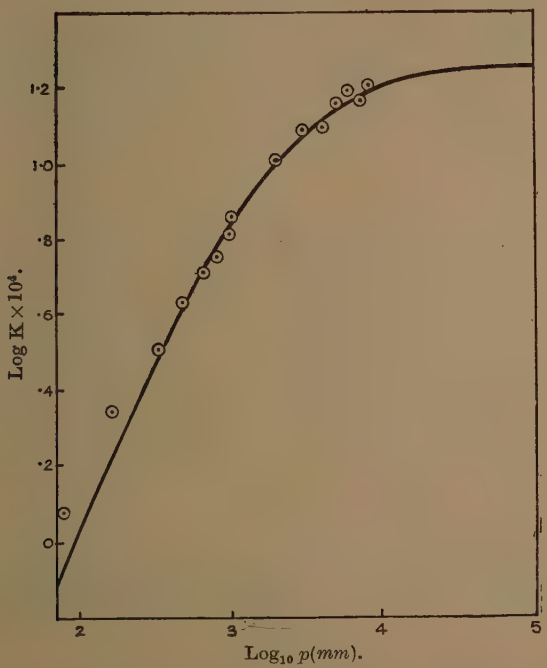

given by Kassel (*loc. cit.*). From the numerical relation taken between p and $\beta\nu$ it is possible to calculate τ.

Since

$$\log_{10} p_{mm} = \log_{10} \beta\nu + 3{\cdot}65,$$

then

$$p_{mm} = 4467\beta\nu$$

$$= 4467\nu\tau\sigma^2 \sqrt{\frac{\pi RT}{M}},$$

where M=molecular weight. Taking M=44 for N_2O, $\sigma^2=10^{-15}$, and using the relation $p_{mm}=1{\cdot}3\times10^{-19}\,\nu T$ and T=980° K., it is found that τ is of the order of 10^{-11} second, this extremely short average life for the activated molecule being the counterpart of the fact that such high pressures are required to maintain a rigorous unimolecular rate in nitrous oxide.

Fig. 2.

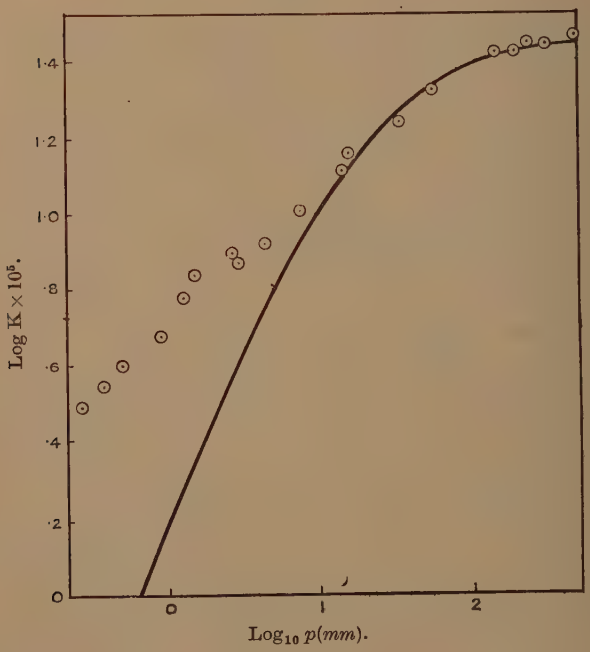

As was anticipated, the agreement in the case of more complex molecules is much poorer. Fig. 2 shows the best agreement that can be obtained with the dissociation of azo-methane by taking

$$\log_{10} K = \log_{10} R(\beta\nu) - 1{\cdot}74.$$
$$\log_{10} p_{mm} = \log_{10} \beta\nu + 1{\cdot}70.$$

The points are the experimental values of Ramsperger for azo-methane at 603° K. as given by Kassel. The

divergence at lower pressures is very wide, and the agreement very much poorer than that given by Kassel's more detailed treatment. Calculating τ as in the previous case, it is found to be of the order of 10^{-8} second.

A rough estimate of τ for other reactions may be obtained from the fact that appreciable departure from strict unimolecular form occurs when $\beta\nu$ is of the order of 10, and by comparing this with the observed pressures at which the reaction rates begin to fall off, a rough value of τ may be arrived at. In this way the values of τ for the unimolecular reactions listed by Kassel are found to be in the range 10^{-6} to 10^{-8} second, indicating that the average life of an activated molecule is of the same order of magnitude as the average life of excited atoms.

4. *Dissociation in the presence of an Inert Gas.*

The analysis of section 2 is easily extended to include the case when the reacting gas is mixed with a gas chemically inert to it. It is assumed that the molecules of the admixed gas can activate and deactivate the reactant molecules. In this case activations and deactivations arise from collisions both with the reactant and inert gas-molecules. Using the suffixes 1 and 2 to denote the original gas and the inert gas respectively, we may write the rate of activation in the form

$$a\nu_1^2+b\nu_1\nu_2, \quad . \quad . \quad . \quad . \quad . \quad . \quad (14)$$

where a and b are independent of ν_1 and ν_2. Assuming, as before, that the rate of dissociation is sufficiently slow, we may put (14) in the form

$$(a+\omega b)\nu_1^2, \quad . \quad . \quad . \quad . \quad . \quad . \quad (15)$$

where $\omega=\nu_2/\nu_1$, and may be termed a "coefficient of dilution." In place of expression (7) we then get for the rate of dissociation

$$\xi=\frac{4\pi}{\tau}\sqrt{\frac{h^3m_1^3}{\pi^3}}(a+\omega b)\nu_1^2\int_0^\infty\frac{c^2e^{-hmc^2}dc}{\frac{c}{\lambda_c}+\frac{1}{\tau}}. \quad . \quad (16)$$

Now the mean free path of a molecule of type 1 and

velocity c in a mixture of molecules of types 1 and 2 is given by

$$\lambda_c = \frac{c}{\Theta_{11} + \Theta_{12}},$$

where

$$\Theta_{1s} = \frac{\sqrt{\pi} \cdot \nu_s \sigma_{1s}^2 \, \psi(c\sqrt{hm_s})}{hm_s c}.$$

Substituting this in (16),

$$\xi = 4\pi \sqrt{\frac{h^3 m_1^3}{\pi^3}} (a + \omega b) \nu_1^2 \times \int_0^\infty \frac{c^2 e^{-hm_1 c^2} \, dc}{1 + \tau\sqrt{\pi} \cdot \left\{ \frac{\sigma_{11}^2 \nu_1 \psi(c\sqrt{hm_1})}{hm_1 c} + \frac{\sigma_{12}^2 \nu_2 \psi(c\sqrt{hm_2})}{hm_2 c} \right\}},$$

or, writing $hm_1 c^2 = x^2$, $\nu_2 = \omega\nu_1$ and $\sqrt{m_2/m_1} = \phi$,

$$\xi = \frac{4\nu_1^2 (a + \omega b)}{\sqrt{\pi}} \times \int_0^\infty \frac{x^2 e^{-x^2} \, dx}{1 + \tau\nu_1 \sqrt{\frac{\pi}{hm_1}} \left\{ \sigma_{11}^2 \frac{\psi(x)}{x} + \frac{\omega\sigma_{12}^2}{\phi} \cdot \frac{\psi(\phi x)}{\phi x} \right\}}. \quad . \quad . \quad . \quad (16)$$

The quantity ϕ is equal to the square root of the ratio of the mass densities of the two gases, *i. e.*, $\phi = \sqrt{\rho_2/\rho_1}$. The collision radii will not be very different from one another, and we take them as being equal without appreciably affecting the argument. Making this approximation, and writing $\beta = \tau\sigma_{11}^2 \sqrt{\frac{\pi}{hm_1}}$, (16) becomes

$$\xi = \frac{4\nu_1^2 (a + \omega b)}{\sqrt{\pi}} \int_0^\infty \frac{x^2 e^{-x^2} \, dx}{1 + \beta\nu_1 \left\{ \frac{\psi(x)}{x} + \frac{\omega}{\phi} \cdot \frac{\psi(\phi x)}{x\phi} \right\}}, \quad (17)$$

and, taking the particular case $\omega = 1$ (*i. e.*, 50 per cent. dilution),

$$\xi = \frac{4\nu_1^2}{\sqrt{\pi}} (a + b) \int_0^\infty \frac{x^2 e^{-x^2} \, dx}{1 + \beta\nu_1 \left\{ \frac{\psi(x)}{x} + \frac{1}{\phi} \cdot \frac{\psi(\phi x)}{\phi x} \right\}}. \quad . \quad (18)$$

The variation of this quantity with ν_1 is of the same type as expression (8), except that the value of ν_1, at which appreciable departure from unimolecular form takes place, will be dependent on ϕ. If ρ_2 is much less than ρ_1, then ϕ is small and $1/\phi$ large. In this case a smaller value of ν_1 will be needed to make the 1 in the denominator of importance to the value of the integral, *i. e.*, a lower value of the pressure will be required in order to cause divergence from the strict unimolecular law. Going back to (17), the magnitude of this change will depend on ω, *i. e.*, it will depend on the amount of foreign gas present. If ρ_2 is increased, $1/\phi$ decreases, and the effect of the foreign gas is diminished. For ϕ equal to or greater than unity the effect becomes very small.

Values of the integral in (17) have been obtained by quadrature for $\beta\nu_1=\infty$ and $\beta\nu_1=1$, with $\omega=1$, and $\phi=0{\cdot}1$

TABLE II.

$\beta\nu$.	K/K_∞.		
	$\omega=0$.	$\omega=1, \phi=1$.	$\omega=1, \phi=0{\cdot}1$.
∞	1·000	1·000	1·000
1·0	·727	·838	·965

and $\phi=1{\cdot}0$. This allows K/K_∞ to be calculated. These values are compared with the case $\omega=0$ in Table II., while fig. 3 shows the curves for K/K_∞ for $\omega=0$ (full line), $\omega=1$, $\phi=0{\cdot}1$ (dotted curve), and $\omega=1$, $\phi=1{\cdot}0$ (chain-dotted curve). It will be seen that addition of a light gas ($\phi=0{\cdot}1$) exerts a powerful effect in maintaining the unimolecular rate. This is in qualitative agreement with Hinshelwood's experiments, where hydrogen is found to exert this influence on the dissociation rate, but not the heavier gases.

There are too many adjustable constants to make it worth while attempting to fit these results to the experimental results, but in any case it is very doubtful whether the effect given by equation (17) is of the right magnitude. Too many important factors have necessarily been left out of account, questions of target area

in particular not having been considered at all. Also there is nothing in expression (17) to indicate that $K_\circ$ in this case is equal to K_∞ for $\omega=0$, as is found experimentally—a point which has already been raised by Hinshelwood [1]. An investigation of this matter would probably require a more detailed view to be taken of the activation processes, and in that case it would certainly be treated more advantageously by the methods

Fig. 3.

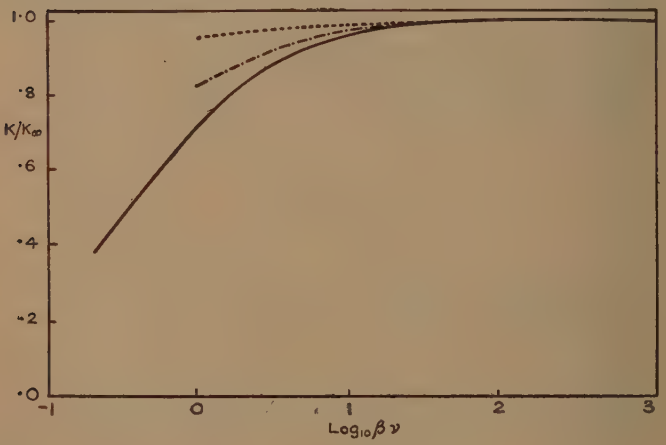

already developed by Rice and Kassel than on the lines given in the present paper.

References.

(1) See Hinshelwood, 'Kinetics of Chemical Change in Gaseous Systems,' 3rd ed., ch. v. Also under ref. 2.
(2) Kassel, 'Kinetics of Homogeneous Gas Reactions,' ch. x.
(3) Lindemann, Trans. Far. Soc. xvii. p. 598 (1922).
(4) Hinshelwood, Proc. Roy. Soc., A, cxiii. p. 230 (1926). (Also (1) above).
(5) O. K. Rice, Proc. Nat. Acad. Sci. xiv. p. 114 (1928).
(6) Ramsperger and Rice, J. Am. Chem. Soc. xlix. p. 1617 (1927); *ibid.* l. p. 617 (1928).
(7) Kassel, J. Phys. Chem. xxxii. p. 225 (1928); *ibid.* xxxii. p. 1065 (1928); see also Kassel's book (ref. 2), ch. v.

XVII. *The Large Roots of* $\cos z = az + c$. *By* RALPH COOPER, *M.A.*, *Ph.D.*, *and* JOHN TODD, *B.Sc.*, *Department of Mathematics, The Queen's University, Belfast, Ireland* *.

I. *Introduction.*

THIS article was suggested by a recent note † in this Journal where the values of 7 roots of small modulus of the equation

$$\cos z = z \quad . \quad . \quad . \quad . \quad . \quad . \quad . \quad . \quad (S)$$

were calculated and where certain conjectures ‡ were made regarding the asymptotic behaviour of the large roots (*i. e.*, the roots with large modulus).

We consider the equation

$$\cos z = az + c, \quad . \quad . \quad . \quad . \quad . \quad . \quad . \quad (1)$$

where $a = \alpha + i\beta$, $c = \gamma + i\delta$ with α, β, γ, δ real and $a \neq 0$, and find it convenient to discuss the cases $\beta = 0$ and $\beta \neq 0$ separately in Section II. and Section III. respectively. It is clear that these cases cover not only (1) itself, but also all the equations obtained from it by replacing $\cos z$ by $\cos kz$, $\cosh kz$, $\sin kz$, or $\sinh kz$, where k is any constant, real or complex. In both cases we establish the existence of an infinity of roots of (1) and, therefore, in particular of (S)—a result which, contrary to Silberstein's statement, does not follow from the mere fact that $\cos z - z$ is an integral function. Our results can be used as illustrations of standard theorems about the distribution of values of integral functions, and in this connexion we notice that they show that $\cos z - az$ has no exceptional values in the Picard sense, and the fact that $\cos z - az$ has no exceptional values in the Borel sense is almost an immediate consequence,

R. (Case $\beta = 0$.)

$$\cos z = \alpha z + \gamma + i\delta. \quad . \quad . \quad . \quad . \quad (1.R)$$

It will be enough to consider the case in which $\alpha > 0$ because the roots of the equation

$$\cos z = -\alpha z + \gamma - i\delta \quad . \quad . \quad . \quad . \quad (1.R\,1)$$

* Communicated by the Authors.

† L. Silberstein, "The Roots of $\cos z = z$," Phil. Mag. (7) xx. pp. 528–531 (1935).

‡ *Ibid.*, last paragraph on p. 531.

are the images in the imaginary axis of those of (1.R). Again, it will only be necessary to consider those roots of (1.R) (with $\alpha>0$) with positive imaginary part because the roots of (1.R) are the images in the real axis of the roots of the equation

$$\cos z = \alpha z+\gamma-i\delta. \quad . \quad . \quad . \quad . \quad . \quad (1.R.2)$$

Our results in their crudest form * are

$$x_n \sim (-1)^n n\pi, \quad . \quad . \quad . \quad . \quad . \quad . \quad (1.R.3)$$

$$y_n \sim \log 2\alpha n\pi, \quad . \quad . \quad . \quad . \quad . \quad . \quad (1.R.4)$$

n being a large positive integer. These results give

$$| x_{n+2}-x_n | \to 2\pi, \quad . \quad . \quad . \quad . \quad . \quad (1.R.5)$$

$$| y_{n+1}-y_n | \to 0. \quad . \quad . \quad . \quad . \quad . \quad (1.R.6)$$

The result (1.R.5) establishes the truth of one † of Silberstein's conjectures, while (1.R.6) shows that another is wrong. The more accurate expressions that we have obtained for x_n, y_n show that $| x_{n+2}-x_n |$ ultimately decreases steadily to 2π (so verifying a third conjecture), and that $y_{n+1}-y_n$ ultimately decreases steadily to zero,

C. (Case $\beta \neq 0$.)

$$\cos z = (\alpha+i\beta)z+\gamma+i\delta \quad . \quad . \quad . \quad . \quad (1.C)$$

The method we use when $\beta=0$ will not apply in this case, and we use a method which at almost every step assumes that $\beta \neq 0$. We have not thought it worth while to carry the approximation so far as in the previous case. The final results, (3.8) and (3.9), are of the same general form as (2.18) and (2.19). Here we point out some differences. A crude form of the results for roots with positive imaginary parts is

$$x_n = 2n\pi+\theta+o(1),$$

$$y_n = \log 2fn\pi+o(1),$$

where f, θ are certain non-zero constants depending on a, c, each having (*not* independently) two possible values

* For more accurate results see (2.18) and (2.19) below. As usual, we write $z=x+iy$, $z_n=x_n+iy_n$, using z_n to denote a root.

† x_{n+1}, x_n have opposite signs, so it is most natural here to consider z_{n+2}, z_n as " successive " roots in respect of this conjecture.

(one of which is positive and the other negative), and n is a large integer of the same sign as f. The presence in x_n, of the number θ, which satisfies $0 < |\theta| < \pi$ shows that here the real parts of the roots no longer approximate to multiples of π. For the limits of the differences we still have 2π, 0, but without carrying the approximations to more terms nothing can be said about the question of whether these limits are ultimately approached monotonically.

II. *The Real Case.*

In this section we consider the large roots of the equation

$$\cos z = \alpha z + \gamma + i\delta, \quad . \quad . \quad . \quad . \quad . \quad (2)$$

where α, γ, δ are real and $\alpha \neq 0$. We have seen above that it is sufficient to consider positive value of α and to examine the roots whose imaginary parts are positive.

Separating (2) into its real and imaginary parts, we obtain

$$\cos x \cosh y = \alpha x + \gamma, \quad . \quad . \quad . \quad . \quad (2.\mathrm{R})$$

$$-\sin x \sinh y = \alpha y + \delta. \quad . \quad . \quad . \quad . \quad (2.\mathrm{I})$$

According as we eliminate the circular or hyperbolic functions these give

$$\left(\frac{\alpha x+\gamma}{\cosh y}\right)^2 + \left(\frac{\alpha y+\delta}{\sinh y}\right)^2 = 1, \quad . \quad . \quad . \quad (2.\mathrm{H})$$

$$\left(\frac{\alpha x+\gamma}{\cos x}\right)^2 - \left(\frac{\alpha y+\delta}{\sin x}\right)^2 = 1. \quad . \quad . \quad . \quad (2.\mathrm{T})$$

It is clear from (2.H) that the roots of large modulus have both x and y large, and, in fact, that $|\alpha x|$ and $\cosh y$ are "about" equal, and, from (2.R), that $\cos x$ and x have the same sign, since α is positive.

We shall first obtain an approximation for y. Using (2.I) we get (2.1), which we substitute in (2.R) to get (2.2), which we substitute in (2.I) to get an equation (2.3) involving y alone:

$$\cos^2 x = 1 - \sin^2 x = \frac{\sinh^2 y - (\alpha y+\delta)^2}{\sinh^2 y}, \quad . \quad . \quad . \quad . \quad (2.1)$$

$$\alpha x + \gamma = \pm \coth y . \{\sinh^2 y - (\alpha y+\delta)^2\}^{\frac{1}{2}}, \quad . \quad . \quad . \quad . \quad (2.2)$$

$$\frac{\alpha y+\delta}{\sinh y} = -\sin\left\{\pm\frac{1}{\alpha}\coth y.[\sinh^2 y-(\alpha y+\delta)^2]^{\frac{1}{2}}-\frac{\gamma}{\alpha}\right\}. \quad (2.3)$$

Since y is positive we can write (2.3) as

$$\frac{\alpha y+\delta}{\sinh y} = \left|\sin\left\{\frac{1}{\alpha}\coth y.[\sinh^2 y-(\alpha y+\delta)^2]^{\frac{1}{2}}\mp\frac{\gamma}{\alpha}\right\}\right|. \quad (2.4)$$

The ambiguities in (2.2), (2.3), (2.4) depend on the sign of $\cos x$—the upper sign being taken when $\cos x$ is positive.

We now introduce the following estimates :

$$\coth y = 1+O(e^{-2y}),$$

$$\{\sinh^2 y-(\alpha y+\delta)^2\}^{\frac{1}{2}} = \sinh y\left(1-\frac{(\alpha y+\delta)^2}{\sinh^2 y}\right)^{\frac{1}{2}}$$

$$= \sinh y+O(y^2e^{-y}),$$

in (2.4) to obtain (2.5), in which we use the first mean value theorem to find (2.6),

$$\frac{\alpha y+\delta}{\sinh y} = \left|\sin\left\{\frac{1}{\alpha}\sinh y+O(y^2e^{-y})\mp\frac{\gamma}{\alpha}\right\}\right|, \quad (2.5)$$

$$\frac{\alpha y+\delta}{\sinh y} = \left|\sin\left(\frac{\sinh y\mp\gamma}{\alpha}\right)\right|+O(y^2e^{-y}). \quad (2.6)$$

We can write (2.6) in the form

$$\sin\left\{\frac{\sinh y\mp\gamma}{\alpha}\right\} = O(y^2e^{-y}), \quad (2.7)$$

which gives

$$\sinh y\mp\gamma = \alpha n\pi+O(y^2e^{-y}), \quad (2.8)$$

where n is a large integer which is positive since y is positive. We obtain

$$e^y = 2\alpha n\pi\left\{1\pm\frac{\gamma}{\alpha n\pi}+o\left(\frac{1}{n}\right)\right\}, \quad (2.9)^*$$

since $e^{-y} = o(1)$ and $O(y^2e^{-y}) = o(1)$.

Taking logarithms in (2.9) we get an approximation for y,

$$y = \log 2\alpha n\pi\pm\frac{\gamma}{\alpha n\pi}+o\left(\frac{1}{n}\right). \quad (2.10)$$

* The equation (2.9), which is fundamental in our discussion, could be obtained alternatively from the dominant terms in (2.26) and the equation (2.R).

From (2.9) and (2.10) we see that the $O(y^2 e^{-y})$ term in (2.8) can be replaced in (2.10) by $O\left(\frac{(\log n)^2}{n}\right)$, so that we have

$$\sinh y = \alpha n\pi \pm \gamma + O\left(\frac{(\log n)^2}{n}\right). \quad . \quad . \quad . \quad (2.11)$$

Using in (2.8) the fact that $e^{-y} = O\left(\frac{1}{n}\right)$, we can improve the error term in (2.10) from $o\left(\frac{1}{n}\right)$ to $O\left(\frac{(\log n)^2}{n^2}\right)$ to give an expression for y better than (2.10):

$$y = \log 2\alpha n\pi \pm \frac{\gamma}{\alpha n\pi} + O\left(\frac{(\log n)^2}{n^2}\right). \quad . \quad . \quad . \quad (2.12)$$

It will be seen shortly that the $\pm$ in (2.12) which originated in (2.2), and so depends on $\cos x$, can be replaced by $(-1)^n$, which is the sign of $\cos x$ when x corresponds to the y given by (2.12).

In this paragraph we shall obtain an estimate for the x corresponding to the y given by (2.12). We substitute this value of y in (2.I) and obtain an expression for $\sin x$ which we simplify in the following manner:

$$\begin{aligned}
\sin x &= -\frac{\alpha y + \delta}{\sinh y} \\
&= -\frac{\alpha\left\{\log 2\alpha n\pi + \frac{\delta}{\alpha} \pm \frac{\gamma}{\alpha n\pi} + O\left(\frac{(\log n)^2}{n^2}\right)\right\}}{\alpha n\pi \pm \frac{\gamma}{\alpha\pi} + O\left(\frac{(\log n)^2}{n}\right)} \\
&= -\frac{1}{n\pi}\left\{\log 2\alpha n\pi + \frac{\delta}{\alpha} \pm \frac{\gamma}{\alpha n\pi} + O\left(\frac{(\log n)^2}{n^2}\right)\right\} \\
&\qquad \times \left\{1 \pm \frac{\gamma}{\alpha n\pi} + O\left(\frac{(\log n)^2}{n^2}\right)\right\}^{-1} \\
&= -\frac{1}{n\pi}\left\{\log 2\alpha n\pi + \frac{\delta}{\alpha} \pm \frac{\gamma}{\alpha n\pi} + O\left(\frac{(\log n)^2}{n^2}\right)\right\} \\
&\qquad \times \left\{1 \mp \frac{\gamma}{\alpha n\pi} + O\left(\frac{(\log n)^2}{n^2}\right)\right\},
\end{aligned}$$

i. e., $$\sin x = -\frac{1}{n\pi}\left\{\log 2\alpha n\pi + \frac{\delta}{\alpha} \mp \frac{\gamma \log 2\alpha n\pi}{\alpha n\pi} \pm \frac{\gamma(\alpha-\delta)}{\alpha^2 n\pi} + O\left(\frac{(\log n)^2}{n^2}\right)\right\}.$$

From this last equation, using the expansion of "$\sin^{-1}x$", it follows that

$$x = N\pi - \frac{(-1)^N}{n\pi}\left\{\log 2\alpha n\pi + \frac{\delta}{\alpha} \mp \frac{\gamma \log 2\alpha n\pi}{\alpha n\pi} \pm \frac{\gamma(\alpha-\delta)}{\alpha^2 n\pi}\right\} + O\left(\frac{(\log n)^2}{n^3}\right), \quad . \quad . \quad (2.13)$$

or, less precisely,

$$x = N\pi + o(1). \quad . \quad . \quad . \quad . \quad . \quad (2.13.1)$$

where N is some positive or negative integer.

We shall identify N with n. From (2.H) we have

$$(\alpha x+\gamma)^2 = \cosh^2 y\left\{1 - \frac{(\alpha y+\delta^2)}{\sinh^2 y}\right\},$$

that is,

$$(\alpha x+\gamma)^2 = \sinh^2 y\left\{1+\frac{1}{\sinh^2 y}\right\}\left\{1-\frac{(\alpha y+\delta)^2}{\sinh^2 y}\right\}. \quad (2.14)$$

Using the results (2.11) and (2.12), it is clear that

$$\left\{1+\frac{1}{\sinh^2 y}\right\} = 1+O\left(\frac{1}{n^2}\right),$$

$$\left\{1-\frac{(\alpha y+\delta)^2}{\sinh^2 y}\right\} = 1+O\left(\frac{(\log n)^2}{n^2}\right).$$

Substituting these in (2.14), we find

$$(\alpha x+\gamma)^2 = \sinh^2 y\left\{1+O\left(\frac{(\log n)^2}{n^2}\right)\right\}, \quad . \quad (2.15)$$

so that we have, again using (2.11),

$$\alpha x+\gamma = \pm\left\{\alpha n\pi \pm \gamma + O\left(\frac{(\log n)^2}{n}\right)\right\}\left\{1+O\left(\frac{(\log n)^2}{n^2}\right)\right\}, \quad . \quad . \quad . \quad (2.16)$$

which gives

$$x = -\frac{\gamma}{\alpha} \pm \left\{n\pi \pm \frac{\gamma}{\alpha} + O\left(\frac{(\log n)^2}{n}\right)\right\}. \quad . \quad (2.17)$$

We can now discuss the various ambiguities of sign which have occurred in our equations. The first $\pm$ in (2.17) was introduced in the passage from (2.15) to (2.16), while the second was brought in by the step from (2.1) to (2.2) and is decided, as we have said, by the fact that the upper (lower) sign is to be taken when $\cos x$ is positive (negative) *.

We compare (2.13) and (2.17) and notice that, save for two exceptions to be discussed presently, we must take in (2.17) either both upper signs or both lower signs; for, if not, then we would have, from (2.17),

$$|x| = n\pi \pm \frac{2\gamma}{\alpha} + o(1),$$

which contradicts (2.13.1). So (2.17) becomes

$$x = \pm n\pi + O\Big(\frac{(\log n)^2}{n}\Big). \quad . \quad . \quad . \quad . \quad (2.17.1)$$

We now compare (2.13.1) and (2.17.1) to see that $N = \pm n$; this we substitute in (2.13) to obtain

$$x = \pm n\pi - \frac{(-1)^n}{n\pi}\{\log 2\alpha n\pi + O(1)\},$$

and from the fact that the ambiguous sign is to be that of x it is clear that the $\pm$ can be replaced by $(-1)^n$. It is now possible to remove all the ambiguities from the equations obtained in the present section; it is only necessary to replace every $\pm$ by $(-1)^n$ and every N by $(-1)^n n$. It will be enough for us to record the desired asymptotic expressions of the real and imaginary parts of the large roots of (2), which are

$$x_n = (-1)^n\left\{n\pi - \frac{\alpha \log 2\alpha n\pi + \delta}{\alpha n\pi}\right\} + \frac{\alpha\gamma \log 2\alpha n\pi - \gamma(\alpha - \delta)}{\alpha^2 n^2 \pi^2} + O\Big(\frac{(\log n)^2}{n^3}\Big), \quad (2.18)$$

$$y_n = \log 2\alpha n\pi + \frac{(-1)^n\gamma}{\alpha n\pi} + O\Big(\frac{(\log n)^2}{n^2}\Big), \quad . \quad . \quad . \quad . \quad (2.19)$$

We now consider the exceptional cases. In the first place we may have $\gamma = 0$: we then obtain (2.17.1) from (2.17) without "linking" the two independent ambiguities

* $\cos x$ cannot be zero for any relevant x because we have, from (2.13.1), that $x = N\pi + o(1)$, which gives $\cos x = (-1)^N + o(1)$.

in (2.17). That the first $\pm$ can be replaced by $(-1)^n$ is found as in the ordinary case, and it is unnecessary to decide the second since it always occurs as a multiplier of γ. The results (2.18) and (2.19) hold in this case (of course with $\gamma=0$). Secondly, we may have $\frac{2\gamma}{d}=r\pi$, where r is some integer, *i.e.*, when we can write (2) in the form

$$\cos z=\alpha\left(z+\frac{r\pi}{2}\right)+i\delta.$$

In this case, by a preliminary transformation of the form $z'=z+m\pi$, we can reduce the given equation to the form (2) with either γ zero or $\frac{2\gamma}{\alpha}$ not a multiple of π when r is even, and to the form

$$\sin z=\alpha z+i\delta \quad . \quad . \quad . \quad . \quad . \quad (2.20)$$

when r is odd; and it is only the last equation with $\alpha>0$ that requires a separate discussion.

Separating the real and imaginary parts, we find

$$\sin x\cosh y=\alpha x, \qquad \cos x\sinh y=\alpha y+\delta,$$

and see that now x and $\sin x$ have the same sign. Using this to remove the ambiguous sign which occurs when we eliminate x, we find in place of (2.7)

$$\sin\left(\frac{\sinh y}{\alpha}\right)=1+O(y^2e^{-y}),$$

from which we find (corresponding to (2.12))

$$y=\log(4n+1)\alpha\pi+O\left(\frac{(\log n)^2}{n^2}\right). \quad . \quad . \quad (2.21)$$

We next find

$$\cos x=\frac{\alpha y+\delta}{\sinh y}$$
$$=\frac{2\log(4n+1)\alpha\pi}{(4n+1)\pi}+\frac{2\delta}{(4n+1)\alpha\pi}+O\left(\frac{(\log n)^3}{n^2}\right),$$

and so, corresponding to (2.13),

$$x=(2N+1)\frac{\pi}{2}+(-1)^{N+1}\left\{\frac{2\log(4n+1)\alpha\pi}{(4n+1)}+\frac{2\delta}{(4n+1)\alpha\pi}\right\}$$
$$+O\left(\frac{(\log n)^3}{n^3}\right). \quad . \quad (2.22)$$

We determine N in terms of n, as before, by finding a rough approximation for x from the equation

$$\alpha^2 x^2 = \cosh^2 y \left\{ 1 - \left(\frac{\alpha y + \delta}{\sinh y} \right)^2 \right\},$$

which gives, corresponding to (2.17),

$$x = \pm (4n+1)\frac{\pi}{2} + O\left(\frac{(\log n)^2}{n} \right). \quad . \quad . \quad (2.23)$$

Comparing (2.22) and (2.23), we see that N is either $2n$ or $-(2n+1)$ *.

All the results stated in (I.R) follow immediately from (2.18) and (2.19) † with the exception, perhaps, of those regarding the monotony of the approach of the differences between the real parts of successive roots to 2π. This is established by observing that (2.18) and (2.19) give ‡

$$| x_{n+2} - x_n | = 2\pi + \frac{2 \log n}{\pi n^2} + O\left(\frac{1}{n^2} \right),$$

$$y_{n+2} - y_n = \frac{2}{n} + O\left(\frac{(\log n)^2}{n^2} \right),$$

while corresponding results in the special case are found from (2.21) and (2.22).

We next indicate (without details) how better approximations can be obtained if required §. We first obtain an accurate expression for $\tan x$ by substituting from (2.R) in (2.I) and using the facts that y and $(\alpha x + \gamma)/\cos x$ are positive. We find

$$-\sin x \cdot \left[\left(\frac{\alpha x + \gamma}{\cos x} \right)^2 - 1 \right]^{\frac{1}{2}} = \alpha \cosh^{-1}\left(\frac{\alpha x + \gamma}{\cos x} \right) + \delta, \quad (2.24)$$

* We can see that this agrees with the facts that x and $\sin x$ have the same sign, and that (2.22) gives $\sin x = (-1)^N + o(1)$.

† Or (2.21) and (2.22) in the special case.

‡ Disregarding terms which are $O(n^{-2})$ the only differences which need examination are those from the logarithmic terms in the first line of (2.18) and the first of these gives the contribution $2 \log n/(\pi n^2)$. The argument for $y_{n+2} - y_n$ from (2.19) is similar,

§ The method to be used here is similar to that used by Hobson (Proc. London Math. Soc. (2), 6 (1908), pp. 349–395, esp. p. 377, ff.) to determine the asymptotic values of the Characteristic Values of a general Sturm-Liouville Differential System and to that used below in our discussion of the complex case.

which gives

$$\tan x = -\frac{1}{x}\left[\log|2\alpha x| - \log|\cos x| + \frac{\delta}{\alpha} + \log\frac{1}{2}\left\{1+\frac{\gamma}{\alpha x}+\left[\left(1+\frac{\gamma}{\alpha x}\right)^2-\frac{\cos^2 x}{\alpha^2 x^2}\right]^{\frac{1}{2}}\right\}\right] \times\left[\left(1+\frac{\gamma}{\alpha x}\right)^2-\frac{\cos^2 x}{\alpha\, x^2}\right]^{-\frac{1}{2}} \quad . \quad . \quad . \quad . \quad . \quad (2.25)$$

By substituting in the right-hand side of (2.25) the value of x given in (2.18) we obtain an estimate of $\tan x$ which gives, by Gregory's series, a better estimation of x than (2.18). Now (2.T) can be written in the form *

$$y+\frac{\delta}{\alpha} = -\left(x+\frac{\gamma}{\alpha}\right)\tan x\left[1-\frac{\cos^2 x}{(\alpha x+\gamma)^2}\right]^{\frac{1}{2}}. \quad (2.26)$$

If we substitute in this the new estimate † for x, we obtain a better one for y than (2.19).

III. *The Complex Case.*

We finally consider the more general equation,

$$\cos z = (\alpha+i\beta)z+\gamma+i\delta, \quad . \quad . \quad . \quad . \quad (3)$$

where $\beta\neq 0$, from which we obtain, separating the real and imaginary parts,

$$\cos x\cosh y = \alpha x-\beta y+\gamma, \quad . \quad . \quad . \quad (3.\mathrm{R})$$

$$\sin x\sinh y = -\beta x-\alpha y-\delta. \quad . \quad . \quad . \quad (3.\mathrm{I})$$

From these we find

$$\left(\frac{\alpha x-\beta y+\gamma}{\cosh y}\right)^2+\left(\frac{\beta x+\alpha y+\delta}{\sinh y}\right)^2 = 1, \quad . \quad (3.\mathrm{H})$$

and so

$$\beta^2x^2 \leqslant x^2(\alpha^2\sinh^2 y+\beta^2\cosh^2 y) \leqslant |\,\mathrm{F}_1(y)\,|+|\,x.\mathrm{F}_2(y)\,|, \quad . \quad . \quad . \quad (3.1)$$

in which F_1, F_2 are integral functions. It follows that, if $|\,y\,|<\mathrm{K}$, $|\,x\,|$ is less than some number K'. Therefore, in

* The ambiguity is removed by our knowledge of approximate values and signs.

† It is, perhaps, worth noting here that a direct substitution for z from (2.18) in (2.26) actually gives a worse approximation for y than (2.19)—the error term being $\mathrm{O}\{(\log n)^3/n^2\}$ instead of $\mathrm{O}\{(\log n)^2/n^2\}$.

examining the asymptotic behaviour of the roots of (3), we can assume, without loss, that $|y|$ is large.

From (3.R) and (3.I) we have

$$\beta \cos x \cosh y + \alpha \sin x \sinh y = -(\alpha^2+\beta^2)y + \beta\gamma - \alpha\delta. \quad (3.2)$$

If we write

$$t = \tan\frac{x}{2}, \quad b = |a|, \quad d = \alpha\delta - \beta\gamma,$$

this becomes

$$t^2\left\{1 - \frac{b^2 y}{\beta\cosh y} - \frac{d}{\beta\cosh y}\right\} - \frac{2\alpha}{\beta} t \tanh y - \left\{1 + \frac{b^2 y}{\beta\cosh y} + \frac{d}{\beta\cosh y}\right\} = 0. \quad (3.3)$$

We now introduce estimates of the hyperbolic terms, assuming that y is positive, as follows :

$$\frac{1}{\cosh y} = 2e^{-y} + O(e^{-3y}), \quad \tanh y = 1 + O(e^{-2y}). \quad (3.3.1)$$

With these the equation (3.3) becomes

$$t^2\left\{1 - \frac{2b^2}{\beta} y e^{-y} - \frac{2d}{\beta} e^{-y} + O(ye^{-3y})\right\} - \frac{2\alpha t}{\beta}\{1 + O(e^{-2y})\} - \left\{1 + \frac{2b^2}{\beta} y e^{-y} + \frac{2d}{\beta} e^{-y} + O(ye^{-3y})\right\} = 0. \quad (3.4)$$

If we write this as $At^2 + 2Bt + C = 0$, we see that

$$B^2 = \frac{\alpha^2}{\beta^2}\{1 + O(e^{-2y})\},$$

$$-AC = 1 + O(y^2 e^{-2y}),$$

and so

$$(B^2 - AC)^{\frac{1}{2}} = \frac{b}{\beta}\{1 + O(y^2 e^{-2y})\}.$$

Therefore the roots of (3.4) are

$$\frac{\frac{\alpha}{\beta}\{1 + O(e^{-2y})\} \pm \frac{b}{\beta}\{1 + O(y^2 e^{-2y})\}}{1 - \frac{2b^2}{\beta} y e^{-y} - \frac{2d}{\beta} e^{-y} + O(ye^{-3y})} = \tau\left\{1 + \frac{2b^2}{\beta} y e^{-y} + \frac{2d}{\beta} e^{-y} + O(y^2 e^{-2y})\right\}, \quad (3.5)$$

in which we have written $\tau = (\alpha \pm b)/\beta$.

For first approximations to the roots of (3) we take in place of (3.5) the following rougher expression for the roots of (3.4) :

$$t=\tau+O(ye^{-y}). \quad . \quad . \quad . \quad . \quad . \quad (3.5.1)$$

If we write $\theta=2\tan^{-1}\tau$ where $-\pi<\theta<\pi$, the first mean value theorem gives

$$x=2n\pi+\theta+O(ye^{-y}), \quad . \quad . \quad . \quad . \quad (3.6)$$

where n is an integer. We now get an equation for y by substituting (3.6) and (3.5.1) in (3.1), getting

$$-\frac{2t\sinh y}{1+t^2}=\beta\{2n\pi+\theta+O(ye^{-y})\}+\alpha y+\delta,$$

$$i.e., \quad 2\sinh y+O(y)=2fn\pi+f\left(\theta+\frac{\alpha y}{\beta}+\frac{\delta}{\beta}\right)+O(ye^{-y}),$$

where we have written $f=-\beta(1+\tau^2)/\tau$ and used the fact that

$$\frac{t}{1+t^2}=\frac{\tau}{1+\tau^2}\{1+O(ye^{-y})\}.$$

Our equation for y reduces to

$$e^y=2fn\pi+O(y). \quad . \quad . \quad . \quad . \quad . \quad (3.7)$$

From this we observe first that the integer n must have the same sign as f; next that n lies between two multiples of e^y, and so $y=O(\log n)$ *. We therefore see that (3.7) gives

$$e^y=2fn\pi\left\{1+O\left(\frac{\log n}{n}\right)\right\}, \quad . \quad . \quad . \quad (3.7.1)$$

$$y=\log 2fn\pi+O\left(\frac{\log n}{n}\right). \quad . \quad . \quad . \quad (3.7.2)\dagger$$

We now use this value of y to get a more accurate value for t than (3.5.1).

* If n is negative, this and all subsequent O-terms are to be read as if they involved $|n|$ in place of n.

† If roots with negative imaginary parts are required we have similar working to that above, but with $e^y, e^{2y}, \ldots$ in place of $e^{-y}, e^{-2y}, \ldots$ and we find that n is of the opposite sign to f, and corresponding to (3.72) we find $y=-\log|2fn\pi|+O(n^{-1}\log n)$. Similar changes have then to be made in the subsequent work.

Substituting from (3.7.2) in (3.5) we find

$$t = \tau\left[1 + \frac{2b^2}{\beta}\frac{\log 2fn\pi}{2fn\pi} + \frac{2d}{\beta}\cdot\frac{1}{2fn\pi} + O\left(\frac{(\log n)^2}{n^2}\right)\right]. \quad . \quad . \quad . \quad (3.7.3)$$

Substituting this in the Taylor expression of $\tan^{-1} t$, we get a better approximation for x than (3.6):

$$x_n = 2n\pi + 2\tan^{-1}\tau + \frac{2(t-\tau)}{1+\tau^2} + O\{(t-\tau)^2\}$$

$$= 2n\pi + \theta - \frac{4b^2}{f}\cdot\frac{\log 2fn\pi}{2fn\pi} - \frac{4d}{f}\cdot\frac{1}{2fn\pi} + O\left(\frac{(\log n)^2}{n^2}\right). \quad . \quad . \quad . \quad (3.8)$$

For y we need first to calculate $(1+t^2)/t$. We have from (3.7.3)

$$\frac{1+t^2}{t}$$

$$= \left[1 + \tau^2\left\{1 + \frac{4b^2}{\beta}\frac{\log 2fn\pi}{2fn\pi} + \frac{4d}{\beta}\cdot\frac{1}{2fn\pi} + O\left(\frac{(\log n)^2}{n^2}\right)\right\}\right]$$

$$\times \frac{1}{\tau}\left[1 - \frac{2b^2}{\beta}\frac{\log 2fn\pi}{2fn\pi} - \frac{2d}{\beta}\cdot\frac{1}{2fn\pi} + O\left(\frac{(\log n)^2}{n^2}\right)\right]$$

$$= \frac{1+\tau^2}{\tau}\left[1 + \frac{2b^2\cos\theta}{\beta}\cdot\frac{\log 2fn\pi}{2fn\pi} + \frac{2d\cos\theta}{\beta}\cdot\frac{1}{2fn\pi} + O\left(\frac{(\log n)^2}{n^2}\right)\right].$$

Therefore (3.1) gives

$$2\sinh y = -\frac{1+\tau^2}{\tau}\left[1 + \frac{2b^2\cos\theta}{\beta}\cdot\frac{\log 2fn\pi}{2fn\pi\beta} + \frac{2d\cos\theta}{\beta}\cdot\frac{1}{2fn\pi} + O\left(\frac{(\log n)^2}{n}\right)\right]$$

$$\times\left[2n\pi\beta + \alpha\log 2fn\pi + \delta + \beta\theta + O\left(\frac{\log n}{n}\right)\right],$$

$$e^y + O\left(\frac{1}{n}\right) = 2fn\pi + \left(\frac{2b^2\cos\theta + f\alpha}{\beta}\right)\log 2fn\pi + \frac{2d\cos\theta + f\delta + f\beta\theta}{\beta} + O\left(\frac{(\log n)^2}{n}\right),$$

$$y_n = \log 2fn\pi + \frac{2b^2\cos\theta + f\alpha}{\beta}\cdot\frac{\log 2fn\pi}{2fn\pi} + \frac{2d\cos\theta + f\delta + f\beta\theta}{\beta\,.\,2fn\pi} + O\left(\frac{(\log n)^2}{n^2}\right). \quad . \quad (3.9)$$

These results (3.8) and (3.9) are the most precise that can be obtained after making the estimations (3.3.1) ; if more precise ones are desired they can be obtained by the same method after taking closer estimates for sech y and tanh y in (3.3).

XVIII. *The Atomic Weight of Element* 93. *By* H. J. Walke, *M.Sc., A.Inst.P., Commonwealth Fellow, Radiation Laboratory, University of California* *.

IT is a well known fact that elements of odd atomic number (other than hydrogen) never have more than two stable isotopes †. Moreover, both isotopes have odd mass numbers (except in the case of elements of odd atomic number less than 8), and, further, the isotope with the higher mass number is always heavier than the lighter by two mass units, *e. g.*, ${}_{29}Cu^{63}$ and ${}_{29}Cu^{65}$, and ${}_{31}Ga^{69}$ and ${}_{31}Ga^{71}$, etc.

In almost every case too the element of even atomic number preceding it in the periodic table has two missing isotopes of corresponding mass numbers. For example, corresponding to ${}_{31}Ga^{69}$ and ${}_{31}Ga^{71}$ the zinc isotopes ${}_{30}Zn^{69}$ and ${}_{30}Zn^{71}$ are absent from the mass spectrum. In previous papers ‡ it has therefore been suggested that these "missing" isotopes are β-radioactive, and it has been shown that it is possible to consider the elements as having been built up by a process of neutron capture and β-radioactivity.

Several elements of odd atomic number are, however, single isotopes, although two isotopes are missing from the mass spectrum of the preceding element of even atomic number. Thus rhodium has only one isotope,

* Communicated by the Author.

† Aston, 'Mass Spectra and Isotopes.'

‡ Walke, Phil. Mag. xviii. p. 795 (1934); xix. p. 33 (1935); xix. p. 341 (1935).

$_{45}Rh^{103}$ *, although two isotopes, $_{44}Ru^{103}$ and $_{44}Ru^{105}$, are missing from the mass range of ruthenium. It was suggested therefore that in these cases the expected heavier isotope, such as $_{45}Rh^{105}$, is also β-radioactive, so that missing isotopes such as $_{44}Ru^{105}$ give rise to two successive β-transformations. Hence we have the following synthesis processes :—

$$_{44}Ru^{103} \rightarrow \beta \rightarrow {}_{45}Rh^{103},$$
$$_{44}Ru^{105} \rightarrow \beta \rightarrow {}_{45}Rh^{105} \rightarrow \beta \rightarrow {}_{46}Pd^{105}.$$

The lightest palladium isotope is then evolved as a result of the emission of β-rays from the missing $_{45}Rh^{104}$. Thus the isotopes can be shown as below :—

Ruthenium....	96, 98, 99, 100, 101, 102	104	
		$\downarrow\beta$	$\downarrow\beta$
Rhodium.....		103	
			$\downarrow\beta$ $\downarrow\beta$
Palladium.....			104, 105, 106, etc.

It is noteworthy that Kourtschatov, Nemenow, and Selinow † have bombarded ruthenium with slow neutrons, and have concluded that both the above reactions occur. Moreover, Fermi and his co-workers ‡ have observed β-radioactivity corresponding to the absorption of slow neutrons by rhodium. This is probably due to $_{45}Rh^{104}$.

This theory has been applied to the synthesis and disintegration of the spontaneously radioactive elements §. By making the hypothesis that the α-radioactive isotopes correspond to the stable isotopes of the non-radioactive elements, the β-radioactive isotopes corresponding to the missing isotopes, it has been shown that the disintegrations of the elements of odd atomic number greater than 82 may be readily understood.

This aspect of the theory, and the close relationship which is shown to exist between the stable and radioactive elements, can perhaps best be understood if applied to the case of protactinium.

The thorium isotopes of mass numbers 230 and 232 are both α-radioactive, though uranium Y ($_{90}Th^{231}$) is short-lived and β-radioactive, being the "missing" thorium synthesis link which results in the evolution

* Dempster, 'Nature,' cxxxv. p. 993 (1935).
† Kourtschatov, Nemenow, and Selinow, *Comptes Rendus*, cc. p. 2162 (1935).
‡ Fermi etc., Proc. Roy. Soc. A, cxlix. p. 522 (1935).
§ Walke, Phil. Mag. xx. p. 25 (1935).

of the "stable" (*i. e.*, α-radioactive) $_{91}Pa^{231}$. The "missing" $_{90}Th^{233}$ would give rise to $_{91}Pa^{233}$, but, like $_{45}Rh^{105}$, this isotope is also β-radioactive and gives rise to $_{92}U^{233}$, as has been verified experimentally by Curie, van Halban junr., and Preiswerk *.

Thus the isotopic relationships can be shown as below :—

Thorium	226. 227, 228, 229, 230	232	
		↓ β	↓ β
Protactinium.		231	
		↓ β	↓ β
Uranium			232, 233, 234, etc.

The similarity between this list and that already given for ruthenium, rhodium, and palladium is striking. (It is to be noted that all the mass numbers listed above are α-radioactive.)

In this connexion it is significant that Fermi † and his co-workers have bombarded $_{92}U^{238}$ with neutrons, and have shown that the new isotope $_{92}U^{239}$ thus produced gives rise to two succeeding β-ray transformations, *i. e.*,

$$_{92}U^{239} \rightarrow \beta \rightarrow {}_{93}\text{EKa} \,.\, Re^{239} \rightarrow \beta \rightarrow {}_{94}\text{EKa} \,.\, Os^{239} \rightarrow ?$$

This suggests that $_{93}$EKa . Re^{239} is the heavier and "missing" isotope of element 93 (*cf.* $_{91}Pa^{233}$, $_{45}Rh^{105}$, etc.). Hence the "stable" (*i. e.*, α-radioactive) isotope of eka-rhenium should have a mass less than 239 by two mass units, *i. e.*, 237. This would suggest, in addition, that $_{92}U^{237}$ is β-radioactive, eka-rhenium being evolved during the cosmic synthesis of the elements when the fairly long-lived α-radioactive $_{92}U^{236}$ captured a neutron, thus:—

$$_{92}U^{236} + n \rightarrow {}_{92}U^{237} \,;\; {}_{92}U^{237} \rightarrow \beta \rightarrow {}_{93}\text{EKa} \,.\, Re^{237}.$$

Thus the α-radioactive eka-rhenium, with atomic weight 237, would be the head of the "missing" series ‡, as below :—

$$_{93}\text{EKa}Re^{237} \rightarrow \alpha \rightarrow {}_{91}Pa^{233} \rightarrow \beta \rightarrow {}_{92}U^{233} \rightarrow \alpha, \text{ etc.}$$

The isotopic range of eka-osmium would thus commence at mass number 238, this isotope being produced as a result of the β-radioactivity of the missing $_{93}$EKa . Re^{238} formed when the α-radioactive isotope captured a neutron.

* Curie, van Halban junr., and Preiswerk, *Comptes Rendus*, cc. p. 2079 (1935).

† Fermi etc., *loc. cit.* A, cxlix. p. 522 (1935).

‡ Walke, Phil. Mag. xix. p. 33 (1935) ; Phil. Mag. xx. p. 25 (1935).

The α-radioactive isotopes of uranium, eka-rhenium, and eka-osmium are therefore probably :—

Uranium	232, 233, 234, 235, 236	238		
		↓β	↓β	
Eka-Rhenium.		237		
			↓β	↓β
Eka-Osmium .			238, 239, 240, etc.	

It appears probable, moreover, that the α-radioactive isotopes of eka-osmium would have mass numbers 238, 239, 240, 241, 242, and 244. The lighter isotopes are probably all short-lived, and may have decayed to form lighter elements. However, $_{94}$EKaOs^{244} might be of long life (*cf.* $_{90}$Th^{232} and $_{92}$U^{238}), and may still exist terrestrially. A search for an α-radioactive substance with atomic weight 244 might result in the discovery of eka-osmium.

XIX. *Notes on the Asymptotic Evaluation of Operational Expressions.* *By* S. Koizumi, *Assistant Professor of the Waseda University, Tokyo* *.

§ 1. *Introduction.*

THE important rôle of the asymptotic series for mathematical and physical researches need not be emphasized here. Unfortunately, however, as for the asymptotic evaluation of operational expressions, "it may be said that the theory is as yet rather unsatisfactory" †, in spite of many researches by Heaviside ‡ himself, Carson §, Wiener ‖, and others.

The so-called Heaviside's rule is used ordinarily to evaluate operational expressions asymptotically, but this rule does not always lead to correct results ¶, and it does not yet appear to the author that the problem has been so clearly and adequately solved that we have an automatic rule giving a correct asymptotic expansion by

* Communicated by the Author.

† J. R. Carson, 'Electric Circuit Theory and the Operational Calculus,' p. 78 (1926).

‡ O. Heaviside, 'Electromagnetic Theory,' ii.

§ J. R. Carson, *loc. cit.*, and "Bell System," Techn. Journ. ix. p. 150 (1930).

‖ N. Wiener, *Math. Annalen*, Bd. cv. p. 579 (1925).

¶ J. R. Carson, "Bell System," Techn. Journ. ix. p. 152 (1930).

purely algebraic operation without special devices. The present paper has as its object to set out the systematic study of an extended Heaviside's rule which will remove ambiguity.

§ 2. *Watson's Lemma.*

It will be shown in the following paragraphs that the asymptotic series, in the sense of Poincaré, of a function can be obtained from its operational expression by virtue of Watson's lemma *, which was established to investigate asymptotic expansions for the parabolic cylinder functions by the method of steepest descents.

For our purpose it is convenient that the lemma be modified slightly in the following form :—

Lemma : Let $G(p)$ be analytic when $|p| \leqslant a+\delta$, where $a>0$, $\delta>0$; and let

$$G(p) = \sum_{n=1}^{\infty} A_n p^{\frac{n}{r}}, \quad . \quad . \quad . \quad . \quad . \quad (1)$$

when $|p| \leqslant a$, r being positive ; also, let

$$|G(p)| < Ke^{b|p|}, \quad . \quad . \quad . \quad . \quad . \quad . \quad (2)$$

where K and b are positive numbers independent of p, when p is on the path of integration Γ shown in fig. 1 and $|p| \geqslant a$. Then the asymptotic expansion,

$$\frac{1}{2\pi i}\int_{\Gamma} e^{tp} G(p)\, dp \sim \sum_{n=1}^{\infty} A_n \Big/ \Gamma\left(-\frac{n}{r}\right) . t^{\frac{n}{r}+1} \quad . \quad (3)$$

is valid in the sense of Poincaré when t is sufficiently large and

$$|\theta| \leqslant \frac{\pi}{2} - \triangle, \quad . \quad . \quad . \quad . \quad . \quad (4)$$

where $\triangle$ is an arbitrary positive number.

For, decomposing the path of integration in three parts, c, L_1, and L_2, as shown in the figure, we have

$$\int_{\Gamma} = \int_{c} + \int_{L_1} + \int_{L_2},$$

* G. N. Watson, Proc. London Math. Soc. xvii. p. 133 (1918), and 'Theory of Bessel Functions,' p. 236 (1922).

where the integral along c will be written as follows:

$$\int_c e^{tp} G(p)\, dp = \sum_{n=1}^{\infty} A_n \int_c e^{tp} p^{\frac{n}{r}}\, dp,$$

when $\rho < a$, using the relation (1).

However, since each term of the right side tends to zero when $\rho \to 0$, we get

$$\int_\Gamma = \int_{L_1} + \int_{L_2} \quad . \quad . \quad . \quad . \quad . \quad . \quad . \quad (5)$$

Let us now consider the integral along L_1,

$$\int_{L_1} = \int_0^\infty \exp(-te^{-i\theta}\rho) . G(e^{i(\pi-\theta)}\rho) . e^{i(\pi-\theta)}\, d\rho. \quad . \quad (6)$$

Fig. 1.

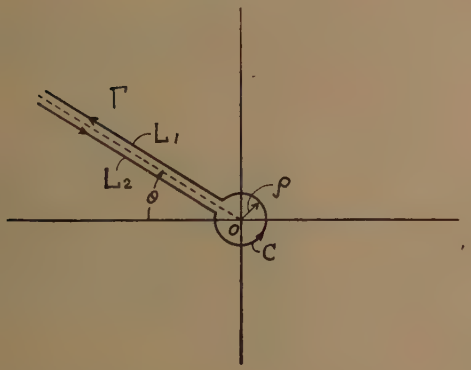

Since, from (1), we have

$$G(e^{i(\pi-\theta)}\rho) = \sum_{n=1}^{\infty} A_n e^{i(\pi-\theta)\frac{n}{r}} \rho^{\frac{n}{r}}, \quad . \quad . \quad . \quad (7)$$

when $|p| = \rho \leqslant a$, and from (2)

$$|G(e^{i(\pi-\theta)}\rho)| < Ke^{b|p|} = Ke^{b\rho}, \quad . \quad . \quad . \quad (8)$$

when $\rho \geqslant a$, we can therefore find by Watson's original lemma * that

* G. N. Watson, *loc. cit.*

$$\int_0^\infty \exp(-te^{i\theta}).\mathrm{G}(e^{i(\pi-\theta)}\rho).e^{i(\pi-\theta)}\,d\rho$$
$$= \sum_{n=1}^{M-1} \mathrm{A}_n e^{i(\pi-\theta)\left(\frac{n}{r}+1\right)}\Gamma\left(\frac{n}{r}+1\right)\Big/(te^{-i\theta})^{\frac{n}{r}+1}+\mathrm{O}\left(\frac{1}{t^{\frac{M}{r}+1}}\right)$$
$$= \sum_{n=1}^{M-1} \mathrm{A}_n e^{i\left(\frac{n}{r}+1\right)\pi}\Gamma\left(\frac{n}{r}+1\right)\Big/t^{\frac{n}{r}+1}+\mathrm{O}\left(\frac{1}{t^{\frac{M}{r}+1}}\right) \quad . \quad (9)$$

when
$$|\arg te^{-i\theta}| = |\theta| \leqslant \frac{\pi}{2}-\triangle.$$

In like manner

$$\int_{L_2} = -\sum_{n=1}^{M-1} \mathrm{A}_n e^{-i\left(\frac{n}{r}+1\right)\pi}\Gamma\left(\frac{n}{r}+1\right)\Big/t^{\frac{n}{r}+1}+\mathrm{O}\left(\frac{1}{t^{\frac{M}{r}+1}}\right). \quad (10)$$

Hence, by (5),

$$\frac{1}{2\pi i}\int_\Gamma e^{tp}\mathrm{G}(p)\,dp = \sum_{n=1}^{M-1} \mathrm{A}_n\Big/\Gamma\left(-\frac{n}{r}\right).t^{\frac{n}{r}+1}+\mathrm{O}\left(\frac{1}{t^{\frac{M}{r}+1}}\right),$$

when $|\theta| \leqslant \frac{\pi}{2}-\triangle$. . . . (11)

§ 3. *Asymptotic Evaluations of Operational Expressions.*

Let $\mathrm{F}(p)$ be a function which has no other singularities than algebraic ones (poles and branch-points) in the finite part of the plane. Making proper cuts, $\mathrm{F}(p)$ may be made a one-valued functian in such plane, and let $\mathrm{F}(p)/p$ be analytic in this semiplane,

$$\mathrm{R}(p) \geqslant \beta;$$

also, let

$$\frac{\mathrm{F}(p)}{p} = \mathrm{O}\left(\frac{1}{p^\gamma}\right), \quad . \quad . \quad . \quad . \quad . \quad . \quad (12)$$

where $\gamma > 0$, when $|p$ is sufficiently large. Then there are the following relations :

$$\mathrm{F}(p) \doteq f(t),$$
$$f(t) = \frac{1}{2\pi i}\int_{\beta-i\infty}^{\beta+i\infty} e^{tp}\frac{\mathrm{F}(p)}{p}\,dp. \quad . \quad . \quad . \quad (13)$$

Now, the path of the above integration will be changed as illustrated in fig. 2, stretching all cuts to the points, the real part of which are $-\infty$.

However, the integrals along the circular arcs at

$|p| = \infty$ will be zero from (12) by Jordan's lemma, and so

$$\frac{1}{2\pi i}\int_{\beta-i\infty}^{\beta+i\infty} e^{tp}\frac{F(p)}{p}dp = \frac{1}{2\pi i}\sum_s \int_{\Gamma_s} e^{tp}\frac{F(p)}{p}dp, \quad . \quad (14)$$

where Γ_s is the path of integration round the branch-point * $p=b_s$ and $\sum_s$ implies taking up all these Γ_s.

Let us now make closer investigations on the integral on Γ_s. Let $p=b_s$ be the pole of order m and the branch-point of order $(r-1)$ † of the function F/p, then

Fig. 2.

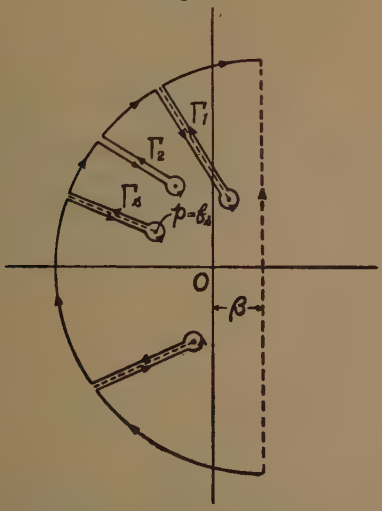

F/p will be expanded about this point in Puiseux's series as follows :

$$\frac{F_s(p)}{p} = \sum_{n=-m}^{\infty} A_n (p-b_s)^{\frac{n}{r}}. \quad . \quad . \quad . \quad (15)$$

Putting $p-b_s=q$, we have

$$f_s = \frac{1}{2\pi i}\int_{\Gamma_s} e^{tp}\frac{F(p)}{p}dp$$

$$= \frac{e^{b_s t}}{2\pi i}\int_{\Gamma} e^{tq}\frac{F(q+b_s)}{q+b_s}dq, \quad . \quad . \quad . \quad . \quad (16)$$

where the path of integration Γ is such as shown in fig. 1.

* Mere poles are included in branch-points.

† When $p=b_s$ is a mere pole we take $r=1$.

If we put

$$G(p)=\frac{F(p)}{p}-\sum_{n=-m}^{0}A_n(p-b_s)^{\frac{n}{r}}, \quad . \quad . \quad (17)$$

then, from (16), we have

$$f_s=\frac{e^{b_st}}{2\pi i}\left\{\int_\Gamma e^{tq}G(q+b_s)\,dq+\sum_{n=-m}^{0}\int_\Gamma e^{tq}A_nq^{\frac{n}{r}}\,dq\right\}. \quad (18)$$

However, when $|p-b_s|$ is sufficiently small, we have, from (15),

$$G(p)=\sum_{n=1}^{\infty}A_n(p-b_s)^{\frac{n}{r}},$$

or

$$G(q+b_s)=\sum_{n=1}^{\infty}A_nq^{\frac{n}{r}},$$

when $|q|$ is sufficiently small. Since from our assumption (12) we can moreover see that $|G(q+b_s)|<Ke^{b|q|}$, when $|q|\geqslant a$, we get the following asymptotic expansion :

$$\frac{1}{2\pi i}\int_\Gamma e^{tq}G(q+b_s)\,dq\sim\sum_{n=1}^{\infty}A_n\Big/\Gamma\left(-\frac{n}{r}\right)t^{\frac{n}{r}+1} \quad . \quad (19)$$

by the preceding lemma.

On the other hand, we have

$$\sum_{n=-m}^{0}\frac{1}{2\pi i}\int_\Gamma e^{tq}A_nq^{\frac{n}{r}}\,dq=\sum_{n=-m}^{0}A_n\Big/\Gamma\left(-\frac{n}{r}\right)t^{\frac{n}{r}+1}.$$

Hence

$$f_s\sim e^{b_st}\sum_{n=-m}^{\infty}A_n\Big/\Gamma\left(-\frac{n}{r}\right)t^{\frac{n}{r}+1}. \quad . \quad . \quad . \quad (20)$$

Thus from (14) we get, finally,

$$f(t)=\sum_s f_s$$

$$\sim\sum_s e^{b_st}\sum_{n=-m}^{\infty}A_n\Big/\Gamma\left(-\frac{n}{r}\right)t^{\frac{n}{r}+1}. \quad . \quad . \quad (21)$$

It can be seen from (21) that f_s of the branch-point (or pole) with the large real part contributes to the integral remarkably when t is large, and it will become sufficient to take notice of the branch-points only which have the largest real part. Especially when the branch-point with

the largest real part is $p=0$, we get the following asymptotic series :

$$f(t)\sim \sum_{n=-m}^{\infty} B_n \Big/ \Gamma\Big(1-\frac{n}{r}\Big)t^{\frac{n}{r}}, \quad . \quad . \quad . \quad (22)$$

where B_n is the coefficient of the series when $F(p)$ is expanded at the origin—that is to say,

$$F(p) = \sum_{n=-m}^{\infty} B_n p^{\frac{n}{r}}. \quad . \quad . \quad . \quad . \quad . \quad (23)$$

Giving to r in (22) the special value 2, we get

$$f(t)\sim \sum_{n=-m}^{1} B_n \Big/ \Gamma\Big(1-\frac{n}{2}\Big)t^{\frac{n}{2}} + \sum_{n=2}^{\infty} B_n \Big/ \Gamma\Big(1-\frac{n}{2}\Big)t^{\frac{n}{2}}.$$

However, since zero and negative integers are zeros of the gamma function, we have

$$f(t)\sim \sum_{n=-m}^{1} B_n \Big/ \Gamma\Big(1-\frac{n}{2}\Big)t^{\frac{n}{2}} + \sum_{k=1}^{\infty} B_{2k+1} \Big/ \Gamma(\tfrac{1}{2}-k).t^{\frac{1}{2}+k},$$

or . . . (24)

$$f(t)\sim \sum_{n=-m}^{1} B_n \Big/ \Gamma\Big(1-\frac{n}{2}\Big)t^{\frac{n}{2}} + \frac{1}{\sqrt{\pi t}} \sum_{k=1}^{\infty} B_{2k+1} \frac{1\cdot 3 \ldots (2k-1)}{(-2t)^k}, \quad (25)$$

using the formula

$$\Gamma(\tfrac{1}{2}-k) = \frac{\sqrt{\pi}(-2)^k}{1\cdot 3 \ldots (2k-1)}.$$

It is obvious that the formula (25), which we have deduced as a special case of the formula (21), is nothing but the result which will be got from Heaviside's rule. Thus his rule leads to the correct result if, and only if, the above assumptions are fulfilled.

Now let us consider

$$F(p) = \frac{p}{\sqrt{p^2+\lambda^2}},$$

where λ is a positive number, as an illustrating example of the application of (21). Making the cuts as shown in fig. 3, we have

$$b_1 = e^{i\frac{\pi}{2}}\lambda \quad \text{and} \quad b_2 = e^{i\frac{3\pi}{2}}\lambda$$

as the branch-point of $F(p)/p$ in the cut plane.

If we put

$$\phi_1(p)=(p-e^{i\frac{3\pi}{2}}\lambda)^{-\frac{1}{2}},$$

we have

$$\phi_1^{(n)}(p)=\frac{\sqrt{\pi}}{\Gamma(\frac{1}{2}-n)}(p-e^{i\frac{3\pi}{2}}\lambda)^{-n-\frac{1}{2}},$$

and so

$$\phi_1^{(n)}(e^{i\frac{\pi}{2}}\lambda)=\frac{\sqrt{\pi}}{\Gamma(\frac{1}{2}-n)(2\lambda e^{i\frac{\pi}{2}})^{n+\frac{1}{2}}},$$

Fig. 3.

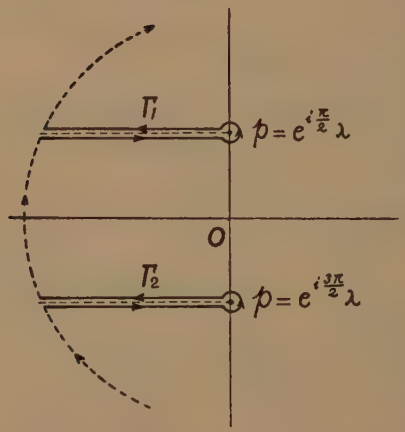

since, along our path of integration,

$$-\pi\leqslant\arg(p-e^{i\frac{3\pi}{2}}\lambda)\leqslant\pi.$$

Thus

$$\frac{\mathrm{F}_1}{p}=\sum_{n=0}^{\infty}\frac{\sqrt{\pi}(p-e^{i\frac{\pi}{2}}\lambda)^{n-\frac{1}{2}}}{n!\,\Gamma(\frac{1}{2}-n)(2\lambda e^{i\frac{\pi}{2}})^{n+\frac{1}{2}}},$$

and so, by (20),

$$f_1\sim e^{i\lambda t}\sum_{n=0}^{\infty}\frac{\sqrt{\pi}}{n!\,\Gamma(\frac{1}{2}-n)(2\lambda e^{i\frac{\pi}{2}})^{n+\frac{1}{2}}\Gamma(\frac{1}{2}-n)t^{n+\frac{1}{2}}}.$$

In like manner, with regard to b_2,

$$f_2 \sim e^{-i\lambda t} \sum_{n=0}^{\infty} \frac{\sqrt{\pi}}{n!\ \Gamma(\frac{1}{2}-n)(2\lambda e^{-i\frac{\pi}{2}})^{n+\frac{1}{2}}\Gamma(\frac{1}{2}-n)t^{n+\frac{1}{2}}}.$$

Thus, by (21),

$$\begin{aligned} f(t) &= f_1+f_2 \\ &\sim \left(\frac{2}{\pi\lambda t}\right)^{\frac{1}{2}} \sum_{n=0}^{\infty} \cos\left(\lambda t-\frac{\pi}{4}-\frac{\pi}{2}n\right)\frac{\pi^2}{n!\ \Gamma^2(\frac{1}{2}-n)(2\lambda t)^n} \\ &= \left(\frac{2}{\pi\lambda t}\right)^{\frac{1}{2}}\left[\cos\left(\lambda t-\frac{\pi}{4}\right)\right. \\ &\qquad \times\left\{\sum_{m=0}^{\infty}(-1)^m\frac{\pi^2}{(2m)!\ \Gamma^2(\frac{1}{2}-2m)(2\lambda t)^{2m}}\right\} \\ &\quad +\sin\left(\lambda t-\frac{\pi}{4}\right) \\ &\qquad \left.\times\left\{\sum_{m=0}^{\infty}(-1)^m\frac{\pi^2}{(2m+1)!\ \Gamma^2(-\frac{1}{2}-2m)(2\lambda t)^{2m+1}}\right\}\right], \end{aligned}$$

that is to say, we have got the asymptotic series for the Bessel function:

$$J_0(\lambda t) \doteq \frac{p}{\sqrt{p^2+\lambda^2}}$$

§ 4. *Summary.*

The above results will be summarized in the following rule:—

Let $F(p)$ *satisfy the following conditions*:

(i.) $F(p)$ *has only algebraic singularities in the finite part of the plane.*

(ii.) *When we make cuts stretched from the branch-points of* $F\ p)$ *to points the real part of which are* $-\infty$, $F(p)/p$ *is a one-valued analytic function in the semiplane*

$$R(p) \geqslant \beta.$$

(iii.) *In this cut plane*

$$\frac{F(p)}{p} = O\left(\frac{1}{p^\gamma}\right),$$

where γ *is positive, when* $|\ p\ |$ *is sufficiently large.*

Further, let $p=b_l\,(l=1, 2 \ldots k)$ *be the branch-points (or poles) of* $\mathrm{F}(p)/p$ *in the cut plane such that this group of the branch-points has the largest real part among all branch-points of* $\mathrm{F}(p)/p$ *; also, let*

$$\frac{\mathrm{F}_l}{p} = \sum_{n=-m_l}^{\infty} \mathrm{A}_{l_n}(p-b_l)^{\frac{n}{r_l}} \quad . \quad . \quad . \quad . \quad \text{(I.)}$$

be the expansion of $\mathrm{F}(p)/p$ *about the point* $p=b_l$. *Then the asymptotic expansion*

$$\mathrm{F}(p) \doteq f(t)$$

$$\sim \sum_{l=1}^{k} e^{b_l t} \sum_{n=-m_l}^{\infty} \mathrm{A}_{l_n} \Big/ \Gamma\left(-\frac{n}{r_l}\right) . t^{-\frac{n}{r_l}+1} \quad . \quad \text{(II.)}$$

is valid in the sense of Poincaré when t *is sufficiently large.*

It will also be found at once that when the series (I.) has the infinitely large radius of convergency the series (II.) is convergent—that is to say,

$$f(t) = e^{b_l t} \sum_{n=-m_l}^{\infty} \mathrm{A}_n \Big/ \Gamma\left(-\frac{n}{r}\right) . t^{-\frac{n}{r}+1} .$$

XX. *Fractional Calculus* : *Fractional Contour Integration.* *By* W. Fabian, *M.A., Ph.D.* *

1. *Introduction.*

FRACTIONAL Contour Integration has not been studied before. The paths of integration taken for the fractional integral were usually rectilinear. They were either along the real axis, such as used by Riemann †, Weyl ‡, Hardy §, Riesz ||, and others, or else were taken along other straight lines in the complex plane, as was done by Hardy and Littlewood ¶ and Hadamard ** ; and the curvilinear paths of integration, used for fractional

* Communicated by the Author.
† *Ges. Werke*, pp. 331–344 (1876).
‡ *Vierteljahrsschrift d. naturf. Ges. in Zurich*, lxii. pp. 296–302 (1917).
§ Messenger of Math. xlvii. pp. 145–150 (1918).
|| *Acta Univ. Hungaricæ* (*Math.*), i. pp. 114–126 (1923).
¶ *Math. Zeitschrift*, xxxiv. pp. 403–439 (1931).
** *Journal de Math.* (4) viii. pp. 101–186 (1892).

integrals for the first time in our last paper *, were not considered closed in that paper. Although fractional integrals along unclosed paths have been expressed as ordinary contour integrals by Laurent †, Bromwich ‡, and Hardy and Littlewood §, the process of taking the fractional integrals themselves along closed curves has not been examined.

In the present paper we discuss fractional integration along closed contours, and we give some instances of the application of the theory. The expression which we obtain for the fractional contour integral includes the form given by the theorem of residues ‖ for ordinary contour integrals as a special case. We use our results to express the Zeta-function of Riemann as fractional contour integrals of derivatives of the Weierstrass's elliptic function $\mathscr{P}(z)$ and of the function $\eta(z)$ as defined by

$$\frac{d\eta(z)}{dz} = -\mathscr{P}(z), \quad \lim_{z\to 0}\left\{\eta(z) - \frac{1}{z}\right\} = 0.$$

The expression of the Zeta-function as a fractional contour integral is of special interest, as this function has been expressed as an ordinary contour integral by Riemann ¶.

2. *Fractional Contour Integration.*

We begin with the general case, in which the integrand of the fractional contour integral may be multiform. The results for uniform integrands will be immediately deduced.

Consider the Riemann's surface associated with $v=f(t)$, where $f(t)$ is a function of the complex variable t. Let a closed contour C be formed on this surface by two simple curves l and L, joining points $t=a$ and $t=z$, which do not cross each other on this surface. The λth integral of $f(z)$ along l is defined ** as

$$\mathrm{D}^{-\lambda}(l_a)f(z) = \frac{\mathrm{D}^{\gamma}}{\Gamma(\lambda+\gamma)}\int_a^z (z-t)^{\lambda+\gamma-1}f(t)\,dt,$$

* Phil. Mag. xx. p. 781 (1935).
† *Nouvelles Annales* (3) iii. p. 240 (1884).
‡ Proc. Lond. Math. Soc. (2) xv. pp. 401–448 (1916).
§ *Math. Zeitschrift*, xxxiv. pp. 403–439 (1931).
‖ See Whittaker and Watson, ' Modern Analysis,' p. 112 (1927).
¶ Whittaker and Watson, ' Modern Analysis,' p. 266 (1927).
** Fabian, Phil. Mag. xx. p. 731 (1935).

where γ is the least integer greater than or equal to zero, such that * $R(\lambda)+\gamma>0$; D stands for $\frac{d}{dz}$, and the differentiation and integration are along l. $f(t)$ is continuous on C in this paper.

Keeping C and z fixed, let the length of L tend to zero, *after* $D^{-\lambda}(l_a)f(z)$ has been evaluated, by letting a move along C until it coincides with z. Then l becomes C. The value of $D^{-\lambda}(l_a)f(z)$, when l has become C by this process, will be denoted by $D^{-\lambda}(C)f(z)$.

THEOREM 7.—*Suppose that $f(z)$ is analytic on and within a closed contour* C *on the Riemann's surface associated with $u=f(z)$, except for isolated singularities within* C *at $b_1, b_2, \ldots b_\rho$, with cycles of $\tau_1, \tau_2, \ldots \tau_p$ roots respectively, at which $f(z)$ can be expanded in a Puiseux's series.*

Then

$$D^{-\lambda-\gamma}(C)f^{(\gamma)}(z)$$

$$=2\pi i \sum_{\rho=1}^{p}\sum_{\sigma_i=1}^{\infty}(-1)^{\sigma_i-1}\tau_\rho A_{\rho,\sigma_i}\frac{(z-b_\rho)^{\lambda-\sigma_i}}{\Gamma(\lambda-\sigma_i+1).(\sigma_i-1)!},$$

where

$$\sum_{\sigma_i=1}^{\infty}\frac{A_{\rho,\sigma_i}}{(z-b_\rho)^{\sigma_i}}$$

is the complete part of terms containing negative integral powers of $(z-b_\rho)$ in the Puiseux's expansion of $f(z)$ at b_ρ.

Also, the value of $D^{-\lambda-\gamma}(C)f^{(\gamma)}(z)$ is finite.

Proof.—Draw round each singularity b_ρ, on the Riemann's surface associated with $v=f(t)$, a simple closed curve T_ρ such that $f(t)$ is analytic on and within T_ρ on this surface, except for the single enclosed singularity at b_ρ, and such that, everywhere on T_ρ, for every ρ,

$$|t-b_\rho|<|z-b_\rho|.$$

On T_ρ we have, for any number σ,

$$\frac{(z-t)^{\lambda+\gamma-1}}{(t-b_\rho)^{\sigma}}=\frac{(z-b_\rho)^{\lambda+\gamma-1}}{(t-b_\rho)^{\sigma}}\left\{1-(\lambda+\gamma-1)\left(\frac{t-b_\rho}{z-b_\rho}\right)\right.$$

$$+\frac{(\lambda+\gamma-1)(\lambda+\gamma-2)}{2!}\left(\frac{t-b_\rho}{z-b_\rho}\right)^2+\ldots.$$

$$\ldots+(-1)^n\frac{(\lambda+\gamma-1)(\lambda+\gamma-2)\ldots(\lambda+\gamma-n)}{n!}\left(\frac{t-b_\rho}{z-b_\rho}\right)^n$$

$$\left.+\ldots.\infty\right\}.$$

* $R(\lambda)$ stands for the real part of λ.

Hence
$$\frac{1}{\Gamma(\lambda+\gamma)}\int_{T_\rho}(z-t)^{\lambda+\gamma-1}\frac{dt}{(t-b_\rho)^\sigma}$$
$$=2\pi i(-1)^{\sigma-1}\tau_\rho\frac{(z-b_\rho)^{\lambda+\gamma-\sigma}}{\Gamma(\lambda+\gamma-\sigma+1).\,(\sigma-1)\,!}$$

if σ is a positive integer, and

$$\frac{1}{\Gamma(\lambda+\gamma)}\int_{T_\rho}(z-t)^{\lambda+\gamma-1}\frac{dt}{(t-b_\rho)^\sigma}=0$$

for all other real values of σ. Consequently, as $f(t)$ can be expanded in a Puiseux's series at b_ρ,

$$\frac{1}{\Gamma(\lambda+\gamma)}\int_{T_\rho}(z-t)^{\lambda+\gamma-1}f(t)\,dt$$
$$=2\pi i\sum_{\sigma_i=1}^{\infty}(-1)^{\sigma_i-1}\tau_\rho A_{\rho,\sigma_i}\frac{(z-b_\rho)^{\lambda+\gamma-\sigma_i}}{\Gamma(\lambda+\gamma-\sigma_i+1).\,(\sigma_i-1)\,!}$$
$$\ldots\ldots\quad(1)$$

By Cauchy's Theorem,

$$D^\gamma D^{-\lambda-\gamma}(C)f(z)=\frac{D^\gamma}{\Gamma(\lambda+\gamma)}\sum_{\rho=1}^{p}\int_{T_\rho}(z-t)^{\lambda+\gamma-1}f(t)dt$$
$$=2\pi i\sum_{\rho=1}^{p}\sum_{\sigma_i=1}^{\infty}(-1)^{\sigma_i-1}\tau_\rho A_{\rho,\sigma_i}\frac{(z-b_\rho)^{\lambda-\sigma_i}}{\Gamma(\lambda-\sigma_i+1).\,(\sigma_i-1)\,!},$$

by (1).

But, integrating $D^{-\lambda-\gamma}(C)f(z)$ by parts γ times, we also have $D^\gamma D^{-\lambda-\gamma}(C)f(z)=D^{-\lambda-\gamma}(C)f^{(\gamma)}(z)$.
The conclusion follows.

For uniform functions $f(z)$ the theorem just proved reduces to

THEOREM 8.—*If $f(z)$ is analytic on and within a closed contour* C, *except for isolated singularities at b_1, b_2, ... b_p within* C,

then
$$D^{-\lambda-\gamma}(C)f^{(\gamma)}(z)$$
$$=2\pi i\sum_{\rho=1}^{p}\sum_{\sigma=1}^{\infty}(-1)^{\sigma-1}A_{\rho,\sigma}\frac{(z-b_\rho)^{\lambda-\sigma}}{\Gamma(\lambda-\sigma+1)\,.\,(\sigma-1)\,!},$$

where
$$\sum_{\sigma=-\infty}^{\infty}\frac{A_{\rho,\sigma}}{(z-b_\rho)^\sigma}$$

is the Laurent's series for $f(z)$ at b_ρ. The value of $D^{-\lambda-\gamma}(C)f^{(\gamma)}(z)$ is finite.

3. *Sums of Series expressed as Fractional Contour Integrals. The Zeta-function of Riemann.*

We shall discuss first the more general case of expressing sums of a certain class of series to n-terms and to infinity as fractional contour integrals, and shall apply the method to the series which defines the Zeta-function of Riemann. The class of series which we consider here is

$$A_1(z-b_1)^k+A_2(z-b_2)^k+\ldots+A_m(z-b_m)^k+\ldots, \quad \text{(I.)}$$

where the numbers A_m, b_m, and k, which may be real or complex, are independent of z, and

$$|b_{m+1}|>|b_m|$$

for all values of m greater than a positive number m_0.

(a) To express the sum of this series to n terms as a fractional contour integral consider a function $\theta(z)$ which is analytic in a region E except for poles at $b_1, b_2, \ldots . b_n$, at which the principal parts of $\theta(z)$ are

$$\frac{A_1}{(z-b_1)^\sigma}, \quad \frac{A_2}{(z-b_2)^\sigma}, \cdots \frac{A_n}{(z-b_n)^\sigma}$$

respectively. Let C_n be a simple closed curve enclosing $b_1, b_2, \ldots b_n$, such that $\theta(z)$ is analytic on and within C_n except for the poles at $b_1, b_2, \ldots b_n$. Theorem 8 gives, for all except negative integral values of k,

$$S_n(z,\ k)=\frac{(-1)^{\sigma-1}}{2\pi i}\,\Gamma(k+1)\,.\,(\sigma-1)\,!\,D^{-k-\sigma-\gamma}(C_n)\theta^{(\gamma)}(z),$$

here γ is the least integer greater than or equal to zero such that $R(k)+\sigma+\gamma>0$, and $S_n(z,\ k)$ denotes the sum of series (I.) to n terms. As we can take the limit when k tends to a negative integer this relation holds for negative integral values of k also.

(b) If we wish to express the sum of series (I.) to infinity as a fractional contour integral we suppose $\theta(z)$ to be analytic in a region E_1 except for poles at $b_1, b_2, \ldots . b_n, \ldots . \infty$, at which the principal parts of $\theta(z)$ are

$$\frac{A_1}{(z-b_1)^\sigma}, \quad \frac{A_2}{(z-b_2)^\sigma}, \cdots \frac{A_n}{(z-b_n)^\sigma}, \ldots \infty$$

respectively. Supposing C_n to be in E_1, we let C_n increase in size indefinitely in such a way that it retains for every

n the property of enclosing $b_1, b_2, \ldots b_n$, such that $\theta(z)$ is analytic on and within C_n except for the poles at $b_1, b_2, \ldots b_n$. If C_∞ denote the contour which C_n ultimately becomes by this process, the expression for $S(z, k)$ in (a) gives for the sum $S(z, k)$ of series (I.) to infinity the form

$$S(z, k) = \frac{(-1)^{\sigma-1}}{2\pi i} \Gamma(k+1) \cdot (\sigma-1)\,!\, D^{-k-\sigma-\gamma}(C_\infty)\theta^{(\gamma)}(z),$$

where γ has the same meaning as in (a).

(c) The Zeta-function of Riemann is defined * when $R(s) \geqslant 1+\delta$, $\delta > 0$, by

$$\zeta(s, z) = \sum_{n=0}^{\infty} \frac{1}{(z+n)^s}.$$

We shall give two expressions of this series as a fractional contour integral.

First, we choose an elliptic function $\mathscr{P}(z)$ which has unity for one of its periods. Using our result in (b) we obtain

$$\zeta(s, z) = -\frac{1}{2\pi i} \Gamma(1-s) \cdot D^{s-2-\gamma}(C_\infty)\mathscr{P}^{(\gamma)}(z), \ldots . \quad \text{(II.)}$$

$$R(s) \geqslant 1+\delta, \quad \delta > 0,$$

where the only poles of $\mathscr{P}(z)$ enclosed by C_∞ are those at

$$0, \quad -1, \quad -2, \ldots . -n, \ldots . \infty,$$

and γ is the least integer greater than or equal to zero such that

$$2 - R(s) + \gamma > 0.$$

As the converse process of evaluating

$$D^{s-2-\gamma}(C_\infty)\mathscr{P}^{(\gamma)}(z)$$

by means of Theorem 8 gives us

$$-\frac{1}{2\pi i} \Gamma(1-s) \cdot D^{s-2-\gamma}(C_\infty)\mathscr{P}^{(\gamma)}(z) = \sum_{n=0}^{\infty} \frac{1}{(z+n)^s},$$

therefore relation (II.) holds for no other values of s than those for which the series

$$\sum_{n=0}^{\infty} \frac{1}{(z+n)^s}$$

converges to $\zeta(s, z)$.

* Whittaker and Watson, ' Modern Analysis,' p. 265 (1927).

To obtain a second expression of $\zeta(s, z)$ as a fractional contour integral, consider the function * $\eta(z)$, defined by

$$\frac{d\eta(z)}{dz} = -\mathscr{P}(z), \quad \lim_{z\to 0}\left\{\eta(z) - \frac{1}{z}\right\} = 0,$$

where $\mathscr{P}(z)$ has unity for one of its periods. $\eta(z)$ has the property of being analytic everywhere except for simple poles at the poles of $\mathscr{P}(z)$, with a residue of 1 at each pole*.

From our result in (*b*)

$$\zeta(s, z) = \frac{1}{2\pi i}\, \Gamma(1-s)\, .\, \mathrm{D}^{s-1-\gamma}(\mathrm{C}_\infty)\eta^{(\gamma)}(z), \quad . \quad \text{(III.)}$$

$$\mathrm{R}(s) \geqslant 1+\delta, \quad \delta > 0,$$

where C_∞ is the same contour as in relation (II.) and γ is the least integer greater than or equal to zero, such that

$$1-\mathrm{R}(s)+\gamma > 0.$$

Relation (III.) holds for no other values of s than those for which the series

$$\sum_{n=0}^{\infty} \frac{1}{(z+n)^s}$$

converges to $\zeta(s, z)$, since, by Theorem 8, the value of $\mathrm{D}^{s-1-\gamma}(\mathrm{C}_\infty)\eta^{(\gamma)}(z)$ is given by

$$\frac{1}{2\pi i}\, \Gamma(1-s)\, .\, \mathrm{D}^{s-1-\gamma}(\mathrm{C}_\infty)\eta^{(\gamma)}(z) = \sum_{n=0}^{\infty} \frac{1}{(z+n)^s}.$$

XXI. *Temperature and Latent Energy in Flame Gases.*

By W. T. David, *Sc.D., M.Inst.C.E.*†

IT has been shown that a thin platinum-rhodium wire (·0005 inch diameter) immersed in the inflamed gases during the pre-pressure period in a gaseous explosion registers a steady temperature for as long as the pre-pressure period lasts ‡. For reasons previously given the steadily maintained temperature is regarded as giving

* Whittaker and Watson, 'Modern Analysis,' p. 445 (1927). In this book this function is denoted by $\zeta(z)$. We use the symbol η, to distinguish this function from the Zeta-function of Riemann.

† Communicated by the Author.

‡ Phil. Mag. xvii. p. 172 ; xviii. p. 228 ; and 'The Engineer,' 1st June, 1934, p. 558.

very approximately the temperature of the inflamed gases when burning at constant pressure. This temperature, however, is many hundreds of degrees Centigrade below the ideal temperature for the flame gases calculated upon the assumption that these gases are merely hot CO_2, H_2O, N_2, etc., and that there is no heat loss †. Experiment has shown that the heat losses are relatively

TABLE I.

Measured Temperature and Latent Energy in Flame Gases resulting from the combustion at constant pressure of various gaseous mixtures for which the ideal calculated temperature is 1900° C. in all cases.

Mixture (percentages).	Measured temperature (°C.).	Difference between ideal and measured temperatures (°C.).	Latent energy per cent. heat of combustion.
1 atmosphere :			
23 CO+77 air	1560	340	20·0
8·63 CH_4+91·37 air	1610	290	16·5
5·25 C_2H_2+94·75 air	1630*	270	15·0
5 atmospheres :			
23 CO+77 air	1680	220	13·5
8·63 CH_4+91·37 air	1675	225	12·5
5·25 C_2H_2+94·75 air	1745*	155	8·0
1 atmosphere :			
16·3 CO+8·15 O_2+75·55 Ar....	1390	510	28
30·6 CO+15·3 O_2+54·1 CO_2 ...	1510	390	23
23·0 CO+16·2 O_2+60·8 N_2 ...	1560	340	20

* Extrapolated results.

negligible, and it is inferred that there exists in flame gases a long-lived latent energy of considerable amount.

Several series of experiments have been completed in which wide variations have been made in the nature of the combustible gas, the pressure at which combustion takes place during the pre-pressure period, and the nature of the diluent gases. From these experiments I have selected for purposes of summary all those for which the ideally calculated flame temperature is 1900° C., and give in Table I. the measured steadily maintained tempera-

† 'Nature,' cxxxv. p. 470.

tures together with the latent energies deduced from them.

It will be seen that the measured temperatures range from 1390° C. to 1745° C. and the latent energies from 8 per cent. of the heat of combustion to as much as 28 per cent.

TABLE II.

Ideal calculated Temperatures and Latent Energy in Flame Gases resulting from the combustion at constant pressure of various gaseous mixtures in which the measured temperature is 1550° C. in all cases.

Mixture (percentages).	Ideal temperature (°C.).	Difference between ideal and measured temperatures (°C.).	Latent energy per cent. heat of combustion.
1 atmosphere :			
22·8 CO+77·2 air	1880	330	20·0
8·25 CH_4+91·75 air	1835	285	16·5
5·0 C_2H_2+95·0 air	1820	270	15·0
6 atmospheres :			
20·7 CO+79·3 air	1760	210	11·5
7·87 CH_4+92·13 air	1760	210	12·5
4·57 C_2H_2+95·43 air	1670	120	8·0
1 atmosphere :			
18·8 CO+9·4 O_2+71·8 Ar	2140*	590	28·5
31·6 CO+15·8 O_2+52·6 CO_2 ...	1940*	390	23·0
22·8 CO+16·2 O_2+61 N_2	1880	330	20·0

* Not allowing for dissociation. As the measured temperature is only 1550° C., dissociation is negligible, and consequently the fairer comparison is with the calculated temperature uncorrected for dissociation.

A similar summary is shown in Table II., except that in this table the basis of selection has been not the same ideally calculated temperature, but the same measured temperature, viz., 1550° C.

The long-lived latent energy would appear to depend upon the following initial conditions: (i.) the nature of the combustible gas; (ii.) the nature of the diluent gases; and (iii.) the pressure at which combustion takes place.

XXII. *On Transverse Vibrations of Long Rods.* *By* Isay A. Balinkin, *B.S.M.E., M.Sc., Ph.D., University of Cincinnati, Department of Physics* *.

I. *Introduction.*

THE mathematical analysis of transverse vibrations of rods goes back to the time of Daniel Bernoulli, who was soon followed by Euler, Poisson, Cauchy, and many others [1], while more recently Lord Rayleigh [2] and Timoshenko [3] made important contributions. The latest complete analysis of the vibrating strip as used in Frahm's tachometer is given by Meyer zur Capellen [4]. A rigorous solution of the differential equation representing vibrating rods involves the method of the calculus of variations, Bessel functions, and transcendental equations. Approximate results, with the use of calculus only, were obtained by Garrett [5] and Barton [6], who made certain simplifying assumptions.

It is proposed to develop here a simple theory establishing a relation between the frequency of an oscillating long blade, its size, and the elastic property of its material. A unified treatment is given for a vibrating long blade, one end of which is clamped, with the axis either in a horizontal or a vertical position. If vertical, the blade is considered vibrating either above or below the fixed end. For each position the frequency is computed when the blade is vibrating alone or with a concentrated load at its free end. Thus six specific cases are presented in theory, and the experimental data are plotted for each case.

II. *Theory.*

In simple theory, given below, the equations are derived for the lowest frequency of long straight rods of uniform cross-section. The deformations are taken to be small and the rotatory inertia of the rod is neglected.

A. *Vibrating Blade with Axis horizontal.*

Consider first a massless blade of length l, with a concentrated load W at its free end, as shown in fig. 1.

* Communicated by the Author.

The static deflexion y' at any point distant x from the origin is

$$y' = -\frac{WX^2}{6EI}(3l-x), \quad . \quad . \quad . \quad . \quad . \quad (1)$$

and the maximum deflexion, y_0', when $x=l$ is

$$y_0' = -\frac{Wl^3}{3EI}, \quad . \quad . \quad . \quad . \quad . \quad . \quad (2)$$

where E is the modulus of elasticity and I is the moment of inertia of the cross-section of the blade about its neutral axis [7].

When an additional displacement y_0 is produced at the free end and the blade released, it will begin to oscillate about its former position of static deformation. The

Fig. 1.

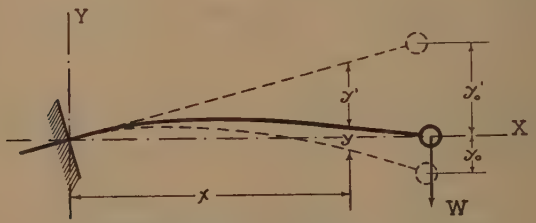

A blade vibrating about a horizontal axis with a concentrated load, W, at the free end.

sum of the kinetic and potential energies is constant for any position of the blade, *i. e.*,

$$\frac{W}{2g}\left(\frac{dy_0}{dt}\right)^2 + \frac{cy_0}{2} = \text{constant}, \quad . \quad . \quad . \quad (3)$$

where g is the acceleration of gravity and c is the spring constant defined as the weight necessary to produce a unit deflexion, *i. e.*,

$$c = \frac{W}{y_0}.$$

The equation of motion is derived from eq. (3) by differentiating it with respect to time, *i. e.*,

$$\frac{d^2y_0}{dt^2} + \frac{g}{y_0}y_0 = 0, \quad . \quad . \quad . \quad . \quad . \quad (4)$$

from which the frequency of vibration, ν, can now be determined:

$$\nu = \frac{1}{2\pi}\sqrt{\frac{g}{y_0'}} = \frac{1}{2\pi}\sqrt{\frac{3EIg}{Wl^3}}. \quad . \quad . \quad . \quad (5)$$

If the effect of the weight of the blade is to be taken into account, it is evident that the frequency of vibration will be decreased. Following the method of Lord Rayleigh, we can calculate the part of the weight W_1 of the blade which is necessary to add to W in order to compensate for the originally considered massless blade.

Let the weight per unit length of the blade be q, i. e., $W_1 = ql$, then the kinetic energy for any element dx of the blade will be

$$\frac{q\,dx}{2g}\left(\frac{dy}{dt}\right)^2, \quad . \quad . \quad . \quad . \quad . \quad . \quad . \quad (6)$$

where y is the additional displacement of any element of the blade from its position under the static load and dy/dt is the velocity of the corresponding element. It is assumed here that the shape of the blade in vibrating is the same as under a concentrated static load at its free end. The relation between a displacement y and y_0' is evidently the same as that given by eqs. (1) and (2):

$$y = y_0\frac{3lx^2 - x^3}{2l^3}. \quad . \quad . \quad . \quad . \quad . \quad (7)$$

The total kinetic energy of the blade can now be found by integrating eq. (6) after a proper substitution of the value for dy/dt from eq. (7):

$$\int_0^l \frac{q}{2g}\left(\frac{dy_0}{dt}\cdot\frac{3lx^2 - x^3}{2l^3}\right)^2 dx = \cdot 236\,\frac{ql}{2g}\left(\frac{dy_0}{dt}\right)^2.$$

Comparing this with the expression for the kinetic energy of the concentrated load given in the first term of eq. (3), we observe that the frequency decrease, due to the weight of the blade, can be compensated by an addition of $\cdot 236W_1$ to the weight of the concentrated load W.

In the extreme case, when $W = 0$, we have

$$\nu = \frac{1}{2\pi}\sqrt{\frac{3EIg}{\cdot 236W_1l^3}}$$

A better approximation can be obtained if we assume that the shape of the blade in vibration is the same as the static curve of the blade under a uniformly distributed weight q per unit length. Then the equivalent weight of the blade is equal to $\cdot 241 W_1$, which differs by only $\cdot 5$ per cent. from the value deduced by a rigorous and considerably more complicated method (3) which gives $\cdot 243 W_1$.

B. *Axis vertical*: *Weight below Support.*

The problem of a blade vibrating in a vertical position is treated again, first by assuming a massless blade

Fig. 2.

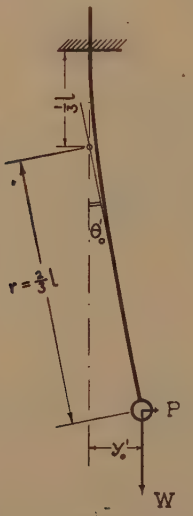

A blade vibrating about a vertical axis with a concentrated load, W, below the support.

with a load concentrated at the free end below the support (fig. 2). In this position the frequency of vibration depends not only upon the elastic forces in the blade itself, but also upon the gravitational force, since the centre of gravity of the system moves in a curve. Indeed, we may justly call this system an "elastic pendulum," since the additional gravitational force is of the same magnitude as that which would act on a simple pendulum

with a length equal to the radius of curvature of the trajectory described by the centroid of the system [9]. This length, r, of the equivalent pendulum can be determined by locating the point of intersection of the tangent to the free end of the blade with the vertical axis of the blade. The deflexion produced by a force P acting perpendicularly to the axis of the massless blade at the free end is given by

$$y_0' = -\frac{Pl^3}{3EI},$$

while the slope is

$$\theta_0' = -\frac{Pl^2}{2EI}.$$

For small deformations $\tan\theta_0' = \sim\theta_0'$ and, therefore,

$$r = \frac{y_0'}{\tan\theta_0'} = \frac{2}{3}l.$$

The spring constant of the elastic pendulum due to the gravitational force is then expressed as

$$c_2 = \frac{W}{r} = \frac{3}{2}\frac{W}{l} \quad \ldots\ldots\ldots \quad (8)$$

The total spring constant of the system is equal to the sum of the elastic spring constant and that of gravitation, *i. e.*,

$$c = \frac{3EI}{l^3} + \frac{3W}{2l},$$

and the resultant frequency is

$$\nu = \frac{1}{2\pi}\sqrt{\frac{3EIg}{Wl^3} + \frac{3}{2}\frac{g}{l}}. \quad \ldots\ldots \quad (9)$$

When the blade vibrates wthout any load attached to its free end, the effect of the gravitational force must be computed for a compound pendulum. Following the same manner of reasoning as for a simple pendulum, but now using the formulæ for uniformly distributed load, the equivalent length of the compound pendulum can be computed to be $3/4\,l$. The spring constant, due to the gravitational force, yields, however, for a compound pendulum exactly the same value as for a simple pendulum, eq. (8).

Thus, in computing the frequency of the blade itself, eq. (9) can be used, in which W is replaced by $0{\cdot}243\ W_1$.

When the effect of the blade and the load is to be considered, the frequency again can be computed from eq. (9), in which $0{\cdot}243W_1$ must be added to W.

C. *Axis vertical : Weight above Support.*

Another interesting case presents itself when the load is located above the fixed end of the blade. In this position the effect of gravity is negative, and, therefore, the frequency of vibration is

$$\nu=\frac{1}{2\pi}\sqrt{\frac{3EIg}{Wl^3}-\frac{3g}{2l}}, \quad . \quad . \quad . \quad . \quad . \quad (10)$$

where the value of W may be replaced by $0{\cdot}243W_1$ or the sum of both, depending upon the circumstances explained in the previous case.

On examining the expression under the radical of eq. (10), it can be observed that for a given value of W there is a critical value of l for which the frequency becomes equal to zero. Solving

$$\frac{3EIg}{Wl^3}-\frac{3g}{2l}=0, \quad . \quad . \quad . \quad . \quad . \quad . \quad (11)$$

we find

$$l_c=\sqrt{\frac{2EI}{W}}. \quad . \quad . \quad . \quad . \quad . \quad . \quad . \quad (12)$$

Thus, when the length of the blade is equal to l, the system will be in neutral equilibrium, and for all values of l greater than the critical value the equilibrium becomes unstable. A slight sidewise force causes the blade to be bent over because the gravitational force is now greater than the elastic force of deformation. From eq. (12) the critical length of the blade with no load can be computed to be

$$l_c=2{\cdot}02\sqrt[3]{\frac{EI}{q}},$$

which is about 1·5 per cent. too high when compared with the result of a rigorous and considerably more complicated solution given by Greenhill [10].

The problem of a blade with the weight above the support is the same as that of a long column under the

action of a vertical thrust. In structural engineering these problems are solved by the classical Euler's formula, which establishes a relation between the length of the column and its maximum safe carrying load,

$$W = \frac{\pi^2}{4}\frac{EI}{l^2} = \sim 2{\cdot}5\,\frac{EI}{l^2}.$$

Euler's relation is derived from static considerations, and it is of interest to make a comparison with the relation between the same variables derived from the principle of dynamic stability. From eq. (12)

$$W = 2\frac{EI}{l^2}.$$

Thus, the safe carrying load as computed from Euler's formula is about 20 per cent. too high.

II. *Experimental Verification.*

The expressions derived in the theoretical part of this paper were verified experimentally for several steel, brass, and wooden blades. The blade was firmly clamped in a vice and a carefully measured length of the blade, whose vibrations could be conveniently counted, was projected horizontally. The number of vibrations counted depended upon the frequency; usually the total duration for one count did not exceed 60 seconds. The vice could then be turned through 90 degrees and the blade set into vibration about a vertical axis. Again the frequency was measured for the two positions of the blade, above and below the support. The length of the blade was then increased by 2 to 5 cm. and the readings taken as before. Near the critical length the measurements were made at closer intervals.

When the length of the blade is increased in a horizontal position there may be an appreciable sag, and it is necessary then to turn the vice through a small angle so that the points of the major portion of the blade vibrate in vertical lines.

Another set of frequency measurements was made with a weight attached to the free end of the blade.

Five-place logarithms were used in computing the results plotted in fig. 3. The blade used was 0·780 cm. thick, 0·116 cm. wide, weighing 0·7045 gm. per cm. The modulus of elasticity for steel was taken as 2×10^9 gm.

per cm.^{2}; the load, W=48·1 gm. The curves show a good agreement for the frequencies as computed from the equations and determined experimentally.

Fig. 3.

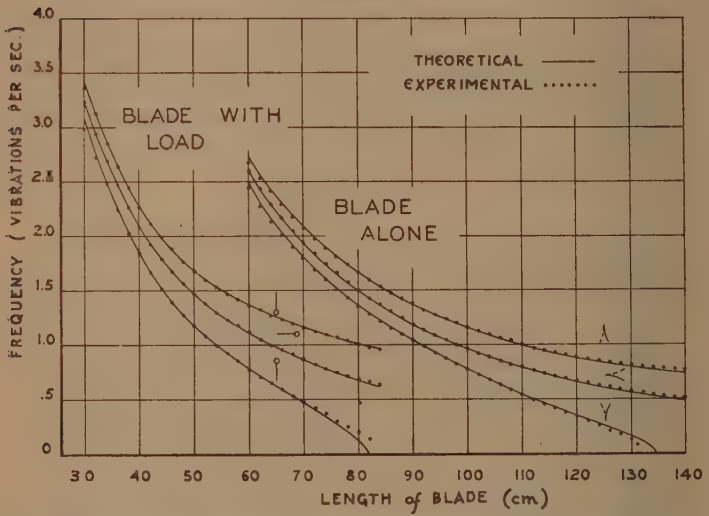

The frequency of a vibrating blade as a function of its length. The blade vibrates with and without a concentrated load at its free end. The theoretical and experimental data are shown for vibrations in three different positions.

In conclusion the writer wishes to express his thanks to H. A. Romanowitz, with whom the contents of this paper were discussed, and who verified experimentally some of the equations.

References.

(1) Todhunter and K. Pearson, ' A History of Elasticity,' i. & ii.
(2) Lord Rayleigh, ' Theory of Sound,' i. ch. viii.
(3) S. Timoshenko, ' Vibration Problems in Engineering,' ch. iv.
(4) W. Meyer zur Capellen, *Ann. der Physik*, xv. p. 1 (1932).
(5) C. A. B. Garrett, Phil. Mag. viii. p. 581 (1904).
(6) E. H. Barton, Phil. Mag. xiv. p. 578 (1907).
(7) C. E. Fuller and W. A. Johnston, ' Applied Mechanics,' xi. p. 189.
(8) B. L. Worsnop and H. T. Flint, ' Advanced Practical Physics,' p. 94.
(9) Ernst Lehr, ' Schwingungstechnik,' § 11.
(10) A. G. Greenhill, Cambridge Phil. Soc. Proc. iv. (1881); also ' Handbuch der Physikalischen und Technischen Mechanik,' Band iv. 1 hälfte, p. 100.

XXIII. *On the Hume-Rothery Conception of the Metallic State.* *By* C. D. Niven, *B.Sc., Ph.D., Asst. Research Physicist, National Research Council Laboratories, Ottawa* *.

1. *Introduction.*

In a paper [1] published three years ago the writer suggested that the correct method of approaching the problem of metallic conduction was by first finding an answer to the question—what is a metal ? The work of Hume-Rothery and others has recently brought to light so many interesting facts about the metallic state that the problem can now be put on an entirely new basis. The necessity of taking structure into account in discussing metallic conduction has recently become more obvious than ever. The temperature-resistance curves for the various metals differ so markedly, that one begins to doubt if it is possible to make a free electron theory fit for all metals, unless the structure—both atomic and crystallographic—be taken into account. Grüneisen [2], for instance, has pointed out that " the metals platinum, palladium, and tantalum exhibit a retarded rise in resistance—while the ferromagnetic metals iron, nickel and cobalt exhibit a very marked rise in resistance up to the Curie Point." Bloch [2], viewing the problem entirely from the standpoint of the free electron theory, draws attention to the fact that the mutual action of electrons cannot be ignored. Thus if the electrons, as well as the atomic residues are to be taken into account, the problem is exceedingly complicated and clear conceptions of the metallic state become very desirable.

2. *The Binding together of Atoms in the Metallic State.*

The essential feature about a metal, when atomic structure considerations are taken into account, is that there is no possible way of grouping the electrons into systems according to the well-known valency laws governing the formation of salts and other chemical compounds. The question then arises as to how atoms behave when they are packed together to form a metal.

* Communicated by the Author.

Hume-Rothery [3] has done an immense amount of work which helps to answer this question; briefly, his conception of the metallic bond is that one electron is shared by more than two atoms. It is found that B group metals incline to crystallize with (8–N) near neighbours—where N is the number of the group. Thus in group VI. B selenium and tellurium crystallize with two near neighbours. The rule is obeyed, according to Hume-Rothery, by the metals in group II. B, by gallium in III. B, by germanium and tin in IV. B, and by the metals in V. B and VI. B, and iodine in VII. B. In the case of groups IV. B, V. B, VI. B, and VII. B it is possible to assume a sort of simple covalent bond, that is to say one electron shared by two atoms; but for the metals in the first, second, and third groups it is necessary to assume that one electron is shared by more than two atoms; this Hume-Rothery conceives to be the true metallic bond.

TABLE I.

Cu	Zn	Ga	Ge	As	Se
Ag	Cd	In	Sn	Sb	Te I
Au	Hg	Tl	Pb	Bi.	

In order to demonstrate clearly which metals obey the (8–N) rule and which do not, the elements under consideration have been set out in Table I.; those which do obey the rule are in block type and those which do not are in ordinary type.

It can be noticed at a glance that group II. B obeys the law more consistently than either group I. B or group III. B, and in this respect resembles V. B, VI. B, and VII. B. It is also well known that electrons build up in systems of 2 and 6 electrons, and the so-called "*p*" system has six electrons in it. One is, therefore, inclined to think that Hume-Rothery's (8–N) rule would represent facts more clearly if it were stated for the groups III. B to VII. B, as follows:—"In crystallizing each atom has (6–N) near neighbours, where N is the number of electrons in the '*p*' system." This more complicated wording gives the same figure for the number of near neighbours, but emphasizes the significance of the rule in so far as atomic structure is concerned.

The Unique Case of Bismuth.

It is now apparent that bismuth holds a unique position in the Mendelejeff's table. Evidence has been given by Hume-Rothery [3] to justify the assumption that the two "*s*" electrons which constitute the second outermost system in thallium, lead, and bismuth remain as part of the core, so that these three elements can be considered as having respectively 1, 2, and 3 valence electrons, not 3, 4, and 5. Bismuth has, therefore, three electrons to share with three near neighbours. Let us consider now a central atom Z and three near neighbours *a*, *b*, and *c*. If one electron from Z is shared with each of *a*, *b*, and *c*, symmetry demands that one electron from each of *a*, *b*, and *c* be shared with Z; and so Z must have six shared electrons. There are now two possibilities; either three groups of two electrons are formed or else groups of six shared electrons are grouped around each bismuth atom. The latter alternative seems preferable in spite of the difficulty of imagining the mechanical model, mainly because the three pairs of electrons, which the other alternative suggests, would imply the common covalent bond of paired electrons and the resultant substance might be expected to be an insulator. If the bismuth atom had normally had five valency electrons instead of three, the core with two "*s*" electrons still attached would have been unstable, and the resulting structure would not be expected to have the unique qualities of bismuth. Thus arsenic with five valence electrons is much more like a normal metal than is bismuth. The latter element appears to owe its exceptional qualities not merely to the fact that it is in the V. B group, but also to the fact that it is in the third long period.

There is a modification of bismuth [4] which occurs when the metal is prepared under very high pressure; prepared under such conditions, we might expect that it might be impossible for the groups of six electrons to form, and in point of fact we find that "high pressure" bismuth has lost some of the "exceptional" qualities of ordinary bismuth.

A system of six electrons is associated with diamagnetism, and the fact that bismuth is so markedly diamagnetic seems to add some weight to the conception

of a system of six shared electrons. This is, furthermore, endorsed by the fact that on melting when the system presumably would get broken down, the diamagnetism decreases enormously.

Some work by Lane [5] on the magneto-resistance of bismuth films at low temperatures shows that there is a distinct discontinuity in the magneto-resistance when the "particle size falls below that of the unit of the secondary structure." On our conception this is presumably when the systems of six shared electrons break down.

It is of interest to emphasize in passing that it is the remarkable stability of the two "*s*" electrons in the second outermost system of the B elements in the third long period which gives to bismuth its definite trivalent character, resulting, apparently, in exceptional metallic properties; and so we might expect that that element, whose position in the periodic table is such that it would have these two "*s*" electrons for its outermost system, might perhaps possess rather unique properties and even resemble a helium atom somewhat. Mercury, of course, is this element; just as helium possesses the lowest melting-point of all gases so mercury possesses the lowest melting-point of all metals. Sidgwick [6], in discussing valency remarks, "Mercury occupies a unique position among metals." Its remarkable preference for the covalent bond is probably connected with the stability of the pair of "*s*" electrons.

4. *The Bearing on Metallic Conduction.*

As mentioned already, Hume-Rothery's conception of the true metallic bond implies that an electron must be shared by more than two atoms. The distinction between such a bond and the type of bond found in bismuth seems sharper than is necessary, especially in view of what has been said above. The type of bond described for bismuth comes into being by the sharing of electrons, and although the resulting structure appears to be of exceptional stability in the case of bismuth, the principle is a general one, and can be readily extended to the cases in which an electron must be shared by more than two atoms. All that we need to hypothesize is that some of the electrons which form a stable grouping

round one atom must be used to complete a stable grouping round another atom. Some of the electrons from the latter, again, must be used to complete another stable grouping, and so on. The difference between such a structure and that of a salt is thus very obvious ; for, in the case of a salt there is no continual travelling of electrons from one atom to another, and thus the structure of a salt lacks the very quality which is obviously necessary for electrical conduction.

Dehlinger [7] describes the bonding of atoms in the metallic state rather lucidly as follows :—" Every one of the bonding electrons of the metallic lattice goes round in the course of time all the atoms of the lattice in the same way, except that a particular atom is somehow favoured by a particular electron."

Such a picture revolutionizes the theory of electrical conduction, for while the electrons are conceived as being perfectly free to move from atom to atom, they are, none the less, intimately related to the atomic cores and to each other. To suggest a mechanical model is out of the question ; it is difficult to imagine what the paths would be like, since there are three dimensions to be taken into consideration. Therefore, all we can hypothesize is, firstly, that the cores of the atom are arranged in a perfectly orderly fashion as demanded by crystal structure data, and, secondly, that there is a net-work of electronic paths in the interspaces over which the electrons, considered in the older theories as free, are compelled to travel, in order that the cores may be held together and that suitable grouping of electrons into systems may occur. Thermal agitation should not now be considered as a crude bombarding of bullet-like atoms, but of vibrations in a " dynamic " electron lattice structure. A net constructed out of perfectly elastic string gives, to some extent, an idea of the structure visualized.

Such a structure would readily transmit any disturbance—electrical or thermal—from one end to the other. The concept of bullet-like electrons contributing to the specific heat is unnecessary, since electrons and atoms must now be considered as belonging to one complete structure—a concept which is very much more compatible with the requirements of the Debye theory of specific heats.

Supposing, now, that an electrical potential be applied

to a metal, it will have some influence on the electrons, which we have assumed to be travelling over perfectly definite paths; indeed, it is conceivably possible that an electron, instead of returning to the particularly favoured atom referred to by Dehlinger, may now be directed to another atom. One might, perhaps, suppose that such a jump would require a certain quantity of energy, and that the current might only flow when the potential gradient reached a certain value. But such a conception appears to be wrong. For if at the moment at which the electron had to make the jump another electron from the atom before was all ready to take its place in connexion with the "favoured" atom, then the electrons could pass along easily. If, however, one atom in a long chain were different from the others, so that the replacing electron arrived just a little too late, then it would stop all the others from permitting the smooth passing on of electrons. This is a logical conclusion from our previous reasoning, and it is just what experiment demonstrates. An amount of impurity amounting to one atom in one hundred atoms in a lineal chain is sufficient to make an appreciable change in the resistance.

Hume-Rothery [8] has pointed out that the hardness of a pure metal is affected by the introduction of an extremely small amount of impurity, and explains the phenomenon by considering that hardness is due to an inability of the atoms to slip past each other—somewhat as balls when piled might do; when one atom cannot slip past owing to the distortion of the lattice as a result of difference in size—then it may prevent, perhaps, one hundred atoms behind it from moving. A small impurity affects both hardness and conductivity, and one might, therefore, be led to suppose that the two phenomena depend on each other. If, however, what has been said above be correct, it would appear that the two phenomena should be accounted for in entirely different ways. The hardness would appear to depend on the size of the foreign atom relative to that of the other atoms, while the electrical conductivity would appear to depend on the periodicity of the electron motion in the foreign atom relative to that in the pure atom.

The effect of impurity would be expected to depend,

therefore, only on the difference in the type of electron motion in the pure atom and in the foreign atom—in other words, on the kind of atom introduced ; the effect should therefore be independent of temperature. This conclusion agrees in general with the experimental data, as it is found that the effect of introducing an impurity is usually to move a temperature-resistance curve up the resistance ordinate, as a whole, without grossly changing its shape.

The more perfectly a crystal of metal is formed the better is found to be its electrical conductivity, and this experimental fact is quite in line with the conception that the more perfectly the electronic motions are in time the more perfectly the metal will conduct.

5. *The Bearing on Superconductivity.*

Our reasoning is thus inclined to lead us to the conclusion that a metal containing absolutely no impurity, crystallized as a perfect single crystal, and free from all thermal agitation should conduct perfectly. Although experimental evidence does certainly indicate a residual resistance at the absolute zero, yet it must be remembered that this is very small, and that, therefore, our conclusions are approximately endorsed by experiment. Most of the resistance in a pure annealed metal is caused by thermal agitation. The circumstance which is harder to explain is how with obvious thermal agitation present does the replacing electron always arrive just at the right moment to permit of perfect conduction in certain metals and alloys. This is the demand of superconductivity. Up to the present superconductivity has been thought to be connected with a sort of process whereby the atoms of the metal became, so to speak, parts of a huge molecule, while in the case of ordinary conduction they were independent. The conceptions of Hume-Rothery, however, point to the sharing of electrons, and, therefore, the atoms cannot be considered as independent of each other.

The appearance of superconductivity is sudden, and resembles in this respect the process of crystallization. One might reason, then, that just as it is not necessary to remove all thermal agitation in order to bring about crystallization, so it is not necessary to remove all thermal agitation in order to allow electronic orbits to synchronize

and thus permit perfect conduction to occur. However, the following experimental evidence clearly shows that the phenomenon of superconductivity must be accounted for by a mechanism which is entirely different from that which explains ordinary conduction.

A study of the data on alloys by Benedicks [9] has shown that, by varying the percentage of alloying metal in a superconductor, one may find in some cases that at a certain percentage the resistance at, say, 20° K., rises to a maximum, while at the same percentage a maximum may be noted in the superconducting transition temperature. This would point to the conclusion that where orbital conditions are such that small thermal agitation disturbs the synchronization to a maximum amount, these very orbital conditions may be the most favourable for the phenomenon of superconductivity to appear. This affords an emphatic proof that the mechanism of superconduction is different from that of ordinary conduction.

What appears so obvious in the case of certain alloys can be noted to a less extent by examining the data on pure metals. Although many obvious exceptions can be found, yet, in general, one is struck by the fact that metals such as mercury or lead, which are rather poor conductors at ordinary temperature, are superconductors at comparatively high temperatures in the low temperature region, while often those elements which are the best conductors of electricity, *e. g.*, copper, silver, gold, and the alkalis are not superconductors at the very lowest temperatures as yet attainable.

The suggestion is put forward that in the case of superconductivity the transition of electrons from atom to atom depends not on the synchronization of jumps from one electronic system to another, but rather on the synchronization of orbits themselves. By making jumps from one system to another the electrons are leaving one path and getting into another. If it were possible that two paths in the atom itself were so close together that an electron could pass from one to the other without any jumping and without causing thereby any thermal agitation, then superconduction might occur. In this connexion Hume-Rothery's [10] observation that the energy levels in A group superconductors are very near together is of interest.

A group superconductors are among a class of elements which have many valencies; this is particularly true of vanadium, niobium and tantalum. These elements lie at the beginning of the transition periods in Mendeljeff's table.

In the case of the B group superconductors these remarks do not apply. With several of these elements, however, there is a marked tendency to covalency, notably in mercury, lead, and aluminium.

References.

(1) Niven, C. D., Canadian Journ. of Research, v. pp. 79–86 (July 1931).
(2) Debye, P., 'The Interference of Electrons,' pp. 53 and 63.
(3) Hume-Rothery, W., Phil. Mag. ser. 7, ix. pp. 65–80 (Jan. 1930).
(4) Bridgman, P. W., Rev. of Mod. Phys. vii. no. 1, p. 25 (Jan. 1935).
(5) Lane, C. T., Phys. Rev. xlv. no. 10, pp. 733–734 (May 1934).
(6) Sidgwick, N. V., 'The Electron Theory of Valency,' p. 264.
(7) Dehlinger, U., *Zeit. für Elektrochem*, xxxviii. p. 149 (March 1932).
(8) Hume-Rothery, W., Phil. Mag. ser. 7, iv. pp. 1017–1045 (Nov. 1927).
(9) Benedicks, C., *Zeit. für Metallkunde*, Jahrg. 25, Heft 9, pp. 197–202 (Sept. 1933).
(10) Hume-Rothery, W., 'The Metallic State,' p. 338.

XXIV. *On an Electro-Magnetic Inertial Ellipsoid associated with the Windings of Electrical Machinery.* By W. H. Ingram, *Columbia University* *.

THE discovery of the analogy between relative angular velocity of commutator and brush in the theory of a commutated electrical nexus and the angular velocity of a system of moving coordinates in dynamics † suggests the possibility of establishing, for the electrical circuits in a machine, an analogy to the inertial ellipsoid of Cauchy and Poinsot in particle dynamics. The purpose of this note is to establish this analogy and to interpret physically the meaning of certain transformations of coordinates in their relation to the ellipsoid.

In the dynamical theory of the three-phase star-connected orthocyclic alternator having, for simplicity, a single pair of field-poles, the kinetic energy contains an expression of the form

$$\mathrm{T}=\tfrac{1}{2}\Sigma\Sigma l_{jk}\dot{q}_j\dot{q}_k \quad (i, j=1, 2, 3), \quad . \quad . \quad . \quad (1)$$

* Communicated by the Author.
† Ingram, Phil. Mag., April 1934, p. 844.

where the self and mutual inductances of the armature circuits are given by the formula

$$l_{jk}=l^*1_{jk}-l_m-l_\mu \cos(\theta_j+\theta_k), \quad . \quad . \quad . \quad (2)$$

where 1_{jk} is a quantity equal to unity when $j=k$ and otherwise zero, l_m is a positive constant, $\theta_i=\theta-2\pi i/3$, and θ the rotor position parameter.

Interpreting (1) as a surface in the space of the $\dot{q}$'s, the cyclic symmetry of the l's implies that the axes of the $\dot{q}$'s must be symmetrically oriented with respect to one of the principal axes *. Therefore the $\dot{q}$-axes, if assumed to be mutually perpendicular, must each make the same angle with this principal axis, about which the ellipsoid obviously must revolve, namely, an angle whose cosine is $\frac{1}{3}\sqrt{3}$. The principal coordinates are obtained projectively, and are

$$\left.\begin{aligned}\dot{\xi}&=\sqrt{\tfrac{2}{3}}(\dot{q}_1\sin\theta_1+\dot{q}_2\sin\theta_2+\dot{q}_3\sin\theta_3),\\ \dot{\eta}&=\sqrt{\tfrac{2}{3}}(\dot{q}_1\cos\theta_1+\dot{q}_2\cos\theta_2+\dot{q}_3\cos\theta_3),\\ \dot{\zeta}&=\sqrt{\tfrac{1}{3}}(\dot{q}_1+\dot{q}_2+\dot{q}_3),\end{aligned}\right\} \quad . \quad . \quad (3)$$

where $\theta_i-\theta_{i+1}=120°$, but where the exact origin for the parametric coordinate θ is of no consequence here.

From the inverse of (3)

$$\left.\begin{aligned}\dot{q}_1&=\sqrt{\tfrac{2}{3}}\dot{\xi}\sin\theta_1+\sqrt{\tfrac{2}{3}}\dot{\eta}\cos\theta_1+\sqrt{\tfrac{1}{3}}\dot{\zeta},\\ \dot{q}_2&=\sqrt{\tfrac{2}{3}}\xi\sin\theta_2+\sqrt{\tfrac{2}{3}}\dot{\eta}\cos\theta_2+\sqrt{\tfrac{1}{3}}\dot{\zeta},\\ \dot{q}_3&=\sqrt{\tfrac{2}{3}}\dot{\xi}\sin\theta_3+\sqrt{\tfrac{2}{3}}\dot{\eta}\cos\theta_3+\sqrt{\tfrac{1}{3}}\dot{\zeta},\end{aligned}\right\} \quad . \quad . \quad (4)$$

it is found readily that (1) can be given the form

$$T=\tfrac{1}{2}(l^*+\tfrac{3}{2}l_\mu)\dot{\xi}^2+\tfrac{1}{2}(l^*-\tfrac{3}{2}l_\mu)\dot{\eta}+\tfrac{1}{2}(l^*-3l_m)\dot{\zeta}^2, \quad . \quad (5)$$

which, as kinetic energy, is positive definite. It follows directly † that the self-inductance for any circuit belonging to a coordinate axis through the centre of the ellipsoid (5) in the direction $\cos\alpha$, $\cos\beta$, $\cos\gamma$ is

$$l_{\alpha,\beta,\gamma}=(l^*+\tfrac{3}{2}l_\mu)\cos^2\alpha+(l^*-\tfrac{3}{2}l_\mu)\cos^2\beta+(l^*-3l_m)\cos^2\gamma, \quad . \quad . \quad . \quad (6)$$

* The axes of the ellipsoid are given by the roots of the so-called "secular equation"

$$\begin{vmatrix} l_{11}-\mu & l_{12} & l_{13}\\ l_{21} & l_{22}-\mu & l_{23}\\ l_{31} & l_{32} & l_{33}-\mu\end{vmatrix}=0.$$

† *Vide* Webster, 'Dynamics,' 2nd ed. p. 231.

where the angles α, β, γ may be functions of the parameter θ.

The inductance given by this theorem is directly measurable when there is a physical correspondence between the values of α, β, γ taken and the terminal connexions of the windings. The diameters that can be directly measured depend upon the type of machine considered. For example, when the direction cosines are $\sqrt{\frac{2}{3}} \sin \theta_i$

Fig. 1.

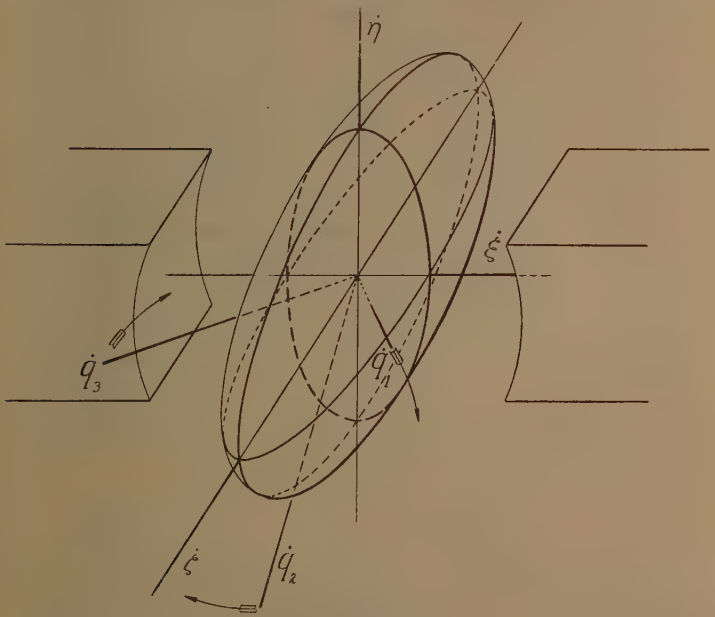

$\sqrt{\frac{2}{3}} \cos \theta_i$, $\sqrt{\frac{1}{3}}$ the corresponding value of l is the self-inductance of the ith armature winding as directly measured at the terminals of a slip-ring machine ; on the other hand, $l_{0,\pi/2,\pi/2}$, $l_{\pi/2,0,\pi/2}$, and $l_{\pi/2,\pi/2,0}$, the principal radii of the ellipsoid, are not directly measurable in the case of such a machine. In the case of a 4-brush commutator machine having an infinite number of independent windings the converse is true at least for $l_{0,\pi/2,\pi/2}$ and $l_{\pi/2,0,\pi/2}$. As such a machine is connected by a Park-Blondel transformation with a three-phase star-connected alternator in which no zero phase-sequent impressed e.m.f. can exist

(as appears from the transformation undergone by the activity function), no corresponding measuring e.m.f. can be applied to the machine to measure $l_{\tau,2,\pi,2,0}$ directly. Although no constraint is implied by the absence of the zero phase-sequent e.m.f. in the slip-ring counterpart of the machine, the behaviour of the machine, since ζ is obviously a normal and isolated coordinate (*i. e.*, does not appear in any cross-product term either in the kinetic energy or in the dissipation function), is essentially identical with that of the three-phase star-connected alternator with the star-point floating.

In contrast to the commutator machine of the foregoing paragraphs, which, to be connected with the star-connected alternator by a Park-Blondel transformation, must have an infinite number of independent internal armature conductors, all (or almost* all) actual commutator machines have continuous armature windings to which the commutator segments are connected at intervals. The internal armature conductors between pairs of commutator segments over-lap to a greater or lesser degree, and between each opposite segment there are always two circuits whose self-inductances are identical, and whose inductances mutual to the field winding are the same.

The kinetic energy function for any three-phase slip-ring machine, either star-connected or delta-connected, will contain terms of the following form :

$$T_a=\tfrac{1}{2}\Sigma\,\Sigma l_{ij}\dot{q}_i\dot{q}_j+\Sigma M_j(\theta)I\dot{q}_j+\tfrac{1}{2}LI^2, \quad . \quad . \quad . \quad (7)$$

where I is the field current and where $M_j=M_0\sin\theta_j$ is the inductance mutual to the field winding and the jth armature current, and where $\dot{q}_j$ is the current flowing in the jth ($j=1, 2, 3$) winding. (The absence of amortisseur circuits is assumed for simplicity.)

In the case of the delta-connected alternator the line currents i_k are connected with the $\dot{q}$'s by the Kirchhoff equations

$$\left.\begin{aligned} i_1&=\dot{q}_2-\dot{q}_3,\\ i_2&=\dot{q}_3-\dot{q}_1,\\ i_3&=\dot{q}_1-\dot{q}_2,\end{aligned}\right\} \quad . \quad . \quad . \quad . \quad . \quad . \quad . \quad (8)$$

* The Thomson-Houston "Spherical-Armature" machine (*circa* 1880) is an exception, for example ; an ingenious three-phase air-blast pump with nozzles at each of the three commutator segments to prevent arcing was integral with this machine.

The line conductors (feeders) have resistance r_f (including the resistance of the brushes and commutator segments) and inductance l_f, so that the total kinetic energy of the system is

$$T=T_a+\tfrac{1}{2}l_f(i_1^2+i_2^2+i_3^2)+\tfrac{1}{2}\Theta\dot{\theta}^2, \quad . \quad . \quad . \quad (9)$$

where Θ is the moment of inertia of the rotor. The corresponding dissipation function is

$$S=\tfrac{1}{2}r\Sigma\dot{q}_k^2+\tfrac{1}{2}r_f\Sigma i_k^2+\tfrac{1}{2}RI^2+\tfrac{1}{2}s\theta^2 \quad . \quad . \quad . \quad (10)$$

and the activity * function, assuming that the machine is operating as a motor, is

$$U=e_k i_k+EI-f\dot{\theta}+N, \quad . \quad . \quad . \quad . \quad (11)$$

where N is a null-function given by the equation

$$-N=\lambda_1(i_1-\dot{q}_2+\dot{q}_3)+\lambda_2(i_2-\dot{q}_3+\dot{q}_1)+\lambda_3(i_3-\dot{q}_1+\dot{q}_2), \quad (12)$$

where the λ's are Lagrangean multipliers corresponding to the equations of constraint (8).

The equations of motion are given by the formula

$$\frac{\partial(U-S)}{\partial\dot{x}}=\frac{d}{dt}\left(\frac{\partial T}{\partial\dot{x}}\right)-\frac{\partial T}{\partial x}, \quad . \quad . \quad . \quad (13)$$

where x stands for each coordinate in (9) in succession, and are

$$\left.\begin{aligned}\lambda_3-\lambda_2&=r\dot{q}_1+\frac{d}{dt}\left(\frac{\partial T_a}{\partial\dot{q}_1}\right),\\ \lambda_1-\lambda_3&=r\dot{q}_2+\frac{d}{dt}\left(\frac{\partial T_a}{\partial\dot{q}_2}\right),\\ \lambda_2-\lambda_1&=r\dot{q}_3+\frac{d}{dt}\left(\frac{\partial T_a}{\partial\dot{q}_3}\right);\end{aligned}\right\} \quad . \quad . \quad . \quad (14\,a)$$

$$e_k-\lambda_k=r_f i_k+l_f\frac{di_k}{dt}; \quad . \quad . \quad . \quad . \quad . \quad (14\,b)$$

$$\left.\begin{aligned}E&=RI+\frac{d}{dt}\left(\frac{\partial T}{\partial I}\right),\\ -f&=s\dot{\theta}+\Theta\ddot{\theta}-\frac{\partial T}{\partial\theta};\end{aligned}\right\} \quad . \quad . \quad . \quad . \quad (14\,c)$$

* I have defined the *activity function* as the algebraic sum of the products of all external forces acting on the system multiplied by their corresponding velocities (Journ. Franklin Inst. ccx. p. 330 (1930). The formula $f_i=\partial U/\partial\dot{x}_i$ is easily establishable by recourse to the principle of virtual work.

where the λ's are potentials with respect to the common point (ground) of the system from which the e.m.f.'s appear as potentials, and are the voltages to ground of the points where the armature winding is tapped.

Substituting the q's given by (14) into (7), (10), and (12) yields, respectively,

$$\mathrm{T}_a=\tfrac{1}{2}(l^*+\tfrac{3}{2}l_\mu)\dot{\xi}^2+\tfrac{1}{2}(l^*-\tfrac{3}{2}l_\mu)\dot{\eta}^2 +\tfrac{1}{2}(l^*-3l_m)\dot{\zeta}^2+\mathrm{M}_0\mathrm{I}\dot{\xi}+\tfrac{1}{2}\mathrm{LI}^2, \quad . \quad . \quad (15)$$

$$\mathrm{S}=\tfrac{1}{2}r(\dot{\xi}^2+\dot{\eta}^2+\dot{\zeta}^2)+\tfrac{1}{2}r_f\Sigma i^2+\tfrac{1}{2}\mathrm{RI}^2+\tfrac{1}{2}s\dot{\theta}^2, \quad . \quad . \quad . \quad (16)$$

$$-\mathrm{N}=\Sigma\lambda_k i_k+\sqrt{2}\Sigma\lambda_k\cos\theta_k\dot{\xi}-\sqrt{2}\Sigma\lambda_k\sin\theta_k\dot{\eta}. \quad . \quad . \quad . \quad (17)$$

Instead of (14 *a*), since the coordinates are quasi-coordinates, there results

$$\left.\begin{aligned} -\sqrt{2}\Sigma\lambda_k\cos\theta_k&=r\dot{\xi}+\frac{d}{dt}\left(\frac{\partial \mathrm{T}_a}{\partial\dot{\xi}}\right)-\dot{\theta}\frac{\partial \mathrm{T}_a}{\partial\dot{\eta}},\\ \sqrt{2}\Sigma\lambda_k\sin\theta_k&=r\dot{\eta}+\frac{d}{dt}\left(\frac{\partial \mathrm{T}_a}{\partial\dot{\eta}}\right)+\dot{\theta}\frac{\partial \mathrm{T}_a}{\partial\dot{\xi}},\\ 0&=r\dot{\zeta}+\frac{d}{dt}\left(\frac{\partial \mathrm{T}_a}{\partial\dot{\zeta}}\right), \end{aligned}\right\} \quad . \quad (18)$$

equations which, together with (8), (14 *b*), and (14 *c*), are the equations of motion of the delta-connected alternator in terms of the Park-Blondel coordinates.

The equations of constraint take the form

$$-i_k=\sqrt{2}\dot{\xi}\cos\theta_k-\sqrt{2}\dot{\eta}\sin\theta_k. \quad . \quad . \quad . \quad (19)$$

The eleven unknowns λ_k, i_k, $\dot{\xi}$, $\dot{\eta}$, $\dot{\zeta}$, I, and θ are given by the eleven equations (18), (14 *b*), (14 *c*), and (19). These general equations (their form is preserved when the different armature windings and the mains are non-symmetrical in the inductances and resistances) may be simplified without difficulty by elimination of the Lagrangean multipliers, and the i_k's when the three phases are symmetrical. Thus, adding the equations (14 *a*), it is found that there results

$$0=r\Sigma\dot{q}_k+l^*\Sigma\ddot{q}_k, \quad . \quad . \quad . \quad . \quad . \quad (20)$$

an equation which leads to the assumption that $\Sigma\dot{q}_k=0$. Whence, from (14 *a*) and (14 *b*), there results the equations for the symmetrical machine,

$$\left.\begin{aligned} e_3-e_2&=(r+3r_f)\dot{q}_1+3l_f\ddot{q}_1+\frac{d}{dt}\left(\frac{\partial T_a}{\partial \dot{q}_1}\right),\\ e_1-e_3&=(r+3r_f)\dot{q}_2+3l_f\ddot{q}_2+\frac{d}{dt}\left(\frac{\partial T_a}{\partial \dot{q}_2}\right),\\ e_2-e_1&=(r+3r_f)\dot{q}_3+3l_f\ddot{q}_3+\frac{d}{dt}\left(\frac{\partial T_a}{\partial \dot{q}_3}\right). \end{aligned}\right\} \quad . \quad (21)$$

The corresponding equations in the Park-Blondel coordinates, still for the symmetrical system, are obtained with the use of (14 *b*) and (19) and are,

$$\left.\begin{aligned} -\sqrt{2}e_k\cos\theta_k&=(r+3r_f)\dot{\xi}+\frac{d}{dt}\left(\frac{\partial T}{\partial \dot{\xi}}\right)-\dot{\theta}\frac{\partial T}{\partial \dot{\eta}},\\ \sqrt{2}e_k\sin\theta_k&=(r+3r_f)\dot{\eta}+\frac{d}{dt}\left(\frac{\partial T}{\partial \dot{\eta}}\right)+\dot{\theta}\frac{\partial T}{\partial \dot{\xi}}. \end{aligned}\right\} \quad . \quad (22)$$

Here T contains the term $\frac{3}{2}l_f(\dot{\xi}^2+\dot{\eta}^2)$ instead of the term $\frac{1}{2}l_f\Sigma\dot{i}^2$.

The Lagrangean multipliers are less easy to eliminate when the machine or its mains are non-symmetrical. Short-circuit problems and stability criteria * then involve the $\delta\lambda_k$'s and the δi_k's as unknowns, as well as the usual variational variables.

The right-hand sides of (18) may be interpreted as appertaining to a 4-brush commutator machine where the coordinates ξ and η are physical. For such a machine, the armature equations take the form

$$\left.\begin{aligned} \kappa_d&=r\dot{\xi}+\frac{d}{dt}\left(\frac{\partial T_a}{\partial \dot{\xi}}\right)-\dot{\theta}\frac{\partial T_a}{\partial \dot{\eta}},\\ \kappa_t&=r\dot{\eta}+\frac{d}{dt}\left(\frac{\partial T_a}{\partial \dot{\eta}}\right)+\dot{\theta}\frac{\partial T_a}{\partial \dot{\xi}}, \end{aligned}\right\} \quad . \quad . \quad . \quad (23\,a)$$

where κ_d and κ_t are new Lagrangean multipliers which also appear in the equations for the feeder-circuits

$$\left.\begin{aligned} e_d-\kappa_d&=r_d\dot{\xi}+l_d\ddot{\xi},\\ e_t-\kappa_t&=r_t\dot{\eta}+l_t\ddot{\eta}. \end{aligned}\right\} \quad . \quad . \quad . \quad (23\,b)$$

* Blondel's important paper (*Rev. Gén. de l'Electricité*, xiii. pp. 339, 389 (1923) on the stability of the synchronous machine showed that variational equations of motion can be obtained with constant coefficients when the the machine is symmetric by the use of the quasi-coordinates ; the situation, however, does not seem to be a general one.

It is to be noted that two of the principal semi-axes of the ellipsoid may be directly measured for such a machine. Conversely, the equations (23 *a*), (23 *b*) may be transformed to true coordinates by means of (3) and (13) after writing down the kinetic energy and dissipation and activity functions in terms of the physical coordinates, forces, and Lagrangean multipliers κ.

When the brush-pairs are not perpendicular, or are moving, the transformations (3) and (4) have to be slightly modified, as has been noted before *.

The Park-Blondel transformation is not the only one of physical significance connected with the ellipsoid. For example, the 3-brush commutator machine is represented by the transformation

$$\dot{q}_i = \Sigma[\tfrac{1}{3} + \tfrac{2}{3}\cos(\theta_i + \theta_j - \beta)]\dot{u}_j, \quad (i, j = 1, 2, 3). \qquad (25)$$

Fig. 2.

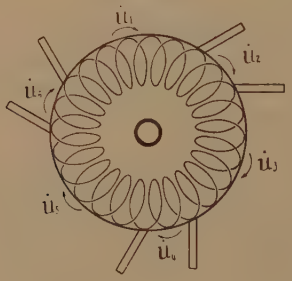

obtained projectively, where the q's are true and the $\dot{u}$'s are quasi-coordinates, $\dot{\theta}$ the angular velocity of the commutator and $\dot{\beta}$ the angular velocity of the brushes. Each coordinate axis for the $\dot{u}$'s is assumed to make the same angle with the ζ-axis, namely, arc cos $\frac{1}{3}\sqrt{3}$. As in the case of the 4-brush machine, the transformed forces and Lagrangean multipliers are obtained with the formula (13) when the physical coordinates are replaced by the true coordinates in the activity function.

The theory may be extended to cases where the number of phases is greater than three ; for example, to the case of fig. 2, where a 6-phase alternator (when the brushes revolve with the commutator) is represented. When there

* Phil. Mag. xvii. p. 848 (1934).

is a difference in the relative velocity of brush and commutator segment, the physical coordinates are given by the equations

$$\left.\begin{aligned} i_{u_{2i-1}} &= \Sigma[\tfrac{2}{3}\cos(\theta-\beta-(i-j)2\pi/3)+\tfrac{1}{3}]\dot{q}_{2i-1}, \\ i_{u_{2i}} &= \Sigma[\tfrac{2}{3}\cos(\theta-\beta-(i-j)2\pi/3)+\tfrac{1}{3}]\dot{q}_{2i}, \end{aligned}\right\}$$

the derivation of which is rather long but not difficult and is connected with the geometry of the associated inertial hyperellipsoid. The equations of motion may be obtained with a formula given by Whittaker * when the dissipation and the constraining forces are taken into account.

This 6-phase alternator, it may be added, goes over into an 8-brush commutator machine under a transformation of the Park-Blondel type with two, as compared with one for the symmetric three-phase alternator, isolated variables. That is, there are two circuits of ζ-type in which no external forces ever appear, and which are not coupled with the active circuits of the machine.

When the brushes of a 4-brush commutator machine have individual active or inactive external connections to ground it is no longer possible to regard the machine as a transform of a three-phase machine. When the brushes rotate with their commutator, there results, obviously, a four-phase slip-ring machine with true coordinates; the quasi-coordinates of the commutator machine are obtained from the true coordinates by a rotation of the coordinate system about a 2-flat perpendicular to the plane of the polar and inter-polar axes †.

It may be stated as a general principle that the true, Park-Blondel and 3-brush coordinates are merely the simpler and more symmetrical examples of an infinite class of possible physical coordinates for machines with the same available number of degrees of freedom and which may be represented by the same slip-ring machine. Given the number of brushes, their spacing, their angular velocity with respect to the commutator, and the angular velocity of the rotor, it becomes merely a problem in the analytics of an ellipsoid to determine the relation between the physical coordinates and the true or any other com-

* Whittaker, 'Dynamics,' 3rd ed. p. 43.

† For the kinematics of such rotations in n-space see Camille Jordan, Bull. Soc. Math. de France, iii. p. 152.

plete system of coordinates. As examples of this procedure it has been shown that the 4-brush (including, of course, the 2-brush) commutator machine with two (or one) external brush circuits and the 3-brush commutator machine have each a dynamically equivalent delta-connected slip-ring representative.

XXV. *Bessel Product Functions.* *By* J. C. Costello *.

§ 1.

DUE to the frequent occurrence of Bessel functions of zero order and semi-imaginary argument in physical problems the combinations of the real and imaginary parts which usually present themselves in numerical work have received considerable attention, being treated as separate functions styled Bessel Product Functions [1], [2]. In particular they have been thoroughly considered and extensively tabulated in the B. A. Report, 1916 [2], [3], [4].

The corresponding functions of order n do not, however, appear to have been investigated, and, as these are of importance in a number of problems treated in recent years [5], [6], [7], [8], etc., they are here briefly considered, primarily with a view to the reduction of labour in future applications.

§ 2. *Solution of Bessel's Equation of Order n and Argument* $xi\sqrt{i}$.

In the case of the functions of zero order the solution has been standardized as

$$y = \mathrm{A}(\mathrm{ber}\, x + i\,\mathrm{bei}\, x) + \mathrm{B}(\ker x + \mathrm{i}\,\mathrm{kei}\, x),$$

where

$$\mathrm{ber}\, x + i\,\mathrm{bei}\, x = \mathrm{J}_0(xi\sqrt{i}) = \mathrm{I}_0(x\sqrt{i})$$

$$= \sum_0^\infty (-1)^r \frac{(x/2)^{4r}}{(2r)!\,(2r)!} + i \sum_0^\infty (-1)^r \frac{(x/2)^{4r+2}}{(2r+1)!\,(2r+1)!},$$

$$\ker x + i\,\mathrm{kei}\, x = \mathrm{G}_0(xi\sqrt{i}) = \mathrm{K}_0(x\sqrt{i})$$

$$= \left(\log \frac{2}{x} - \gamma\right) \mathrm{ber}\, x + \frac{\pi}{4}\,\mathrm{bei}\, x$$

* Communicated by the Author.

$$+\sum_1^\infty (-1)^r \frac{(x/2)^{4r}}{(2r)!\,(2r)!}\left(1+\frac{1}{2}+\cdots\frac{1}{2r}\right)$$

$$+i\left\{\left(\log\frac{2}{x}-\gamma\right)\operatorname{bei} x-\frac{\pi}{4}\operatorname{ber} x\right.$$

$$\left.-\sum_1^\infty (-1)^r \frac{(x/2)^{4r+2}}{(2r+1)!\,(2r+1)!}\left(1+\frac{1}{2}+\cdots\frac{1}{2r+1}\right)\right\}.$$

In the case of the functions of orders higher than zero the solution has not been definitely standardized. Whitehead [9] has taken as the solution

$$y=\mathrm{AJ}_n(xi\sqrt{i})+\mathrm{BH}_n(xi\sqrt{i}),$$

but the forms

$$y=\mathrm{CJ}_n(xi\sqrt{i})+\mathrm{DG}_n(xi\sqrt{i})$$

or

$$y=\mathrm{EI}_n(x\sqrt{i})+\mathrm{FK}_n(x\sqrt{i})$$

appear to have been those used in actual applications. The second of these three has been the most widely used, and the real and imaginary parts to this have been termed by McLachlan [10] ber_n, bei_n, ker_n, kei_n, giving

$$\mathrm{ber}_n x+i\,\mathrm{bei}_n x=\mathrm{J}_n(xi\sqrt{i})=i^n\mathrm{I}_n(x\sqrt{i})$$

$$=\left\{\sum_0^\infty (-1)^r \frac{(x/2)^{n+2r}}{r!\,(n+r)!}\cos\tfrac{3}{4}(n+2r)\pi\right\}$$

$$+i\left\{\sum_0^\infty (-1)^r \frac{(x/2)^{n+2r+2}}{r!\,(n+r)!}\sin\tfrac{3}{4}(n+2r)\pi\right\}$$

$$\mathrm{ker}_n x+i\,\mathrm{kei}_n x=\mathrm{G}_n(xi\sqrt{i})=i^n\mathrm{K}_n(x\sqrt{i})$$

$$=\left\{\left(\log\frac{2}{x}-\gamma\right)\mathrm{ber}_n x+\frac{\pi}{4}\mathrm{bei}_n x\right.$$

$$+\frac{1}{2}\sum_0^{n-1}(-1)^r\frac{(n-r-1)!}{r!}\left(\frac{2}{x}\right)^{n-2r}\cos\tfrac{3}{4}(n+2r)\pi$$

$$+\frac{1}{2}\sum_0^\infty (-1)^r\frac{(x/2)^{n+2r}}{r!\,(n+r)!}$$

$$\left.\times\left(1+\frac{1}{2}+\cdots\frac{1}{r}+1+\frac{1}{2}+\cdots\frac{1}{n+r}\right)\cos\tfrac{3}{4}(n+2r)\pi\right.$$

$$+i\left\{\left(\log\frac{2}{x}-\gamma\right)\mathrm{bei}_n x-\frac{\pi}{4}\mathrm{ber}_n x\right.$$

$$+\frac{1}{2}\sum_{0}^{n-1}(-1)^r\frac{(n-r-1)!}{r!}\left(\frac{2}{x}\right)^{n-2r}\sin\tfrac{3}{4}(n+2r)\pi$$

$$-\frac{1}{2}\sum_{0}^{\infty}(-1)^r\frac{(x/2)^{n+2r}}{r!\,(n+r)!}$$

$$\times\left(1+\frac{1}{2}+\ldots\frac{1}{r}+1+\frac{1}{2}+\ldots\frac{1}{n+r}\right)$$

$$\times\sin\tfrac{3}{4}(n+2r)\pi\Big\}.$$

It would have been more logical to adopt as the first and second solutions the modified functions

$$i^{-\frac{3n}{2}}J_n(xi\sqrt{i}) \quad \text{and} \quad i^{\frac{3n}{2}}G_n(xi\sqrt{i}),$$

when the resulting expressions for the real and imaginary parts would have been identical in form with the ber, bei, ker, kei functions, and so more reasonably denoted by the terms ber_n, bei_n, etc. In addition they would be considerably simpler and more compact—*e. g.*, for $\mathrm{ber}_n x$ we should have

$$\mathrm{ber}_n x=\sum_{0}^{\infty}(-1)^r\frac{(x/2)^{n+4r}}{(2r)!\,(n+2r)!}$$

instead of

$$\mathrm{ber}_n x=\cos\frac{3n\pi}{4}\sum_{0}^{\infty}(-1)^r\frac{(x/2)^{n+4r}}{(2r)!\,(n+2r)!}$$

$$-\sin\frac{3n\pi}{4}\sum_{0}^{\infty}(-1)^r\frac{(x/2)^{n+4r+2}}{(2r+1)!\,(n+2r+1)!}$$

(as obtained on expanding the trigonometric term above). However, there is probably little prospect of obtaining the standardization of this form, and as the values of the product functions are the same whether the modified or unmodified functions be used, the matter need not further concern us here.

§ 3. *Definitions of Product Functions.*

The functions of the *first kind* are:

$$\mathrm{X}_n^{(b)}(x)=\mathrm{ber}_n{}^2 x+\mathrm{bei}_n{}^2 x=\mathrm{J}_n.\mathrm{conj}\,\mathrm{J}_n,$$

$$\mathrm{V}_n^{(b)}(x)=\mathrm{ber}_n{}'^2 x+\mathrm{bei}_n{}'^2 x=\mathrm{J}_n'.\mathrm{conj}\,\mathrm{J}_n',$$

$$Z_n^{(b)}(x) = \mathrm{ber}_n x\, \mathrm{ber}_n' x + \mathrm{bei}_n x\, \mathrm{bei}_n' x$$
$$= \tfrac{1}{2}(J_n'.\mathrm{conj}\, J_n + J_n.\mathrm{conj}\, J_n')$$
$$W_n^{(b)}(x) = \mathrm{ber}_n x\, \mathrm{bei}_n' x - \mathrm{bei}_n x\, \mathrm{ber}_n' x$$
$$= \frac{1}{2i}(J_n'.\mathrm{conj}\, J_n - J_n.\mathrm{conj}\, J_n').$$

The functions of the *second kind* are :

$$X_n^{(k)}(x) = \mathrm{ker}_n^2 x + \mathrm{kei}_n^2 x = G_n.\mathrm{conj}\, G_n,$$
$$V_n^{(k)}(x) = \mathrm{ker}_n'^2 x + \mathrm{kei}_n'^2 x = G_n'.\mathrm{conj}\, G_n',$$
$$Z_n^{(k)}(x) = \mathrm{ker}_n x\, \mathrm{ker}_n' x + \mathrm{kei}_n x\, \mathrm{kei}_n' x$$
$$= \tfrac{1}{2}(G_n'.\mathrm{conj}\, G_n + G_n.\mathrm{conj}\, G_n'),$$
$$W_n^{(k)}(x) = \mathrm{ker}_n x\, \mathrm{kei}_n' - \mathrm{kei}_n x\, \mathrm{ker}_n' x$$
$$= \frac{1}{2i}(G_n'.\mathrm{conj}\, G_n - G_n.\mathrm{conj}\, G_n').$$

The *mixed kind* functions are :

$$\left.\begin{aligned} X_n^{(r)}(x) &= \mathrm{ber}_n x\, \mathrm{ker}_n x + \mathrm{bei}_n x\, \mathrm{kei}_n x \\ X_n^{(u)}(x) &= \mathrm{bei}_n x\, \mathrm{ker}_n x - \mathrm{ber}_n x\, \mathrm{kei}_n x \end{aligned}\right\} X_n^{(r)}(x) + iX_n^{(u)}(x)$$
$$= J_n.\mathrm{conj}\, G_n,$$
$$\left.\begin{aligned} V_n^{(r)}(x) &= \mathrm{ber}_n' x\, \mathrm{ker}_n' x + \mathrm{bei}_n' x\, \mathrm{kei}_n' x \\ V_n^{(u)}(x) &= \mathrm{bei}' x\, \mathrm{ker}_n' x - \mathrm{ber}_n' x\, \mathrm{kei}_n' x \end{aligned}\right\} V_n^{(r)}(x) + iV_n^{(u)}(x)$$
$$= J_n'.\mathrm{conj}\, G_n',$$
$$\left.\begin{aligned} Z_n^{(r)}(x) &= \tfrac{1}{2}(\mathrm{ber}_n\, \mathrm{ker}_n' + \mathrm{ber}_n'\, \mathrm{ker}_n + \mathrm{bei}_n\, \mathrm{kei}_n' + \mathrm{bei}_n'\, \mathrm{kei}_n) \\ Z_n^{(u)}(x) &= \frac{1}{2i}(\mathrm{bei}_n \mathrm{ker}_n' + \mathrm{bei}_n'\, \mathrm{ker}_n - \mathrm{ber}_n\, \mathrm{kei}_n' - \mathrm{ber}_n' \mathrm{kei}_n) \end{aligned}\right\}$$
$$Z_n^{(r)}(x) + iZ_n^{(u)}(x) = \tfrac{1}{2}(J_n'.\mathrm{conj}\, G_n + J_n.\mathrm{conj}\, G_n'),$$
$$\left.\begin{aligned} W_n^{(r)}(x) &= \tfrac{1}{2}(\mathrm{ber}_n\, \mathrm{kei}_n' + \mathrm{bei}_n'\, \mathrm{ker}_n - \mathrm{bei}_n \mathrm{ker}_n' - \mathrm{ber}_n'\, \mathrm{kei}_n) \\ W_n^{(u)}(x) &= \tfrac{1}{2}(\mathrm{ber}_n \mathrm{ker}_n' + \mathrm{bei}_n'\, \mathrm{kei}_n - \mathrm{bei}_n'\, \mathrm{kei}_n - \mathrm{ber}_n'\, \mathrm{ker}_n) \end{aligned}\right\}$$
$$W_n^{(r)}(x) + iW_n^{(u)}(x) = \frac{1}{2i}(J_n'.\mathrm{conj}\, G_n - J_n.\mathrm{conj}\, G_n').$$

In the above the argument $xi\sqrt{i}$ is to be understood for J_n, G_n, the dash $'$ denotes differentiation with regard to x,

and the prefix conj denotes the conjugate of the function to which it is prefixed.

§4. *Recurrence Formulæ satisfied by the Product Functions.*

By means of the Bessel function recurrence formulæ it may be shown that the following recurrence formulæ are satisfied by the product functions. (In this and subsequent sections where the distinguishing bracketed index is omitted the functions X_n, V_n, Z_n, W_n may be of any of the four kinds, provided of course that in any one equation the functions are all of the same kind.)

$$W_{n-1}+W_{n+1}=2Z_n,$$

$$X_{n-1}+X_{n+1}=2V_n,$$

$$Z_{n-1}+Z_{n+1}=2W_n-\frac{2}{x}V_n+\frac{4n^2}{x^2}Z_n,$$

$$V_{n-1}+V_{n+1}=2X_n-\frac{4}{x}W_n+\frac{4(n^2+1)}{x^2}V_n-\frac{16n^2}{x^3}Z_n.$$

We have also :

$$W_{n-1}-W_{n+1}=\frac{2n}{x}X_n,$$

$$X_{n-1}-X_{n+1}=\frac{4n}{x}Z_n,$$

$$Z_{n-1}-Z_{n+1}=\frac{2n}{x}V_n-\frac{4n}{x^2}Z_n,$$

$$V_{n-1}-V_{n+1}=\frac{4n}{x}W_n-\frac{8n}{x^2}V_n+\frac{8n(n^2+1)}{x^3}Z_n.$$

From these by subtraction we obtain

$$W_{n+1}=Z_n-\frac{n}{x}X_n,$$

$$X_{n+1}=V_n-\frac{2n}{x}Z_n,$$

$$Z_{n+1}=W_n-\frac{(n+1)}{x}V_n+\frac{2n(n+1)}{x^2}Z_n,$$

$$V_{n+1}=X_n-\frac{2(n+1)}{x^2}W_n+\frac{2(n+1)^2}{x}V_n-\frac{4n(n+1)^2}{x^3}Z_n.$$

Similarly, by addition, formulæ giving functions of the $(n-1)$th order in terms of those of the nth order are obtained, and by repeated substitution formulæ giving the functions of the $(n\pm r)$th order in terms of the nth order may be obtained.

§ 5. *Relations among Derivatives of Product Functions.*

Using the properties of the parent functions the first derivatives of the product functions are readily obtained. They are

$$W_n'=X_n-\frac{1}{x}W_n, \quad X_n'=2Z_n,$$

$$Z_n'=V_n-\frac{1}{x}Z_n, \quad V_n'=2W_n-\frac{2}{x}V_n+\frac{4n^2}{x^2}Z_n.$$

By repeated differentiation (multiplying across each time by x) the following relations among the derivatives of higher orders are obtained :—

$$W_n^N+\frac{N}{x}W_n^{N-1}=X_n^{N-1}+\frac{N-1}{x}X_n^{N-2}, \quad X_n^N=2Z_n^{N-1},$$

$$Z_n^N+\frac{N}{x}Z_n^{N-1}=V_n^{N-1}+\frac{N-1}{x}V_n^{N-2},$$

$$V_n^N+\frac{2N}{x}V_n^{N-1}+\frac{N(N-1)}{x^2}V_n^{N-2}$$

$$=2W^{N-1}+4\frac{(N-1)}{x}W^{N-2}$$

$$+2\frac{(N-1)(N-2)}{x^2}W^{N-3}+\frac{4n^2}{x^2}Z_{n-1}.$$

The cyclic nature of these relations, and, indeed, of the functions in general, is apparent, and renders elimination a comparatively simple process (§ 6).

§ 6. *Differential Equations satisfied by the Product Functions.*

From the relations of the preceding section it is evident that the functions W_n, X_n, Z_n are solutions of linear differential equations and that these equations are of the fourth order. The relation in the case of V_n^N being non-

linear, except when $n=0$, when it becomes so, the equation solved by V_n is linear only when $n=0$, being in general an integro-differential equation, of a type however which is very simple.

Eliminating W_n, Z_n, V_n and their derivatives between successive derivates of W_n (each expressed in terms of Z_n and its derivates only), we obtain:

$$x^4W_n^{IV}+4x^3W^{III}-(4n^2-1)x^2W_n^{II}-(4n^2-1)xW_n^{I}+W\{(4n^2-1)-4x^4\}=0.$$

Proceeding similarly in the case of X_n (the derivates being expressed in terms of V_n and its derivates only), we obtain:

$$x^4X_n^{IV}+4x^3X_n^{III}-(4n^2-1)x^2X_n^{II}+(4n^2-1)xX_n^{I}-4x^4X=0.$$

The equations for Z_n and V_n may be similarly obtained by eliminating W_n, X_n, and their derivatives (1st and 2nd) after expressing Z_n, V_n...Z^{IV}, V^{IV} in terms of W...W^{II} and $X-X^{II}$ respectively, but they may be more conveniently obtained by making use of the differential equations already obtained for W_n, X_n, and the first two recurrence formulæ. The equations are:

$$x^4Z_n^{IV}+4x^3Z_n^{III}-(4n^2+3)x^2Z_n^{II}+(12n^2-3)xZ_n^{I}-Z\{(12n^2-3)+4x^4\}=0,$$

$$x^4V_n^{IV}+4x^3V_n^{III}-(4n^2+3)x^2V_n^{II}+(20n^2+3)xV_n^{I}-V(64n^2+4x^4)+\frac{128n^2}{x^2}\int xV_n dx=0.$$

§ 7. *Ascending Power Series.*

By solution in series of the foregoing equations ascending power series convergent for all values of x are obtained. Each equation has four independent solutions, viz., the functions of the first kind, second kind, and mixed (real and unreal) kinds. The various solutions are distinguished by comparison with the expressions obtained by multiplying out the first few terms of the ber_n etc. functions. Obtaining the entire series by direct multiplication would be, however, much more laborious than solving the equations.

In the case of the functions of the *first kind* simple series very suitable for computation are obtained :

$$W_n^{(b)}(x) = \sum_0^\infty \frac{(x/2)^{2n+4r+1}}{r!\ (n+r)!\ (n+2r+1)!},$$

$$X_n^{(b)}(x) = \sum_0^\infty \frac{(x/2)^{2n+4r}}{r!\ (n+r)!\ (n+2r)!},$$

$$Z_n^{(b)}(x) = \sum_0^\infty \frac{(x/2)^{2n+4r-1}}{r!\ (n+r)!\ (n+2r-1)!},$$

$$V_n^{(b)}(x) = \sum_0^\infty \frac{(n+2r)(x/2)^{2n+4r-2}}{r!\ (n+r)!\ (n+2r-1)!}.$$

In the the case of the functions of the *second* and *mixed* kinds the series are, however, relatively cumbersome and difficult of computation. The values for order zero have, however, been tabulated for the functions of the second kind $W_0^{(k)}$, $X_0^{(k)}$, $V_0^{(k)}$, $Z_0^{(k)}$, and for the functions $V_0^{(r)}$, $V^{(u)}$, and the series for these and for the remaining mixed kind functions given. [Ref. 2. Values for $x=0$ to $x=10$, with interval 0·2. Six significant figures.]

For the range of orders likely to be required in any practical application it is much easier to compute from these zero order functions, using the recurrence formulæ of § 5, and it does not seem necessary therefore to devote space to the series for these functions. (For large values of the argument the simple asymptotic formulæ of the next section may, however, be advantageously applied.)

§ 8. *Descending Power Series (Asymptotic).*

From the well-known asymptotic expansion for $J_n(x)$, or by direct solution in series of Bessel's equation with the substitution $y=\exp(\int u\,dx)$, asymptotic series for $\mathrm{ber}_n x$, $\mathrm{bei}_n x$ are obtained (much more easily by the latter method).

$$\mathrm{ber}_n x = \frac{\epsilon^{\alpha_n}}{\sqrt{(2\pi x)}}\cos\beta_n, \quad \mathrm{bei}_n x = \frac{\epsilon^{\alpha_n}}{\sqrt{(2\pi x)}}\sin\beta_n,$$

where

$$\alpha_n = \frac{x}{\sqrt{2}} - \frac{(4n^2-1)}{8\sqrt{2}x} - \frac{(16n^4-104n^2+25)}{384\sqrt{2}x^3}$$

$$- \frac{(16n^4-56n^2+13)}{128x^4} + \frac{(64n^6-1840n^4+4748n^2-1073)}{5120\sqrt{2}x^5} \cdots,$$

$$*\beta_n = \frac{x}{\sqrt{2}} + \frac{(6n-1)\pi}{8} + \frac{(4n^2-1)}{8\sqrt{2}x} + \frac{(4n^2-1)}{16x^2}$$

$$- \frac{(16n^4-104n^2+25)}{384\sqrt{2}x^3} - \frac{(64n^6-1840n^4+4748n^2-1073)}{5120\sqrt{2}x^5} \cdots$$

From these the expansions of the product functions of the first kind are readily obtained. They are:

$$X_n^{(b)}(x) = \frac{\epsilon^{2\alpha_n}}{2\pi x}, \quad W_n^{(b)}(x) = \frac{\epsilon^{2\omega_n}}{2\sqrt{2.\pi x}},$$

$$Z_n^{(b)}(x) = \frac{\epsilon^{2\zeta_n}}{2\sqrt{2.\pi x}}, \quad V_n^{(b)}(x) = \frac{\epsilon^{2\eta_n}}{2\pi x},$$

where α_n is as given above, and

$$\omega_n = \frac{x}{\sqrt{2}} - \frac{(4n^2-1)}{8\sqrt{2}x} + \frac{(4n^2-1)}{16x^2} - \frac{(16n^4+88n^2-23)}{384\sqrt{2}x^3}$$

$$- \frac{(16n^4-8n^2+1)}{128x^4} + \frac{(64n^6-3120n^4+5388n^2-1153)}{5120\sqrt{2}x^5} \cdots,$$

$$\zeta_n = \frac{x}{\sqrt{2}} - \frac{(4n^2+3)}{8\sqrt{2}x} + \frac{(4n^2-3)}{16x^2} - \frac{(16n^4-200n^2+81)}{384\sqrt{2}x^3}$$

$$+ \frac{(16n^2-9)}{128x^4} + \frac{(64n^6+400n^4-5978n^2+1179)}{5120\sqrt{2}x^5} \cdots,$$

$$\eta_n = \frac{x}{\sqrt{2}} - \frac{(4n^2+3)}{8\sqrt{2}x} + \frac{n^2}{2x^2} - \frac{(16n^4+392n^2-63)}{384\sqrt{2}x^3}$$

$$- \frac{(96n^2-27)}{128x^4} + \frac{(64n^6+1680n^4-8532n^2+1899)}{5120\sqrt{2}x^5} \cdots.$$

The expansion of W_n is obtained by making use of $W_n/X_n = \beta_n' \equiv \frac{d}{dx}\left(\arctan\frac{\mathrm{bei}_n}{\mathrm{ber}_n}\right)$. Writing $W_n = \frac{\epsilon^{2\omega}}{2\sqrt{2.\pi x}}$ we have $2(\omega_n - \alpha_n) = \log(\beta_n'\sqrt{2})$, and on expanding the logarithm and adding $2\alpha_n$ we obtain $2\omega_n$.

In the case of Z_n we have $Z_n = \frac{1}{2}X_n'$; also, taking logs. of and differentiating $\epsilon^{2\alpha} = 2\pi x X_n$, we have $Z_n/X_n = \alpha_n' - \frac{1}{2x}$.

* *Note.*—If the modified function $i^{-\frac{3n}{2}} J_n(xi\sqrt{i})$ is used the term $\frac{6n\pi}{8}$ disappears from β_n.

Putting $Z_n = \frac{\epsilon^{2\zeta_n}}{2\pi x}$, and proceeding as for W_n, we get the value of $2\zeta_n$.

In the case of V_n we make use of the relation (§ 5) $V_n = \frac{1}{x}\frac{d}{dx}(xZ_n)$. Hence, putting $V = \frac{\epsilon^{2\eta_n}}{2\pi x}$, we have $2\eta_n = 2\zeta_n + \log(\zeta_n'\sqrt{2})$.

As regards the functions of the *second kind*, since $\ker_n$ and kei_n are given by the series for ber_n bei_n on replacing x by $-x$ and $\sqrt{\frac{1}{2\pi}}$ by $\sqrt{\frac{\pi}{2}}$, it is obvious that $W_n^{(k)}$, $X_n^{(k)}$, $Z_n^{(k)}$, $V_n^{(k)}$ are given by the above series on making the same replacements.

Finally, with regard to the *mixed kind* functions; since the differential equations (§ 6) are unchanged on substituting ix for x (or, of course, $-x$), the same coefficients occur in these functions as in those of the first and second kinds, different powers of x being, however, absent in different functions. The expansions are:

$$X_n^{(r)}(x) = \frac{\epsilon^{A_n}}{2x}\cos B_n, \qquad V_n^{(r)}(x) = \frac{\epsilon^{C_n}}{2x}\cos D_n,$$

$$X_n^{(u)}(x) = \frac{\epsilon^{A_n}}{2x}\sin B_n, \qquad V_n^{(u)}(x) = \frac{\epsilon^{C_n}}{2x}\sin D_n,$$

$$W_n^{(r)}(x) = \frac{\epsilon^{E_n}}{2\sqrt{2}.x}\cos F_n, \qquad Z_n^{(r)}(x) = \frac{\epsilon^{G_n}}{2\sqrt{2}.x}\cos H_n,$$

$$W_n^{(u)}(x) = \frac{\epsilon^{E_n}}{2\sqrt{2}.x}\sin F_n, \qquad Z_n^{(u)}(x) = \frac{\epsilon^{G_n}}{2\sqrt{2}.x}\sin H_n,$$

where

$$A_n = \left\{ -\frac{(16n^4 - 56n^2 + 13)}{64x^4} \cdots \right\},$$

$$B_n = \left\{ x\sqrt{2} + \frac{(4n^2-1)}{4\sqrt{2}x} - \frac{(16n^4 - 104n^2 + 25)}{192\sqrt{2}x^3} - \frac{(64n^6 - 1840n^4 + 4748n^2 - 1073)}{2560\sqrt{2}x^5} \right\},$$

$$C_n = \left\{ -\frac{(96n^2 - 27)}{64x^4} \cdots \right\},$$

$$D_n = \left\{ x\sqrt{2} + \frac{(4n^2+3)}{4\sqrt{2x}} - \frac{(16n^4+392n^2-63)}{192\sqrt{2x^3}} - \frac{(64n^6+1680n^4-8532n^2+1899)}{2560\sqrt{2x^5}} \cdots \right\},$$

$$E_n = \left\{ \frac{(4n^2-1)}{8x^2} - \frac{(16n^4-8n^2+1)}{64x^4} \cdots \right\},$$

$$F_n = \left\{ x\sqrt{2} + \frac{(4n^2-1)}{4\sqrt{2x}} - \frac{(16n^4+88n^2-23)}{192\sqrt{2x^3}} - \frac{(64n^6-3120n^4+5388n^2-1153)}{2560\sqrt{2x^5}} \cdots \right\},$$

$$G_n = \left\{ \frac{(4n^2-3)}{8x^2} + \frac{(16n^2-9)}{64x^4} \cdots \right\},$$

$$H_n = \left\{ x\sqrt{2} + \frac{(4n^2+3)}{4\sqrt{2x}} - \frac{(16n^4-200n^2+81)}{192\sqrt{2x^3}} - \frac{(64n^6+400n^4-5972n^2+1179)}{2560\sqrt{2x^5}} \right\}.$$

References.

(1) A. Russell, 'Alternating Currents,' i. ch. 7 (2nd ed.).
(2) British Association Report, 1916, p. 108.
(3) H. Savidge, "Tables of Ber, Bei, Ker, and Kei Functions," Proc. Phys. Soc. (Nov. 1909).
(4) S. Butterworth, "Evaluation of Ber, Bei, and Allied Functions," Proc. Phys. Soc. (1913).
(5) S. Butterworth, "A. C. Resistance of Short Coils," Trans. Roy. Soc. A, coxxii. p. 57.
(6) J. R. Carson, "Wave Propagation over Parallel Wires," Phil. Mag. xli. p. 607.
(7) G. Mie, "Elektrische Wellen an Zwei Parallelen Drahten," Pog. *Ann.* p. 201 (1900).
(8) S. P. Mead, "Wave Propagation over Parallel Tubular Conductors," Bell Syst. Tech. Jour. p. 325 (1925).
(9) C. S. Whitehead, "On a Generalisation of the Functions Ber, Bei, Ker, and Kei," Quart. Journ. Math. no. 168 (1911).
(10) N. W. McLachlan, 'Bessel Functions for Engineers.'

May 1935.

XXVI. *Notices respecting New Books.*

Elements of Strength of Materials. By Professors S. Timoshenko and G. H. MacCullough. [Pp. v+350.] (Macmillan and Company, Limited. Price 14*s*.)

THIS book embodies in a concise and convenient form the more elementary aspects of the subject that is so fully dealt with in Professor Timoshenko's 'Strength of Materials' (two volumes). The work is designed primarily as a text-book for undergraduate courses in strength of materials in American Colleges and Schools of Engineering.

Considerable attention is devoted to combined stresses, shear, riveted joints, torsion, shearing force, and bending moment for dead and live loads, stresses and deflexions of beams. Both the classical method of successive integration and the area-moment method of determining the deflexion of beams are presented. It is gratifying to note that the authors have included the conjugate beam (or elastic weights) method for solving problems in deflexions, and that Mohr's Theorem is fully discussed in the text. The method of superposition for finding deflexions and statically indeterminate reactions is also given in some detail. Some space is devoted to the determination of tensile and compressive stresses in statically indeterminate structures and to the application of Mohr's circle for solving graphicallly problems relating to combined stresses. In the treatment of columns a complete logical analysis is given, in addition to the usual examination of the more common empirical formulæ. The book concludes with a chapter on the elements of the strain-energy theory, with application to statically indeterminate structures, and a short chapter on the mechanical and physical properties of materials.

The authors have rightly emphasized the importance of fundamental principles in the study of this subject, and have continually indicated the limitations in the applications of the theory and formulæ. Each chapter is accompanied by a good selection of illustrative problems, while at the end of each chapter there are a liberal number of admirable problems. In spite of the fact that the authors have presented the material to conform with American practice and have made no reference to British Standard specifications, the book may be recommended as a first course in Strength of Materials in most Engineering Schools and Universities. The increasing use in recent years of the mathematical theory of elasticity, in contrast with empirical rules, in solving engineering problems and in machine design calculations has created a need for a book of this type, in which a more comprehensive view of the

fundamental concepts and methods of stress analysis is so ably presented.

The Diffraction of Light, X-Rays, and Material Particles. By C. F. Meyer. [Pp. 473+xiv.] (Published by the Cambridge University Press, England, and the University of Chicago Press, U.S.A. Price 22*s.* 6*d.*)

This book has been written and produced in an exceedingly attractive manner. Approximately two-thirds of it is devoted to the diffraction of light, and the remaining third to the diffraction of X-rays and of material particles. The treatment of the optical section is fuller than is usual in books dealing with optics generally; in particular, the methods of mounting gratings and the different kinds of errors which may arise are fully discussed. The explanations given are clear and simple and depend largely on the use of graphical rather than more mathematical methods.

Wherever one opens the book the details are excellent, but certain misgivings arise when one considers it more broadly. Students requiring so extensive a knowledge of diffraction will generally be able to follow more advanced methods of treatment, while more elementary students who will profit by the simple treatment will usually not require such an extensive book. On the other hand, it may well be argued that the student who finds the average book on optics too concise will obtain here a full account which may be of great help to him, and hence the book will probably be a very useful reference work for students.

The book is less satisfactory than it might have been in that insufficient attention is given to many points of similarity between optical and X-ray diffraction; a book which includes both branches of optics could reasonably be expected to give more space to such similarities. In fact one of the great advantages of bringing together these two branches of the subject in a single book is that it enables points of similarity to be adequately dealt with, whereas other books can only mention such matters very briefly. For example, optical diffraction by a slit and X-ray diffraction by an atom have several points of similarity. The Abbe treatment of the theory of the microscope is similar to the application of Fourier analysis to the determination of crystal structures. Lattice distortion in crystals might be correlated with errors in the ruling of a grating. The reviewer thinks that this lack of correlation detracts somewhat from a book which in other ways is really excellent.

[*The Editors do not hold themselves responsible for the views expressed by their correspondents.*]

THE

LONDON, EDINBURGH, AND DUBLIN

PHILOSOPHICAL MAGAZINE

AND

JOURNAL OF SCIENCE.

[SEVENTH SERIES.]

SUPPLEMENT, FEBRUARY 1936.

XXVII. *A Method for determining the Optical Constants of Crystals and Examples of its Application to certain Organic Compounds.*

By R. G. Wood, *M.Sc.*, *and* S. H. Aylieffe, *Ph.D.* *

1. *Introduction.*

In Part I. of this paper is described a method which has been developed for the determination of the optical constants of small crystals by immersion in a suitable liquid. The method has been used with the specially designed microscope stage-goniometer described by the authors in a recent paper [1]. The goniometer is a modified form of one manufactured by Messrs. James Swift and Son, Ltd., and by its use it is possible to ensure that the crystal is accurately orientated with respect to the plane of polarization of the incident light when determining the principal refractive indices.

A large amount of work has been published giving optical data for organic crystals, mostly for purposes of chemical identification. The measurements have either been made on powdered crystals or else the refractive indices determined corresponding to the extinction directions on the most prominent face. Such measurements are sufficient for the purpose in view, and in many

* Communicated by Prof. W. L. Bragg, M.A., F.R.S.

cases the principal refractive indices of the crystal are not given. Examples will be found in a paper by Davies and Hartshorne [2], in which references to earlier work are listed. The object of the present work has been to determine the principal refractive indices (α, β, γ) and the orientation of the indicatrix, in order to supplement the information given by X-rays and assist in elucidating the crystal structure.

In Part II. of the paper are given the results obtained in applying the method to the following organic compounds :—Picryl aniline, picryl *p*-toluidine (yellow and red forms), diphenyl ether, and diphenyl sulphone. The results for picryl aniline and picryl *p*-toluidine form a sequel to the crystallographic and X-ray investigations on these substances recently published by the authors with N. M. Cullinane [3]. The crystallographic measurements on the other two substances are included in the present paper.

Part I.

2. *General Description of Method.*

In the case of a biaxial crystal the fundamental constants to be determined are (i.) the values of the three principal refractive indices, (ii.) the orientation of the indicatrix with respect to the crystallographic axes.

Organic crystals are usually small and often have their faces imperfectly formed, so that it is necessary to use a polarizing microscope for their optical examination and an immersion method for determining their refractive indices. For this purpose it is necessary to orientate the crystal accurately with respect to the axis of the microscope and then immerse it in a liquid whose refractive index can be varied. The Becke line or other test shows in which direction the index of the liquid must be changed in order to attain an exact match with the crystal for the particular direction of vibration of the incident light. When the crystal has been matched the index of the liquid can be measured with a refractometer or by using a comparison crystal as described later (§ 4). By repeating the process for three suitable orientations of the crystal the three principal indices can be determined.

It may happen that the highest index γ is too great to be matched with any convenient liquid. In this

case measurements of α and β and the optic axial angle serve to give γ by calculation from the formula

$$\frac{1}{\gamma^2} = \frac{1}{\beta^2} - \left(\frac{1}{\alpha^2} - \frac{1}{\beta^2}\right)\cot^2 \mathrm{V}. \quad . \quad . \quad . \quad . \quad (1)$$

In this formula V is the angle between the circular section of the indicatrix and the plane containing the axes α and β. If the crystal has positive birefringence V is less than 45°, the γ-axis is the acute bisectrix, and 2V is the acute angle between the optic axes. If the crystal has negative birefringence V is greater than 45°, the γ-axis is the obtuse bisectrix, and 2V is the obtuse angle between the optic axes. In the present paper the optic axial angle is tabulated as the acute angle between the optic axes. The optic axial angle is therefore equal to 2V for a positive crystal and to 180° −2V for a negative crystal.

The derivation of γ from formula (1) will not be very accurate if α and β are nearly equal and the crystal is strongly positive, for in these circumstances the calculated value of γ depends on the accurate determination of the small quantity $\beta - \alpha$. Further, if the liquid corresponding to β has an index too great for measurement with an ordinary refractometer the formula (1) cannot be applied. For these reasons it is usually preferable to use the graphical method described in the following paragraph for determining γ (and, if necessary, β also).

3. *Determination of the Principal Refractive Indices.*

The determination of the principal refractive indices is made with the crystal mounted on the special microscope stage-goniometer to which reference has already been made. With this apparatus the crystal, while immersed in a suitable liquid, may be rotated through accurately measurable angles about an axis perpendicular to the axis of the microscope.

If possible it is best to mount the crystal on the microscope stage-goniometer with the plane of the optic axes perpendicular to the horizontal axis of rotation. The β-axis of the indicatrix will then be in the axis of rotation, and the three refractive indices and the optic axial angle can be measured without any further

alteration in the mounting of the crystal, as follows :— β is found by setting the polarizing nicol so that the incident light vibrates in a plane parallel to the horizontal axis of rotation (the crystal will then be in an extinction position when observed through the analysing nicol). The equality of index between an immersion liquid of index β and the crystal will hold for all settings of the crystal with respect to rotation about the horizontal axis. The optic axial angle is measured directly by bringing the points of emergence of the optic axes (the "eyes") in turn into coincidence with the intersection of the cross-wires of the microscope, while the crystal is immersed in a liquid of index β. The angle through which the crystal is rotated is then equal to the optic axial angle. From the directions of emergence of the optic axes it is easy to set the crystal so that the α- and γ-axes of the indicatrix are parallel to the stage of the microscope, for the bisectrices of the optic axial angle define the directions of α and γ. For each of these settings in turn an immersion liquid is found, if possible, whose index is the same as that of the crystal for light vibrating parallel to α or γ respectively.

If both α and γ can be measured equation (1) serves as a check on the values of α, β, γ, and V. If γ is too high for measurement it may be calculated from equation (1). As already mentioned, however, it is usually better to use a graphical method, which will now be described :—

With the crystal mounted as before it is immersed in a series of liquids whose indices increase in steps of about 0·01. The crystal is rotated about the horizontal axis until a match for each liquid is obtained, and the angle θ from the position in which the α-axis is parallel to the stage is measured.

If μ is the refractive index of the liquid which matches the crystal for a setting θ, then

$$\frac{1}{\mu^2}=\frac{1}{\gamma^2}+\left(\frac{1}{\alpha^2}-\frac{1}{\gamma^2}\right)\cos^2\theta, \quad . \quad . \quad . \quad (2)$$

so that $1/\mu^2$ varies linearly with $\cos^2\theta$. The observed values of $1/\mu^2$ are then plotted against $\cos^2\theta$, and the straight line thus obtained extrapolated to $\theta=90°$ to obtain γ. α and β are given by the values of μ corresponding to $\theta=0°$ and $\theta=$V respectively. In this way it is possible to determine β and γ, even though they are

both outside the range of the refractometer. It is only necessary to have a liquid which will match β, so that the optic axial angle can be determined accurately.

The orientation of the indicatrix with respect to the crystallographic axes is found either from the extinction angles on suitable faces or from the directions of emergence of the optic axes. For this purpose it is necessary to know the relation between the scale-reading on the stage-goniometer and the orientation of the faces parallel to the axis of rotation. This can easily be found by an arrangement similar to that employed in Hutchinson's universal goniometer [1], which enables the scale-readings to be taken when each of the faces in turn is parallel to the microscope stage. A note describing the method has been communicated to the 'Journal of Scientific Instruments' [5].

Every crystal presents a special problem, and difficulties may arise, for example, on account of peculiarities of habit which make it impossible to mount the crystal in the orientation desired. The second part of this paper contains examples of such difficulties.

4. *Measurement of a High Index of Refraction of a Liquid.*

When the indices of a crystal have been determined by the graphical method described in the preceding paragraph it is obvious that the crystal can be employed in the reverse way to measure the refractive index of a liquid lying between α and γ. The crystal forms what is effectively a solid medium whose refractive index, for the proper direction of vibration of the incident light, varies continuously from α to γ as the crystal is rotated about the axis β. Indices of liquids up to the value of γ can thus be measured by finding the setting θ at which a match is obtained with the liquid under examination. The index of the liquid, μ, is then found from the graph or from equation (2).

To find θ it is necessary to know the goniometer scale-reading corresponding to the setting for which α is parallel to the plane of the microscope stage. This can be found either from the scale-readings for the optic axes (as described in § 3) or by obtaining a match with a liquid of known refractive index μ' as near that of the unknown

liquid as possible. In the latter method if the scale-reading corresponding to μ' is θ', while the angle corresponding to μ' obtained from the graph of $1/\mu^2$ against $\cos^2\theta$ is θ'', the reading for which α will be parallel to the plane of the stage will be $\theta' - \theta''$. The second method is usually preferable, since it is less affected by small errors in the microscope and mounting of the crystal, and it is not necessary to obtain an exact match with β.

The accuracy with which the refractive index of a liquid can be measured in this way is evidently of the same order as that in determining the index of a crystal. After matching a crystal it is not necessary to remove the drop of liquid from the cell in order to find its index, so that errors due to temperature change and evaporation are minimized.

Picryl *p*-toluidine (yellow form) was found to be a very suitable crystal to use in this way, and it was employed in all the work to be described when it was necessary to find the index of refraction of a liquid outside the range of the refractometer. Any crystal may be used, however, provided it is sufficiently birefringent and has a well-formed zone of faces parallel to the axis β of the indicatrix.

Part II.

5. In this part are given the results of measurements made on a number of organic crystals by the methods just described. The following substances have been examined in sodium light:—Picryl *p*-toluidine (yellow form), picryl aniline, diphenyl ether, and diphenyl sulphone (§§ 6–9). The other form of picryl *p*-toluidine is deep red and opaque to sodium light, so that measurements with that light were not possible. The measurements on yellow picryl *p*-toluidine were therefore repeated with red light, in order that comparative measurements on the two forms might be obtained (§§ 10 and 11).

Numerical values of the refractive indices and the optic axial angle are given for these substances, while the orientation of the indicatrix and the directions of the optic axes (E_1, E_2) are indicated in each case on a stereographic projection. The refractive index is estimated to be correct to within two or three units in the third decimal place, while the optic axial angle is correct to about $\frac{1}{4}°$.

6. *Picryl p-toluidine (yellow form),*

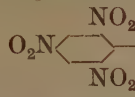

This substance crystallizes in monoclinic needles elongated along the crystallographic symmetry axis b, which

Fig. 1.

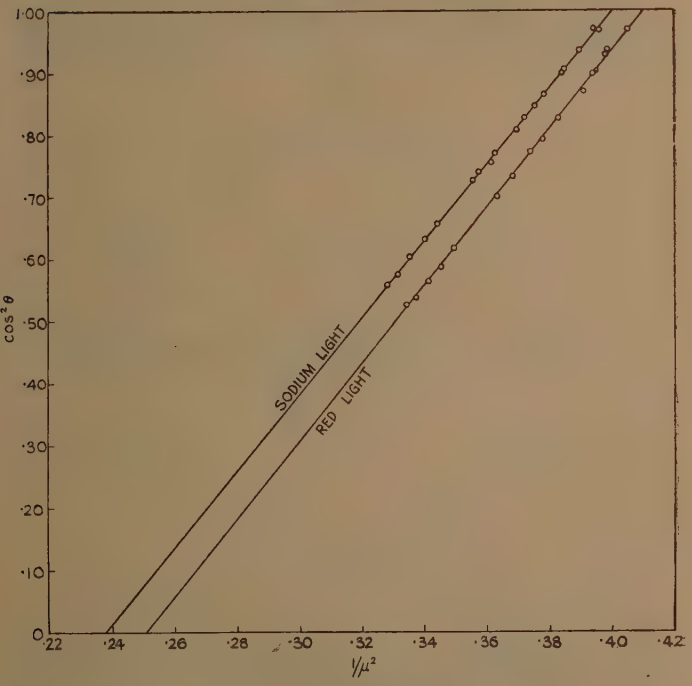

Graphs of $1/\mu^2$ against $\cos^2\theta$.

coincides with the β-axis of the indicatrix. Since there is a well-formed zone of faces around b the crystal could easily be mounted as described in § 3, with β in the axis of rotation.

The index α could be measured directly by immersion in a solution of potassium mercuric iodide in water. A match for β was obtained by using a solution of sulphur in methylene iodide. The refractive index of this solution

was, however, too great for measurement on the Abbe refractometer used, so that the values of β and γ were determined by the graphical method of § 3.

The observed values of $1/\mu^2$ are plotted against those of $\cos^2\theta$ in fig. 1. The extrapolation to $\theta=V$ to obtain β is very small. The extrapolation to $\theta=90°$ to obtain γ is rather large, but justifiable, as the position of the straight line is clearly defined. This extrapolation is equivalent to calculating γ from α, β, and the optic axial angle, but more accurate, since it depends on more readings. The points on the graph of fig. 1 were obtained from three

Fig. 2.

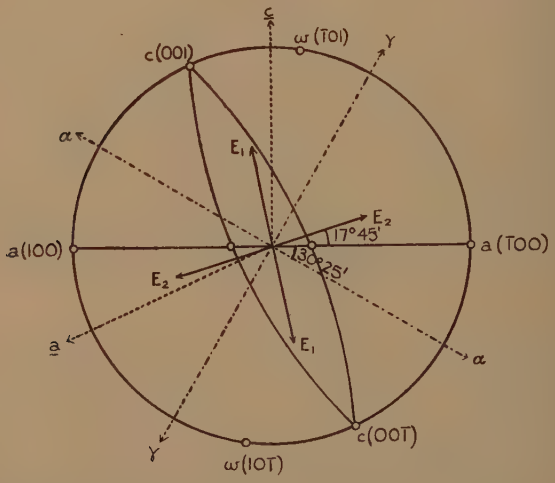

Stereographic projection of picryl *p*-toluidine (yellow form).

different crystals, and the points fit equally closely to the straight line, showing that the line obtained is independent of the specimen used.

The numerical values of the constants are :—

$\alpha=1{\cdot}580$, $\beta=1{\cdot}747$, $\gamma=2{\cdot}052$.

Optic axial angle $=83°\ 45'=2V$.

The birefringence is positive.

An optic axis emerged at an angle $12°\ 40'$ with the normal to (001). This fixes the orientation of the optic axes and therefore the axes of the indicatrix. The

optic axes and the axes of the indicatrix are shown in stereographic projection in fig. 2.

7. *Picryl Aniline*, O_2N(C$_6$H$_3$(NO_2)$_2$)—NH—(C$_6$H$_5$).

Two apparently different forms of this substance have been described, viz., prisms and needles. These have, however, been shown to be identical by X-ray methods [3], and the present optical examination confirms

Fig. 3.

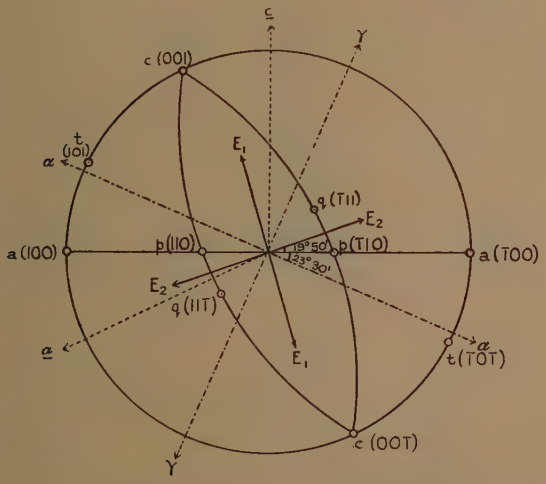

Stereographic projection of picryl aniline.

that conclusion. The crystals are monoclinic, the symmetry axis b coinciding with β. On account of the difference in habit a different method of mounting was used for each variety.

(a) *Needle Form.*—The needles of picryl aniline are elongated along the c-axis which is perpendicular to β. Making this the axis of rotation, β can be set in the plane of the stage by observing the interference figure and can then be measured. Rotation through 90° about the horizontal axis then brings α and γ into position for measurement.

(b) *Prism Form.*—The ortho-zone is developed on this form of the substance, which can therefore easily be mounted with β parallel to the horizontal axis of the stage-goniometer, and the standard procedure followed. Measurements were also made on this form mounted in the same way as the needle form, *i. e.*, to rotate about the *c*-axis.

The measurements on both forms gave the same numerical results within experimental error. The value of γ was calculated from α, β, and the optic axial angle, since α and β could be measured accurately and were widely separated.

Fig. 4.

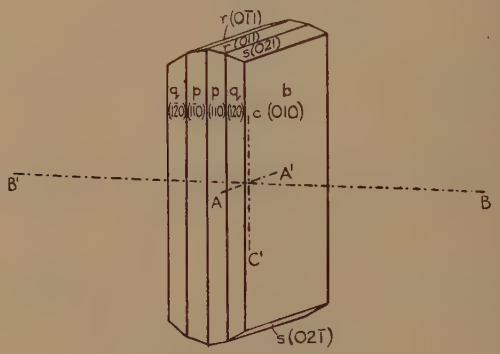

Typical crystal of diphenyl ether.

The numerical values are as follows :—

$\alpha = 1{\cdot}549$, $\beta = 1{\cdot}800$, $\gamma = 2{\cdot}168$.

Optic axial angle $= 86° 35' = 180° - 2V$.

The birefringence is negative.

The orientation of the indicatrix is shown in the stereographic projection, fig. 3.

8. *Diphenyl Ether*, .

This substance crystallizes in the orthorhombic system, the crystals being usually elongated parallel to the *c*-axis, which coincides with the axis β of the indicatrix. A typical crystal is illustrated in fig. 4.

The interfacial angles are given in the following table, which represents the mean of observations on seven crystals :—

b (010)		b (010)	61° 27′
q (120)	54° 7′	s (021)	13° 18′
p (110)	16° 3′	r (011)	30° 22′
p (1$\bar{1}$0)	39° 43′	r (0$\bar{1}$1)	

The axial ratios are :—

$$a : b : c = 0{\cdot}361 : 1 : 0{\cdot}273.$$

Fig. 5.

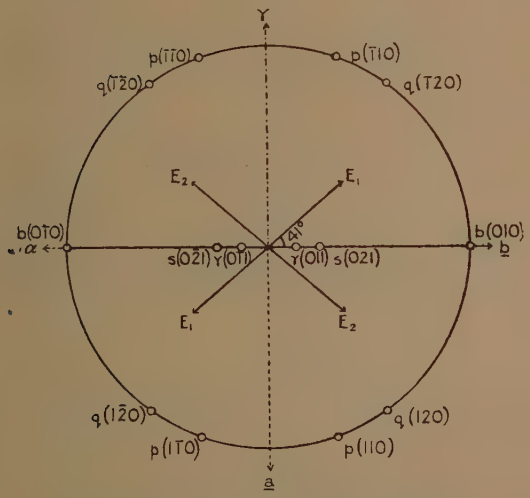

Stereographic projection of diphenyl ether.

These are calculated from the angles bp (70° 8′) and br (74° 44′) most frequently measured.

The crystal was mounted with β in the axis of rotation, and since all the indices were within the range of the liquids available all the constants could be determined with this one mounting, and no extrapolation was necessary. The value of β was most susceptible to inaccuracy in orientation and was therefore calculated from the other measurements in the final results. This gave a value for β of 1·658 compared with the measured value 1·656. The low melting-point of diphenyl ether (28° C.) makes

the mounting of the crystals rather difficult, but the accuracy of the mounting can be tested by observing the interference figure as the crystal is rotated.

The numerical values are as follows :—

$\alpha = 1{\cdot}617$, $\beta = 1{\cdot}658$, $\gamma = 1{\cdot}691$.

Optic axial angle $= 82° 0' = 180° - 2V$.

The birefringence is negative.

The orientation of the indicatrix is shown in the stereographic projection, fig. 5.

Fig. 6.

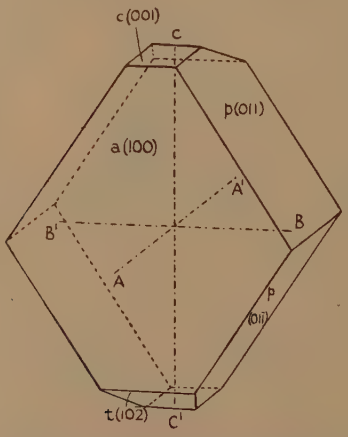

Typical crystal of diphenyl sulphone.

9. *Diphenyl Sulphone*, $C_6H_5—SO_2—C_6H_5$.

This substance crystallizes in monoclinic plates with the *b*-axis, which coincides with β, in the plane of the plate. A typical crystal is illustrated in fig. 6.

The interfacial angles (mean of observations on eight crystals) are as follows :—

a (100)	81° 43′*	*c* (001)	55° 9′	*a* (100)	85° 21′
c (001)	26° 14′*	*p* (011)	69° 48′*	*p* (011)	
t (10̄2)		*p* (01̄1)			

The axial ratios and angle calculated from the angles marked with an asterisk are :—

$$a : b : c = 1{\cdot}56 : 1 : 1{\cdot}45,$$
$$\beta = 98^\circ\ 17'.$$

For the optical examination the axis β was mounted in the axis of rotation and the standard method applied. Since α is close to β the graphical method was necessary to find γ.

Fig. 7.

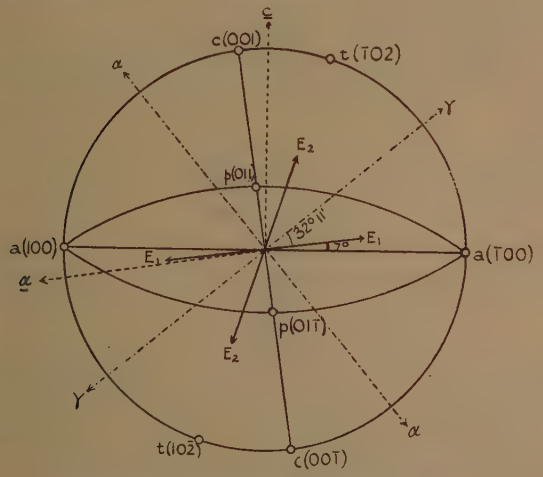

Stereographic projection of diphenyl sulphone.

The numerical results are as follows :—

$\alpha = 1{\cdot}606$, $\beta = 1{\cdot}632$, $\gamma = 1{\cdot}703$.

Optic axial angle $= 64^\circ\ 20' = 2V$.

The birefringence is positive.

The orientation of the indicatrix is shown in the stereographic projection, fig. 7.

10. *Measurements in Red Light.*

All the preceding measurements have been made in the light from a sodium-vapour lamp. For reasons given in § 5 it was necessary to repeat the measurements

on the yellow form of picryl *p*-toluidine in red light. As no source of monochromatic red light of sufficient intensity was available the measurements were made in the light of a 60 watt lamp after passing through a Wratten α-filter. This transmits only wave-lengths greater than 6500 Å., the brightest portion being in the neighbourhood of 6700 Å.

In using the immersion liquids with this light small corrections had to be made to allow for the dispersion of the liquids. Apart from this the work is identical with what has already been described, so that only the results need be quoted.

The values of $1/\mu^2$ plotted against $\cos^2\theta$ for the yellow form of picryl *p*-toluidine in red light are shown in fig. 1. The points lie on a straight line below the line for sodium light.

The numerical values of the constants for yellow picryl *p*-toluidine in red light are as follows :—

$\alpha = 1{\cdot}560$, $\beta = 1{\cdot}719$, $\gamma = 1{\cdot}998$.

Optic axial angle $= 84° 30' = 2V$.

The birefringence is positive.

11. *Picryl p-toluidine* (*red form*).

The red form of picryl *p* toluidine is entirely different in structure from the yellow. The crystals consist of monoclinic needles elongated along the crystallographic axis *c*. The symmetry axis *b* coincides with the α-axis of the indicatrix, while the β-axis is in the symmetry plane, making a small angle with *c*. On account of the crystal habit a special method had to be applied, since it was only feasible to mount the crystals with the needle axis *c* in the axis of rotation. The optic axes then emerged symmetrically on each side of the *b*-axis, but since the plane of the optic axes was not perpendicular to the needle axis they could not be made to pass through the intersection of the cross-wires of the microscope. Instead, they passed through points placed symmetrically to the right and left of the intersection of the cross-wires. It was therefore easy to set the bisectrix α in the plane of the stage of the microscope and measure the index α. A rotation through 90° then brought the plane of β and γ into the plane of the

stage. β was measured by comparison with a solution of sulphur in methylene iodide, while γ was obtained by calculation.

The optic axial angle was measured by bringing each "eye" in turn on to the cross-wire, while the crystal was immersed in a liquid of index β. If 2 A′ is the angle of rotation, the optic axial angle, 2 A, is given by

$$\tan A = \tan A'/\cos\psi \quad . \quad . \quad . \quad . \quad . \quad (3)$$

In this formula ψ is the angle between the plane of the optic axes and the plane normal to the axis of rotation,

Fig. 8.

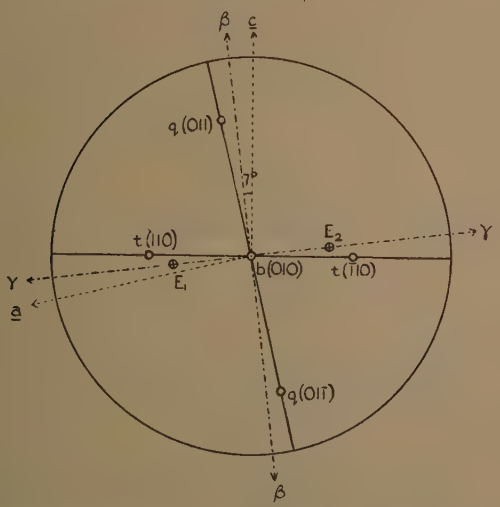

Stereographic projection of picryl *p*-toluidine (red form).

i. e., between *c* and β. The value of ψ is found from the extinction angles made with the needle axis (*c*) when the plane containing β and γ is parallel to the plane of the stage.

The numerical values are as follows :—

$\alpha = 1{\cdot}557$, $\beta = 1{\cdot}769$, $\gamma = 2{\cdot}041$

$2A' = 85° 3'$, $\psi = 7°$.

Optic axial angle $= 85° 30' = 180° - 2V$.

The birefringence is negative.

The orientation of the indicatrix is shown in the stereographic projection, fig. 8.

12. *Summary of Measurements.*

Substance.	Light.	α.	β.	γ.	Optic axial angle.	Sign.	Crystal system.
Picryl aniline.	Sodium.	1·549	1·800	2·168	86° 35′	—	Monoclinic.
Picryl *p*-toluidine (yellow).	Sodium.	1·580	1·747	2·052	83° 45′	+	„
„	Red.	1·560	1·719	1·998	84° 30′	+	
Picryl *p*-toluidine (red).	Red.	1·557	1·769	2·041	85° 30′	—	„
Diphenyl ether.	Sodium.	1·617	1·658	1·691	82° 0′	—	Orthorhombic.
Diphenyl sulphone.	Sodium.	1·606	1·632	1·703	64° 20′	+	Monoclinic.

13. This paper describes the measurement of the optical constants of a number of organic crystals by means of the immersion method, using a polarizing microscope and a special microscope stage-goniometer.

The thanks of the authors are due to Prof. R. T. Dunbar for his continued help throughout the research and to Prof. W. J. Jones for the loan of apparatus. We should also like to thank Prof. W. L. Bragg, F.R.S., for his interest in the work.

References.

(1) Wood and Ayliffe, J. Sci. Inst. xii. p. 194 (1935).
(2) Davies and Hartshorne, J. Chem. Soc. 1830 (1934).
(3) Wood, Ayliffe, and Cullinane, Phil. Mag. xix. p. 405 (1935).
(4) Hutchinson, Min. Mag. xvi. p. 100 (1911).
(5) Wood and Ayliffe, J. Sci. Inst. xii. p. 299 (1935).

Physics Department,
University College, Cardiff.
August 1935.

XXVIII. *On the Mutual Energy in Systems of Vibrating Particles, and a Suggestion regarding Electrostatic Energy.* *By* E. Taylor Jones, *D.Sc., Professor of Natural Philosophy in the University of Glasgow* *.

THE problem of the mutual action between two small spheres immersed in an incompressible fluid, each sphere vibrating radially, *i. e.*, expanding and contracting, but having no translational motion, was considered by H. A. Lorentz †, who showed that the expression for the energy of the liquid contains a term proportional to the product of the vibratory velocities of the spheres, the coefficient of this term being inversely proportional to the distance between the centres of the spheres. It was shown by Lorentz that the spheres attract each other if their pulsations are in the same phase, and repel if they are in opposite phase. It is probably for this reason, viz., the attraction of similar and the repulsion of unlike particles, that the question of a possible application of the theory to the explanation of electrostatic phenomena does not appear to have been pursued further.

At the present time, however, the question assumes a new interest owing to the fact that there is strong experimental evidence to show that electrons possess oscillatory properties. The numerous experiments on electron diffraction which have been carried out in recent years leave no room for doubt that an electron, when in translatory motion, is accompanied by a system of waves which extend from it into the surrounding space, and have a wave-length determinable by diffraction experiments. There can be little doubt that such waves exist also when the electron is at rest, and that the electron as the centre of such a wave system may be regarded as itself an oscillator having the frequency of the waves surrounding it. This frequency is generally admitted to have the value indicated by the quantum-relativity relation $\nu_0 = m_0 c_0^2/h = 1{\cdot}24 \cdot 10^{20}$, m_0 being the rest-mass of an electron, c_0 the velocity of light *in vacuo*, and h Planck's constant.

At the present time a stationary electron is regarded as the centre of two independent fields of influence,

* Communicated by the Author.

† 'Lectures on Theoretical Physics,' i. pp. 62–68 (1927).

viz., the oscillatory field of the system of waves just referred to and its steady unidirectional electrostatic field which determines its action upon other electrons. It is natural to enquire whether these two fields are not essentially the same, *i. e.*, whether the electrostatic attractions and repulsions of stationary electrons cannot be traced to the interaction of the wave-systems with which they are associated.

As the basis of such an enquiry it must be supposed that two electrons can act upon each other with a definite average unidirectional force in the line joining them when their vibrations are in the same or in opposite phase, and that the work done in causing them to approach each other is proportional to the increase of their common frequency arising from the mutual action between them. It is also assumed that the mutual energy of two electrons having no translatory motion is proportional to the product of the *displacements* in their vibratory movements, so that if these displacements are represented by x and y the equations of motion (after division by the vibratory "mass," supposed the same for both) may be written

$$\left.\begin{aligned} \ddot{x}+ax+by=0 \ldots \\ \ddot{y}+ay+bx=0 \ldots \end{aligned}\right\} \quad \ldots\ldots \quad (1)$$

The coefficient a represents $4\pi^2\nu_0^2$, ν_0 being the frequency of an electron at rest and far removed from other electrons, and b may be called the "coupling" of the electrons regarded as a pair of interacting vibrators. The magnitude of b will depend upon the distance of the electrons apart, and we assume that b is inversely proportional to this distance.

Assuming $x=\mathrm{A}e^{\mathrm{int}}$, $y=\mathrm{B}e^{\mathrm{int}}$, we find from equations (1)

$$\begin{aligned} (-n^2+a)\mathrm{A}+b\mathrm{B}=0, \\ (-n^2+a)\mathrm{B}+b\mathrm{A}=0, \end{aligned}$$

which give for the two common frequencies

$$n^2=4\pi^2\nu^2=a\pm b,$$

and for the amplitudes

$$\begin{aligned} \mathrm{A}=\mathrm{B} \text{ if } n^2=a+b, \\ \mathrm{A}=-\mathrm{B} \text{ if } n^2=a-b. \end{aligned}$$

With the type of coupling here assumed, in which the mutual action of the electrons depends upon the displacements rather than upon the velocities in their vibratory movements, it follows therefore that when the electrons are vibrating with their higher frequency $n_1/2\pi$, given by

$$n_1^2 = a + b,$$

they are in the same phase. They are therefore electrons of the same sign, and their mutual energy is increased when they are caused to approach each other. In other words, two electrons having the frequency $\nu_1 (= n_1/2\pi)$ vibrate in the same phase and repel each other. On the other hand, two electrons vibrating in opposite phase have their energy and frequency diminished when they approach, and they therefore attract each other *.

We shall see that at all ordinary distances b is very small in comparison with a. At such distances therefore we have, to a high degree of approximation,

$$n_1 = 2\pi\nu_1 = \sqrt{a} + \frac{b}{2\sqrt{a}},$$

and since $\sqrt{a} = 2\pi\nu_0$, the increase of energy consequent upon the approach of two similar electrons from an infinite distance is

$$2h(\nu_1 - \nu_0) = \frac{2hb}{4\pi\sqrt{a}} \quad . \quad . \quad . \quad . \quad . \quad (6)$$

$$= \frac{hk}{2\pi r\sqrt{a}}$$

if k is the coupling at unit distance.

If this is equated to the electrostatic energy $E_1 (= e^2/r)$ we have

$$e^2 = \frac{hk}{2\pi\sqrt{a}} \quad . \quad . \quad . \quad . \quad . \quad . \quad . \quad (7)$$

* If the coupling is such that the mutual energy depends upon the velocities the equations of motion are

$$\ddot{x} + ax + b\ddot{y} = 0,$$
$$\ddot{y} + ay + b\ddot{x} = 0.$$

The frequencies are $\frac{a}{1 \pm b}$, the phases being the same in the lower- and opposite in the higher-frequency mode. Particles of like sign therefore attract, those of unlike sign repel, as in the problem discussed by H. A. Lorentz.

From this relation and the known values of e, h, and a we deduce the value of k for two electrons, viz., $k=1{\cdot}7\,.\,10^{29}$ c.g.s. Since $\nu_0=1{\cdot}24\,.\,10^{20}$, the value of a is $4\pi^2\,.\,1{\cdot}24^2\,.\,10^{40}$, *i. e.*, $6{\cdot}07\,.\,10^{41}$, and at 1 cm. the ratio b/a is therefore about $2{\cdot}8\,.\,10^{-13}$.

Similarly, the approach of two unlike electrons involves the performance of work

$$2h(\nu_2-\nu_0)=-\frac{hk}{2\pi r\sqrt{a}} \quad . \quad . \quad . \quad . \quad . \quad . \quad . \quad (8)$$
$$=-e^2/r,$$

leading to the same value $hk/2\pi\sqrt{a}$ for the square of the charge.

According to the views here suggested, therefore, two electrons repel each other if they have the same phase, attract if they are opposite in phase, and behave at moderate distances as if the electric charge of each were equal to $\sqrt{hk}/2\pi\sqrt{a}$.

Since $\sqrt{a}=2\pi\nu_0=m_0c_0^2/h$, the expression for the charge may be written

$$e=\frac{h}{2\pi c_0}\sqrt{\frac{k}{m_0}}, \quad . \quad . \quad . \quad . \quad . \quad (9)$$

in which m_0 is the mass of an electron at rest and far removed from other electrons. The magnitude of the repulsive force between two electrons at distance r is

$$-\frac{d\mathrm{E}_1}{dr}=\frac{h^2k}{4\pi^2c_0^2m_0r^2} \quad . \quad . \quad . \quad . \quad . \quad (10)$$

Whatever be the nature of the mechanism of this force it appears to require that the electron fields shall experience a certain distortion when in presence of each other which, owing to the variation in the value of b, would result in a slight excess of frequency on the nearer over that on the further sides. Such distortion must be supposed to exist whenever an electron experiences a resultant force owing to the proximity of other charges.

So long as two electrons are separated by a moderate distance the mutual force between them, according to the view which regards them as coupled oscillators, follows the usual law. They behave as if their charges were constant, and the attraction between two electrons of opposite sign is equal to the repulsion of a pair of like sign at the same distance. But these statements do not

hold good if the distance between the electrons is extremely small. If this distance is so short that b is not very small in comparison with a, the expression for the frequency becomes, in the case of two similar electrons,

$$\nu_1 = \frac{1}{2\pi}\sqrt{a+\frac{k}{r}}, \quad \ldots\ldots \quad (11)$$

and the mutual energy is

$$2h(\nu_1-\nu_0) = \frac{h}{\pi}\left(\sqrt{a+\frac{k}{r}}-\sqrt{a}\right). \quad \ldots \quad (12)$$

The repulsion of the electrons is therefore

$$-\frac{dE_1}{dr} = \frac{hk}{2\pi r^2}\frac{1}{\sqrt{a+k/r}}. \quad \ldots\ldots \quad (13)$$

The force is therefore no longer inversely proportional to the square of the distance. The factor $1/\sqrt{1+k/ar}$ which represents the deviation is about 0·99 at $r = 10^{-11}$ cm. and about 0·88 at 10^{-12} cm. if k/a has the same value $2{\cdot}8 \cdot 10^{-13}$ as at ordinary distances.

If the two electrons are of opposite sign the expression for their mutual energy at very short distances becomes

$$E_2 = 2h(\nu_2-\nu_0) = \frac{h}{\pi}\left(\sqrt{a-k/r}-\sqrt{a}\right),$$

and the attraction is

$$\frac{dE_2}{dr} = \frac{hk}{2\pi r^2\sqrt{a}}\cdot\frac{1}{\sqrt{1-k/ar}}.$$

This force is greater than that given by the law of inverse squares if the charge is regarded as having the normal value of $\frac{h}{2\pi c_0}\sqrt{\frac{k}{m_0}}$. Also the attraction is greater than the repulsion between two electrons of the same sign at the same distance, the ratio of the attraction to the repulsion being

$$\sqrt{\frac{1+k/ar}{1-k/ar}}, \quad \ldots\ldots \quad (14)$$

which is equal to 2 if the distance r is about $4{\cdot}7 \cdot 10^{-13}$ cm.

The theory indicates that the greatest possible value of the coupling b of two electrons is a, which would be attained (the above numerical values being assumed)

if r were about $2{\cdot}8 \cdot 10^{13}$ cm. If this close approach occurred the electrons would, if of opposite sign, presumably annihilate each other, since their frequency would be zero. There is some experimental evidence indicating that such annihilation of electrons can take place, with emission of two quanta of radiation *.

Another effect indicated by this theory is that the mass of each of two electrons depends upon their distance apart. Since the mass is proportional to the frequency, the fractional increase of mass for two electrons of the same sign is, at a moderate distance r,

$$\begin{aligned} \frac{m_1-m_0}{m_0} &= \frac{\nu_1-\nu_0}{\nu_0} \\ &= \frac{k}{2ar} \\ &= \frac{1{\cdot}4 \cdot 10^{-13}}{r} \quad . \quad . \quad . \quad . \quad . \quad . \quad . \quad . \quad (15) \end{aligned}$$

At atomic distances, that is at about 10^{-8} cm., the change of mass is of the order $10^{-5}\ m_0$. For much shorter distances the more exact expression for the frequency must be used, giving

$$\frac{m_1-m_0}{m_0} = \sqrt{1+\frac{k}{ar}} - 1. \quad . \quad . \quad . \quad (16)$$

The increase of mass indicated by the theory is therefore, for two electrons of like sign, about 1·4 per cent. at 10^{-11} cm. and about 13 per cent. at 10^{-12} cm.

Similarly, for two electrons of opposite sign we find that the fractional diminution of mass is $k/2ar$ at moderate distances and $1-\sqrt{1-k/ar}$ at very short distances.

Turning now to systems consisting of more than two electrons, it is to be remembered that, according to the assumptions of this theory, electrons can exert steady average force upon each other only if they have the same frequency. The solution of the problem must therefore begin with the determination of the common frequencies of all the electrons forming the system. The simplest cases are those in which all the electrons are similarly situated, sign as well as position being taken into account, with regard to the others. We will begin with the case

* J. Thibaud, *Comptes Rendus*, cxcvii. p. 1629 (1933); F. Joliot, *J. de Phys. et le Rad.* v. p. 299 (1934).

of three electrons at equal distances $l\,(=k/b)$ from one another. The equations of motion are

$$\left.\begin{aligned}\ddot{x}+ax+by+bz=0\ldots\\ \ddot{y}+ay+bx+bz=0\ldots\\ \ddot{z}+az+bx+by=0\ldots\end{aligned}\right\}\quad\ldots\quad(17)$$

Substituting $x=Ae^{int}$, $y=Be^{int}$, $z=Ce^{int}$, eliminating A, B, and C, and writing N for n^2-a, we find the equation for the frequencies

$$(N-2b)(N+b)^2=0.\quad\ldots\quad(18)$$

The three frequencies of the system are therefore given by

$$\left.\begin{aligned}n_1^2=a+2b\ldots\\ n_2^2=a-b\ldots\\ n_3^2=a-b\ldots\end{aligned}\right\}\quad\ldots\quad(19)$$

For the amplitudes the equations are

$$\left.\begin{aligned}-NA+bB+bC=0\ldots\\ bA-NB+bC=0\ldots\\ bA+bB-NC=0\ldots\end{aligned}\right\}\quad\ldots\quad(20)$$

In the first mode $N=2b$, and equations (20) give $A=B=C$, so that all the amplitudes are equal and the three electrons oscillate in the same phase. They are evidently electrons of the same sign. The frequency ν_1 in the first mode is

$$\sqrt{a}+\frac{2b}{4\pi\sqrt{a}},$$

and the mutual energy of the system is

$$3h(\nu_1-\nu_0)=\frac{3hk}{2\pi l\sqrt{a}}.$$

If this is equated to the electrostatic energy $3e^2/l$ we arrive at the same expression (9) for the charge.

In the second or third mode N is equal to $-b$, and equations (20) for the amplitudes reduce to

$$A+B+C=0.\quad\ldots\quad(21)$$

This may be interpreted as indicating that two of the particles have equal amplitudes but are opposite in phase, the third particle having zero amplitude in this mode. We suppose that y and z are in opposite phase (fig. 1)

representing electrons of opposite sign, so that equation (21) reduces to

$$\left.\begin{aligned} B+C=0 \ldots \\ A=0 \ldots \end{aligned}\right\} . \quad . \quad . \quad . \quad . \quad (22)$$

The particle x is to be regarded as having no mutual energy with the others in this mode, so that, since the frequency is given by $n_2^2=a-b$, the total mutual energy of the system is

$$2h(\nu_2-\nu_0)=-\frac{hb}{2\pi\sqrt{a}},$$

corresponding by (7) to the electrostatic energy $-e^2/l$. *

If the system consists of four electrons at the corners of a square of side $l\,(=k/b)$ and diagonal $r\,(=k/c)$, the equations of motion are

$$\left.\begin{aligned} \ddot{x}+ax+by+cz+bu=0 \ldots \\ \ddot{y}+ay+bx+bz+cu=0 \ldots \\ \ddot{z}+az+cx+by+bu=0 \ldots \\ \ddot{u}+au+bx+cy+bz=0 \ldots \end{aligned}\right\} . \quad . \quad . \quad (24)$$

Fig. 1.

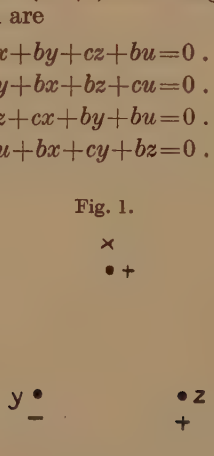

Proceeding as before, and writing N for n^2-a, we find that the equation for the frequencies reduces to

$$(N-2b-c)(N+2b-c)(N+c)^2=0. \quad . \quad . \quad (25)$$

The four frequencies of the system are given by

$$\left.\begin{aligned} n_1^2=a+2b+c \ldots \\ n_2^2=a-2b+c \ldots \\ n_3^2=n_4^2=a-c \ldots \end{aligned}\right\} . \quad . \quad . \quad . \quad . \quad (26)$$

* If x is positive there is no reason for choosing y and z rather than y and x (fig. 1) as the oscillating pair, and it is probable that x and z oscillate alternately in the mode $a-b$.

For the amplitudes we have

$$\left.\begin{aligned} -NA+bB+cC+bD&=0\ldots\\ bA-NB+bC+cD&=0\ldots\\ cA+bB-NC+bD&=0\ldots\\ bA+cB+bC-ND&=0\ldots \end{aligned}\right\}\quad\ldots\quad(27)$$

In the first mode N is $2b+c$, and it follows from equations (27) that

$$A=B=C=D.$$

In this mode therefore the amplitudes are all equal and the particles all vibrate in the same phase. This mode evidently represents the state of four particles all of the same sign. The frequency ν_1 in the first mode is given by

$$\begin{aligned} n_1^2&=a+2b+c\\ &=4\pi^2\nu_1^2, \end{aligned}$$

and the mutual energy, if the distances are not extremely small, is

$$4h(\nu_1-\nu_0)=\frac{h(2b+c)}{\pi\sqrt{a}}.$$

The electrostatic energy is $4\frac{e^2}{l}+2\frac{e^2}{r}$, and since $b=k/l$, $c=k/r$, we find as before

$$e^2=\frac{hk}{2\pi\sqrt{a}}.$$

For the second mode we substitute $-2b+c$ for N in (27), and find

$$\left.\begin{aligned} A+B&=0\ldots\\ A-C&=0\ldots\\ B-D&=0\ldots \end{aligned}\right\}\quad\ldots\quad(28)$$

In the second mode therefore each electron is opposite in sign to its two neighbours, and diagonally opposite electrons have the same sign. The frequency ν_2 in this mode is given by

$$\begin{aligned} n_2^2&=a-2b+c\\ &=4\pi^2\nu_2^2, \end{aligned}$$

and the mutual energy is

$$4h(\nu_1-\nu_0)=-\frac{h(2b-c)}{\pi\sqrt{a}}.$$

Equating this to the electrostatic energy $-4\frac{e^2}{l}+2\frac{e^2}{r}$ we again find the usual expression (9) for the charge.

In the third and fourth modes N is equal to $-c$, and equations (27) reduce to

$$A+C-B+D=0, \quad . \quad . \quad . \quad . \quad . \quad (28)$$

which may be regarded as meaning that each electron differs in sign from the one diagonally opposite to it. The two diagonal pairs now oscillate with frequency given by $n_3{}^2=a-c$, and the mutual energy $4h(\nu_3-\nu_0)$ is $-hc\,\pi\sqrt{a}$. The electrostatic energy in this case is $-2e^2/r$, so that the charge again has the usual value (9).

Another possible interpretation of equations (28), however, is that while x and z are opposite in sign ($A+C=0$), the other two particles y and u have zero amplitudes ($B=D=0$) in the mode $a-c$. This would occur if y and u were of the same sign, in which case they would vibrate in phase with each other and with the frequency given by $n^2=a+c$. This frequency is not included in equation (25), which gives the frequencies of the whole system, but is to be regarded as a "partial oscillation" affecting only a portion of it. In this state of the system one of the electrons is different in sign from the other three, and the system may be regarded as consisting of two diagonal pairs, independent in energy, vibrating with frequencies given by $n^2=a\pm c$. The mutual energy of this system is zero, in agreement with the value of the electrostatic energy.

A system having similar properties is that of four particles placed at the corners of a regular tetrahedron. If b is the coupling for any pair the equation for N ($=n^2-a$) is

$$(N-3b)(N+b)^3=0. \quad . \quad . \quad . \quad . \quad (29)$$

The frequencies are therefore given by

$$\left.\begin{aligned} n_1{}^2&=a+3b \ldots \\ n_2{}^2=n_3{}^2&=n_4{}^2=a-b \ldots \end{aligned}\right\} . \quad . \quad . \quad . \quad (30)$$

The first mode corresponds to the case in which all four particles are of the same sign, and the energy equation leads to the usual expression (9) for the charge. The other three modes represent systems in which two of the particles are of opposite sign. In one case the system may, as in the system of four particles forming

a square, be regarded as consisting of two pairs vibrating in the mode $a-b$, in another as a pair oscillating in this mode with a partial oscillation in the mode $a+b$ superposed upon the other two. In the former case the mutual energy of the system is $-hb/\pi\sqrt{a}$, agreeing with the electrostatic energy $-2e^2/l$ if e^2 has the usual value. In the latter case the mutual energy and the electrostatic energy are both zero.

It is clear that there are many systems of this kind, in which the particles form figures of regular form, some of the frequencies of which can be expressed at once in terms of the coefficients a, b, c, ... In the case of eight particles at the corners of a cube, for example, two of the frequencies are given by

$$n_1^2=a+3b+3c+d,$$
$$n_2^2=a-3b+3c-d,$$

where b is the coupling of two particles on the same side of the cube, c that of two diagonally opposite particles on the same face, and d that of two diagonally opposite in the cube. The first mode represents a system in which all the particles are of the same sign, the second one in which each particle differs in sign from the one diagonally opposite to it and also from the three particles nearest to it. Similarly, a system consisting of a large number of similar particles uniformly distributed over the surface of a sphere has a frequency given by $n^2=a+\Sigma b$, and the mutual energy $\Sigma h(\nu_1-\nu_0)$ will agree with the electrostatic energy if the charge has the value given by (7) or (9).

In systems of non-regular form, however, the energy relation, obtained by equating the mutual vibrational energy (calculated in the same way from the frequency of the whole system) to the electrostatic energy, does not usually lead, or leads only approximately, to the same expression for the charge. One case of this kind is that of three particles forming an isosceles triangle. If the particle x is at the vertex, y and z at the ends of the base (fig. 2), and if $b\ (=k/r)$ is the coupling of two particles on one side, $c(=k/l)$ that of those on the base, the equations of motion are

$$\left.\begin{aligned}\ddot{x}+ax+by+bz=0\ \ldots\\ \ddot{y}+ay+bx+cz=0\ \ldots\\ \ddot{z}+az+bx+cy=0\ \ldots\end{aligned}\right\}\ \ldots\ldots\ldots\quad(31)$$

and the equation for the frequencies, with $N=n^2-a$, is

$$(N^2-cN-2b^2)(N+c)=0. \quad . \quad . \quad . \quad (32)$$

If N_1, N_2 are the positive and negative roots of the equation

$$N^2-cN-2b^2=0,$$

the three frequencies of the system are given by

$$\left.\begin{aligned} n_1^2&=a+N_1 \ldots \\ n_2^2&=a+N_2 \ldots \\ n_3^2&=a-c \ldots \end{aligned}\right\} \quad . \quad . \quad . \quad . \quad . \quad . \quad (33)$$

The amplitude equations reduce to the following :—

In the first mode

$$B=C=\frac{N_1}{2b}A,$$

Fig. 2.

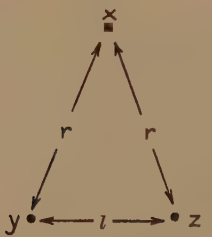

and since N_1 is positive all three particles are of the same sign.

In the second mode

$$B=C=\frac{N_2}{2b}A,$$

and, N_2 being negative, the particles y and z are opposite in sign to x.

In the third mode, if b is not equal to c,

$$B+C=0,$$

and

$$A=0,$$

that is the particles y and z are opposite in sign and x has no mutual energy with them *.

* The condition $A=0$ may be satisfied by supposing either that the amplitude of x is zero in this mode, in which case x would have the frequency $\sqrt{a}/2\pi$, or that the phase of x differs by $\pi/2$ from those of y and z.

If in the third mode b is equal to c then $A+B+C=0$. This case, which is that of three equidistant particles, one being different in sign from the other two, has already been considered.

In fig. 3 the curves N_1, N_2 show values of these quantities for values of the ratio b/c over the whole range, *i. e.*, from 0 ($r=\infty$) to 2 ($r=l/2$). If the three particles were regarded as having, in all the configurations of the

Fig. 3.

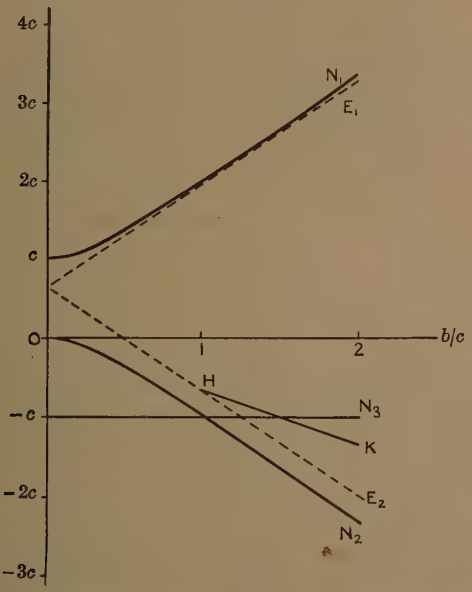

Frequency and energy curves for system of three particles.

system, each one quantum of energy, the total mutual vibrational energy of the system would be, in the first mode,

$$3h(\nu_1-\nu_0)=\frac{3h\mathrm{N}_1}{4\pi\sqrt{a}}$$
$$=\frac{3e^2\mathrm{N}_1}{2lc},$$

if e^2 is written for $hk/2\pi\sqrt{a}$ in accordance with equation (7). If the mutual vibrational energy were equal to the

electrostatic energy E_1, the curve N_1 in fig. 3 would represent the quantity $2lcE_1/3e^2$.

But

$$E_1 = \frac{e^2}{l} + \frac{2e^2}{r}$$
$$= \frac{e^2}{l}\left(1+\frac{2l}{r}\right)$$
$$= \frac{e^2}{l}\left(1+\frac{2b}{c}\right),$$

so that $2lcE_1\ 3e^2$ is equal to $\frac{2}{3}\left(1+\frac{2b}{c}\right)$.

Values of this quantity are indicated in fig. 3 by the straight line marked E_1, which, while it agrees approximately with the N_1 curve over most of its length, coincides with it at only one point, viz. the point for which $b=c$, at which the E_1 line touches the curve. The difference is greatest at $b=0$ ($r=\infty$), and the reason for the divergence at this point is evident. When x is infinitely far from y and z its amplitude in the first mode is zero, and the mutual energy of the system in this mode is equivalent to two quanta instead of three. In fig. 3 therefore the value of N_1 for $b=0$ should be reduced by one-third, which brings the N_1 and E_1 curves into agreement at this point. As x approaches y and z from infinity the system changes from a state in which two of the particles are vibrating in the mode $a+c$ (the third being in its undisturbed mode a) to one in which all three particles are vibrating in the mode $a+2c$ which exists when $b=c$. In these two states the mutual vibrational energy is equal to the electrostatic energy if the charge has the usual value (9), but the question is as to the manner in which the system changes from one of these states to the other. It might be thought that as soon as b becomes appreciable the system changes suddenly and permanently from the state in which two only of the particles are vibrating in the mode $a+c$ to that in which all three are oscillating in the mode $a+N_1$, but this would involve an abrupt increase of the energy for which there is no apparent reason. It is more probable that if the mode $a+N_1$ appears when b is small it will not be permanent, but will give place to $a+c$ (two particles) again, and that the system will fluctuate

between the two modes until the mode $a+2c$ is established. During this period of unsteadiness the mutual energy fluctuates between the values $hc/2\pi\sqrt{a}$ and $3h\mathrm{N}_1/4\pi\sqrt{a}$, the average value increasing gradually, and it is suggested that this average value represents the electrostatic energy.

Another small discrepancy between the N_1 and E_1 curves appears when b is greater than c ($r<l$). It is greatest when $b=2c$, *i. e.*, when x is in the line yz, the value of N_1 then being $3{\cdot}372\,c$, that of $2lc\mathrm{E}_1/3e^2$ $3{\cdot}333\,c$. It may arise from the appearance of another partial oscillation (in the mode $a+b$ for example) which would have the effect of slightly altering the average value of the mutual energy. Otherwise, if such partial oscillation does not appear at this stage, the theory indicates a small departure of the charge from the usual value (9).

In the second mode x is opposite in sign to y and z, and the electrostatic energy is $\dfrac{e^2}{l}-\dfrac{2e^2}{r}$, so that $2lc\mathrm{E}_2/3e^2$ is equal to $\dfrac{2}{3}c\left(1-\dfrac{2b}{c}\right)$. This quantity is represented in fig. 3 by the straight line E_2. It will be seen that the N_2 and E_2 curves, while running generally parallel over the greater part of their length, do not come into contact. It is clear, however, that there are two configurations of the system in which the mutual energy agrees with the electrostatic energy, the charge having the usual value (9), viz. when $b=0$ and when $b=c$. In each of these states the mutual energy is confined to two of the particles instead of being shared by all three. In the former y and z are vibrating in the mode $a+c$ (which does not appear at all as a possible value of $a+\mathrm{N}_2$), the third particle x having its undisturbed frequency $\sqrt{a}/2\pi$. In the latter the two particles x and y (or x and z) are vibrating in the mode $a-c$, the third having no mutual energy with them, this being in fact the case, already considered, of three equidistant particles one differing in sign from the other two. It seems reasonable to suppose that in passing from one of these states to the other the system fluctuates between the first of these two modes and the mode $a+\mathrm{N}_2$, in which all three particles can simultaneously vibrate. The average mutual energy meanwhile changes gradually

from $hc/2\pi\sqrt{a}$ to $-hc/2\pi\sqrt{a}$, in accordance with the change of electrostatic energy which is from e^2/l to $-e^2/l$.

The range of the energy fluctuation is clearly greater in the second mode than that suggested in connexion with the first. The smallest value of the range occurs at $b=0$, and is represented in fig. 3 by $2c/3$ in the second mode and $c/3$ in the first.

We have seen that when $b=c$ the particle x vibrates with y or with z, or with the two alternately, in the mode $a-c$. It is probable that, since there is no sudden withdrawal of energy from the system, this kind of 2-particle vibration will continue when b is greater than c, the mode being now $a-b$, so that the system will fluctuate between this mode and $a+\mathrm{N}_2$, which now reappears as a possible mode of vibration of all three particles. In these conditions the energy of the system will fluctuate between that of two particles in the mode $a-b$ and that of three particles in the mode $a+\mathrm{N}_2$. The upper limit of this energy fluctuation is represented in fig. 3 by the straight line HK, the ordinate of which is $2b/3$. It is possible that the average value of the energy during these fluctuations represents the electrostatic energy when b is between c and $2c$.

It appears that in the theory of the oscillations of the 3-particle system there is in some of its configurations an indeterminateness in regard to the type of vibration existing at any particular time. It arises from the fact that partial oscillations can appear in the system which do not affect all three components, and which in some cases do not appear in the frequency equation of the whole system. The suggestion that these partial oscillations give rise to fluctuations in the mode of vibration of the system concerns of course the ordinary theory of the vibrations as well as the question of its possible application to the theory of electrostatic phenomena.

In the third mode of the system the frequency is independent of b, the value of N_3 being constant and equal to $-c$. This is represented in fig. 3 by the horizontal line N_3, which intersects the N_2 curve at the point for which $b=c$. In this configuration the second and third modes are of course equivalent. The mutual energy in the third mode is $-hc/2\pi\sqrt{a}$, which is equal to the constant electrostatic energy $-e^2/l$ if the charge has the normal value given by (9).

In a similar manner fig. 4 shows the relations for a system of four particles, one (x) at the vertex, the others at the ends of the base sides, of a triangular pyramid. The base side is $l(=k/c)$, and the height of the pyramid is supposed to vary from zero to infinity. If b is the coupling of x with any one of the other particles the frequency equation is .

$$(\mathrm{N}^2-2c\mathrm{N}-3b^2)(\mathrm{N}+c)^2=0,$$

Fig. 4.

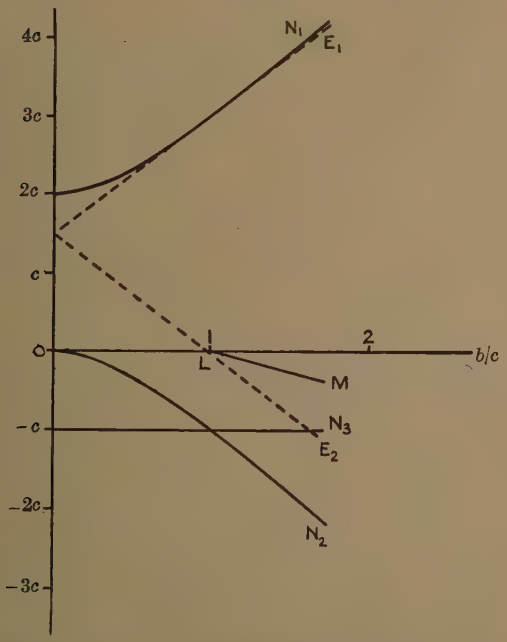

Frequency and energy curves for system of four particles.

and the four frequencies of the system are given by

$$n_1^2=a+\mathrm{N}_1,$$
$$n_2^2=a+\mathrm{N}_2,$$
$$n_3^2=n_4^2=a-c,$$

where N_1, N_2 are the positive and negative roots of the equation

$$\mathrm{N}^2-2c\mathrm{N}-3b^2=0.$$

The first mode corresponds to the case in which all four particles are of the same sign, the second to that in which the particle x at the vertex differs in sign from the other three.

The electrostatic energy in these two modes is

$$\left.\begin{matrix} E_1 \\ E_2 \end{matrix}\right\} = 3\frac{e^2}{l}\left(1 \pm \frac{b}{c}\right),$$

and the straight lines marked E_1, E_2, in fig. 4 represent values of $E_1 lc/2e^2$ and $E_2 lc/2e^2$, which would be equal to N_1 or N_2 if the energy $h(\nu_1 - \nu_0)$ or $h(\nu_2 - \nu_0)$ were possessed by each of the four particles, and if e^2 had the normal value $hk/2\pi\sqrt{a}$. The discrepancies between the N and E curves in the first and second modes in fig. 4 are similar to those seen in fig. 3, and are to be accounted for in a similar manner if b is less than c. When $b=c$ the particle x oscillates with any one of the three particles at the base in the mode $a-c$, the other two having the partial mode $a+c$. In this state the system has zero energy, as shown by the E_2 line intersecting the horizontal axis at this point.

When b is greater than c the particle x may (again owing to the absence of any sudden withdrawal of energy from the system) be supposed to continue to vibrate with one of the other three, now in the mode $a-b$, the other two continuing in the mode $a+c$, but $a+N_2$ reappears as a mode of the whole system, so that the energy fluctuates between that of two partial modes $a-b$, $a+c$, and that of four particles in the mode $a+N_2$. The upper limit of this energy fluctuation is indicated in fig. 4 by the straight line LM, the ordinate of which is $\frac{1}{2}(c-b)$. The lower limit is of course represented by the curve N_2. It is suggested that the average mutual energy during these fluctuations diminishes gradually and represents the electrostatic energy E_2.

The third and fourth modes of this system, $n_3^2 = n_4^2 = a-c$, indicate cases in which two of the particles at the base of the pyramid are of opposite sign, the other two having no mutual energy with them but oscillating as a partial system in the mode $a-b$ if they are unlike, or $a+b$ if they are similar in sign. In these cases the system must be divided into two parts, the mutual energy of each of which is equal to the electrostatic energy of the same part on the basis of equation (7) or (9).

The present communication is concerned with the question of the possibility of interpreting the electrostatic energy of systems of electrons in terms of the interactions of vibrating particles. The examples here given show that this kind of interpretation is suitable in many cases. Whether it is so in problems of a more general character is a matter for further enquiry.

Natural Philosophy Department,
The University, Glasgow.

XXIX. *Magnetic Studies on Graphite and Graphitic Oxides.* *By* N. Ganguli, *M.Sc., Research Scholar, Indian Association for the Cultivation of Science, Calcutta* *.

1. *Introduction.*

GRAPHITE crystal belongs to the hexagonal system and has a perfect basal cleavage. It occurs in nature in the form of thin plates parallel to the basal plane. The crystal exhibits remarkable magnetic and electrical properties. It has an abnormally large diamagnetic susceptibility along the hexagonal axis, its value, according to recent measurements by Guha and Roy †, being about -22×10^{-6}, whereas for directions in the basal plane the susceptibility is only $-0{\cdot}4\times10^{-6}$. The susceptibility of the other crystalline form of carbon, namely, diamond, is near about the latter value. Electrically graphite is a good conductor, whereas diamond is an insulator. These anomalous properties of graphite are presumably due to the characteristic layered lattice structure of the crystal, in which the weak bindings between the successive layers or networks of carbon atoms are of the metallic type (as contrasted with the three valencies of the carbon atoms in the plane of the network, which are homopolar). Any change in the structure of the crystal that would affect these metallic linkages may therefore be expected to have considerable influence on the abnormal diamagnetism. The well-known "swelling" of graphite on treatment with a

* Communicated by Prof. K. S. Krishnan, D.Sc.
† Ind. Journ. Phys. viii. p. 345 (1934).

mixture of concentrated nitric and sulphuric acids is one such, since the "swelling" is generally attributed to the creeping in of oxygen atoms between the carbon layers, which separate out (along the hexagonal axis) as a consequence, the metallic linkages between them being broken thereby. An indefinite diminution in the size of the crystal also conduces to a similar lateral expansion along the hexagonal axis.

The magnetic behaviour of graphite under these and other influences has been studied by us in detail, and an account of these studies is given in the following pages.

2. *The Magnetic Anisotropy of Graphite.*

Guha and Roy have measured the magnetic anisotropy of a number of well-developed single crystals of graphite. Their method of measurement was the same as that described by Krishnan, Guha, and Banerjee in their recent papers *. The crystal is suspended with its basal plane vertical in a uniform magnetic field, at the end of a fine quartz fibre attached to a graduated torsion-head. The crystal tends to bring its basal plane to parallelism with the field, showing that the specific susceptibility of the crystal along directions in the basal plane, say $\chi_\perp$, is greater (algebraically) than that along the vertical axis, $\chi_{||}$. The torsion-head is suitably rotated, so that in the natural setting position of the crystal in the field the torsion of the fibre is zero. If now the torsion-head is rotated from this position slowly, for some position of it the crystal would suddenly turn round. This corresponds to an inclination of the plane of the crystal at 45° to the direction of the field, since in this position the couple due to the field, acting on the crystal, passes through a maximum value, equal to $\frac{1}{2}m\mathrm{H}^2(\chi_\perp-\chi_{||})$, where m is the mass of the crystal and H is the field. If α is the angle through which the torsion-head has been rotated from its initial position corresponding to zero torsion, it is evident that the above maximum couple due to the field will be equal to $c(\alpha-\pi/4)$, where c is the torsional constant of the fibre. Therefore

$$\chi_\perp-\chi_{||}=\frac{(2\alpha-\pi/2)c}{m\mathrm{H}^2} \quad . \quad . \quad . \quad . \quad . \quad . \quad (1)$$

* Phil. Trans. A, ccxxxi. p. 235 (1933); ccxxxii. p. 99 (1934); ccxxxiv. p, 265 (1935).

By rotating the torsion-head in both the clockwise and the anticlockwise directions, α can be accurately determined, and therefore $\chi_\perp - \chi_{||}$.

In view of the importance of this quantity the measurements were repeated by us with a large number of specially chosen crystals. The values of $\chi_\perp - \chi_{||}$ obtained in these measurements were slightly different for different crystals, and ranged from 21×10^{-6} to 22×10^{-6} per gm. They are in agreement with the values obtained by Guha and Roy.

3. *Susceptibility of Graphite along Directions in the Basal Plane.*

$\chi_\perp - \chi_{||}$ being now known, if we can measure in addition the absolute value of either $\chi_\perp$ or $\chi_{||}$ both of them are known. Since $\chi_\perp$ is numerically very much smaller than $\chi_{||}$ it is desirable to choose $\chi_\perp$ for this measurement.

An accurate measure of $\chi_\perp$ is difficult to obtain, for the following reasons. We have to use the natural crystals, and even the best ones contain traces of iron, which would tend to lower slightly their diamagnetism. Any imperfection in the crystal—the crystal flakes, being flexible, are easily liable to distortion—will, on the other hand, tend to raise numerically the value of $\chi_\perp$ at the expense of $\chi_{||}$.

We have measured $\chi_\perp$ for some fifteen crystals. Since our crystals were found to be slightly more diamagnetic along this direction than those measured by Guha and Roy, we had to adopt a different method of measurement from theirs. The present measurements were made with a magnetic balance of the Curie type. The balance consisted of a long thin aluminium beam suspended from a torsion-head by means of a thin phosphor-bronze strip about 30 cm. long. The point of attachment of the suspension strip to the beam was considerably to one side of its centre, so that the lengths of the two arms were very different. The crystal was suspended by a long stout glass fibre from the end of the longer arm in the manner to be described below. A small brass weight sliding on the shorter arm served to keep the beam horizontal. A mirror attached to the phosphor-bronze

strip near its lower end served, with the usual reflecting arrangements, for the measurements of the rotation of the beam. The crystal was suspended in the centre of a Curie non-homogeneous magnetic field in such a manner as to have its plane vertical and along the direction of the field and normal to the direction of the gradient of the field. The beam of the torsion balance was in the vertical plane of the crystal flake.

When the field was put on, the crystal naturally moved laterally along the direction of the field gradient. and could be brought back to its original position by a suitable rotation of the torsion-head, the latter rotation θ giving a measure of the lateral force acting on the crystal. The crystal was then replaced by a thin plate of glass of about the same dimensions, having a volume susceptibility of about $-0{\cdot}4\times10^{-6}$, which could be determined easily by the modified Rabi method * by magnetically balancing it with a suitable aqueous solution of potassium chloride or iodide. The glass plate was adjusted to occupy exactly the same position as was originally occupied by the graphite flake. When the field was put on, the glass plate moved laterally, and the torsion-head was suitably rotated in the same manner as before so as to bring the plate to its original position corresponding to zero field. Let θ_0 be the angle in this case. If m be the mass of the graphite, and if m_0 be the mass, ρ the density, and k the *volume* susceptibility (determined by the Rabi method), of the glass plate, then the *specific* susceptibility of graphite along its plane is plainly given by the relation

$$\chi_\perp = \frac{m_0\theta}{m\theta_0}\times\frac{k}{\rho} \quad . \quad . \quad . \quad . \quad . \quad . \quad . \quad (2)$$

Some fifteen crystals of graphite were measured by this method, and the values of $\chi_\perp$ ranged from $-0{\cdot}49\times10^{-6}$ to $-0{\cdot}51\times10^{-6}$. We may therefore adopt the value

$$\chi_\perp = -0{\cdot}50\times10^{-6} \text{ per gm.}$$

Combining this result with that obtained in the previous section we obtain the following values for the two principal susceptibilities of graphite :—

$$\chi_{\parallel} = -22\times10^{-6} \text{ per gm.,}$$
$$\chi_\perp = -0{\cdot}5_0\times10^{-6} \quad ,,$$

* See Krishnan, Guha, and Banerjee, *loc. cit.*

4. *The Principal Susceptibilities of Fine Graphite Particles by the Goetz Method.*

It has been found by Paramasivan *, Vaidyanathan †, and others ‡, working with graphite powder, that as the size of the particles diminishes the susceptibility of the powder also diminishes numerically. For extremely fine particles, *e. g.*, colloidal carbon or soot, the susceptibility is only $-0{\cdot}5\times10^{-6}$ per gm. This would mean that the mean susceptibility of a single crystal of graphite, namely $(\chi_{\parallel}+2\chi_{\perp})/3$, which has a value $-\frac{22+2\times0{\cdot}5}{3}=-7{\cdot}7\times10^{-6}$ per gm. when the size of the crystal is large, comes down to $-0{\cdot}5\times10^{-6}$ for an extremely small particle. It would be of great interest to determine how the principal susceptibilities $\chi_{\perp}$ and $\chi_{\parallel}$ of the crystal individually vary with the size of the crystal.

The changes in susceptibility begin to be appreciable only when we go to sizes below about $2\,\mu$. For particles of this size the method of measurement described in the previous section is evidently not applicable. There is an elegant method devised by Goetz § which can be adopted for measurements with such small particles. His method is as follows. The fine particles are dispersed in a gelatine solution, which is allowed to solidify in the presence of a strong uniform horizontal magnetic field. The individual crystallites of graphite will naturally set themselves with their basal planes parallel to the field. If, further, during this process of solidification of the gelatine solution in the field, the containing vessel is kept rotating slowly about a vertical axis, all the crystallites will have their planes horizontal ||. The resulting solid will therefore contain embedded in it a number of graphite particles oriented in the same manner, and by measuring the susceptibility of this solid along the crystallite planes and along the normal to the planes, and correcting for that of the medium, the principal susceptibilities of the particles $\chi_{\perp}$ and $\chi_{\parallel}$ can be calculated.

* Ind. Journ. Phys. iv. p. 139 (1929).
† 'Nature,' cxxiv. p. 762 (1929); and cxxv. p. 820 (1930); also Ind. Journ. Phys. v. p. 559 (1930).
‡ Ramachandra Rao, Ind. Journ. Phys. vi. p. 241 (1931).
§ Phys. Rev. xl. p. 1053 A (1932).
|| Goetz, Phys. Rev. xlv. p. 282 (1934).

We have determined by this method the susceptibility of very finely powdered carbon. Molten paraffin was found to be a suitable medium for the dispersion of the particles. A specimen of spectroscopic carbon from Adam Hilger, of known purity, was finely powdered and dispersed in the molten paraffin, in a narrow vertical test-tube, which was kept rotating slowly about its axis in a large uniform horizontal magnetic field, and slowly allowed to cool. The paraffin cylinder containing oriented particles was then detached from the tube by breaking the latter and divided into shorter cylinders. The principal susceptibilities of these cylinders were measured as follows :—(1) By suspending the cylinder with its axis horizontal its magnetic anisotropy was determined by the same method as was described in Section 2 ; (2) the absolute susceptibility along a direction perpendicular to the axis of the cylinder was determined by the Rabi method. Similar measurements were made for also pure paraffin solidified in the same manner in the magnetic field. This is necessary in order to correct for any feeble anisotropy that may be developed in pure paraffin due to its solidification in the magnetic field.

Suppose that m gm. of the mixture contains m_g gm. of carbon and $m-m_g$ gm. of paraffin. Let ρ be the density of the mixture and ρ_p that of pure paraffin, k the volume susceptibility of the mixture, k_p that of pure paraffin (determined by the Rabi method). Then the specific susceptibility of graphite for the particular direction, viz., $\chi_\perp$ is given by the relation

$$\chi^\perp = \frac{1}{m_g}\left[\frac{mk}{\rho} - \frac{(m-m_g)k_p}{\rho_p}\right] \quad . \quad . \quad . \quad . \quad (3)$$

In one experiment ·2081 gm. (m) of the mixture contained ·0094 (m_g) gm. of carbon. The values of the other quantities were

$\rho = \cdot 913, \quad \rho_p = \cdot 892$;

$k = -0{\cdot}652 \times 10^{-6}$ per c.c., $k_p = 0{\cdot}646 \times 10^{-6}$ per c.c.

Therefore

$$\chi_\perp = -0{\cdot}5 \times 10^{-6} \text{ per gm.}$$

Measurements on the magnetic anisotropy of the same paraffin-carbon block gave, after correcting for the

feeble anisotropy developed in pure paraffin allowed to solidify similarly in the magnetic field, for the carbon

$$\chi_{\perp}-\chi_{\parallel}=0{\cdot}4\times10^{-6} \text{ per gm.}$$

Thus we obtain for the spectroscopic carbon

$$\chi_{\parallel}=-0{\cdot}9\times10^{-6} \text{ per gm.,}$$

$$\chi_{\perp}=-0{\cdot}5\times10^{-6} \quad ,,$$

5. *The Principal Susceptibilities of "Blue Graphite."*

A small well-developed single crystal of graphite was weighed, and its two principal susceptibilities were measured as described in the previous sections. The crystal was then treated with a mixture of concentrated sulphuric and nitric acids for some hours. In some of the experiments pinches of powdered potassium chlorate were added to the acid mixture from time to time. As is well known the crystal undergoes some remarkable changes during this treatment; it swells up, loses its brilliancy, and the colour changes from black to green, and finally to blue, in reflected light. The resulting piece of "blue graphite" retained more or less the same shape as the original crystal of graphite. It was taken out of the acid mixture, washed in running water for over twelve hours, and, after preliminary drying, was kept in a dessicator for a day.

The principal susceptibilities were now measured in the same manner as described in the previous sections, and compared with the corresponding values for the same crystal before the acid treatment.

The results for three crystals treated with $HNO_3+H_2SO_4$ are given in the following table :—

TABLE I.

No. of crystal.	Wt. in milligrams. Before treatment.	Wt. in milligrams. After treatment.	Period of treatment.	Magnetic constants $\times 10^6$ per gm. For graphite. $\chi_{\perp}-\chi_{\parallel}$.	For graphite. $\chi_{\perp}$.	For blue graphite. $\chi_{\perp}-\chi_{\parallel}$.	For blue graphite. $\chi_{\perp}$.
			hours.				
1 ...	52	71	7	21	−0·50	0·93	−0·5
2 ...	25	34	12	21	−0·50	0·91	−0·5
3 ...	11	15	18	21	−0·50	0·92	−0·5

A study of the X-ray diffraction of these crystals showed in the first place that they were practically single crystals; the diffraction pattern was similar to that of untreated graphite, except that the $(00l)$ spacings were much greater in blue graphite than in graphite.

Thus, for directions in the basal plane, the specific susceptibility of "blue graphite" is the same as that of graphite before treatment. On the other hand, along the vertical axis of the crystal the abnormal susceptibility is almost completely destroyed.

It should be mentioned here that, although the magnetic anisotropy, $\chi_\perp - \chi_{||}$, of "blue graphite" is less than one-twentieth of that of graphite, it is by no means small when compared with that of other diamagnetic substances. In fact with reference to the latter substances the anisotropy of blue graphite should be considered quite large.

For later theoretical discussions it would be more convenient to express the value of $\chi_\perp - \chi_{||}$ for blue graphite *in terms of its carbon content*; the values given in the table would then correspond to

$$\chi_\perp - \chi_{||} = 1{\cdot}2 \text{ to } 1{\cdot}3 \times 10^{-6} \text{ per gm. content of carbon.}$$

Two crystals of graphite were also treated with a mixture of $HNO_3 + H_2SO_4 + KClO_3$. The resulting blue graphite had practically the same magnetic constants as the other specimens, viz.,

$$\chi_\perp = -0{\cdot}5 \times 10^{-6} \text{ per gm. of blue graphite,}$$

$$\chi_\perp - \chi_{||} = 1{\cdot}2 \times 10^{-6} \text{ per gm. content of carbon in blue graphite.}$$

6. *Magnetic Susceptibility of Graphitic Acid.*

Further oxidation of graphite, as is well known, converts it into the brown graphitic acid. With graphite crystals of the usual small size the oxidation does not proceed very far beyond the "blue" stage, and in order to facilitate further oxidation we have to start with very finely powdered graphite. The resulting graphitic acid is not soluble to an appreciable extent in any of the usual solvents. Hence it was not possible to study the magnetic properties of single crystals of this substance, and measurements were confined to the powder only.

A specimen of graphitic acid obtained from Messrs. Fraenkel and Landau, Berlin, was freed from iron by repeated treatment with concentrated hydrochloric acid. The powder was washed thoroughly and dried.

The magnetic susceptibility of the powder was determined by the Gouy method, by weighing the dry powder packed uniformly in a long narrow test-tube of uniform bore, in a magnetic field, and comparing it with the weight due to the field acting on water contained in the same test-tube suspended under the same conditions in the field.

The specific susceptibility of the powder of graphitic acid was found to be

$$-0{\cdot}54\times10^{-6} \text{ per gm.}$$

7. *The Abnormal Unidirectional Diamagnetism of Graphite.*

In this and the following sections we shall attempt to correlate the experimental results with the structure of the crystals. Considering firstly graphite, the most striking result is its abnormal diamagnetism along the vertical axis, viz., -22×10^{-6} per gm. Along perpendicular directions the susceptibility of graphite is quite normal, $-0{\cdot}50\times10^{-6}$ per gm., which is almost exactly the same as that of diamond, $-0{\cdot}49\times10^{-6}$.

The abnormal diamagnetism of graphite along the vertical axis may be attributed, as was mentioned in the introduction, to the peculiar structure of the crystal. The carbon atoms are closely packed in the basal planes in the form of a regular hexagonal network, the distance between adjacent C-atoms in the plane, equal to the side of the hexagon, being 1·42 Å. The successive layers of carbon atoms, however, are widely separated, the distance between them being 3·41 Å. The C-atoms in alternate layers are exactly above and below one another, while the atoms in adjacent layers are so disposed that half the atoms in each layer are above half the atoms in the layer below, the other half being directly above the centres of the hexagons of the lower layer. Thus three of the valencies of the carbon atom are in the basal plane and are equivalent, and they are generally taken to be homopolar. The fourth valencies, which feebly link together the successive layers, are supposed to be of the

" metallic " type, *i. e.*, the corresponding electrons are more or less free *. Hofmann and others have suggested that each layer of carbon atoms is a metallic poly-ion and that the different layers are held together by the metallic electrons as in metals. Further, if we assume that these metallic electrons in graphite are capable of easy displacement in the basal plane but not in the perpendicular direction, then under the influence of a magnetic field incident along the hexagonal axis these electrons will precess, in the Larmor sense, in very large orbits, and thus the abnormal diamagnetism along the hexagonal axis is explained.

We have mentioned that graphite is a good conductor of electricity. This is to be expected from the presence of free electrons. If, however, as we have assumed, these metallic electrons are capable of easy displacement in the basal plane and not along the perpendicular direction, we should expect the conductivity of graphite to be large only when the electric current is in the basal plane. This result has not been directly verified. It is known, however, that while the electrical resistivity of powdered graphite is 140×10^{-5} ohm-cm., that for the single crystal, when the electric current is along directions in the basal plane, is much smaller, namely, 3·9 to $6\ 0 \times 10^{-5}$ ohm-cm.

8. *The " Swelling " of Graphite.*

The " swelling " of graphite under the action of various oxidizing agents has been studied by Hofmann †, Thiele ‡, and others §. There is considerable difference of opinion regarding the nature of the chemical reaction that takes place, specially with reference to the question whether any definite compound is formed. Recent chemical and X-ray studies by Hofmann, however, show definitely that during this reaction oxygen atoms creep between the network of carbon atoms, the distances between adjacent layers increasing as a consequence, and thus leading to the swelling. Due to the introduction of these oxygen atoms the metallic linkages

* See U. Hofmann and A. Frenzel, *Koll. Zeit.* lviii. p. 8 (1932).
† *Koll. Zeits.* lxi. p. 297 (1932).
‡ *Koll. Zeits.* lxvi. p. 129 (1931).
§ For a good account of the subject see C. H. Desch's ' Chemistry of Solids ' (1934), p. 180, or J. T. Randall's ' Diffraction of X-rays ' (1934), p. 192.

between adjacent carbon layers will be broken, the electrons released thereby being probably utilized now in binding chemically or quasi-chemically the oxygen atoms to the carbons. This would be equivalent to freezing the metallic electrons of the original graphite, and would therefore tend to quench the abnormal diamagnetism. This is probably the explanation of the very much smaller anisotropy of blue graphite as compared with that of graphite.

It should be remarked here that the change in the diamagnetism of graphite on oxidation cannot be due to the para-magnetism of the oxygen, which goes into combination, since the diminution of the diamagnetic susceptibility is almost wholly along the vertical axis, the diamagnetism along directions in the basal plane remaining unaltered. Conversely this experimental result suggests that the contribution of the oxygen which goes into combination with graphite to form blue graphite is either very feebly paramagnetic, or diamagnetic as in organic compounds. (Pascal's value for oxygen in organic compounds is $-4{\cdot}6\times10^{-6}$ per gm. atom.)

9. *The Magnetic Anisotropy of Blue Graphite compared with that of Condensed Benzene Nuclei.*

Recent X-ray investigations by Robertson and others show that in aromatic hydrocarbons containing condensed benzene nuclei, *e. g.*, anthracene, chrysene, 1·2 ; 5·6-dibenzanthracene, the benzene rings have a regular hexagonal structure, the size of the hexagon being practically the same as that of the hexagonal network of carbons in graphite. If in blue graphite there is no abnormal diamagnetism due to free electrons its magnetic anisotropy should be characteristic of the network of carbon atoms, and the question naturally arises how this anisotropy compares with that of organic molecules containing several condensed benzene nuclei.

Krishnan and Banerjee have studied the magnetic anisotropy of a number of such hydrocarbons in the crystal state, and have given in their paper * values for the principal susceptibilities of the molecules of these hydrocarbons. They find that the two principal susceptibilities in the plane of the molecule are nearly equal

* In course of publication in Phil. Trans. A.

and numerically much smaller than that along the normal to the plane. We shall denote the former two susceptibilities of the molecule by k_1 and k_2 ($k_1=k_2$), and the latter by k_3. The values of the k's for some typical molecules, taken from Krishnan and Banerjee's paper, are given in the following table :—

TABLE II.

Magnetic Anisotropies of Molecules containing Condensed Benzene Nuclei. The unit for the k's is 10^{-6} c.g.s. e.m.u.

Molecule.	Per gm. molecule.			Per gm. atom of carbon.
	$k_1=k_2$.	k_3.	k_1-k_3.	k_1-k_3.
Benzene (C_6H_6)	−37	−91	54	9
Naphthalene ($C_{10}H_8$) ..	−41	−187	146	15
Anthracene ($C_{14}H_{10}$)...	−49	−273	224	16
Phenanthrene ($C_{14}H_{10}$).	−74	−240	166	12
Chrysene ($C_{18}H_{12}$)	−88	−306	218	12
Pyrene ($C_{16}H_{10}$)	−81	−303	222	14

The figures given in the last column vary naturally from molecule to molecule, but they give us an idea of the value to be expected for a molecule containing many close-packed benzene rings. We can easily see that the value obtained by us for "blue graphite," namely $1{\cdot}2$ to $1{\cdot}3\times10^{-6}$ per gm. content of carbon, which would be equal to 15×10^{-6} per gm. atom of carbon, is quite consistent with this value.

10. *Graphitic and Mellitic Acids.*

The influence of further oxidation to graphitic acid on the anisotropy could not be followed, since single crystals of graphitic acid could not be obtained. An attempt to measure the anisotropy of graphitic acid by the Goetz method also did not give consistent results ; the anisotropy, however, is lower than that of blue graphite for the same carbon content. This result would seem to suggest that at these stages of oxidation, besides the breaking up of the metallic bindings which

have already occurred at the earlier stages of oxidation, there is a tendency for some of the co-valent links in the basal plane also to break up, and for the hexagonal network of carbons to separate into discrete benzene rings, for which the anisotropy would be much smaller, namely, 9×10^{-6} per gm. atom of carbon or $0{\cdot}75\times10^{-6}$ per gm. of it.

The end product of the oxidation is the well-known mellitic acid. Though this compound is freely soluble in water attempts to prepare crystals of this compound have also not been successful.

11. *Dependence of the Anisotropy of Graphite on Particle Size.*

We have referred in an earlier section to the work of Paramasivan and others, which show a diminution in the diamagnetism of graphite powder with particle size. Our measurements by the Goetz method give for spectroscopic carbon a mean susceptibility of $-0{\cdot}6\times10^{-6}$, as compared with $-7{\cdot}7\times10^{-6}$ for large crystals of graphite, thus supporting Paramasivan's conclusions. We further find that for the block of oriented crystallites in paraffin obtained by the Goetz method, $\chi_\perp$ has the value $-0{\cdot}5\times10^{-6}$, which is practically the same as for large-sized crystals ; it is only $\chi_{||}$, which has an abnormal diamagnetism of -22×10^{-6} for large crystals, which comes down, viz., to $-0{\cdot}9\times10^{-6}$. The following observations also support this conclusion. A few fine particles of graphite were dispersed in a concentrated aqueous solution of potassium iodide, of susceptibility $-0{\cdot}9\times10^{-6}$ per c.c., contained in a narrow tube of about 2 mm. diameter. This tube was kept in a strongly inhomogeneous magnetic field obtained between the usual conical pole pieces of the electromagnet brought very close together. Watching a small crystallite under the microscope and putting on the field the particle was found to turn round and move away from the central or strongest part of the field. This shows that for the direction which sets along the field, namely, in the basal plane, the crystallite is diamagnetic with reference to the solution—that is, its $\chi_\perp$ cannot be numerically less than $0{\cdot}9\times10^{-6}$ per c.c. Since the density of graphite $=2{\cdot}3$ this would mean that for the crystallite $\chi_\perp$ should be numerically greater

than $0{\cdot}4\times10^{-6}$; and the value $-0{\cdot}5\times10^{-6}$ obtained by the Goetz method is therefore consistent with it.

12. *Influence of Swelling and of Diminution of Crystallite Size compared.*

Thus the effect of diminution of particle size is very similar to that of swelling. In both cases the susceptibility in the basal plane remains practically unaffected, while it is the abnormal diamagnetism along the "*c*"-axis that is almost completely destroyed. The connexion between the two phenomena is probably closer than is apparent at first sight. Randall and Rooksby * find, from a study of the X-ray diffraction of fine carbon, that as the size of the particle diminishes the spacing along the "*c*"-axis, *i. e.*, between the adjacent carbon layers, increases, and they suggest that this is due to a weakening of the fourth valency of carbon. Of course the particles that they have experimented with are very much smaller in size than the ones we are considering here, but the effect may be present in a small degree in the larger crystallites also. If this view is correct the influence of diminution of particle size and that of "swelling" on the abnormal diamagnetism of graphite are due to essentially the same cause, namely, the breaking up of the feeble metallic linkages.

Summary.

The principal susceptibilities of graphite crystal along its vertical axis and along directions in the basal plane have been measured and are found to be equal to -22×10^{-6} and $-0{\cdot}5\times10^{-6}$ respectively per gm.

When the crystal is treated with a mixture of concentrated sulphuric and nitric acids to form "blue graphite" the abnormal diamagnetism along the vertical axis is nearly destroyed, whereas the diamagnetism along directions in the basal plane remains practically unaltered.

The anisotropy of "blue graphite" is found to be of the same order of magnitude as in aromatic molecules containing several condensed benzene nuclei, viz., $1{\cdot}3\times10^{-6}$ per gm. content of carbon.

A diminution in the size of graphite particle has nearly the same effect as oxidation, namely, to destroy the

* Randall, *loc. cit.* p. 192.

abnormal diamagnetism along the vertical axis without appreciably affecting that along directions in the basal plane.

The above quenching of the abnormal diamagnetism of graphite along the vertical axis on oxidation or on diminution of particle size may be attributed to a breaking up of the metallic linkages in graphite which are responsible for its abnormal diamagnetism.

In conclusion, I wish to express my very sincere thanks to Prof. K. S. Krishnan for suggesting the problem and for his continued help and interest throughout the progress of the work.

210 Bowbazar Street, Calcutta.
30th April, 1935.

XXX. *The Application of Debye's Theory of Polar Molecules to Solid Dielectrics.* *By* B. J. O'Kane, *Ph.D., B.Eng.* (*From the Department of Electrical Engineering, University of Liverpool* *.)

Summary.

The paper deals with the results of tests on three fatty acids—palmitic, oleic, and stearic. The variation of power factor and permittivity with temperature at constant frequency and with frequency at constant temperature are shown. The frequency range was from 11,000 cycles per second to 12·5 megacycles per second. Measurements of the D.C. conductivity were also taken. The Debye dipole theory has been shown to be applicable to certain solid non-crystalline dielectrics by Gemant [4], assuming that the substance has a finite viscosity. It was found that if the ordinary expression giving the ratio between the viscosities of liquids at different temperatures was applied in the expression given by Debye for the power factor of a dielectric, in terms of the internal viscosity of the medium in which the dipole is assumed to move, that the calculated curves for variation of power factor with temperature agreed closely with those obtained by experiment both for the pure oleic acid and

* Communicated by Prof. E. W. Marchant, D.Sc., F.C.G.I.

for mixtures of oleic and palmitic, and oleic and stearic acids. It would appear, therefore, that there is some property of the substance analogous to the macroscopic viscosity of liquids which obeys the ordinary rules for variation with temperature. With this assumption the Debye theory can be applied to solid dielectrics.

Introduction.

IN the past few years a great deal of research has been carried out in order to arrive at some theory to explain the anomalous behaviour of dielectrics in an electric field. Two papers have been published giving a *résumé* of the work done and the conclusions that may be drawn from the experiments [1] [2]. The theory which would appear to explain the various phenomena most satis-

Fig. 1.

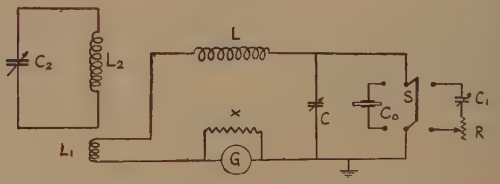

factorily is that put forward by Debye [3]. This postulates the presence in the dielectric of permanent electric dipoles which become orientated on the application of a field. Work on liquid dielectrics has led to an extensive knowledge of their behaviour, but there has been very little work done on solid dielectrics. In the present paper the results of tests on materials of known chemical constitution are given showing the variation of power factor and permittivity with temperature and frequency. The substances used were the pure fatty acids, palmitic, oleic, and stearic. Palmitic and stearic acid are solid at room-temperature, oleic being liquid.

Apparatus.

The measurements were carried out by the substitution method [4]. The circuit diagram is shown in fig. 1. The electrode assembly was contained in a large screening

box (fig. 2) which was adapted for use in the temperature measurements. The box itself was placed in a large wooden container and lagged with about two inches of granulated cork. The higher temperatures were produced by the heater elements A, B, of the ordinary type. The hot air flowed upwards behind the baffle-plates C, D, and was deflected down on to the sample from the lid

Fig. 2.

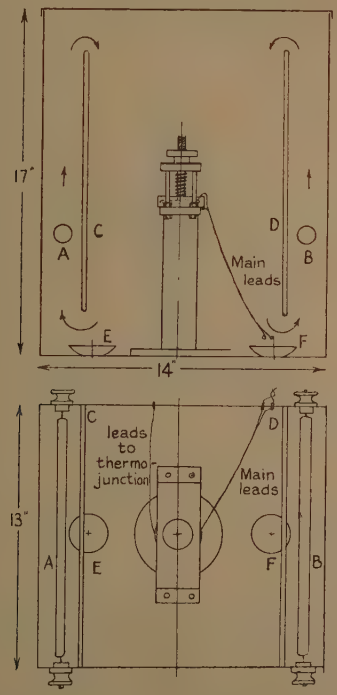

of the box. In this way a uniform heat flow could be attained. The low temperatures were eventually found to be most satisfactorily obtained by the use of solid carbon dioxide. As there was a danger of this dissolving in the acids it was placed in two flat tins which were connected to each other and to a pipe leading out to the atmosphere. The tins were so arranged that they dropped

down behind the two baffles C, D, and so did not disturb the screening arrangements. A dish of calcium chloride was placed in the large box to absorb the moisture deposited as the air in the tin cooled down.

The test electrodes are shown in fig. 3. The plates CC′ are of brass, silver-plated to withstand the action of the acids. The distance pieces BB′ and the threaded rod R are also of brass, thus making the whole assembly self compensating for changes in temperature; for when the rod R and the plates CC′ expand the gap

Fig. 3.

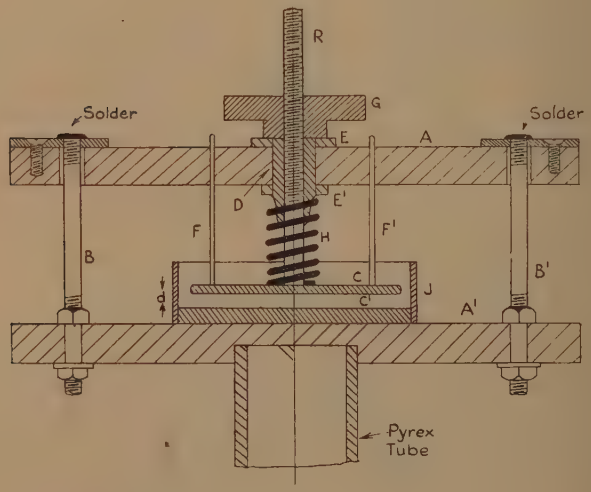

between the plates tends to diminish, but this effect is compensated by the tendency to increase the gap due to the expansion of BB′. The only error therefore is that due to the expansion of a length of brass equal to the gap width. The percentage change over a temperature range of 100° C. is therefore only $\frac{0{\cdot}00001\times 100\times 100\times d}{d}$ $=0{\cdot}1$ per cent. The cross-pieces AA′ are of seven-ply wood to prevent warping. G is a milled head for adjusting the gap and H a coil spring to maintain a pressure on the top plate. The rods FF′ prevent the top plate from rotating while adjustments are being made. The power

factor was determined from the difference in effective series resistance of the test condenser and the standard air condenser at resonance. The test condenser was first adjusted to a capacity equal to the capacity when the sample was in place. The effective series resistance of the test condenser as an air condenser was then measured. The difference between this and the resistance when the test condenser contained the sample gave the effective resistance of the sample. A correction was also made for any error in the measured capacity caused by the inductance of the leads, as the lay-out was not perfectly symmetrical. The current in the resonant circuit was indicated by a low-resistance Duddell thermo-galvanometer.

The substance was introduced into the test condenser by heating up the whole assembly to a temperature above the melting-point (in the case of palmitic and stearic acids) and then pouring in the liquid gently, keeping the condenser tilted to avoid trapping any air. The capacity was then adjusted by means of the milled head and the material allowed to cool down slowly. No trouble was experienced due to the formation of voids as the substance contracted. The same procedure was carried out in the case of the oleic acid. This, of course, could be introduced at room-temperature.

Results.

Fig. 4 shows the variation of power factor and permittivity with temperature at 6·3 and 12·5 megacycles per second for a sample of oleic acid which was badly oxidized. The curves in fig. 5 show the effect of oxidation. The original sample gave curve A, and after successive heatings in air the power factor gradually rose until it attained the values shown by curve C. The permittivity was not affected to the same extent. The temperature at which the power factor maximum occurs remains practically unaltered during the oxidation process. This agrees with previous work on this subject [6]. The oleic acid in the condition given by curve C, fig. 5, was then mixed with various proportions of stearic acid which had a very low loss. Any loss in the mixtures can therefore be taken to be due to the oleic acid only, and, if the mixtures are not heated to too high a temperature,

it can be assumed that the oleic acid will not oxidize any further.

Fig. 4.

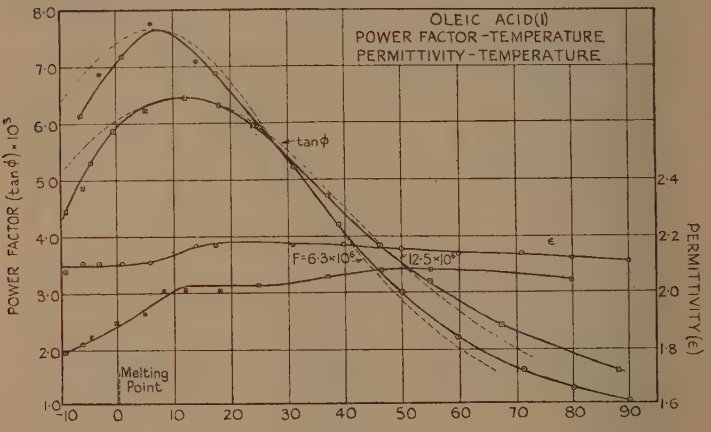

Fig. 5.

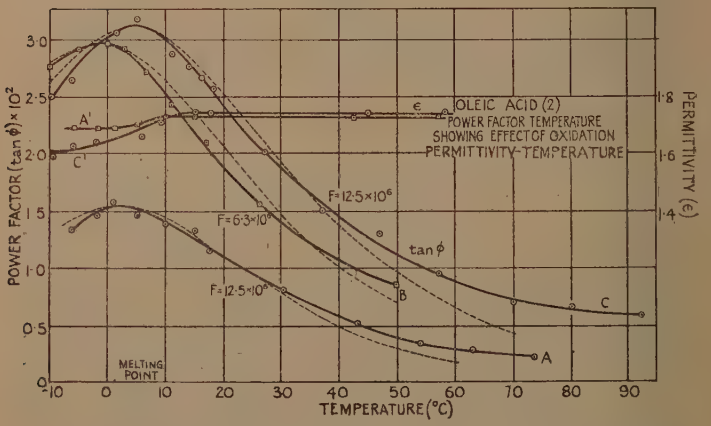

The variation of power factor with temperature for mixtures containing various percentages of oleic acid with stearic acid (ranging from 15 per cent. to 60 per cent.) are shown in figs. 6 and 7. Fig. 8 shows the variation of permittivity with temperature for mixtures of oleic

Fig. 6.

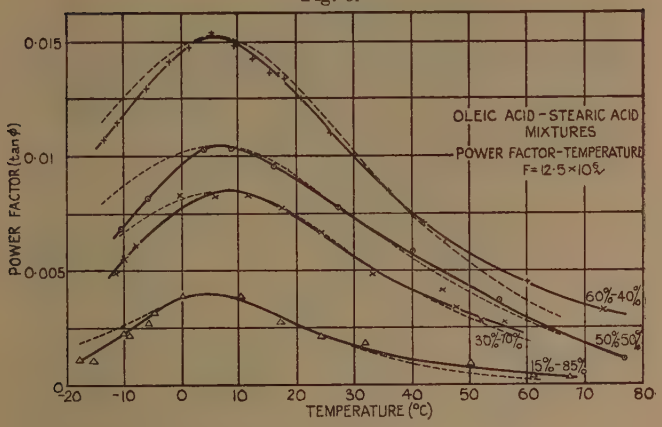

Fig. 7.

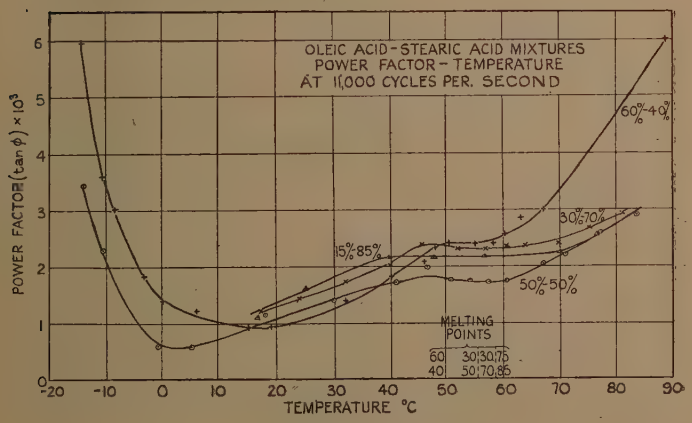

Fig. 8.

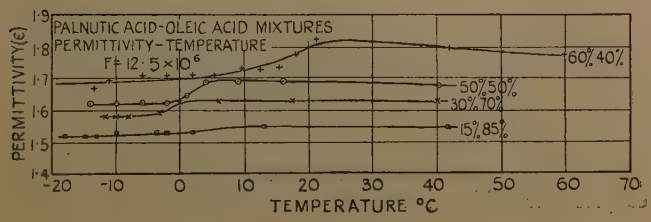

Fig. 9.

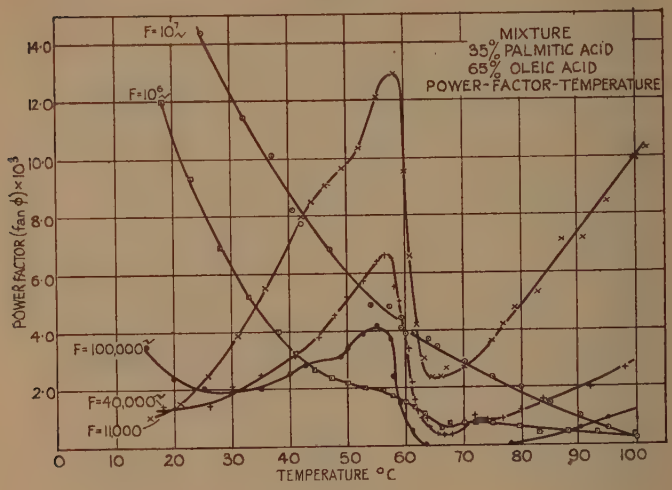

Fig. 10.

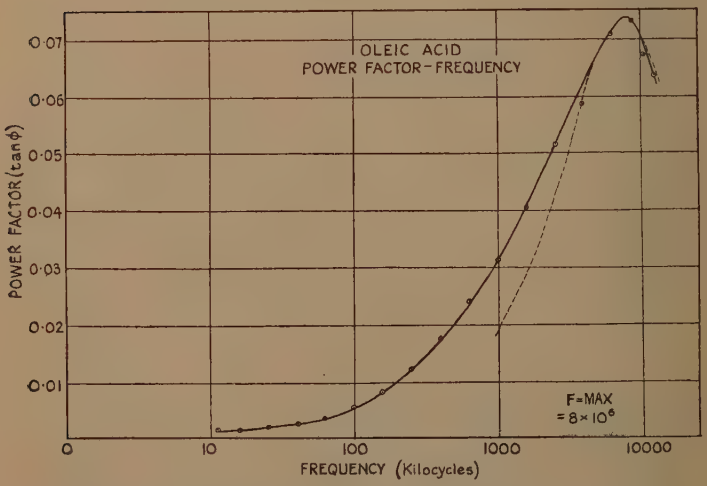

and palmitic acids at 12·5 megacycles per second. The variation of power factor with temperature for a mixture of palmitic acid and oleic acid is given in fig. 9.

Frequency-power factor curves are given in figs. 10, 11, and 12. Fig. 10 is for the oleic acid shown in fig. 4; fig. 11 is for a 60 per cent. oleic, 40 per cent. stearic mixture; and fig. 12 is for the palmitic-oleic mixture.

Fig. 11.

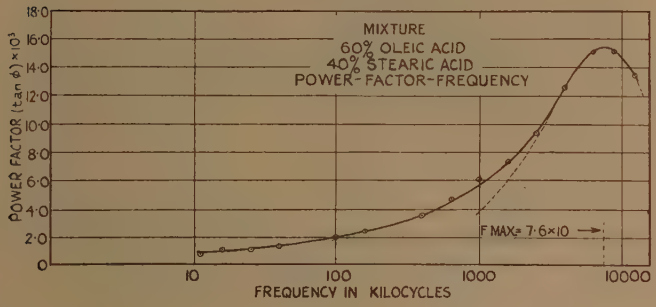

Fig. 12.

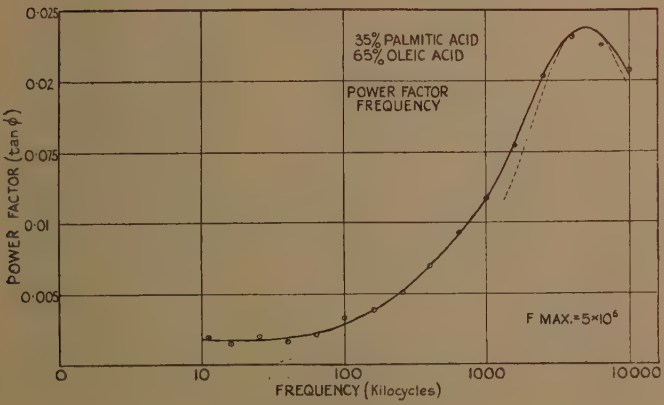

Discussion of Results.

In the Debye theory [3], as applied to liquid solvents, the polar molecule is assumed to be a sphere rotating in a viscous fluid. This has a characteristic frequency ν given by $\nu\tau = 1$, where τ is known as the relaxation time. τ is given by the equation

$$\tau = \frac{4\pi a^3 \eta}{kT},$$

where

a=radius of the polar molecule.

η=viscosity (or inner frictional constant) of the solvent.

T=absolute temperature.

k=Boltzmann's constant.

At the point where the maximum occurs in the power factor-frequency curve taken at constant temperature

$$\omega\tau = 1,$$

where

$$\omega = 2\pi f_{\max.}$$

and

$f_{\max.}$=frequency at which the maximum power factor occurs.

The value of this maximum can be shown to be

$$\tan\phi = \frac{\epsilon_1 - \epsilon_0}{2\sqrt{\epsilon_1\epsilon_0}},$$

where

ϵ_1=dielectric constant (or permittivity) at low frequencies,

and ϵ_0=dielectric constant at very high frequencies.

The same equation will hold for the power factor maximum when we consider the variation of power factor with temperature at constant frequency.

We can develop an equation to show the variation of power factor with frequency to determine whether it agrees with the observed results. The power factor is given by [3]

$$\tan\phi = \frac{(\epsilon_1 - \epsilon_0)x}{\epsilon_1 + \epsilon_0 x^2},$$

where

$$x = \frac{\epsilon_1 + 2}{\epsilon_0 + 2}\omega\mathrm{T}.$$

From this we obtain the relation

$$\tan\phi = \frac{\epsilon_1 - \epsilon_0}{\sqrt{\epsilon_1\epsilon_0}} \cdot \frac{\mathrm{C}\omega\mathrm{T}}{\mathrm{C}^2 + \omega^2\mathrm{T}^2},$$

where

$$\mathrm{C} = \sqrt{\frac{\epsilon_1}{\epsilon_0}\left(\frac{\epsilon_1 + 2}{\epsilon + 2}\right)}.$$

As there is no great difference between ϵ_0 and ϵ_1 we can say that C is approximately unity ;

$$\therefore \quad \tan \phi = \frac{\epsilon_1 - \epsilon_0}{\sqrt{\epsilon_1 \epsilon_0}} \cdot \frac{\omega T}{1+\omega^2 T^2},$$

but

$$\tan \phi_{max.} = \frac{\epsilon_1 - \epsilon_0}{2\sqrt{\epsilon_1 \epsilon_0}},$$

$$\tau = \frac{1}{2\pi f_{max.}},$$

and

$$\omega = 2\pi f ;$$

$$\therefore \quad \tan \phi = 2 \tan \phi_{max.} \times \frac{\frac{f}{f_{max.}}}{1+\left(\frac{f}{f_{max.}}\right)^2}$$

$$= 2 \tan \phi_{max.} \times \frac{f f_{max.}}{f^2_{max.} + f^2}.$$

The frequency curves (shown dotted) in figs. 10, 11, and 12 are calculated from this equation, the maximum height of the measured and calculated curves being made equal (*i. e.* = $\tan \phi_{max}$). It will be seen that the calculated curves fall below the observed curves as the frequency decreases. This is probably due to the fact that another source of loss, namely conduction, begins to have an effect at lower frequencies. Another possible explanation is that the whole of the molecule does not rotate, so that the conception of a rotating sphere will not be applicable.

The more interesting curves are those showing the variation of power factor with temperature at constant frequency. Although it is not possible to obtain an exact relation between power factor and temperature we can arrive at an approximate equation. It is difficult to define the meaning of the term " viscosity of the solvent" when we are dealing with a solid. Jackson [7] has used Debye's equations and obtains values for some variable which he calls the " apparent viscosity." This appears to behave in the same manner as the macroscopic viscosity, and it is proposed to use the ordinary equation for the variation of viscosity with temperature in calculating

the variation of power factor with temperature of the solid mixtures. This equation is

$$\frac{\eta}{\eta_m} = \sqrt{\frac{\mathrm{T}}{\mathrm{T}_m}}\, \epsilon^{c\frac{\mathrm{T}_m-\mathrm{T}}{\mathrm{T}_m\mathrm{T}}}$$

where η_m, T_m are the viscosity and temperature at any given temperature (in our case at the point of maximum power factor); η, T are the viscosity and temperature at any other point. Now we know that

$$\tan\phi = 2\tan\phi_{\max.} \times \frac{ff_{\max.}}{f_{\max.}^2+f^2},$$

but

$$f = \frac{k\mathrm{T}}{8\pi^2a^3\eta},$$

and

$$f_{\max.} = \frac{k\mathrm{T}_m}{8\pi^2a^3\eta_m},$$

$$\tan\phi = 2\tan\phi_{\max.} \frac{\frac{\mathrm{T}}{\eta}\frac{\mathrm{T}_m}{\eta_m}}{\left(\frac{\mathrm{T}_m}{\eta_m}\right)^2+\left(\frac{\mathrm{T}}{\eta}\right)^2}.$$

Dividing by $\left(\frac{\mathrm{T}}{\eta}\right)^2$,

$$\tan\phi = 2\tan\phi_{\max.} \frac{\frac{\eta}{\eta_m}\frac{\mathrm{T}_m}{\mathrm{T}}}{1+\left(\frac{\mathrm{T}_m}{\mathrm{T}}\frac{\eta}{\eta_m}\right)^2}.$$

Substituting for $\frac{\eta}{\eta_m}$,

we get

$$\tan\phi = 2\tan\phi_{\max.} \frac{\sqrt{\frac{\mathrm{T}_m}{\mathrm{T}}}\,\epsilon^{c\frac{\mathrm{T}_m-\mathrm{T}}{\mathrm{T}\mathrm{T}_m}}}{1+\epsilon^{2c\left(\frac{\mathrm{T}_m-\mathrm{T}}{\mathrm{T}\mathrm{T}_m}\right)}}.$$

Now, for small variations of T about T_m, assume that $\mathrm{T}=\mathrm{T}_m$, except in the difference $\mathrm{T}_m-\mathrm{T}$ let this difference be $-t$.

Then

$$\tan\phi = 2\tan\phi_{\max.} \frac{\epsilon^{-\alpha t}}{1+\epsilon^{-2\alpha t}},$$

where

$$\alpha = \frac{c}{TT_m},$$

$$\therefore \quad \tan\phi = \tan\phi_{max.} \frac{2}{\epsilon^{\alpha t} + \epsilon^{-\alpha t}},$$

$$= \frac{\tan\phi_{max.}}{\cosh \alpha t}.$$

By taking one or two points on the curve we can find an average value for α, and putting this in the equation, draw the theoretical curves. The calculated results are shown by the dotted curves in figs. 4, 5, and 6. It will be seen from the figures that the calculated values agree fairly closely with the observed values, even for the solid mixtures, at temperatures up to 50° C. The calculated curves tend to be lower than the observed ones as the temperature rises. This is due to the fact that the assumption $T = T_m$ leads to an appreciable error as the temperature difference increases.

It will be noted that in the case of the oleic acid alone (fig. 4), and for the mixtures (fig. 6). the calculated values are higher than the observed values below the melting-point of the oleic (2° C.). This is probably due partly to the solidification of the oleic acid and also to an alteration in the structure of the crystals on passing this point. In both cases the constant α would be affected.

The only explanation for the large changes in power factor at 60° C. (approximately the melting-point of the palmitic acid), shown in fig. 9 for the palmitic-oleic mixture, seems to be a change in conductivity. When, however, D.C. measurements were made the D.C. conductivity changed rapidly at 43° C. (the melting-point of the mixture), but did not show any unusual variation at 60° C. On the other hand, the fact that the discontinuity disappears as the frequency increases suggests that the changes are due to conduction effects. The magnitude of the sudden variation in power factor is plotted against frequency in fig. 13, showing how it decreases as the frequency rises.

A similar effect is seen in fig. 7, which gives the variation of power factor with temperature for the mixtures of oleic and stearic at 11,000 cycles per second. In this case the curve does not fall steeply at the melting-point

of the stearic, but instead flattens out. The length of the horizontal portion decreases as the amount of oleic acid present increases, showing that the irregularities are due to the presence of the stearic acid. It was found that at 4×10^5 cycles per second the irregularities had disappeared and the curve was quite smooth, which is in agreement with the explanation given above.

It is interesting to calculate the change $\epsilon_1-\epsilon_0$ from the observed value of the power factor maximum, using the formula

$$\tan\phi_{\max.}=\frac{\epsilon_1-\epsilon_0}{2\sqrt{\epsilon_1\epsilon_0}},$$

Fig. 13.

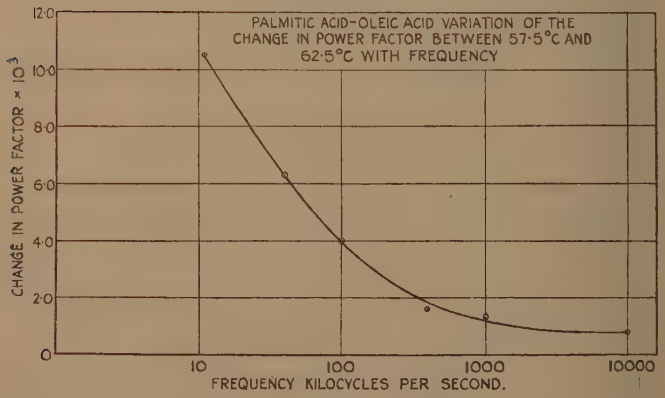

and compare it with the result obtained from the permittivity measurements. They can be tabulated as follows:—

	Measured values of $\epsilon_1-\epsilon_0$.	Calculated from $\tan\phi_{\max.}$.
Oleic acid (1)	0·23	0·245
Oleic acid (2)	0·13	0·10
60–40 per cent. mixture .	0·12	0·053
50–50 per cent. „ .	0·07	0·035
30–70 per cent. „ .	0·05	0·0266

It will be seen that while the first two agree fairly closely the calculated values for the mixtures are only about half of those obtained from the permittivity measurements. This may be due to the existence of a number of different relaxation times, as the polar molecules in the mixture may not all be orienting under the same conditions. Race [6] showed that the existence of, say, five slightly different relaxation times would reduce the observed power factor maximum to about 60 per cent. of what it would be if there were only one time. The permittivity would not, however, be affected.

Conclusions.

It appears that, although Debye's theory was put forward originally to explain the behaviour of liquid dielectrics, it can be applied without modification to solid dielectrics on the assumption that they possess some property which can be termed the " apparent viscosity," which behaves in the same manner as the ordinary macroscopic viscosity of a liquid.

The experimental work in connexion with this paper has been conducted in the Laboratories of Applied Electricity in the University of Liverpool, under the direction of Professor Marchant. The author is also indebted to Professor Hilditch for his assistance in supplying pure samples of the fatty acids, and to Mr. W. J. Shutt, of the Department of Physical Chemistry. He also wishes to express his thanks for the grants received from the Department of Scientific and Industrial Research, which have made this work possible.

Bibliography.

(1) L. Hartshorn, Journal I.E.E. lxiv. p. 1152 (1926).
(2) W. Jackson, Journal I. E. E. lxxv. p. 93 (1934).
(3) P. Debye, " Polar Molecules," Chemical Catalogue Co. New York (1928).
(4) A. Gemant, Phil. Mag. xix. p. 746 (April 1935).
(5) D. W. Dye, ' Dictionary of Applied Physics,' ii. p. 675.
(6) H. H. Race, Journ. Phys. Chem. xxxvi. p. 1928 (1932).
(7) W. Jackson, Proc. Roy. Soc. cl. p. 197 (1935).

XXXI. *Electromagnetic Waves from a Point Source.* *By* W. T. Howell, *M.Sc.**

HERTZ [1] showed theoretically that a certain degree of variation of intensity of spherical electromagnetic waves over the wave-front is compatible with Maxwell's equations, and verified it experimentally. He further showed that variation of the amplitudes of the electric and magnetic force components along the wave-front is accompanied by deviations from the inverse first-power law of their variation with distance from the source, as well as by deviations of their phase-velocities from the velocity of light as ordinarily understood. The object of this paper is to study these deviations for spherical electromagnetic waves of the most general type, and to note some consequences of such deviations.

§1. *Detailed Expressions for the Forces.*

It may be shown that a general solution of Maxwell's equations is expressed in spherical polar coordinates by the following scheme [2] :—

$$\left.\begin{aligned} \mathrm{E}_1 &= \iota\frac{\partial \mathrm{U}'}{r\,\partial\theta} - \frac{\partial \mathrm{V}}{r\sin\theta\,\partial\phi}, & \mathrm{E}_2 &= \iota\frac{\partial \mathrm{U}'}{r\sin\theta\,\partial\phi} + \frac{\partial \mathrm{V}}{r\,\partial\theta}, \\ & & \mathrm{E}_3 &= \iota k(\mathrm{U}''+\mathrm{U}), \\ \mathrm{H}_1 &= -\frac{\partial \mathrm{U}}{r\sin\partial\theta\phi} + \iota\frac{\partial \mathrm{V}'}{r\,\partial\theta}, & \mathrm{H}_2 &= \frac{\partial \mathrm{V}}{r\partial\theta} + \iota\frac{\partial \mathrm{U}'}{r\sin\theta\,\partial\phi}, \\ & & \mathrm{H}_3 &= \iota k(\mathrm{V}''+\mathrm{V}), \end{aligned}\right\} \quad (1.1)$$

where E, H represent the electric and magnetic forces, suffixes 1, 2, 3 stand for θ, ϕ, r in that order, and accents denote differentiations with respect to kr. U and V are of similar form, and we may take for U the expression

$$\mathrm{U} = \sum_{n=1}^{\infty}\sum_{m=0}^{n} \mathrm{U}_{nm},$$

where

$$\mathrm{U}_{nm} = (\mathrm{C}_n \mp \iota\mathrm{S}_n)\mathrm{X}_{nm}\exp\iota(kct+\alpha_{nm}) + (\mathrm{C}_n \mp \iota\mathrm{S}_n)\mathrm{Y}_{nm}\exp\iota(kct+\beta_{nm}). \quad . \quad . \quad (1.2)$$

with

$\mathrm{X}_{nm} = \mathrm{A}_{nm}\mathrm{P}_n^m(\cos\theta)\cos m\phi$, $\quad \mathrm{Y}_{nm} = \mathrm{B}_{nm}\mathrm{P}_n^m(\cos\theta)\sin m\phi$, A_{nm}, B_{nm}, α_{nm}, β_{nm} being arbitrary constants, $\mathrm{P}_n^m(\cos\theta)$ the usual associated Legendre function of order n and

* Communicated by G. A. Schott, F.R.S.

class m according to Ferrers' definition, whilst the functions $C_n(kr)$, $S_n(kr)$ are given by

$C_n(kr)=(-)^n\sqrt{(\frac{1}{2}\pi kr)}J_{-n-\frac{1}{2}}(kr)$, $S_n(kr)=\sqrt{(\frac{1}{2}\pi kr)}J_{n+\frac{1}{2}}(kr)$, $J_\nu(z)$ being the ordinary Bessel function of order ν and argument z. We shall speak of the disturbance represented by U_{nm} as being of "Electric" type, of order n, and class m, and shall omit the suffixes whenever no confusion can result. We shall also write for all values of the suffix n

$$p=\sqrt{(C^2+S^2)},\ q=\sqrt{(C'^2+S'^2)},\ \psi=\tan^{-1}\frac{S}{C},\ \chi=\tan^{-1}\frac{S'}{C'},$$

the square roots being taken positively, whilst the angles ψ, χ are taken to lie between $\pm\pi/2$.

Then written at full length the ter U_{nm} and the electric and magnetic forces components derived from it by (1.1) become respectively, only real parts being taken,

$$\left.\begin{aligned}
U_{nm}&=p_n\{X_{nm}\cos(kct-\psi_n+\alpha_{nm})\\
&\qquad+Y_{nm}\cos(kct-\psi+\beta_{nm})\},\\
E_1&=\frac{q_n}{r}\left\{\frac{\partial X_{nm}}{\partial\theta}\cos\left(kct-\chi_n+\alpha_{nm}+\frac{\pi}{2}\right)\right.\\
&\qquad\left.+\frac{\partial Y_{nm}}{\partial\theta}\cos\left(kct-\chi_n+\beta_{nm}+\frac{\pi}{2}\right)\right\},\\
E_2&=\frac{q_n}{r}\left\{\frac{\partial X_{nm}}{\sin\theta\partial\phi}\cos\left(kct-\chi_n+\alpha_{nm}+\frac{\pi}{2}\right)\right.\\
&\qquad\left.+\frac{\partial Y_{nm}}{\sin\theta\partial\phi}\cos\left(kct-\chi_n+\beta_{nm}+\frac{\pi}{2}\right)\right\},\\
E_3&=\frac{n(n+1)p_n}{kr^2}\left\{X_{nm}\cos\left(kct-\psi_n+\alpha_{nm}+\frac{\pi}{2}\right)\right.\\
&\qquad\left.+Y_{nm}\cos\left(kct-\psi_n+\beta_{nm}+\frac{\pi}{2}\right)\right\},\\
H_1&=-\frac{p_n}{r}\left\{\frac{\partial X_{nm}}{\sin\theta\partial\phi}\cos(kct-\psi_n+\alpha_{nm})\right.\\
&\qquad\left.+\frac{\partial Y_{nm}}{\sin\theta\partial\phi}\cos(kct-\psi_n+\beta_{nm})\right\},\\
H_2&=\frac{p_n}{r}\left\{\frac{\partial X_{nm}}{\partial\theta}\cos(kct-\psi_n+\alpha_{nm})\right.\\
&\qquad\left.+\frac{\partial Y_{nm}}{\partial\theta}\cos(kct-\psi_n+\beta_{nm})\right\},\\
H_3&=0.
\end{aligned}\right\}\quad(1.3)$$

The ambiguity of sign has been removed, since we shall be dealing in what follows with divergent waves. These equations show that the amplitudes and phases of the typical terms in the expressions for the forces all involve the functions C_n, S_n. We see also that while the radial force decreases approximately as the inverse square of the distance, both the transverse electric components decrease as the inverse first power. We thus expect that the transverse forces will produce discernible effects at such distances from the source that the radial force has ceased to be important. We also see that all constituent disturbances of the same order but different classes are propagated in the same way. We note in passing that Hertz's harmonic oscillator is given in our scheme by $V=0$, $n=1$, $m=0$, *i. e.*, it is of electric type, of order unity, and class zero.

§2. *The Functions* p, q, ψ, χ.

We shall need the chief properties of these functions in order to study the variation with kr of the amplitude, intensity, and phase.

Writing z for kr, and using the equations of definition, we obtain

$$\left.\begin{aligned}
&\chi-\psi=\tan^{-1}\frac{1}{pp'},\\
&\psi' = \frac{CS'-C'S}{C^2+S^2}=p^{-2},\\
&\chi' = \frac{C'S''-C''S'}{C'^2+S'^2}=\left\{1-\frac{n(n+1)}{z^2}\right\}q^{-2},\\
&pp'=CC'+SS',\\
&qq'=C'S''+S'C''=-\left\{1-\frac{n(n+1)}{z^2}\right\}pp',\\
&q^2 =C'^2+S'^2=(pp')'-CC''-SS''\\
&\qquad=\frac{1}{2}\frac{d^2}{dz^2}p^2+\left\{1-\frac{n(n+1)}{z^2}\right\}p^2,
\end{aligned}\right\}\quad (2.1)$$

the order being equal to n throughout. These equations enable us to express ψ', χ', and q^2 in terms of p^2 and its differential coefficients with respect to kr. The

function $p_n^2(z)$ is a polynomial, and is given by Lorentz's[3] Summation formula

$$p_n^2(z) = \sum_{m=0}^{n} \frac{1.3 \ldots (2m-1)}{2.4 \ldots (2m)} \cdot \frac{(n+m)!}{(n-m)!} z^{-2m}. \qquad (2.2)$$

It thus follows by the last equation of (2.1) that $q_n^2(z)$ is also a polynomial. Some tables of these polynomials $p_n^2(z)$ and $q_n^2(z)$ are given in B. A. Reports[4].

The function $p_n^2(z)$ when z is real is monotonic decreasing, being infinite at the origin and unity at infinity. The function $q_n^2(z)$ when z is real also tends to unity as z increases without limit, and to infinity as z approaches zero, but is not monotone and has a minimum value for $z=\sqrt{n(n+1)}$, this last property being evident from the B. A. tables as well as from the fifth equation (2.1). The values of ψ' and χ' are now given by the second and third equations (2.1); ψ' is monotone increasing continuously from zero for infinitely small values of r, to unity for infinitely large values, but χ' is not monotone, diminishing from zero for infinitely small values of r to a negative minimum, and thereafter increasing continuously through zero to unity for infinitely great values of r. For large values of n Lorentz's summation formula and its derivatives become hopelessly inconvenient for calculation of p_n^2 and q_n^2 owing to the number of terms necessary to secure accuracy. We thus require asymptotic expressions for $p_n^2(z)$ and $q_n^2(z)$ for n large. Those required for this paper are :—

(1) When $z-n-1/2$ is great compared with $z^{1/3}$:

$$p_n^2(z) \sim \sigma^{-1}\left\{1 - \frac{1+4\gamma^2}{8z^2\sigma^6} + \frac{27+472\gamma^2+592\gamma^4+64\gamma^6}{128z^4\sigma^{12}} \cdots\right\}, \qquad (2.3)$$

$$q_n^2(z) \sim \sigma\left\{1 + \frac{1+4\gamma^2+2\gamma^4}{8z^2\sigma^6} - \frac{29+480\gamma^2+696\gamma^4+160\gamma^6}{128z^4\sigma^{12}} \cdots\right\}, \qquad (2.4)$$

where

$$\gamma = \frac{n+\frac{1}{2}}{z}, \quad \sigma = +\sqrt{(1-\gamma^2)}.$$

(2) When $|\, z-n-1/2\,|$ is of lower order than $z^{1\,3}$:

$$p_n^2(z)\sim 1{\cdot}2572z^{1/3}\left(1+\frac{4\zeta-10\zeta^3}{15z}\right)$$
$$-1{\cdot}1546\left(\zeta-\frac{1-21\zeta^2+35\zeta^4}{70z}\right)$$
$$+\frac{1{\cdot}0606}{z^{1/3}}\left(\zeta^2-\frac{3\zeta-35\zeta^3+35\zeta^5}{105z}\right)+\ldots, \quad (2.5)$$

$$q_n^2(z)\sim\frac{1{\cdot}0606}{z^{1/3}}\left(1+\frac{3\zeta-4\zeta^2}{3z}\right)+\frac{1{\cdot}1546}{z}\left(\zeta^2-\frac{3}{10}\right)$$
$$+\frac{1{\cdot}2572}{z^{5/3}}\left(\frac{5}{3}\zeta^4-\frac{9}{4}\zeta^2-\frac{37}{100}\right)+\ldots, \quad (2.6)$$

where $n+\frac{1}{2}=z-\zeta$.

(3) When $n+\frac{1}{2}-z$ is great compared with $z^{1/3}$:

$$p_n^2(z)\sim\frac{1}{\sinh\alpha}\left\{\tfrac{1}{4}\epsilon^{2\nu(\tanh\alpha-\alpha)}+\epsilon^{-2\nu(\tanh\alpha-\alpha)}\right\}+\ldots, \quad (2.7)$$

$$q_n^2(z)\sim\sinh^2\alpha\, p_n^2(z)+\ldots, \quad (2.8)$$

where $z=(n+\frac{1}{2})\operatorname{sech}\alpha$.

It has not been found necessary for our purpose to use appropriate approximations for the case when $|\, z-n-\frac{1}{2}\,|$ is of the same order as $z^{1\,3}$, so that these have not been derived.

§3. *Variation of Intensity and Amplitude with Distance from the Source.*

We may take as intensity factors for spherical waves of "Electric" type

$$\frac{q_n^2(z)}{z^2}\ \text{for}\ \mathrm{E}_{1nm},\ \mathrm{E}_{2nm};\quad \frac{[n(n+1)]^2p_n^2(z)}{z^4}\ \text{for}\ \mathrm{E}_{3nm};$$

and

$$\frac{p_n^2(z)}{z^2}\ \text{for}\ \mathrm{H}_{1nm},\quad \mathrm{H}_{2nm}.$$

All three intensity factors depend on the order n and upon $kr=z=2\pi r/\lambda$, which determines the variation with the distance r from the source, as well as the dependence on the wave-length at infinity. From the properties of $p_n^2(z)$ and $q_n^2(z)$ described in the previous section we see that the second and third expressions are monotone decreasing

functions of kr, tending to infinity as kr approaches zero and tending to zero like z^{-4} and z^{-2} respectively as kr increases without limit. On the other hand, the first expression is only monotone for small values of n. When n is greater than some value between 5 and 10 this function decreases from infinity for $z=0$ to a minimum at a value of z slightly greater than the critical distance $r=\frac{\lambda\sqrt{n(n+1)}}{2\pi}$, at which $q_n^2(z)$ has its minimum, rises rapidly to a maximum, then falls off to zero like z^{-2}. It is of special importance that for large values of n $\frac{q_n^2(z)}{z^2}$ on reaching its minimum rises rapidly to its maximum, then falls off slowly to zero. To get an idea of the magnitudes involved in the variation of the transverse intensity factor $\frac{q_n^2(z)}{z^2}$ we can use the first term of the asymptotic expansion as an approximation. This will have a maximum for $\frac{d}{dz}\left(\frac{\sigma}{z^2}\right)=0$, that is for $r=\frac{1\cdot22(n+\frac{1}{2})\lambda}{2\pi}$ the value of $\frac{q_n^2(z)}{z^2}$ at the maximum being approximately $\frac{\cdot385}{(n+\frac{1}{2})^2}$. This suggests that if we took $(n+\frac{1}{2})\frac{q_n(z)}{z}$ as our amplitude factor instead of $\frac{q_n(z)}{z}$ its maximum value would be constant, 0·385 approximately for all n provided n is large. This would also take account of the factor $\frac{\partial X_{nm}}{\partial\theta}$, which is of the order of nX_{nm}. This behaviour of the transverse intensity factor is shown in the figure, in which the functions $\left[\frac{n+\frac{1}{2}}{z}p_n(z)\right]^2$ and $\left[\frac{(n+\frac{1}{2})}{z}q_n(z)\right]^2$ are plotted for a range of values of n and z.

§4. *The Wave-fronts and Phase-velocities.*

We see from equations (1.3) that, apart from constants, the phases of E_{3nm}, H_{1nm}, H_{2nm}, and E_{1nm}, E_{2nm}, are respectively equal to $kct-\psi_n$ and $kct-\chi_n$. Thus the

wave-fronts are spheres concentric with the source, and at any one sphere the phases of the transverse electric forces differ from those of the other forces involved for the same order. Formulæ suitable for calculating ψ_n and χ_n have been given by Macdonald [5], and it may be shown that for all n, $\psi_n(kr)$ slowly increase from zero at

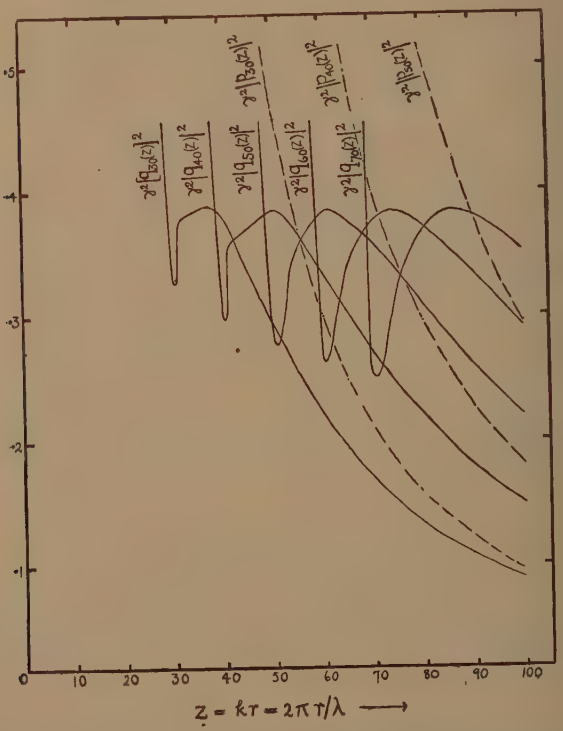

Graphs illustrating the chief properties of $\gamma^2[p_n(z)]^2$ and $\gamma^2[q_n(z)]^2$ for large values of the order n and argument z derived from the appropriate formulæ given in the text.

the origin to approximately $\frac{\pi}{6}$ near the critical point, $z=\sqrt{n(n+1)}$ thereafter being asymptotic to $z-(n+\frac{1}{2})\frac{\pi}{2}$. The second phase angle χ_n slowly decreases from zero to

a negative minimum near the critical point equal to approximately $-\frac{\pi}{6}$ for all n, thereafter being asymptotic to $z-(n+3/2)\frac{\pi}{2}$. The velocity of any particular wave-front $\dot{r}$ away from the source is determined from the condition that the corresponding phase remains unaltered, and is defined to be the corresponding phase velocity[6]. Thus for E_3, H_1, H_2 the phase velocity is $\dot{r}_1=\frac{C}{\psi'}=cp^2$, whilst for E_1, E_2 the phase velocity is

$$\dot{r}_2=\frac{c}{\chi'}=\frac{cq^2}{1-\frac{n(n+1)}{z^2}}.$$

From the character of the functions p, q determined in §2 we deduce that the first phase velocity is a monotonic decreasing function of r, infinitely great at the origin and tending to c, the velocity of light, as r increases without limit. The second, *i. e.*, transverse phase velocity, is negative infinity at the origin, increasing at first to a negative maximum, then decreasing again to negative infinity as kr approaches $\sqrt{n(n+1)}$. As kr passes through this critical value the phase velocity jumps to positive infinity, thereafter decreasing monotonically to c, the rate of decrease in both cases being more rapid the higher the order n.

§5. *Concentration of Radiation.*

The factors arising from spherical harmonic terms in the amplitudes of the six force components are :—

$$\frac{\partial X_{nm}}{\partial\theta},\quad \frac{\partial X_{nm}}{\sin\theta\partial\phi},\quad X_{nm},\quad \frac{\partial X_{nm}}{\sin\theta\partial\phi},\quad \frac{\partial X_{nm}}{\partial\theta},\quad 0,$$

where X_{nm} is of the form $(A_{nm}\cos m\phi+B_{nm}\sin m\phi)$ $P_n{}^m(\cos\theta)$, and n takes on any positive integral value, while m takes any integral value $\leqslant n$. These show that the radiation due to a spherical harmonic constituent of any disturbance is emitted principally along certain directions from the source. By summation over an infinite set of such constituents taken with suitable co-

efficients it is obviously possible to obtain an electromagnetic field in which one of the forces is an arbitrary function of position on a sphere about the source. Thus let us suppose for simplicity that over the sphere $r=r_0$ E_1 is given by

$$\left.\begin{aligned} E_1 &= \cos kct \\ &= 0 \end{aligned}\right\} \quad \text{for} \quad \left\{\begin{aligned} &0 \leqslant \theta \leqslant \pm\alpha, \\ &\pm\alpha < \theta \leqslant \pm\pi. \end{aligned}\right\} \quad . \quad (5.1)$$

Then we can write

$$E_1 = \sum_{n=0}^{\infty} A_n P_n^1(\cos\theta) \cos kct,$$

where

$$A_n = \frac{2n+1}{n(n+1)} \int_{-\alpha}^{\alpha} P_n^1(\cos\theta)\, d(\cos\theta),$$

i. e.,

$$A_n \sim \frac{4\alpha}{2n+1} J_0\{(n+\tfrac{1}{2})\alpha\},$$

when α is small and n is large; so that by equations (1.3) we may write

$$\left.\begin{aligned} E_1 &= \sum_{n=0}^{\infty} A_n P_n(\cos\theta) \frac{r_0}{q_n(kr_0)} \\ &\qquad \times \frac{q_n(kr)}{r} \cos\left(kct - \chi_n + \alpha_n + \frac{\pi}{2}\right), \\ E_3 &= \sum_{n=0}^{\infty} A_n P_n(\cos\theta) \frac{r_0}{q_n(kr_0)} \\ &\qquad \times \frac{p_n(kr)}{kr^2} n(n+1) \cos\left(kct - \psi_n + \alpha_n + \frac{\pi}{2}\right), \\ H_2 &= \sum_{n=0}^{\infty} A_n P_n^1(\cos\theta) \frac{r_0}{q_n(kr_0)} \\ &\qquad \times \frac{p_n(kr)}{r} \cos(kct - \psi_n + \alpha_n), \end{aligned}\right\} \quad . \quad (5.2)$$

where $\alpha_n = \chi_n(kr_0) - \dfrac{\pi}{2}$ and all the other forces vanish identically. These equations constitute a solution of Maxwell's equations for free space, giving as intense a concentration of the transverse electric force as we please in the neighbourhood of the positive pole of the wave-front of radius r_0, where r_0 may have any value

we please. The solution may be made as exact as we please by taking a sufficient number of terms of the series, provided the latter converge. This solution may be further generalized by making the transverse force vary in any manner over the selected wave-front of radius r_0 bounded by the small circle of angular radius α. The effect of this change will obviously be to change the relative magnitudes of the several spherical harmonic terms in the series, and in this way it may prove possible to make any convenient set of terms dominant over all the rest, say those whose orders lie between n_1 and n_2. Thus if all the values of n between these limits be large and lie between kr_0 and a value about 0·7 of it, then, according to the result given in §3, the value of the factor $r_0 q_n(kr)/r q_n(kr_0)$ will differ little from unity for a certain range of n and r, so that the factors containing r reduce very nearly to the cosine of $kct-\chi_n(kr)+\chi_n(kr_0)$. Now this reduces to kct for $r=r_0$, and to the same value at the distance r at a subsequent time $t'=t+[\chi^n(kr)-\chi_n(kr_0)]/ck$. In other words the concentrated disturbance behaves as if it had travelled from the wave-front of radius r_0 to the wave-front of radius r in the time $t'-t$ practically unchanged, provided only that $r-r_0$ is not too large. Hence, if the coefficients of the series can be adjusted so as to satisfy the conditions specified above, we can obtain a solution of Maxwell's equations for free space which represents a centre of concentration, movable through a limited distance. From the approximation for A_n given above we see that a large number of terms would have to be taken to secure a good approximation. Although the transverse electric force is concentrated at the wave-front of radius r_0, the other force components are not, as we see from equations (5.2), nor does the concentration of the transverse electric force itself extend to any great distance from that wave-front. The time average of the radial Poynting flux $\frac{ck}{4\pi} E_1 H_2$ is given at the wave-front $r=r_0$ by

$$\frac{ck}{8\pi} f(\cos\theta) \sum_{n=1}^{\infty} A_n \frac{P_n{}^1(\cos\theta)}{q_n{}^2(kr)_0},$$

so that this is concentrated in this neighbourhood, while the remaining component is easily seen to vanish. This

solution, representing concentration of spherical electromagnetic waves, includes that given in 1922 by Oseen [7].

§6. *The Outflow of Energy and Angular Momentum.*

From the expressions for the forces derived in §1 we may write down the components of the Poynting flux in the ordinary conventional units $\Pi_1 = \frac{c}{4\pi}(E_2H_3 - E_3H_2)$, etc. Generally, of course, both E and H will consist of sums of terms of both electric and magnetic types derived as shown before from two functions U and V. For the sake of brevity we shall confine ourselves to the case where the disturbance is represented by

$$U = p_n\{X_{nm}\cos(kct-\psi_n+\alpha_{nm})+Y_{nm}\cos(kct-\psi_n+\beta_{nm}) + X_{nl}\cos(kct-\psi_n+\alpha_{nl})+Y_{nl}\cos(kct-\psi_n+\beta_{nl})\}, \quad (6.1)$$

and shall be concerned only with the time average of the Poynting flux written Π. On integrating over the sphere of radius r we find that the average rate of radiation arising from a wave-function of type (6.1) is

$$\frac{ck}{8\pi}n(n+1)\{a_{nm}^2+b_{nm}^2+a_{nl}^2+b_{nl}^2\}, \quad . \quad . \quad . \quad (6.2)$$

where $\dfrac{A_{nm}}{B_{nm}} = \dfrac{a_{nm}}{b_{nm}} \cdot \sqrt{\dfrac{2n+1}{2\pi}} \cdot \dfrac{(n-m)!}{(n+m)!}$.

This is dependent only upon the amplitudes and order of the disturbance, and independent of r. The *total* energy radiated out over a sphere of radius r per unit time is not independent of r. Calculated on the assumption that the energy per unit volume in the field is $\frac{1}{8\pi}(E^2+H^2)$ this turns out to be

$$\frac{ck}{16\pi}n(n+1)(a_{nm}^2+b_{nm}^2+a_{nl}^2+b_{nl}^2) \times \left[p_n^4\left\{1+\frac{n(n+1)}{k^2r^2}\right\}+q_n^4\left\{1-\frac{n(n+1)}{k^2r^2}\right\}^{-1}\right]; \quad (6.3)$$

for kr large this expression reduces to the average rate of radiation as expected; at the origin it is positively infinite, and as kr increases it decreases through zero

to negative infinity at the critical distance $kr=\sqrt{n(n+1)}$. As kr passes through this value the expression changes from negative to positive infinity, thereafter decreasing rapidly to the above expression for the average rate of radiation. Thus the *total* radiation over the surface of a sphere of radius r is a discontinuous function of kr, and for a certain region, bounded on the outside by the critical distance, the radial flow of energy is towards the source. We next derive expressions for the outflow of moment of momentum about three mutually perpendicular axes over the sphere of radius r. The moment of momentum per unit volume in the field is given by

$$\mathrm{M}=\left[r.\frac{\Pi}{c^2}\right].$$

If we multiply M by the element of volume in spherical polars, and set $dr=\dot{r}\,dt=cp_n^2dt$, then integrate over the sphere of radius r, we get the moment of momentum transferred through the sphere of radius r in time $dt=dr/cp_n^2$. Thus the moment of momentum, M_x, M_y, M_z, about the axes of $x\ y\ z$ respectively transferred through the sphere of finite radius r per unit time are given by

$$\left.\begin{aligned}
\mathrm{M}_x&=\frac{rp_n^2}{c}\int_0^{2\pi}d\phi\int_{-\frac{\pi}{2}}^{\frac{\pi}{2}}r^2\sin\theta(\bar{\Pi}_2\cos\theta\cos\phi+\bar{\Pi}_1\sin\phi)d\theta,\\
\mathrm{M}_y&=\frac{rp^{n2}}{c}\int_0^{2\pi}d\phi\int_{-\frac{\pi}{2}}^{\frac{\pi}{2}}r^2\sin\theta(\bar{\Pi}_2\cos\theta\sin\phi-\bar{\Pi}_1\cos\phi)d\theta,\\
\mathrm{M}_z&=\frac{rp_n^2}{c}\int_0^{2\pi}d\phi\int_{-\frac{\pi}{2}}^{\frac{\pi}{2}}r^2\sin\theta(-\bar{\Pi}_2\sin\theta)d\theta.
\end{aligned}\right\}\quad\ldots\quad(6.4)$$

On substituting the expressions for Π we find that for $m>0$, $\mathrm{M}_z=0$ except when $l=m$, and $\mathrm{M}_x=\mathrm{M}_y=0$ except when $l=m\pm1$.

Thus for $l=m$ $\mathrm{M}_x=\mathrm{M}_y=0$ and

$$\mathrm{M}_z=\frac{n(n+1)p_n^4(kr)}{8\pi}\,.\,4\,a_{nm}b_{nm}\sin(\alpha_{nm}-\beta_{nm});\quad(6.5)$$

while for $l=m-1$ we get $M_z=0$ and

$$\left.\begin{aligned} M_x=&-\frac{n(n+1)p_n^4(kr)}{8\pi}\sqrt{n(n+1)-m(m-1)}\\ &\{a_{nm}b_{nm-1}\sin(\alpha_{nm}-\beta_{nm-1})+a_{nm-1}b_{nm}\sin(\alpha_{nm-1}-\beta_{nm})\},\\ M_y=&-\frac{n(n+1)p_n^4(kr)}{8\pi}\sqrt{n(n+1)-m(m-1)}\\ &\{a_{nm}a_{nm-1}\sin(\alpha_{nm}-\alpha_{nm-1})+b_{nm}b_{nm-1}\sin(\beta_{nm}-\beta_{nm-1})\}. \end{aligned}\right\} \quad . \quad . \quad . \quad (6{\cdot}6)$$

These expressions give the amounts of angular momentum about the axes of x, y, and z, radiated out per unit time across the sphere of radius r, arising from a potential of specified type, and we may pass by summation over integral values of n and $m \leqslant n$ to that radiated out from a point source in any general type of disturbance. It will be noted that ratio

$$\frac{\text{Angular momentum radiated over sphere of radius } r}{\text{Energy radiated out over sphere of radius } r}$$

is only independent of r for kr approaching infinity when $p_n \to 1$.

Results of a somewhat similar character to the above expressions for rate of radiation of angular momentum have been published by Conway [8], but they do not show the dependence of the value of the angular momentum components upon the distance from the origin.

Mathematical Appendix.

The Asymptotic Series for $p_n^2(z)$ and $q_n^2(z)$.

The expression for $p_n^2(z)$ when $(z-n-\frac{1}{2})$ is greater than $z^{1/3}$ is deduced in the following way :—

Multiply together the asymptotic expansions for $H_\nu^1(\sec\beta)\,H_\nu^2(\sec\beta)$ [9], we get

$$p_n^2(z) \sim \sigma^{-1}\left\{1-\frac{1+4\gamma^2}{8z^2\sigma^6}+\ldots,\right.$$

where

$$z=(n+\tfrac{1}{2})\sec\beta\,;\ \cos\beta=\gamma=\frac{n+\frac{1}{2}}{z}\,;\ \sin\beta=+\sqrt{1-\gamma^2}=\sigma.$$

To find the next term in the series we may proceed by evaluating two more terms in the expansions for $H_\nu^1(\sec\beta)$, or more directly as follows :—

We arrange the summation formula

$$p_n^2(z)=\sum_{m=0}^{n}\frac{1.3\ldots 2m-1}{2.4\ldots 2m}\cdot\frac{(n+m)!}{(n-m)!}z^{-2m}$$

as a double series, proceeding according to descending powers of z and ascending powers of γ. We find that the series of ascending powers of γ corresponding to z^{-4} converges and can be summed.

Writing down the first four terms in the coefficient of z^{-4}, we have

$$\frac{1.3}{2.4}\frac{9}{16}+\frac{1.3.5}{2.4.6}\frac{259}{64}(2\gamma)^2+\frac{1.3.5.7}{2.4.6.8}\frac{1974}{256}(2\gamma)^4$$
$$+\frac{1.3.5.7.9}{2.4.6.8.10}\cdot\frac{8778}{1024}\cdot(2\gamma)^6+\ldots.$$

We expect this series to be summable, and a fairly simple function of $(1-\gamma^2)^{-\frac{13}{2}}$, and the easiest way of finding this function is by straightforward division.

Hence

$$p_n^2(z)\sim\frac{1}{\sigma}-\frac{1+4\gamma^2}{8z^2\sigma^7}+\frac{27+472\gamma^2+592\gamma^4+64\gamma^6}{128z^4\sigma^{13}}.$$

Using the relation

$$q_n^2(z)=\frac{1}{2}\frac{dz}{dz^2}p_n^2(z)+\left\{1-\frac{n(n+1)}{z^2}\right\}p_n^2,$$

and carrying out the straightforward differentiation we get the expression (2.4).

In the same way we derive the appropriate formulæ when $|z-n-\frac{1}{2}|$ is of smaller order than $z^{1/3}$, *i. e.*, equations (2.5) and (2.6).

In the case when $(n+\frac{1}{2}-z)$ is greater than $z^{1/3}$ we deduce by straightforward analysis [10]

$$p_n^2(z)\sim\frac{\epsilon^{2\nu(\tanh\alpha-\alpha)}}{4\sinh\alpha}\left\{1+\frac{3-5\coth^2\alpha}{12z\sinh\alpha}+\cdots\right\}$$
$$+\frac{\epsilon^{2\nu(\tanh\alpha-\alpha)}}{\sinh\alpha}\left\{1-\frac{3-5\coth^2\alpha}{12z\sinh\alpha}+\cdots\right\},$$

$$q_n^2(z) \sim \epsilon^{2\nu(\tanh\alpha-\alpha)} \frac{\sinh\alpha}{4}\left\{1+\frac{3+7\coth^2\alpha}{12z\sinh\alpha}+\ldots\right\}$$

$$+\epsilon^{-2\nu(\tanh\alpha-\alpha)}\sinh\alpha\left\{1+\frac{3-17\coth^2\alpha}{12z\sinh\alpha}+\ldots\right\},$$

where $\nu=n+\frac{1}{2}$; $z=\nu\,\mathrm{sech}\,\alpha$.

The following integrals are required in §6 :—

$$I_1=\int_{-1}^{1}\left[\left(\frac{\partial P_n^m}{\partial\theta}\right)^2+\frac{m^2(P_n^m)^2}{1-\mu^2}\right]d\mu,$$

$$I_2=\int_{-1}^{1}\mu\frac{P_n^m P_n^{m-1}}{\sqrt{1-\mu^2}}\,d\mu,$$

$$I_3=\int_{-1}^{1}\left(P_n^m\frac{\partial P_n^{m-1}}{\partial\theta}-P_n^{m-1}\frac{\partial P_n^m}{\partial\theta}\right)d\mu.$$

Using the recurrence relations [11], and noting that

$$P_n^{m+2r}(\mu)=(-)^p\frac{(n-m)!}{(n-m-2p)!}P_n^m(\mu)+BP_{n-2}^m(\mu)+\ldots,$$

we readily find on applying the orthogonality relations

$$I_1=\frac{2}{2n+1}\frac{(n+m)!}{(n-m)!}n(n+1),$$

$$I_2=\frac{2}{2n+1}\frac{(n+m)!}{(n-m)!}\frac{1}{(n+m)},$$

$$I_3=-\frac{2}{n+m}\frac{(n+m)!}{(n-m)!}.$$

References.

(1) Hertz, 'Electric Waves' (English translation), p. 137.
(2) Bromwich, Phil. Mag. ser. 6, xxxviii. p. 151 (1919).
(3) Lorentz (L.), 'Œuvres,' tome 1, p. 403.
(4) B. A. Reports, p. 87 (1914); p. 97 (1916); p. 263 (1925).
(5) Macdonald, Phil. Trans. Roy. Soc. A, ccx. p. 113 (1910).
(6) Brillouin, 'Propagation de l'électricité,' p. 301 (1910).
(7) Oseen, *Ann. der Phys.* F. 4, Bd. lxix. p. 202 (1922).
(8) Conway, Proc. R. I. A. xli Sect. A, no. 2, p. 8 (1932).
(9) Watson, 'Theory of Bessel Functions,' § 8·42.
(10) Watson, 'Theory of Bessel Functions,' § 8·4.
(11) Bateman, Part. Diff. Equations of Math. Phys. p. 360.

XXXII. *The Plastic Deformation of Cadmium Single-Crystals.* *By* R. Roscoe, *Ph.D., Assistant Lecturer in Physics, University College, London* *.

Introduction.

THE general nature of the plastic deformation of cadmium single-crystals has already been elucidated by Boas and Schmid †. In this paper attention is directed to two phenomena which seem to have escaped observation up to the present. The crystals used were in the form of wires, prepared by a method to be described in a forthcoming publication, while the method used in determining the orientation of the crystal axes has already been described by the writer ‡. Metal of two widely different degrees of purity was used, viz., cadmium containing 0·11 per cent. of lead and 0·03 per cent. of zinc, and some very pure cadmium supplied by Messrs. Adam Hilger, Ltd., in which the impurities did not amount to more than one part in a million.

In simple plastic extension the " critical shear stress " for a particular rate of glide is defined as the shear stress over the glide-planes, resolved in the glide direction, initially necessary to produce this rate of glide. It is measured, together with the strain-hardening, by means of a recording extensometer. Both these quantities are found to depend on the rate of deformation of the crystals, although not to a very marked extent. The two lower curves in fig. 1 represent the critical shear stress (S_0) and the upper curve the stress (S_3) necessary to maintain the deformation after an amount of glide of 300 per cent. has taken place. The points marked with squares correspond to the very pure cadmium.

The Bending of Single-Crystal Wires.

The ease with which single-crystals bend under their own weight is remarkable. Thus, if a single-crystal wire of cadmium half a millimetre in diameter is placed upon a smooth surface, with one end projecting over the

* Communicated by Prof. E. N. da C. Andrade, F.R.S.
† Boas and Schmid, *Zeits. f. Phys.* liv. p. 16 (1929).
‡ Roscoe and Hutchings. Phil. Mag. vii. p. 703 (1933).

edge, and is then moved until several centimetres of its length are overhanging, the crystal bends suddenly. If this operation is performed quickly the deformation is confined to a very limited region close to the supporting surface. Microscopic examination of this bent part of the wire reveals a clear set of glide planes which are crystallographically identical with those operative in ordinary longitudinal extension (the basal plane of the hexagonal structure). The formation of these glide-planes is a

Fig. 1.

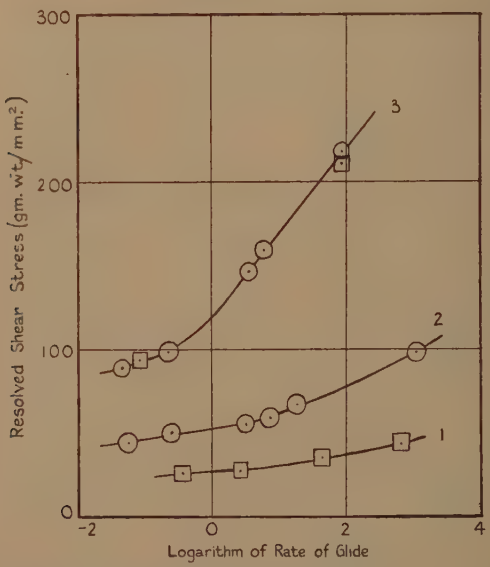

Curve 1.—Critical shear stress of pure cadmium.
,, 2.—Critical shear stress of cadmium with 0·1 per cent. lead.
,, 3.—Shear stress after glide of 300 per cent.

necessary preliminary to local bending of the crystal. Table I. shows measurements on some single-crystal wires of cadmium (containing 0·11 per cent. of lead and 0·03 of zinc, corresponding to curve 2 in fig. 1) which were bent under their own weight in this manner. The first column contains the length (l) of wire projecting in each case.

The distribution of the shear stress over a cross-section of the wire at the point of bending consists of two

parts :—(1) A uniform shear stress necessary to balance the *weight* of the projecting portion, of magnitude ρgl, where "ρ" is the density of the material. This has a shear component over the glide-planes (the mean shear stress) lying between $\rho gl \cdot \sin\chi_0$ and $\rho gl \cdot \sin^2\chi_0$, where "$\chi_0$" is the angle between the glide-planes and the axis of the wire. (2) A distribution of normal stress necessary to balance the *couple* exerted by the projecting portion. This stress varies linearly from $2\rho gl^2/r$ at the highest point to $-2\rho gl^2/r$ at the lowest point of the circumference,

Table I.

Lengths of Single-Crystal Wires which bend under their own Weight.

Radius of wire 0·24 mm.
Density of cadmium 8·64 gm./c.c.

l (cm.).	χ_0.	α.	Mean shear stress (gm. wt./mm.^{2}).	Max. shear stress (gm. wt./mm.^{2}).
7·93	13·4	17	0·16	96
6·78	22·0	25	0·22	104
5·67	48·0	20	0·36	108
6·36	56·9	15	0·46	129
6·96	67·8	15	0·61	118

"r" being the radius of the wire. To this there corresponds a linear distribution of shear stress over the glide-planes, of which the component in the glide direction varies between

$$\pm \frac{\rho gl^2}{r} \sin 2\chi_0 \cdot \cos\alpha,$$

where α is the angle between the glide direction and the major axis of the glide ellipses.

The greatest possible value for the mean shear stress over the glide-planes (viz. $\rho gl \cdot \sin\chi_0$) is calculated in each case, and the results are shown in the fourth column of Table I. These figures are a hundredfold less than the values of the shear stress necessary to produce simple extension (*i. e.*, when the shear stress is uniformly

distributed), and show a consistent variation with the orientation of the crystal axes. In contrast to this the figures for the maximum shear stress, $\frac{\rho g l^2}{r} \sin 2\chi_0 . \cos \alpha$, do not show a systematic variation with the angle χ_0.

In making these measurements the wires were pushed forward quite rapidly, so that the bending was sudden. The rate of glide which occurred is estimated as between 500 and 5000 per cent. per sec. The critical shear stresses in simple extension corresponding to these rates of glide are 90 and 115 gm. wt./mm.^{2} respectively (from fig. 1), comparing quite well with the extreme values for the maximum stress given in the table, viz. 96 and 129 gm. wt./mm.^{2}. From this agreement it is inferred that when the stress over a glide-plane is not uniform slipping is determined by the *maximum* value of the resolved shear stress upon it.

The Effect of Oxide Films.

As has been pointed out by the author * the strength of single crystal wires of cadmium can be greatly increased by superficial oxidation. Thus, if air is admitted into the tubes in which single-crystals are grown, a marked increase in the critical shear stress of the wires results. While the admission of oxygen alone produces the same effect, the presence of pure nitrogen, carbon dioxide or water-vapour does not alter the plastic properties of the crystals in the least. It is immaterial whether the oxidation of the crystals takes place during growth or subsequently, and slow oxidation at room-temperatures ultimately produces as much effect as heating in air near to the melting-point. Removal of the oxide film by brushing the surface with dilute sulphuric acid reduces the critical shear stress to the ordinary value for wires with bright surfaces. If the film is removed in this manner from a short section of an oxidized crystal, which is then stretched, the deformation is confined to this region until a considerable amount of glide has occurred, although no appreciable diminution in the area of cross-section is produced by the action of the acid.

During the extension of oxidized wires this increased

* 'Nature,' cxxxiii. p. 912 (1934).

strength is maintained. The following table of results for a series of wires oxidized to varying extents shows the critical shear stress (S_0) required to start the glide, as defined above, and the shear stress (S_3) necessary to maintain it when an amount of glide of 300 per cent. has taken place. The crystals were all stretched at approximately the same rate, and the corresponding values of S_0 and S_3 for unoxidized wires (read off from the graph, fig. 1) are included in the table.

TABLE II.

The Strength of Oxidized Cadmium Crystals.

Rate of glide=0·5 per cent. per sec.
Wire radius=$\frac{1}{4}$ mm.

Colour of oxide.	S_0.	S_3.
(Unoxidized)	50	102
Pale orange	75	121
Orange	79	130
,, ...	82	115
,, ...	84	127
,, ...	84	142
Brown	95	140
,, ...	95	162
,, ...	99	145
,, ...	106	147
,, ...	122	241
,, ...	122	251

It is hard to obtain really uniform oxidation of the surface, and these results no doubt owe their lack of consistency to this cause. The thickness of each film is estimated by comparison of its appearance with those of three standard oxidized wires, coloured pale orange, orange, and brown respectively. By oxidizing a series of wires of known surface area in small glass tubes containing air at various pressures an upper limit to the thickness of film corresponding to each colour is obtained. The tubes are baked out *in vacuo* previous to being filled with air at known pressure. From the volume of each tube the amount of oxygen present is calculated, and hence an upper limit to the thickness of the film

is deduced. Out of a number of such figures the lowest are picked out and given below :—

Pale orange film	Less than 20 atoms thick.
Orange film	Less than 400 atoms thick.
Brown film	Less than 1200 atoms thick.

For a particular thickness of oxide the critical shear stress depends on the thickness of the wire itself. Thus it is highest for very thin wires and decreases as the radius

Fig. 2.

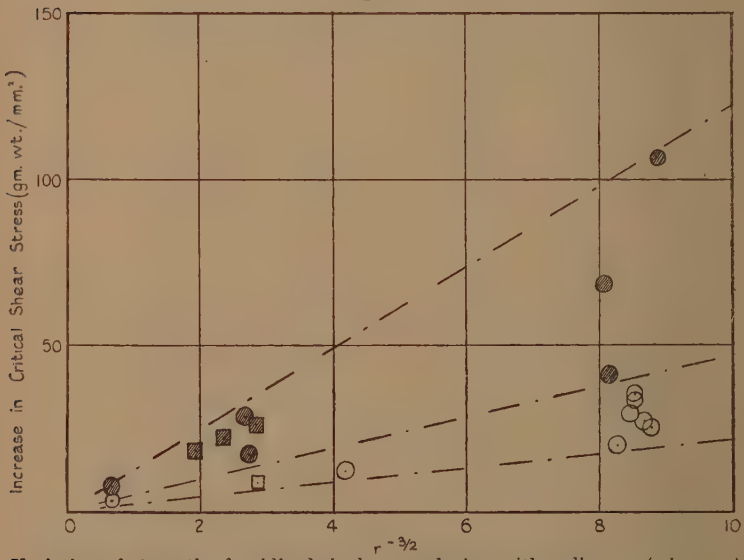

Variation of strength of oxidized single-crystal wires with radius r. (r in mm.)

increases, until for very thick wires it has the same value as in the case of bright crystals. It is, of course, only the *increase* in the critical shear stress which is dependent upon the gauge of the wire, the strength of unoxidized crystals being quite independent of it. This variation with the radius (r) is shown in fig. 2 for a series of wires which were all stretched at approximately the same rate. The shaded points represent results for wires with brown films, the unshaded orange. Since these arbitrary colours each cover considerable ranges of thickness of oxide (viz. 20–400 and 400–1200 atoms),

it is only to be expected that the points should cover a considerable area of the graph, but by using values of $r^{-3/2}$ as abscissæ it is found possible to divide the shaded and unshaded points into two well-defined regions separated by straight lines drawn from the origin. Although an exact statement of the law of variation of the increase in strength with the radius of the wires cannot be made from these results it is clear that the increase in shear stress decreases according to an inverse power of the radius lying between the first and the second.

The points marked with circles are for cadmium containing 0·11 per cent. of lead and 0·03 per cent. of zinc, while those marked with squares refer to crystals in which the impurities only amount to one part in a million. From the relative positions of these points it is clear that the phenomenon is not affected appreciably by small amounts of impurities.

Discussion.

The independence of the increase in the critical shear stress of the orientation of the crystal axes in the wire indicates that if the effect were produced by the actual strength of the oxide film the resistance to shear and not the tensile strength of the oxide would be involved. The resistance to shear necessary to produce the observed strengthening would have to be between 3×10^9 and 3×10^{10} dynes/cm.^{2}, that is to say of the same order as the tensile strength of steel. Also the figures in Table II. show that the increase in shear stress rises rather than falls during the deformation. After an amount of glide of 300 per cent. so thin a film must be completely ruptured and incapable of withstanding any stress at all, yet the shear stress rises still higher above the normal. These considerations would seem to indicate that the crystal is affected by the oxide to some considerable depth below its surface. The existence of "faults" or "cracks" in the crystal lattice has been postulated by various writers to explain the low tensile strength of materials *, and the penetration of the oxide into those cracks which are present on the surface seems to afford a satisfactory explanation of the phenomenon; for if the cracks are sealed up by the

* A. Joffé, 'International Conference on Physics, London, 1934,' ii. p. 77.

oxidation an outer layer of the crystal of the same order of thickness as the length of a crack would be expected to possess a relatively high strength compared to the interior. By assuming for this layer the maximum strength displayed by cadmium under any circumstances—the tenacity of the polycrystalline metal, 7×10^8 dynes/cm.^{2}—it can be estimated that the oxygen atoms of an orange film penetrate from a half to one micron into the interior of the lattice, and those of a brown film from one to two microns. These distances are of the order of the lengths of cracks demanded by Joffé's theory.

Summary.

It is concluded from observations on the bending of single-crystal wires that, when the stress over the glide-planes of a crystal is not uniform, slip begins when the *maximum* value of the resolved shear stress reaches the critical value for deformation under uniform stresses. Measurements show that surface oxidation of cadmium single-crystals produces an increase in their resistance to plastic deformation which cannot be due to the cohesion of the oxide film. It is suggested that the added strength has its origin in the healing of submicroscopic cracks by the film.

In conclusion, the writer desires to express his warmest thanks to Prof. E. N. da C. Andrade for his valuable direction and advice throughout this work. A grant from the Department of Scientific and Industrial Research is gratefully acknowledged.

XXXIII. *An Apparent Regularity in β-ray Reflexion.*

By Samuel C. Curran, *M.A., B.Sc., Metcalfe Research Fellow, Glasgow University* *.

[Plate II.]

Introduction.

THE present paper discusses an effect of experimental importance which appeared in the course of an investigation of the diffraction of β-rays by thin films, and is shown to be explicable theoretically as due to

* Communicated by Prof. E. Taylor Jones, D.Sc.

reflexion of the rays by a certain portion of the apparatus. By the term reflexion is meant the multiple scattering of the β-rays from a surface, the reflected rays being those scattered back away from the surface. The reflected β-particles causing the phenomenon are shown to have velocities approximately the same as the incident particles, the energy loss in the multiple scattering process being therefore small. It is shown that the photographs obtained in the investigation can be used to deduce the relative reflecting powers of various materials by a simple photographic method.

Apparatus.

The apparatus was designed initially for the purpose of investigating the diffraction of β-rays, but some minor

Fig. 1.

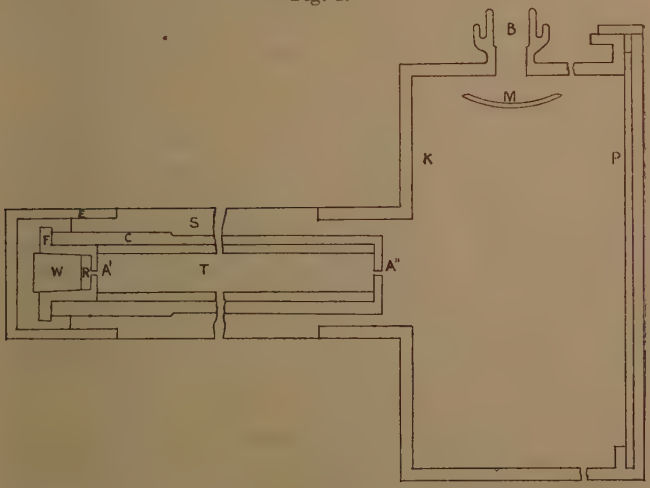

modifications have been made. The essential features are shown diagrammatically in fig. 1, which, in order to show details of certain parts, is not drawn to scale.

S is a soft iron shielding tube to prevent magnetic fields deflecting the β-particles. C is a tube of brass which fits into and is held by S. It is closed by a thin brass plate, $\frac{1}{2}$ mm. thick, at its right-hand end. At the centre of this plate is a small circular aperture A″, $\frac{1}{2}$ mm. in diameter. C in turn contains the tube T, and

the left-hand end of C is occupied by a short flanged tube F having a small aperture A′, the same as A″. Within F is the source R, which rests in a narrow groove immediately behind A′, and is held in position by the plug W. The system is finally closed at this end by the cap E fitting over S. The main body of the camera is denoted by K and the pump connexion by B. The latter is covered by a metal screen M to prevent light from entering the apparatus and fogging the plates. The photographic plate-holder is on the extreme right of the figure, and contains the plate P. Most of the joints are screw-joints, sealed with "Picien." The main dimensions are:—Length of tube T, 8 cm.; distance from A″ to P, 35 cm.; bore of tube T, 1 to 6 mm.; diameter of K, 9 cm. The camera was larger than required for purposes of measurement, the advantage being that the larger the dimensions the clearer the background on the plates. The pumping system consisted of a rotary oil-pump backing a two-stage oil-diffusion pump, using Apiezon oil B, and capable of producing vacua down to 10^{-7} mm. of mercury. Between the pumping system and the camera was inserted a discharge-tube for pressure measurement, it being found necessary to isolate this by means of stopcocks, as running the discharge was found to fog the plates. The customary leak to the atmosphere was inserted between the discharge-tube and the camera. The body of the camera was held vertical, source-end uppermost, by supports not shown in fig. 1. A system of grooves was cut in the various parts S, C, T, W, to allow free passage of air in pumping, any pressure on the radon capillary R, with consequent risk of breakage, being thereby avoided. The apparatus as described is similar to that used in diffraction experiments except for several minor modifications introduced for the better analysis of the effect obtained. In particular the tube T, at the inner surface of which the observed reflexion took place, could be removed and tubes of different materials and internal diameters inserted in its place.

Sources of β-rays.

Various sources of β-radiation were tried in an attempt to secure the most suitable type for this experiment, but it was soon found that the chief drawback to almost

all of these was lack of intensity. Radium itself in a small glass tube was tried, but with no great success, as large supplies were not available. Specially prepared active deposit sources were used also, and although these were very intense their short period of activity made their use inconvenient, as a plate of the required density could seldom be obtained with less than about six of these preparations. This meant that the process of taking an exposure was tedious, as the system had to be let up to atmospheric pressure every time a fresh active wire was inserted. The sources which were finally adopted were radon capillaries, which liberated β-particles of energy corresponding to about 130,000 volts upwards, the range of velocity being determined by the usual semicircular focussing apparatus. Each radon capillary was generally used twice, its activity falling in the course of the exposures from about 60 to 40 mc. and from about 40 to 10 mc.

Experimental Procedure.

The radon capillary was first placed in the holder immediately behind aperture A′, and then plug W was inserted to hold it in position. The source-end of the camera was then sealed with "Picien," the plate was inserted, and the apparatus exhausted. The vacuum in the course of an exposure was usually sufficient to wipe out a discharge with 70,000 volts between the electrodes. Exposures were long, varying between one day and four days according to the initial activity of the source and the plate density required. The method adopted for measuring the source intensity was that described by Chalmers (Brit. Journ. of Rad. vol. vii. no. 84, pp. 755–763, Dec. 1934), the microammeter reading indicating rapidly and accurately the activity of the radon capillaries.

The photographs obtained showed a very strong central spot surrounded by a ring in all cases, and the appearance of the ring suggested that it might be due to β-ray diffraction. Fig. 2 (*a*) (Pl. II.) is a photograph taken with a carbon tube of 4 mm. bore in the above apparatus, and fig. 2 (*b*) (Pl. II.) is one taken with a brass tube in a second smaller camera. The diametral line in the latter case is interesting, as it arises from the fact that the

groove containing the radon capillary was cut rather deep, so that the very high energy β-particles were able to penetrate to a certain extent the plate at A′. This meant that these rays formed a kind of pin-hole image of the source on the plate after passing through A″.

In the first place it had to be established that it was actually the β-rays which were causing the effect, as three types of radiation were present, namely, beta, gamma, and light. The light referred to is the green fluorescence of the capillary. The effect of the β-rays was separated from that of the γ-rays and light by applying a strong magnetic field across the body of the camera. When this was done the ring was entirely absent and a very weak central spot remained, probably marking the point where the fluorescent light reached the plate. (It should be mentioned here that sometimes with bright metal tubes a weak outer ring was present, formed by regular reflexion of the light at the middle portion of T.) It was next proved that the ring was caused by the tube T, this being verified by removing it and showing that the ring was then absent from the plates. To prove that T was affecting the β-particles entering at A′ was the next step, as it was possible that the circle formed by the β-rays might arise from a secondary action of the γ-radiation impinging on the surface of T and liberating β-rays by the photoelectric or the Compton effect. This was done by putting between the aperture A′ and T a thin plate of glass just sufficiently thick to absorb the β-rays, while allowing the γ-rays to enter the cylinder. In this case the ring was absent and a weak central spot remained, which was not due to β-rays as it did not deflect in a magnetic field, and which was possibly due, as mentioned above, to the weak fluorescence of the source. The γ-ray effect in the apparatus was practically negligible, as the camera was purposely constructed on generous lines to reduce the effect to a weak background on the plates. The variation of the diameter of the circle was investigated, brass tubes of different diameters being used. In all cases it was found that the diameter of the circle varied directly as the internal diameter of the tube T, which was varied from 1 to 6 mm. Measurements were taken at the inner edge of the ring in this case. Thus we have the following specimen figures for brass :—

Diameter of cylinder (cm.).	Diameter of ring (cm.).
0·2	0·9
0·4	1·8
0·6	2·7

Different metals—lead, copper, iron, aluminium—and also carbon were substituted for brass. The size of the β-ray ring for any one particular diameter of tube was found to be the same for the various materials, but a variation in the intensity of the ring was noticed when photographs were taken under similar conditions with different substances. Finally, the constitution of the primary beam and the ring was studied, and several photographs taken with magnetic fields across the path of the beam on its way to the plate. The central spot was drawn out into a short line with several dark maxima on it. These corresponded to the well known maxima of intensity in the β-ray spectrum of radium B—that is, those with energies equivalent to $1{\cdot}529\times10^5$, $2{\cdot}067\times10^5$, $2{\cdot}638\times10^5$ volts. This showed that the spot consisted almost entirely of β-rays. At the same time the ring lost its circular form and had the appearance of two lines running parallel to the denser central line of the undeflected β-particles. The three lines were of the same form and approximately equal in length, this proving that the reflected β-rays had velocities approximately equal to those in the primary beam.

The Theory of the Effect.

Calculation showed that the ring obtained in these experiments could not be due to regular diffraction of the β-rays by the lattice planes of the metal tube T.

Thus, if we consider the primary beam as striking the surface of the tube at B in fig. 3 and being diffracted in the direction BA″, we find that the observed angle of deflexion ϕ would agree with that calculated from the wave-length h/mv and the spacing of the lattice planes (as in diffraction experiments) only if the electrons were at the most of velocity equivalent to 10,000 volts,

and would be very different from the value of ϕ for β-rays. The correct explanation of the phenomonen seems to lie in the geometrical distribution of the electrons reflected from the inner surface of the tube. Thus, consider fig. 4.

Suppose a ray enters at A′ and impinges on the cylinder at A. Let AA″ represent a reflected β-particle leaving A and meeting the plate at a distance R from the central spot on the plate, marked by the point where A′A″ meets the plate, represented by the line at distance L from A″. Suppose A is distant x from A″, and let us

Fig. 3.

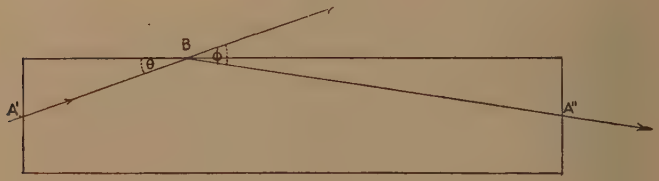

Fig. 4.

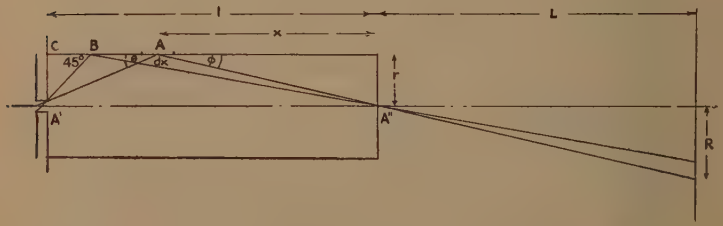

consider a small element dx of the cylindrical surface around A. Let θ be the angle of incidence and ϕ the angle of the reflected ray to the surface. It is assumed that electrons impinge on the element and are diffusely reflected—that is, with equal intensity in all directions independently of the direction of incidence of the rays on any element such as that at A. AA″ represents one of these diffusely scattered electrons travelling in the direction required to reach the plate through A″. The other reflected β-particles from the element, which is really acting as a source of reflected electrons, are absorbed for the most part by the surrounding walls of the tube. Now the number of rays from A′ to elemental cylinder of length $dx \propto 2\pi r\, dx \sin\theta$. Hence

number of reflected rays passing through A'' $\propto dx \sin\theta . dx \sin\phi$, in accordance with what is said above about the nature of the reflexion. But

$$\tan\theta = \frac{r}{l-x} \quad \text{and} \quad \tan\phi = \frac{r}{x};$$

$\therefore$ number reflected

$$\propto \frac{r^2}{\sqrt{[r^2+(l-x)^2][r^2+x^2]}} . (dx)^2,$$

that is,

$$\propto \frac{(dx)^2}{\sqrt{[r^2+x^2][r^2+(l-x)^2]}},$$

since r is constant for any particular tube. The rays from the element dx cover an annular element of the plate whose area

$$= \pi \left[\frac{r^2 L^2}{\left(x - \frac{dx}{2}\right)^2} - \frac{r^2 L^2}{\left(x + \frac{dx}{2}\right)^2} \right] = \pi r^2 L^2 \frac{2dx}{x^3}$$

to a first approximation. Hence number of rays hitting unit area of the plate

$$\propto \frac{(dx)^2}{\sqrt{[r^2+(l-x)^2][r^2+x^2]}} \cdot \frac{x^3}{dx},$$

that is,

$$\propto \frac{x^3\, dx}{\sqrt{[r^2+x^2][r^2+(l-x)^2]}}.$$

If we assume that the blackening of the plate is proportional to the number of particles hitting unit area, we obtain the function

$$I = \frac{x^3}{\sqrt{[r^2+x^2][r^2+(l-x)^2]}}$$

as a measure of the density of the plates for various values of x, or, alternatively, for various values of R, since $R = r \cdot \frac{L}{x}$.

We are therefore in a position to plot the intensity distribution on the photographic plate by plotting the function I against R. It is to be noticed that there is a maximum value of x corresponding to the β-ray which

just enters through the aperture A′, and since it is a circular one of $\frac{1}{2}$ mm. diameter in a plate $\frac{1}{2}$ mm. thick this limiting value corresponds to $\theta=45°$, as shown at B. This in turn determines a minimum value of R, and inside a circle of this radius no reflected β-rays are detected on the plate. To take a particular case: suppose the function I is graphed against R, as in fig. 5, for a tube of r 0·2 cm., where L=35 cm., l=8 cm. The minimum

Fig. 5.

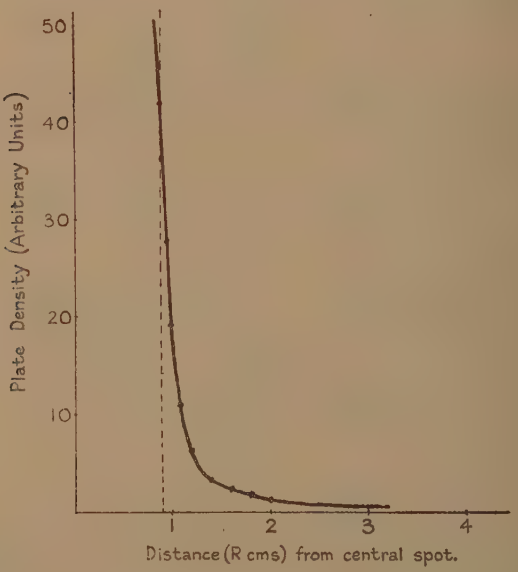

value of R in this case is that for $x=(8{\cdot}0-0{\cdot}2)$ cm., *i. e.*, for $x=7{\cdot}8$ cm., and $=0{\cdot}2\times\frac{35}{7{\cdot}8}$ cm., $=0{\cdot}90$ cm. This is indicated by the broken line in the figure.

The function

$$\mathrm{I}=\frac{x^3}{\sqrt{[(0{\cdot}2)^2+(8{\cdot}0-x)^2]\,[(0{\cdot}2)^2+x^2]}}$$

for this value of r, and it is seen that, starting at R=0·9 cm., the curve falls very rapidly, indicating that the plate

density will decrease rapidly outside of R = 0·9 cm.; and, since there are no reflected β-particles inside this radius, we have a sudden increase in plate density at R = 0·9 cm., with a rapid decrease for greater values of R. This exactly corresponds to the density distribution on the plates obtained in the experiments. In the case $r = 0{\cdot}2$ cm., for example, the inner edge of the ring was at a distance R = 0·9 cm. from the central spot. and was sharply defined, while the outer edge of the ring was more diffuse.

The equation $R = \frac{r \cdot L}{x}$ shows that the inner edge of the circle, corresponding approximately to $x = l$, neglecting the end-correction BC discussed above (fig. 4), should vary directly as r, since we have $R = r \cdot (L/l)$, and this agrees with the measurements given.

Finally, a remark might be added on the other experimental observation, the difference in intensity of the rings with tubes of different materials under similar conditions of exposure. The method can be utilized as a convenient means of measuring the relative reflecting powers of the different substances composing the tubes with β-rays. By photometry we can find the ratio of the maximum intensity in the ring to the intensity of the central spot, and this figure gives a measure of the reflecting powers of the various substances. The strength of the source and other variables are taken into account automatically by this device, and the only error is the slight background effect produced on the plates by light and γ-radiation. This error can be eliminated by subtracting the background intensity from the other measurements if greater accuracy is desired. The method is free from the difficulties associated with delta-rays and so on in the electrical methods of determining reflecting powers.

The writer is much indebted to Prof. E. Taylor Jones, under whose supervision the work was carried out, for his valuable help and advice. The experiment was performed in the Research Laboratories of the Natural Philosophy Department at the University of Glasgow.

XXXIV. *Magnetic Forces in a Rectangular Circuit.* By Forrest F. Cleveland *, *Department of Physics, University of Kentucky, Lexington, Kentucky, U.S.A.* †

Abstract.

The standard force equation, and Ampère's force equation for the magnetic force between current elements, are applied to determine the forces in a rectangular circuit, one side of which is mechanically separable from the other three. In order to explain the observed forces by the use of the standard equation, it is necessary to make the doubtful assumption that a part of the rectangular circuit can lift itself. Ampère's equation gives a reasonably correct value of the forces without the necessity of making this assumption.

Introduction.

STRAINS and stresses in a hypothetical medium (the ether) were assumed by Faraday as a means of explaining electric and magnetic forces. In spite of rapid development of the "action at a distance" theory in the hands of Ampère, Weber, and others, Maxwell chose to develop electromagnetic theory in terms of the concepts of Faraday. The remarkable success of his theory, involving the prediction of the electromagnetic waves discovered by Hertz, caused the earlier "action at a distance" theory to be largely forgotten.

Notwithstanding its great success, the Maxwell theory has several recognized weaknesses, among which are the following:—(*a*) It makes action and reaction not equal and opposite for elements of a circuit (or for isolated moving charges); (*b*) it requires continuous radiation from an electron rotating about a positive nucleus.

The first difficulty was not very serious so long as the ether was regarded as a reality and Newton's Third Law was not known to hold for atomic phenomena. But now that the existence of the ether is open to serious doubt, and that the laws of mechanics are known to hold for many atomic phenomena, it seems worth while to examine the theory critically with a view to the elimination of this difficulty.

* Now at Lynchburg College, Lynchburg, Virginia.
† Communicated by the Author.

As for item (*b*), it is to be hoped that atomic and electromagnetic theories may not continue to be divorced, but that the present theory may be modified, or a new theory developed, in such a way as to include both types of phenomena.

One point of inquiry in such a critical study is the magnetic force equation. The standard equation for the magnetic force exerted by a closed circuit on a current element **ds** is

$$\mathbf{df}=i/c(\mathbf{ds}\times\mathbf{H}), \quad . \quad . \quad . \quad . \quad . \quad . \quad (1)$$

where **H**, the magnetic field due to a closed circuit, is defined by the equation

$$\mathbf{H}=i'/c\int(\mathbf{ds}'\times\mathbf{r})/r^3,$$

r being the distance between **ds** and **ds′**. Since equation (1) is well verified by experience, it is customary to assume that the equation

$$\mathbf{d^2f}=ii'/c^2r^3[\mathbf{ds}\times(\mathbf{ds}'\times\mathbf{r})]=i/c(\mathbf{ds}\times\mathbf{dH}) \ast \quad . \quad . \quad (2)$$

will give the correct value for the force between two current elements †. In writing this equation it is definitely assumed that Newton's law of action and reaction is not valid for elements of current. This assumption may be seriously questioned on the grounds that the law holds, not only for closed circuits, but also for the impacting charged particles in nuclear phenomena and for the moving charged particles in the Bohr theory of the atom. Moreover, the law of action and reaction is frequently used in deducing the force on a current element due to a magnetic pole, in spite of the fact that neither the pole nor the current element constitute a closed circuit ‡.

Another expression for the force between current

* Zeleny and Page (Phys. Rev. xl. p. 305 (1932)) state that "Maxwell's equations lead unambiguously to the equation $\mathbf{dH}=i'/cr^3(\mathbf{ds}'\times\mathbf{r})$. As Slater and Frank ('Introduction to Theoretical Physics,' McGraw Hill Book Co., 1933, p. 233) point out, this expression gives the same results as the integral form, $\mathbf{H}=i'/c\int(\mathbf{ds}'\times\mathbf{r})/r^3$, only for closed circuits; and that for open circuits the correct expression might equally well be $\mathbf{dH}=i'/cr^3(\mathbf{ds}'\times\mathbf{r})+d\mathbf{V}$ where the integral of $d\mathbf{V}$ about a closed circuit vanishes.

† See, for example, Mason and Weaver, 'The Electromagnetic Field,' University of Chicago Press, 1929, p. 184, and Zeleny and Page, Phys. Rev. xl. p. 305 (1932).

‡ See, for example, Page and Adams, 'Principles of Electricity,' D. Van Nostrand Co., 1931, p. 243.

elements is the original equation proposed by Ampère, and which, according to Maxwell *, is "a formula from which all the phenomena may be deduced, and which must always remain the cardinal formula of electrodynamics." Written in vector form, it is †

$$\mathrm{d^2f}=(-ii'/c^2r^3)\mathrm{r}[2(\mathrm{ds}\,.\,\mathrm{ds}')-3/r^2\,(\mathrm{ds}\,.\,\mathrm{r})(\mathrm{ds}'\,.\,\mathrm{r})]. \quad . \quad (3)$$

Here the force is entirely along r, and hence the law of action and reaction is assumed to hold. As in the case of equation (2), this expression leads to a correct value for the force exerted by a closed circuit; the two equations are always contradictory, however, when neither circuit is closed.

It seems interesting and worth while to attempt to discover whether equation (3) has any advantages over equation (2) as an expression for the force between current elements. One way of doing this is to apply both equations to the determination of the force exerted by a part of a circuit upon another part of the same circuit. A simple case is that of a rectangular circuit, one side of which is mechanically separable from the other three.

Ampère performed an experiment with this kind of a circuit, the movable side consisting of a bridge floating in mercury troughs; when current was allowed to traverse the circuit, the bridge moved so as to lengthen the circuit. Maxwell ‡ mentions that this experiment is sometimes used to prove that Ampère's formula is more correct than Grassmann's (which gives no force between elements in the same straight line), and states that it can favour one expression no more than the other, since only a *closed circuit* is involved; both the Ampère and Grassmann expressions give the same results for a closed circuit.

Maxwell evidently had in mind that the *closed circuit* produced a field and then ceased its responsibility, the field in turn acting on the bridge. From the present point of view that one current element (or isolated moving charge) acts ultimately on another, letting the field assume secondary importance, and avoiding any implication as to just how the action is transmitted from one

* James Clerk Maxwell, 'A Treatise on Electricity and Magnetism' (third edition), Oxford, Clarendon Press (1904), ii. p. 175.

† See Mason and Weaver, *loc. cit.* pp. 173–185.

‡ James Clerk Maxwell, *loc. cit.* p. 319.

element to the other, Maxwell's statement is definitely untenable; for the two force equations have been proven to give the same results only in the case of a closed circuit plus an element of another circuit, while Ampère's experiment clearly involves the action of *one part* of a circuit on *another part of itself*.

The Rectangular Circuit.

Consider the rectangular circuit ABCD in a vertical plane (fig. 1), AC and BD being much longer than the other two sides. The customary procedure for finding the force on AB, by the use of equation (2), is to find the

Fig. 1.

field **H** due to the entire circuit ABCD, substitute this value of **H** into equation (1), and integrate along AB. Since **H** is perpendicular to AB, and lies in a horizontal plane through AB, the force is downward.

To find the reacting force on the three sides, one would obtain the field at an element of the three sides due to ABCD and proceed as above. Now since the field at AC and BD is horizontal and perpendicular to these conductors, there will be no vertical force exerted on them. Hence the force of reaction is the upward force exerted on CD; from the symmetry of the problem, action and reaction between the mechanically separable parts would from this viewpoint be equal and opposite.

But since CD produces no field at any element of itself, and since AB is so far from CD as to produce a negligible force upon it, then the force on CD must be due to AC and BD, which are rigidly connected to CD. Thus the customary manner of applying equation (2) leads to the result that a part of a circuit can *lift itself* *.

One may attempt to apply equation (2) in such a way as to avoid this result. For example, one could find the partial field **H** at AB due to the other three sides and substitute this value of **H** into equation (1) to find the vertical force on AB. Conversely, to find the force exerted by AB on the three sides, one would find the partial field at the three sides due to AB and use this value in determining the force on the three sides. But since the field due to AB at AC and BD is perpendicular to these conductors, and since AB is so far from CD as to produce a negligible field there, this procedure yields the result that there is a negligible vertical force on the three sides. Thus, on the basis of this viewpoint, one arrives at the conclusion that *action and reaction are not equal* for the mechanically separable parts of the circuit.

If one applies Ampère's expression, equation (3), to the calculation of the downward force exerted on AB by the three sides, one obtains the equation

$$\begin{aligned} F = 2i^2/c^2\{L^2/d(L^2+d^2)^{\frac{1}{2}} \\ +\log\,[d+(d^2+L^2)^{\frac{1}{2}}]\,/\,[a+(a^2+L^2)^{\frac{1}{2}}] \\ -d/(d^2+L^2)^{\frac{1}{2}}+a/(a^2+L^2)^{\frac{1}{2}}-\log\,d/a\}, \end{aligned} \qquad . \; . \; . \quad (4)$$

where L is the length of AB or CD, d is the length of AC and BD, and a is a small length left out of the integration because, for physical reasons, it is known that the elements concerned are not infinitely close together †. Since in equation (3) the entire force is

* It may be argued that the effect of the field cannot be localized in such a manner; this is obviously done, however, as soon as one assumes equation (2). During the process of integration one may sum up first the forces on CD due to elements **ds**′ along CD—the net force is zero; then one may sum up the forces on CD due to elements **ds**′ along AB; because of the large distance this force is negligible; hence the reaction on CD must be due to forces exerted by elements **ds**′ along AC and BD.

† A similar small length must be left out in applying equation (2), since the field of the vertical currents at the ends of AB, in the ideal circuit considered, would otherwise be infinite.

along r, the reacting force on the three sides is equal and opposite to the force on AB. Thus Ampère's equation leads to the result that *action and reaction are equal and opposite* for the mechanically separable parts.

Measurement of the Forces.

In order to determine whether action and reaction were equal and opposite for the mechanically separable

Fig. 2.

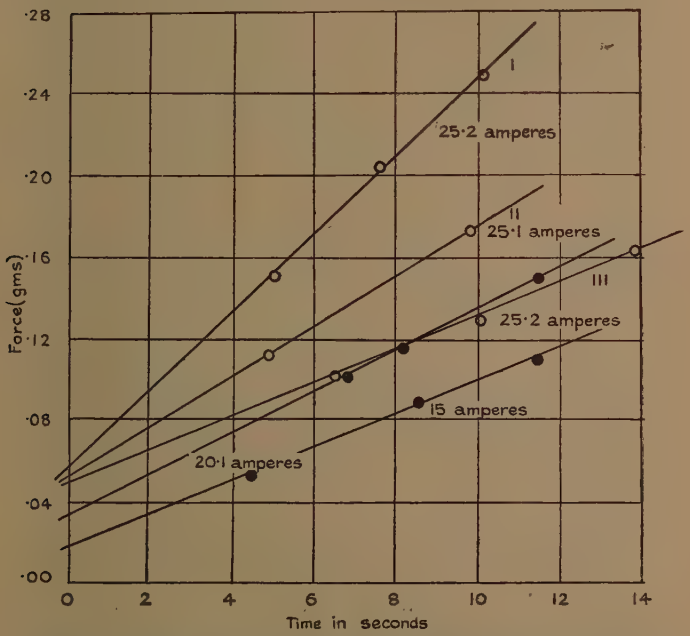

Variation in the total force on the single side with time. The three lines through the plain circles were obtained at a current very close to 25·2 amperes. It should be noted that while the slope of the three lines has changed, due to variations in the experimental conditions, the intercepts are the same within the limits of error in the experiment.

The lines through the heavy circles are for lower values of the current. Each circle represents the mean of from five to ten readings. The intercepts represent the true magnetic force.

parts, the forces were measured. This was accomplished by connecting each of the parts in turn to the arms

of a beam-balance. Connexion between the parts was made by the use of mercury cups. A heating effect in these cups caused the measured force to increase linearly with time; consequently it was necessary to plot the observed forces against the time, as shown in figs. 2 and 3, in order to obtain the true magnetic forces as intercepts at the $t=0$ axis.

Fig. 3.

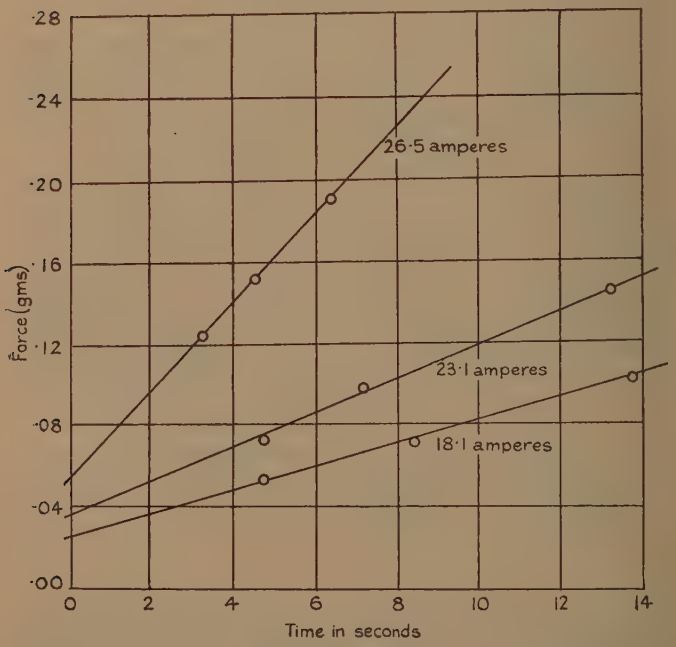

Increase in the total force on the three sides with time for different values of the current. Each point represents the mean of from five to ten readings. The intercepts represent the true value of the magnetic force.

The magnetic forces so obtained are given in Table I., and are shown graphically in fig. 4. It was not surprising to find that action and reaction were equal and opposite because, since the law is valid for closed circuits, it is reasonable to expect it to hold for macroscopic parts of circuits.

It is possible to estimate the value of the small length a left out of the integration in equation (4) for the experimental circuit used. If one imagines the current to flow through AB in horizontal filaments which turn

TABLE I.

Action.			Reaction.		
f (gm.).	i (amp.).	i^2.	f (gm.).	i (amp.).	i^2.
0·048	25·2	636	0·055	26·5	702
0·032	20·1	405	0·036	23·1	533
0·016	15·0	225	0·026	18·1	328

Fig. 4.

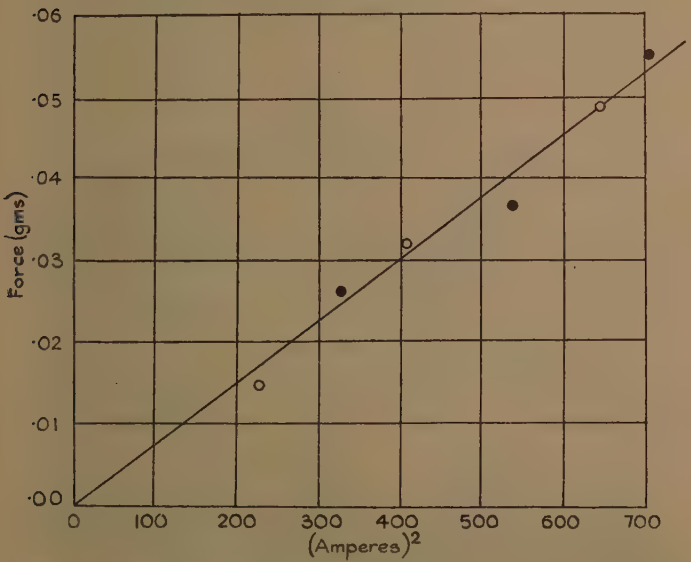

Force action and reaction between one side of a rectangular circuit and the other three sides. The plain circles represent the force on the single side and the heavy circles represent the force on the three sides.

at right angles to enter the vertical rods AC and BD, then the uppermost one of these horizontal filaments, which is roughly equivalent to a narrow stream of

electrons, might be a distance of 10^{-8} cm. from the corresponding filament in the vertical rods. The bottom of the brass rod used for AB was between 0·2 and 0·4 cm. from the end of the vertical rods, and hence the lowest horizontal filament would be at a distance of about 0·3 cm. from the corresponding vertical filament. Thus the average gap between the horizontal and vertical filaments would be about 0·15 cm. Substituting this value of a into equation (4) and solving for fc^2/i^2, the slope of the line in fig. 4, one obtains $8{\cdot}2\times10^{-5}$. The experimental value obtained from fig. 4 is $7{\cdot}55\times10^{-5}$.

Considering the assumptions made in estimating the value of a, this is a satisfactory agreement. If the distance from the bottom of the rod AB to the end of the vertical rods AC and BD had been taken to be 0·400 cm., as may actually have been the case, the average value of a would have been 0·200 cm.; this value of a gives a value of $7{\cdot}65\times10^{-5}$ for the slope of the line in fig. 4.

Discussion of Results.

The experimental results show clearly that, as one should expect, action and reaction are equal and opposite for the mechanically separable parts of the rectangular circuit. It follows from the foregoing discussion that in order to explain the results on the basis of the standard force equation for current elements, equation (2), it is necessary to make the doubtful assumption that *a part of a macroscopic circuit can lift itself*.

On the other hand, Ampère's expression, equation (3), gives a reasonably correct value for the forces without the necessity of making such an assumption. Since it leads to correct results for closed circuits, and also, in this case at least, for parts of circuits, the possibility of equation (3) being a correct expression for the force between current elements (or isolated moving charges) seems worthy of serious consideration *.

If Ampère's equation is correct, there must be a component of the magnetic force parallel to any element of a circuit, the parallel forces cancelling when the

* As a matter of fact, Maxwell concludes (*loc. cit.*, section 527, p. 174) that Ampère's equation "is undoubtedly the best, since it is the only one which makes the forces on the two elements not only equal and opposite, but in the straight line which joins them."

integration is taken about the entire circuit. Hering *, several years ago, described qualitative experiments which he claimed to indicate the presence of such a force. The results of the present work give quantitative evidence for the existence of the parallel force, unless one makes the unreasonable assumption, pointed out above, that a part of a macroscopic circuit can lift itself †.

In the standard force equation the entire force is perpendicular to the current element; hence, if the parallel force exists, this equation is definitely not valid as an expression for the force between current elements.

The author desires to express his appreciation to Prof. F. W. Warburton for his suggestion of this line of investigation, and for his continued interest and helpful criticisms throughout the course of the work.

XXXV. *The Ster and Stei Functions.* *By* N. W. McLachlan, *D.Sc.*, *M.I.E.E.*, *and* A. L. Meyers, *B.Sc.*, *A.M.I.E.E.*‡

STRUVE'S function of order ν is defined to be

$$\mathbf{H}_\nu(z) = \sum_{r=0}^{\infty} (-1)^r \frac{(\frac{1}{2}z)^{\nu+2r+1}}{\Gamma(r+\frac{3}{2})\Gamma(\nu+r+\frac{3}{2})} \quad . \quad . \quad . \quad (1)$$

If z is replaced by $zi^{3/2}$, we define the ster and stei functions of order ν, in Cartesian coordinates, by the relationship

$$\mathbf{H}_\nu(zi^{\pm 3/2}) = \mathrm{ster}_\nu z \pm i\,\mathrm{stei}_\nu z, \quad . \quad . \quad . \quad . \quad (2)$$

* C. Hering, Trans. of the Amer. Inst. of Elec. Engineers, xlii. p. 311 (1923).

† Ampère's force equation has been successfully applied by Pietenpol and Westerfield (Phys. Rev. xxxviii. p. 2280 (1931)) in the calculation of the torque on a rotating magnet, and by V. Bush (Journal of Mathematics and Physics, Mass. Inst. of Tech. v. p. 129 (1926)) in the calculation of the rate of precession of the orbit of an electron rotating about a massive nucleus and in explaining the results of the Kaufmann-Bucherer experiment without the necessity of assuming a variant mass. There is, to our knowledge, no case in which the Ampère equation is known to give incorrect results, either for partial or complete circuits.

‡ Communicated by the Authors.

these two functions being particular integrals of the differential equations

$$\frac{d^2y}{dz^2}+\frac{1}{z}\frac{dy}{dz}+\left(\mp i-\frac{\nu^2}{z^2}\right)y=\frac{i^{\pm 3(\nu+1)/2}z^{\nu-1}}{2^{\nu-1}\sqrt{\pi}\Gamma(\nu+\frac{1}{2})}. \quad . \quad (3)$$

Putting $\nu=0$, and writing $zi^{3/2}$ for (z) in (1), we obtain

$$\mathbf{H}_0(zi^{3/2})$$

$$=\frac{2i^{3/2}}{\pi}\left\{\frac{z}{1^2}+\frac{z^3i}{1^2.3^2}-\frac{z^5}{1^2.3^2.5^2}-\frac{z^7i}{1^2.3^2.5^2.7^2}+\cdots\right\}$$

$$=\frac{\sqrt{2}(i-1)}{\pi}\left\{\frac{z}{1^2}-\frac{z^5}{1^2.3^2.5^2}+\cdots\right.$$

$$\left.+i\left[\frac{z^3}{1^2.3^2}-\frac{z^7}{1^2.3^2.5^2.7^2}+\cdots\right]\right\}. \quad . \quad (4)$$

Hence

$$\operatorname{ster} z=-\frac{\sqrt{2}}{\pi}\left\{\frac{z}{1^2}+\frac{z^3}{1^2.3^2}-\frac{z^5}{1^2.3^2.5^2}\right.$$

$$\left.-\frac{z^7}{1^2.3^2.5^2.7^2}+\cdots\right\}, \quad . \quad (5)$$

and

$$\operatorname{stei} z=\frac{\sqrt{2}}{\pi}\left\{\frac{z}{1^2}-\frac{z^3}{1^2.3^2}-\frac{z^5}{1^2.3^2.5^2}\right.$$

$$\left.+\frac{z^7}{1^2.3^2.5^2.7^2}+\cdots\right\}. \quad . \quad (6)$$

Similarly we get

$$\operatorname{ster}_1 z=\frac{2}{\pi}\left\{\frac{z^4}{1^2.3^2.5}-\frac{z^8}{1^2.3^2.5^2.7^2.9}+\cdots\right\}, \quad . \quad (7)$$

$$\operatorname{stei}_1 z=-\frac{2}{\pi}\left\{\frac{z^2}{1^2.3}-\frac{z^6}{1^2.3^2.5^2.7}+\cdots\right\}. \quad . \quad . \quad (8)$$

Differentiating we obtain

$$\frac{d\operatorname{ster} z}{dz}=\operatorname{ster}' z=-\frac{\sqrt{2}}{\pi}\left\{1+\frac{z^2}{1^2.3}-\frac{z^4}{1^2.3^2.5}\right.$$

$$\left.-\frac{z^6}{1^2.3^2.5^2.7}+\cdots\right\}, \quad . \quad (9)$$

and

$$\frac{d\,\mathrm{stei}\,z}{dz}=\mathrm{stei}'z=\frac{\sqrt{2}}{\pi}\left\{1-\frac{z^2}{1^2.3}-\frac{z^4}{1^2.3^2.5}+\frac{z^6}{1^2.3^2.5^2.7}+\cdots\right\}. \quad (10)$$

From (9) and (10), by addition and subtraction,

$$\mathrm{ster}'z+\mathrm{stei}'z=\sqrt{2}\,\mathrm{stei}_1 z, \quad (11)$$

$$\mathrm{ster}'z-\mathrm{stei}'z=\sqrt{2}\left(\mathrm{ster}_1 z-\frac{2}{\pi}\right). \quad (12)$$

From (11) and (12)

$$\mathrm{ster}'z=\frac{1}{\sqrt{2}}\left(\mathrm{ster}_1 z+\mathrm{stei}_1 z-\frac{2}{\pi}\right), \quad (13)$$

$$\mathrm{stei}'z=\frac{1}{\sqrt{2}}\left(\mathrm{stei}_1 z-\mathrm{ster}_1 z+\frac{2}{\pi}\right). \quad (14)$$

From (13) and (14)

$$\mathrm{ster}'^2 z+\mathrm{stei}'^2 z=\left(\mathrm{ster}_1 z-\frac{2}{\pi}\right)^2+\mathrm{stei}_1{}^2 z, \quad (15)$$

$$\mathrm{ster}'^2 z-\mathrm{stei}'^2 z=2\,\mathrm{stei}_1 z\left(\mathrm{ster}_1 z-\frac{2}{\pi}\right), \quad (16)$$

$$\mathrm{ster}\,z=-\frac{\sqrt{2}z}{\pi}+\frac{1}{\sqrt{2}}\int_0^z(\mathrm{ster}_1 z+\mathrm{stei}_1 z)\,dz. \quad (17)$$

$$\mathrm{stei}\,z=\frac{\sqrt{2}z}{\pi}+\frac{1}{\sqrt{2}}\int_0^z(\mathrm{stei}_1 z-\mathrm{ster}_1 z)\,dz. \quad (18)$$

We also have

$$\frac{d}{dz}(z\,\mathrm{ster}'z)=-\left[\frac{\sqrt{2}}{\pi}+z\,\mathrm{stei}\,z\right], \quad (19)$$

or

$$z\,\mathrm{ster}'z=-\frac{\sqrt{2}z}{\pi}-\int_0^z z\,\mathrm{stei}\,z\,dz\,; \quad (20)$$

and $$\frac{d}{dz}(z\,\mathrm{stei}'z)=\frac{\sqrt{2}}{\pi}+z\,\mathrm{ster}\,z, \quad . \quad . \quad . \quad . \quad . \quad (21)$$

or $$z\,\mathrm{stei}'z=\frac{\sqrt{2}z}{\pi}+\int_0^z z\,\mathrm{ster}\,z\,dz. \quad . \quad . \quad (22)$$

Using (19) and (21), the following integrals can be evaluated :

$$\begin{aligned}\int_0^z z\,\mathrm{ster}^2 z\,dz&=\int_0^z \mathrm{ster}\,z\,.(z\,\mathrm{ster}\,z)\,dz\\&=\int_0^z \mathrm{ster}\,z\left[-\frac{\sqrt{2}}{\pi}dz+d(z\,\mathrm{stei}'z)\right]\\&=-\frac{\sqrt{2}}{\pi}\int_0^z \mathrm{ster}\,z\,dz+z\,\mathrm{ster}\,z\,\mathrm{stei}'z\\&\qquad-\int_0^z z\,\mathrm{ster}'z\,\mathrm{stei}'z\,dz\,; \quad . \quad (23)\end{aligned}$$

$$\begin{aligned}\int_0^z z\,\mathrm{stei}^2 z\,dz&=\int_0^z \mathrm{stei}\,z\,(z\,\mathrm{stei}\,z)\,dz\\&=-\int_0^z \mathrm{stei}\,z\left[\frac{\sqrt{2}}{\pi}dz+d(z\,\mathrm{ster}'z)\right]\\&=-\frac{\sqrt{2}}{\pi}\int_0^z \mathrm{stei}\,z\,dz-z\,\mathrm{ster}'z\,\mathrm{stei}\,z\\&\qquad+\int_0^z z\,\mathrm{ster}'z\,\mathrm{stei}'z\,dz. \quad . \quad (24)\end{aligned}$$

From (23) and (24), by addition, we get

$$\begin{aligned}\int_0^z z(\mathrm{ster}^2 z+\mathrm{stei}^2 z)dz&=z[\mathrm{ster}\,z\,\mathrm{stei}'z-\mathrm{ster}'z\,\mathrm{stei}\,z]\\&\qquad-\frac{\sqrt{2}}{\pi}\int_0^z(\mathrm{ster}\,z+\mathrm{stei}\,z)\,dz. \quad . \quad (25)\end{aligned}$$

In like manner it can be shown that

$$\begin{aligned}\int_0^z z\,(\mathrm{ster}'^2 z+\mathrm{stei}'^2 z)\,dz&=z[\mathrm{ster}\,z\,\mathrm{ster}'z+\mathrm{stei}\,z\,\mathrm{stei}'z]\\&\qquad+\frac{\sqrt{2}}{\pi}\int_0^z(\mathrm{ster}\,z-\mathrm{stei}\,z)\,dz. \quad . \quad (26)\end{aligned}$$

Since

$$\mathbf{H}_\nu(zi^{3/2}) = \sum_{r=0}^{\infty} \frac{(-1)^r (\frac{1}{2}z)^{\nu+2r+1} i^{3(\nu+2r+1)/2}}{\Gamma(r+\frac{3}{2})\Gamma(\nu+r+\frac{3}{2})}, \quad . \quad (27)$$

we obtain immediately

$$\mathrm{ster}_\nu z = \sum_{r=0}^{\infty} \frac{(-1)^r (\frac{1}{2}z)^{\nu+2r+1} \cos \frac{3}{4}(\nu+2r+1)\pi}{\Gamma(r+\frac{3}{2})\Gamma(\nu+r+\frac{3}{2})} \quad . \quad (28)$$

$$= \sum_{r=0}^{\infty} \frac{(\frac{1}{2}z)^{\nu+2r+1} \cos \frac{3}{4}(\nu+\frac{2}{3}r+1)\pi}{\Gamma(r+\frac{3}{2})\Gamma(\nu+r+\frac{3}{2})}, \quad . \quad . \quad . \quad (29)$$

and

$$\mathrm{stei}_\nu z = \sum_{r=0}^{\infty} \frac{(-1)^r (\frac{1}{2}z)^{\nu+2r+1} \sin \frac{3}{4}(\nu+2r+1)\pi}{\Gamma(r+\frac{3}{2})\Gamma(\nu+r+\frac{3}{2})} \quad . \quad (30)$$

$$= \sum_{r=0}^{\infty} \frac{(\frac{1}{2}z)^{\nu+2r+1} \sin \frac{3}{4}(\nu+\frac{2}{3}r+1)\pi}{\Gamma(r+\frac{3}{2})\Gamma(\nu+r+\frac{3}{2})} \cdot \quad . \quad . \quad . \quad (31)$$

The most important recurrence and integral formulæ are

$$z\,\mathrm{ster}_\nu' z = -\nu\,\mathrm{ster}_\nu z - \frac{z}{\sqrt{2}}(\mathrm{ster}_{\nu-1} z + \mathrm{stei}_{\nu-1} z), \quad . \quad (32)$$

$$z\,\mathrm{stei}_\nu' z = -\nu\,\mathrm{stei}_\nu z + \frac{z}{\sqrt{2}}(\mathrm{ster}_{\nu-1} z - \mathrm{stei}_{\nu-1} z), \quad . \quad (33)$$

$$z\,\mathrm{ster}_{\nu+1} z = -\sqrt{2}\nu(\mathrm{ster}_\nu z - \mathrm{stei}_\nu z) - z\,\mathrm{ster}_{\nu-1} z + \frac{2(\frac{1}{2}z)^{\nu+1} \cos \frac{3}{4}\nu\pi}{\sqrt{\pi}\Gamma(\nu+\frac{3}{2})}, \quad . \quad . \quad . \quad (34)$$

$$z\,\mathrm{stei}_{\nu+1} z = -\sqrt{2}\nu(\mathrm{ster}_\nu z + \mathrm{stei}_\nu z) - z\,\mathrm{stei}_{\nu-1} z + \frac{2(\frac{1}{2}z)^{\nu+1} \sin \frac{3}{4}\nu\pi}{\sqrt{\pi}\Gamma(\nu+\frac{3}{2})}, \quad . \quad . \quad . \quad (35)$$

$$\int^z z^\nu \,\mathrm{ster}_{\nu-1} z\, dz = -\frac{1}{\sqrt{2}} z^\nu (\mathrm{ster}_\nu z - \mathrm{stei}_\nu z), \quad . \quad (36)$$

$$\int^z z^\nu \,\mathrm{stei}_{\nu-1} z\, dz = -\frac{1}{\sqrt{2}} z^\nu (\mathrm{ster}_\nu z + \mathrm{stei}_\nu z). \quad . \quad (37)$$

From the differential equation we obtain, at once, the relationships

$$\mathrm{ster}_\nu'' z + \frac{1}{z}\mathrm{ster}_\nu' z + \mathrm{stei}_\nu z - \frac{\nu^2}{z^2}\mathrm{ster}_\nu z = \frac{(\frac{1}{2}z)^{\nu-1} \cos \frac{3}{4}(\nu+1)\pi}{\sqrt{\pi}\Gamma(\nu+\frac{1}{2})}, \quad . \quad . \quad . \quad (38)$$

$$\mathrm{stei}_\nu''z+\frac{1}{z}\mathrm{stei}_\nu'z-\mathrm{ster}_\nu z-\frac{\nu^2}{z^2}\mathrm{stei}_\nu z=\frac{(\frac{1}{2}z)^{\nu-1}\sin\frac{3}{4}(\nu+1)\pi}{\sqrt{\pi}\Gamma(\nu+\frac{1}{2})}. \quad . \quad . \quad (39)$$

It can also be shown that

$$\mathrm{ster}\,z=i\,\mathrm{stei}\,(zi), \quad . \quad . \quad . \quad . \quad . \quad . \quad (40)$$

$$\mathrm{stei}\,z=i\,\mathrm{ster}\,(zi), \quad . \quad . \quad . \quad . \quad . \quad . \quad (41)$$

$$\mathrm{ster}'\,z=-\mathrm{stei}'\,(zi), \quad . \quad . \quad . \quad . \quad . \quad . \quad (42)$$

$$\mathrm{stei}'\,z=-\mathrm{ster}'\,(zi). \quad . \quad . \quad . \quad . \quad . \quad . \quad (43)$$

Asymptotic Formulæ for $\mathrm{ster}_\nu z$ *and* $\mathrm{stei}_\nu z$.

When z is large enough *

$$\mathbf{H}_\nu(zi^{3/2})\doteqdot \mathrm{Y}_\nu(zi^{3/2})+\frac{1}{\pi}\sum_{r=0}^{n-1}\frac{\Gamma(r+\frac{1}{2})}{\Gamma(\nu+\frac{1}{2}-r)}\left(\frac{2}{z}\right)^{1+2r-\nu}e^{-3\pi(1+2r-\nu)i/4}, \quad . \quad . \quad . \quad . \quad (44)$$

provided $\mathrm{R}(n+\frac{1}{2}-\nu)\geqslant 0$.

Taking $\mathrm{Y}_\nu(zi^{3/2})$ first we have

$$\mathrm{Y}_\nu(zi^{3/2})=\tfrac{1}{2}i[\mathbf{H}_\nu^{(2)}(zi^{3/2})-\mathbf{H}_\nu^{(1)}(zi^{3/2})]. \quad . \quad . \quad (45)$$

The asymptotic formula for the second Hankel function is

$$\mathbf{H}_\nu^{(2)}(zi^{3/2})\doteqdot\sqrt{\frac{2}{\pi z}}e^{-3\pi i/8}.e^{-zi^{5/2}+(1/4+\nu/2)\pi i} \times[\zeta_\nu(zi^{3/2})-i\xi_\nu(zi^{3/2})], \quad . \quad . \quad (46)$$

so

$$\mathbf{H}_\nu^{(2)}(zi^{3/2})\doteqdot\sqrt{\frac{2}{\pi z}}e^{z/\sqrt{2}}.e^{i(z/\sqrt{2}-\pi/8+\nu\pi/2)}[\zeta_\nu-i\xi_\nu], \quad . \quad (47)$$

where

$$\zeta_\nu(u)=1-\frac{(4\nu^2-1^2)(4\nu^2-3^2)}{2\,!\,(8u)^2}+\ldots+\mathrm{R}_p, \quad . \quad . \quad . \quad . \quad (48)$$

$$\xi_\nu(u)=\frac{(4\nu^2-1^2)}{1\,!\,8u}-\frac{(4\nu^2-1^2)(4\nu^2-3^2)(4\nu^2-5^2)}{3\,!\,(8u)^3}+\ldots+\mathrm{R}_s, \quad . \quad . \quad . \quad (49)$$

and $u=zi^{3/2}$.

* Watson, ' Theory of Bessel Functions,' p. 333.

Also

$$H_\nu^{(1)}(zi^{3/2}) \doteqdot \sqrt{\frac{2}{\pi z}}\, e^{-z/\sqrt{2}} . e^{-i(z/\sqrt{2}+5\pi/8+\nu\pi/2)}[\zeta_\nu + i\xi_\nu] . \quad (50)$$

As a first approximation (50) can be neglected in comparison with (47), so that (45) becomes

$$Y_\nu(zi^{3/2}) \doteqdot \frac{e^{z/\sqrt{2}}}{\sqrt{2\pi z}} . e^{i(z/\sqrt{2}+3\pi/8+\nu\pi/2)}[\zeta_\nu - i\xi_\nu] . \quad (51)$$

$$\zeta_\nu(zi^{3/2}) = 1 - \frac{B}{z^4} + \frac{D}{z^8} - \ldots + i[-A/z^2 + C/z^6 - E/z^{10} + \ldots] \quad (52)$$

$$= P(z) + iQ(z), \quad (53)$$

where $A = (4\nu^2 - 1^2)(4\nu^2 - 3^2)/2!\,8^2$,

$B = (4\nu^2 - 1^2) \ldots (4\nu^2 - 7^2)/4!\,8^4$,

and so on.

$$\xi_\nu(zi^{3/2}) = \frac{1}{\sqrt{2}}[-A_1/z - B_1/z^3 + C_1/z^5 + D_1/z^7 - \ldots] + \frac{i}{\sqrt{2}}[-A_1/z + B_1/z^3 + C_1/z^5 - \ldots] . \quad (54)$$

$$= P_1(z) + iQ_1(z), \quad (55)$$

where

$$A_1 = \frac{(4\nu^2 - 1^2)}{1!\,8}, \quad B_1 = (4\nu^2 - 1^2)(4\nu^2 - 3^2)(4\nu^2 - 5^2)/3!\,8^3,$$

and so on.

Hence from (51), (53), and (55)

$$Y_\nu(zi^{3/2}) \doteqdot \frac{e^{z/\sqrt{2}}}{\sqrt{2\pi z}} \{(\cos\alpha + i\sin\alpha)[(P + Q_1) - i(P_1 - Q)]\}, \quad (56)$$

where $\alpha = (z/\sqrt{2} + \frac{3}{8}\pi + \frac{1}{2}\nu\pi)$.

From (44) and (56) we obtain the asymptotic formulæ, for $\mathrm{ster}_\nu z$ and $\mathrm{stei}_\nu z$, to the approximation indicated above, as follows :—

$$\mathrm{ster}_\nu z \doteqdot \frac{e^{z/\sqrt{2}}}{\sqrt{2\pi z}}[(P + Q_1)\cos\alpha + (P_1 - Q)\sin\alpha] + \frac{1}{\pi}\sum_{r=0}^{n-1} \frac{\Gamma(r + \frac{1}{2})}{\Gamma(\nu + \frac{1}{2} - r)} \left(\frac{2}{z}\right)^{1+2r-\nu} \cos\tfrac{3}{4}(1 + 2r - \nu)\pi \quad (57)$$

and

$$\mathrm{stei}_\nu z \doteq \frac{e^{z/\sqrt{2}}}{\sqrt{2\pi z}}[(\mathrm{P}+\mathrm{Q}_1)\sin\alpha-(\mathrm{P}_1-\mathrm{Q})\cos\alpha] - \frac{1}{\pi}\sum_{r=0}^{n-1}\frac{\Gamma(r+\frac{1}{2})}{\Gamma(\nu+\frac{1}{2}-r)}\left(\frac{2}{z}\right)^{1+2r-\nu}\sin\tfrac{3}{4}(1+2r+\nu)\pi. \quad . \quad . \quad . \quad (58)$$

If $\mathrm{H}_\nu^{(1)}(zi^{3/2})$ in (45) is included in the asymptotic formulæ it is necessary to add to $\mathrm{ster}_\nu z$

$$\frac{-e^{-z/\sqrt{2}}}{\sqrt{2\pi z}}[(\mathrm{P}-\mathrm{Q}_1)\cos\beta+(\mathrm{P}_1+\mathrm{Q})\sin\beta], \quad . \quad (59)$$

and to $\mathrm{stei}_\nu z$

$$\frac{e^{-z/\sqrt{2}}}{\sqrt{2\pi z}}[(\mathrm{P}-\mathrm{Q}_1)\sin\beta-(\mathrm{P}_1+\mathrm{Q})\cos\beta], \quad . \quad (60)$$

where $$\beta=(z/\sqrt{2}+\tfrac{1}{8}\pi+\tfrac{1}{2}\nu\pi).$$

Polar Form of $\mathbf{H}_\nu(zi^{\pm 3/2})$.

This is treated in like manner to that of the functions $\mathrm{J}_\nu(zi^{3/2})$ and $\mathrm{K}_\nu(zi^{1/2})$ *.

By definition

$$\mathbf{H}_\nu(zi^{\pm 3/2})=\mathrm{S}_\nu(z)\,e^{\pm i\psi_\nu(z)}=\mathrm{ster}_\nu z \pm i\,\mathrm{stei}_\nu z, \quad . \quad (61)$$

so that

$$\mathrm{ster}_\nu z=\mathrm{S}_\nu(z)\cos\psi_\nu(z), \quad . \quad (62)$$

$$\mathrm{stei}_\nu z=\mathrm{S}_\nu(z)\sin\psi_\nu(z), \quad . \quad (63)$$

$$\sqrt{\mathrm{ster}_\nu{}^2 z+\mathrm{stei}_\nu{}^2 z}=\mathrm{S}_\nu(z), \quad . \quad (64)$$

$$\psi_\nu(z)=\tan^{-1}(\mathrm{stei}\,z/\mathrm{ster}\,z), \quad . \quad (65)$$

and $$-\psi_\nu(z)=\tan^{-1}(-\mathrm{stei}\,z/\mathrm{ster}\,z). \quad . \quad (66)$$

From a recurrence formula for Struve's function

$$\mathbf{H}_0{}'(zi^{3/2})=2/\pi-\mathbf{H}_1(zi^{3/2})=2/\pi-\mathrm{S}_1(z)e^{i\psi_1(z)},$$

so

$$\frac{1}{i^{3/2}}\frac{d}{dz}\{\mathbf{H}_0(zi^{3/2})\}=2/\pi-\mathrm{S}_1(z)e^{i\psi_1(z)},$$

and, therefore,

$$\mathrm{ster}'\,z+i\,\mathrm{stei}'\,z=-(2/\pi)\,e^{-\frac{1}{4}\pi i}+\mathrm{S}_1(z)e^{i\{\psi_1(z)-\frac{1}{4}\pi\}}. \quad (67)$$

* McLachlan, 'Bessel Functions for Engineers,' p. 122.

Thus

$$\mathrm{ster}'\, z=-\frac{\sqrt{2}}{\pi}+\mathrm{S}_1(z)\cos\left[\psi_1(z)-\tfrac{1}{4}\pi\right], \quad . \quad (68)$$

and

$$\mathrm{stei}'\, z=\frac{\sqrt{2}}{\pi}+\mathrm{S}_1(z)\sin\left[\psi_1(z)-\tfrac{1}{4}\pi\right]. \quad . \quad . \quad (69)$$

From (68) and (69) we get

$$\mathrm{ster}'^2 z+\mathrm{stei}'^2 z=4/\pi^2+\mathrm{S}_1{}^2(z)-(4/\pi)\mathrm{S}_1(z)\cos\psi_1(z), \quad (70)$$

and

$$\mathrm{ster}'^2 z-\mathrm{stei}'^2 z=-(4/\pi)\mathrm{S}_1(z)\sin\psi_1(z)+\mathrm{S}_1{}^2(z)\sin\{2\psi_1(z)\}. \quad . \quad . \quad . \quad (71)$$

Also from (62), (63), (68), and (69) it can be shown that

$$\mathrm{ster}\, z\ \mathrm{ster}'\, z+\mathrm{stei}\, z\ \mathrm{stei}'\, z=\mathrm{S}_0\mathrm{S}_1\cos(\psi_1-\psi_0-\tfrac{1}{4}\pi) -\frac{2}{\pi}\mathrm{S}_0\cos(\psi_0+\tfrac{1}{4}\pi), \quad . \quad (72)$$

and

$$\mathrm{ster}\, z\ \mathrm{stei}'\, z-\mathrm{ster}'\, z\ \mathrm{stei}\, z=\mathrm{S}_0\mathrm{S}_1\sin(\psi_1-\psi_0-\tfrac{1}{4}\pi) +\frac{2}{\pi}\mathrm{S}_0\sin(\psi_0+\tfrac{1}{4}\pi), \quad . \quad (73)$$

the argument z for the S and ψ functions being understood.

By aid of a recurrence formula for $\mathbf{H}_\nu(z)$ we obtain

$$\mathrm{ster}_\nu'\, z=\tfrac{1}{2}\{\mathrm{S}_{\nu+1}\cos(\psi_{\nu+1}-\tfrac{1}{4}\pi)-\mathrm{S}_{\nu-1}\cos(\psi_{\nu-1}-\tfrac{1}{4}\pi)\} +\frac{(\frac{1}{2}z)^\nu\cos\frac{3}{4}\pi(\nu+1)}{\sqrt{\pi}\Gamma(\nu+\frac{3}{2})}, \quad . \quad . \quad (74)$$

and

$$\mathrm{stei}_\nu'\, z=\tfrac{1}{2}\{\mathrm{S}_{\nu+1}\sin(\psi_{\nu+1}-\tfrac{1}{4}\pi)-\mathrm{S}_{\nu-1}\sin(\psi_{\nu-1}-\tfrac{1}{4}\pi)\} +\frac{(\frac{1}{2}z)^\nu\sin\frac{3}{4}\pi(\nu+1)}{\sqrt{\pi}\Gamma(\nu+\frac{3}{2})}. \quad . \quad . \quad (75)$$

By using other recurrence formulæ for $\mathbf{H}_\nu(z)$, $\mathrm{ster}_\nu'\, z$ and $\mathrm{stei}_\nu'\, z$ can be expressed differently from (74) and (75).

To differentiate $\mathrm{S}_\nu(z)$ and $\psi_\nu(z)$ with respect to z we have

$$\mathbf{H}_\nu'(z)=-\frac{\nu}{z}\mathbf{H}_\nu(z)+\mathbf{H}_{\nu-1}(z),$$

so

$$\frac{d\mathbf{H}_\nu(zi^{3/2})}{dz}=-\frac{\nu}{z}\mathbf{H}_\nu(zi^{3/2})-e^{-\pi i/4}\mathbf{H}_{\nu-1}(zi^{3/2}). \quad . \quad (76)$$

Thus

$$\frac{d}{dz}\{S_\nu(z)\,e^{i\psi_\nu(z)}\}=[S_\nu'+i\psi_\nu'\,S_\nu]\,e^{i\psi_\nu} \quad . \quad . \quad . \quad (77)$$

$$=-\frac{\nu}{z}S_\nu\,e^{i\psi_\nu}-S_{\nu-1}\,e^{i[\psi_{\nu-1}-\pi/4]}. \quad (78)$$

Equating real and imaginary parts in (77) and (78), we obtain

$$\frac{d}{dz}S_\nu(z)=S_\nu'(z)=-S_{\nu-1}(z)\cos(\psi_\nu-\psi_{\nu-1}+\tfrac{1}{4}\pi)-\frac{\nu}{z}S_\nu(z), \quad (79)$$

and

$$\frac{d}{dz}\psi_\nu(z)=\psi_\nu'(z)=\frac{S_{\nu-1}(z)}{S_\nu(z)}\sin(\psi_\nu-\psi_{\nu-1}+\tfrac{1}{4}\pi). \quad . \quad (80)$$

Two additional expressions for these derivatives can be found by using other recurrence formulæ. As a particular case we have

$$\frac{d}{dz}S_0(z)=S_1\cos(\psi_1-\psi_0-\tfrac{1}{4}\pi)-\frac{2}{\pi}\cos(\psi_0+\tfrac{1}{4}\pi), \quad (81)$$

$$\frac{d}{dz}\psi_0(z)=\frac{S_1}{S_0}\sin(\psi_1-\psi_0-\tfrac{1}{4}\pi)+\frac{2}{\pi}\sin(\psi_0+\tfrac{1}{4}\pi). \quad . \quad (82)$$

Struve Function with imaginary argument $\mathbf{H}_\nu(zi)$.

From (1), using Watson's notation, we obtain

$$\left.\begin{aligned}\mathbf{L}_\nu(z)&=i^{-(\nu+1)}\,\mathbf{H}_\nu(zi)=e^{-(\nu+1)\pi i/2}\,\mathbf{H}_\nu(zi),\\&=\sum_{r=0}^{\infty}\frac{(\frac{1}{2}z)^{\nu+2r+1}}{\Gamma(r+\frac{3}{2})\Gamma(\nu+r+\frac{3}{2})}.\end{aligned}\right\} \quad . \quad . \quad (83)$$

Using the recurrence and other formulæ associated with Struve's function the following are easily obtained :

$$z\mathbf{L}_\nu'(z)=\nu\mathbf{L}_\nu(z)+z\mathbf{L}_{\nu+1}(z)+\frac{2(\frac{1}{2}z)^{\nu+1}}{\sqrt{\pi}\Gamma(\nu+\frac{3}{2})}. \quad (84)$$

$$z\mathbf{L}_\nu'(z)=-\nu\mathbf{L}_\nu(z)+z\mathbf{L}_{\nu-1}(z) \quad . \quad . \quad . \quad (85)$$

$$2\mathbf{L}_\nu'(z)=\mathbf{L}_{\nu-1}(z)+\mathbf{L}_{\nu+1}(z)+\frac{(\frac{1}{2}z)^\nu}{\sqrt{\pi}\Gamma(\nu+\frac{3}{2})}. \quad (86)$$

$$\frac{2\nu\mathbf{L}_\nu(z)}{z}=\mathbf{L}_{\nu-1}(z)-\mathbf{L}_{\nu+1}(z)-\frac{(\frac{1}{2}z)^\nu}{\sqrt{\pi}\Gamma(\nu+\frac{3}{2})}. \quad (87)$$

$$\mathbf{L}_0'(z)=2/\pi+\mathbf{L}_1(z). \quad . \quad . \quad . \quad . \quad . \quad . \quad (88)$$

$$\int^z z^\nu \mathbf{L}_{\nu-1}(z)\,dz = z^\nu \mathbf{L}_\nu(z), \quad \text{or} \quad \frac{d}{dz}\{z^\nu \mathbf{L}_\nu(z)\} = z^\nu \mathbf{L}_{\nu-1}(z). \quad . \quad . \quad . \quad (89)$$

$$\left.\begin{aligned} &\int^z z^{-\nu}\mathbf{L}_{\nu+1}(z)\,dz = z^{-\nu}\mathbf{L}_\nu(z) - z/2^\nu\sqrt{\pi}\Gamma(\nu+\tfrac{3}{2}), \\ \text{or} \quad &\\ &\frac{d}{dz}\{z^{-\nu}\mathbf{L}_\nu(z)\} = z^{-\nu}\mathbf{L}_{\nu+1}(z) + 1/2^\nu\sqrt{\pi}\Gamma(\nu+\tfrac{3}{2}). \end{aligned}\right\} \quad . \quad (90)$$

$$\mathbf{L}_\nu(z) = \frac{2(\frac{1}{2}z)^\nu}{\sqrt{\pi}\Gamma(\nu+\frac{1}{2})}\int_0^{\pi/2} \sinh(z\cos\theta)\sin^{2\nu}\theta\,d\theta, \quad (91)^*$$

$$\mathrm{R}(\nu) > -\tfrac{1}{2}$$

$$= \frac{2(\frac{1}{2}z)^\nu}{\sqrt{\pi}\Gamma(\nu+\frac{1}{2})}\int_0^1 (1-t^2)^{\nu-1}\sinh zt\,dt. \quad . \quad . \quad (92)$$

$$\mathrm{R}(\nu) > -\tfrac{1}{2}$$

$$\int_0^z \mathbf{L}_0(z)\,dz = \frac{2}{\pi}\int_0^{\pi/2}\left[\frac{\cosh(z\sin\theta)-1}{\sin\theta}\right]d\theta. \quad . \quad (93)$$

$$\mathrm{I}_\nu(z) - \mathbf{L}_\nu(z) = \frac{2(\frac{1}{2}z)^\nu}{\sqrt{\pi}\Gamma(\nu+\frac{1}{2})}\int_0^{\pi/2} e^{-z\left\{\begin{smallmatrix}\cos\theta\\ \sin\theta\end{smallmatrix}\right.}\begin{cases}\sin^{2\nu}\theta\,d\theta\\ \cos^{2\nu}\theta\end{cases}. \quad (94)$$

$$\mathrm{R}(\nu) > -\tfrac{1}{2}$$

$$\mathbf{L}_\nu''(z) + \frac{1}{z}\mathbf{L}_\nu'(z) - \left(1+\frac{\nu^2}{z^2}\right)\mathbf{L}_\nu(z) - \frac{(\frac{1}{2}z)^{\nu-1}}{\sqrt{\pi}\Gamma(\nu+\frac{1}{2})} = 0. \quad (95)$$

$$\mathbf{L}_0(z) = \frac{4}{\pi}\sum_{n=0}^{\infty}(-1)^n\frac{\mathrm{I}_{2n+1}(z)}{2n+1}. \quad . \quad . \quad . \quad . \quad . \quad . \quad . \quad . \quad (96)$$

$$\mathbf{L}_{1/2}(z) = -\sqrt{\frac{2}{\pi z}} + \mathrm{I}_{-1/2}(z) = \sqrt{\frac{2}{\pi z}}[\cosh z - 1]. \quad (97)$$

$$\mathbf{L}_{-1/2}(z) = \mathrm{I}_{1/2}(z) = \sqrt{\frac{2}{\pi z}}\sinh z. \quad . \quad . \quad . \quad . \quad . \quad . \quad . \quad (98)$$

We also have

$$\mathbf{L}_\nu(zi^{\pm 1/2}) = \mathrm{S}_\nu(z)\,e^{\pm i[\psi_\nu(z) \mp (\nu+1)\pi/2]}. \quad . \quad . \quad . \quad . \quad . \quad . \quad . \quad (99)$$

Asymptotic Formula for $\mathbf{L}_\nu(z)$.

From (44) and (83), when z is large enough, we have

$$\mathbf{L}_\nu(z) \doteqdot e^{-(\nu+1)\pi i/2}\mathrm{Y}_\nu(zi) + \frac{1}{\pi}\sum_{r=0}^{n-1}\frac{\Gamma(r+\frac{1}{2})}{\Gamma(\nu+\frac{1}{2}-r)}\left(\frac{2}{z}\right)^{1+2r-\nu} e^{-(r+1)\pi i}. \quad . \quad . \quad . \quad (100)$$

* This formula is also given in Watson's 'Bessel Functions,' p. 329.

We have

$$\mathrm{H}_\nu^{(2)}(zi) \doteqdot \sqrt{\frac{2}{\pi z}}\, e^{-\pi i/4}.e^{z+(1/4+\nu/2)\pi i}[\zeta_\nu(zi)-i\xi_\nu(zi)],$$

$$\doteqdot \sqrt{\frac{2}{\pi z}}\, e^{z}.e^{\nu\pi i/2}[\zeta_\nu(zi)-i\xi_\nu(zi)], \quad . \quad . \quad . \quad (101)$$

$\zeta_\nu(u)$ and $\xi_\nu(u)$ being given in (48) and (49).

We also have

$$\mathrm{H}_\nu^{(1)}(zi) \doteqdot \sqrt{\frac{2}{\pi z}}\, e^{-z}.e^{-\pi(\nu+1)i/2}[\zeta_\nu(zi)+i\xi_\nu(zi)]. \quad (102)$$

Thus from (45), (101), and (102)

$$e^{-\pi(\nu+1)i/2}\,\mathrm{Y}_\nu(zi) \doteqdot \frac{1}{\sqrt{2\pi z}}\{e^{z}[\zeta_\nu(zi)-i\xi_\nu(zi)] - e^{-z}.e^{-(\nu+1/2)\pi i}[\zeta_\nu(zi)+i\xi_\nu(zi)]\}, \quad (103)$$

where

$$\zeta_\nu(zi) = 1+\mathrm{A}/z^2+\mathrm{B}/z^4+\ldots,$$

and

$$\xi_\nu(zi) = -i[\mathrm{A}_1/z+\mathrm{B}_1/z^3+\mathrm{C}_1/z^5+\ldots],$$

giving

$$\zeta_\nu(zi)+i\xi_\nu(zi) = [1+\mathrm{A}_1/z+\mathrm{A}/z^2+\mathrm{B}_1/z^3+\mathrm{B}/z^4+\ldots] = \mathrm{P}_2(z), \quad . \quad . \quad . \quad (104)$$

and

$$\zeta_\nu(zi)-i\xi_\nu(zi) = [1-\mathrm{A}_1/z+\mathrm{A}/z^2-\mathrm{B}_1/z^3 +\mathrm{B}/z^4-\ldots] = \mathrm{P}_2(-z). \quad . \quad . \quad (105)$$

Hence (103) can be written

$$e^{-\pi(\nu+1)i/2}\,\mathrm{Y}_\nu(zi) \doteqdot \frac{1}{\sqrt{2\pi z}}\{e^{z}\,\mathrm{P}_2(-z)-e^{-z}\,e^{-(\nu+1/2)\pi i}\,\mathrm{P}_2(z)\}; \quad . \quad . \quad . \quad (106)$$

so that from (100) and (106) we finally obtain

$$\mathbf{L}_\nu(z) \doteqdot \frac{1}{\sqrt{2\pi z}}\{e^{z}\,\mathrm{P}_2(-z)-e^{-z}.e^{-(\nu+1/2)\pi i}\,\mathrm{P}_2(z)\} + \frac{1}{\pi}\sum_{r=0}^{n-1}(-1)^{r+1}\frac{\Gamma(r+\frac{1}{2})}{\Gamma(\nu+\frac{1}{2}-r)}\left(\frac{2}{z}\right)^{1+2r-\nu}, \quad (107)$$

provided $\mathrm{R}(n+\frac{1}{2}-\nu) \geqslant 0$.

In another paper the results given herein are used to evaluate integrals involving Bessel functions.

XXXVI. *Integrals involving Bessel and Struve Functions.* *By* N. W. McLachlan, *D.Sc.*, *M.I.E.E.*, *and* A. L. Meyers, *B.Sc.*, *A.M.I.E.E.**

1. CONSIDER the two differential equations

$$z\frac{d^2x}{dz^2}+\frac{dx}{dz}+(l^2z^2-\nu^2)\frac{x}{z}=f(z), \quad . \quad . \quad . \quad (1)$$

and

$$z\frac{d^2y}{dz^2}+\frac{dy}{dz}+(k^2z^2-\nu^2)\frac{y}{z}=0, \quad . \quad . \quad . \quad . \quad (2)$$

where $f(z)$ is any function of z. The particular integral of (1) depends upon $f(z)$, whilst the two solutions of (2) are Bessel functions of real, imaginary, or complex argument according to the value of k. Following Lommel, and multiplying (1) by y, (2) by x, and subtracting, we get

$$(k^2-l^2)\int^z (xy)z\,dz+\int^z yf(z)\,dz=z\left[y\frac{dx}{dz}-x\frac{dy}{dz}\right]. \quad (3)$$

If $k=l$, (3) reduces to the form

$$\int^z yf(z)\,dz=z\left[y\frac{dx}{dz}-x\frac{dy}{dz}\right]. \quad . \quad . \quad . \quad (4)$$

Since $f(z)$ is equal to the l.h.s. of (1), (4) can also be written

$$\int^z y\left[zx''+x'+(l^2z^2-\nu^2)\frac{x}{z}\right]dz=z[yx'-xy'], \quad . \quad (5)$$

the accent denoting differentiation with respect to z.

The relationship

$$\int^z z^{\nu+1}\mathrm{J}_\nu(z)\left[\mathrm{B}''(z)+\left(\frac{2\nu+1}{z}\right)\mathrm{B}'(z)+\mathrm{B}(z)\right]dz$$
$$=z^{\nu+1}[\mathrm{B}'(z)\,\mathrm{J}_\nu(z)+\mathrm{B}(z)\,\mathrm{J}_{\nu+1}(z)], \quad . \quad (6)$$

to which (5) is akin, was obtained by Sonine, and is given in Watson's 'Theory of Bessel Functions,' p. 132. In (6) $\mathrm{J}_\nu(z)$ may be replaced by any cylinder function.

In (4), since y represents any Bessel function, if the

* Communicated by the Authors.

particular integral of (1) can be put in a suitable form, integrals of the type

$$\int^z \mathrm{J}_\nu(kz)\, f(z)\, dz, \quad \int^z \mathrm{Y}_\nu(kz)\, f(z)\, dz, \quad \int^z \mathrm{K}_\nu(kz)\, f(z)\, dz$$

can be evaluated.

Suppose we wish to evaluate

$$\int^z (lz)^\nu \mathrm{J}_\nu(lz)\, dz, \quad \text{then} \quad f(z)=\mathrm{A}z^\nu,$$

where A is a constant. If we put

$$\mathrm{A}=l^{\nu+1}/2^{\nu-1}\sqrt{\pi}\Gamma(\nu+\tfrac{1}{2})$$

the particular integral of (1) is Struve's function $\mathbf{H}_\nu(lz)$. Hence from (4) we obtain

$$\int^z (lz)^\nu \mathrm{J}_\nu(lz)\, dz = 2^{\nu-1}\sqrt{\pi}\Gamma(\nu+\tfrac{1}{2})z[\mathrm{J}_\nu(lz)\, \mathbf{H}_\nu'(lz) - \mathbf{H}_\nu(lz)\, \mathrm{J}_\nu'(lz)]. \quad . \quad . \quad (7)^*$$

Using recurrence formulæ for $\mathrm{J}_\nu'(lz)$ and $\mathbf{H}_\nu'(lz)$, (7) can be written in other ways, two of which are

$$\int^z (lz)^\nu \mathrm{J}_\nu(lz)\, dz = 2^{\nu-1}\sqrt{\pi}\Gamma(\nu+\tfrac{1}{2})z[\mathrm{J}_{\nu+1}(lz)\, \mathbf{H}_\nu(lz) - \mathbf{H}_{\nu+1}(lz)\, \mathrm{J}_\nu(lz)] + \mathrm{J}_\nu(lz)\, (lz)^{\nu+1}/l(2\nu+1), \quad . \quad . \quad . \quad (8)$$

$$= 2^{\nu-1}\sqrt{\pi}\Gamma(\nu+\tfrac{1}{2})z[\mathrm{J}_\nu(lz)\, \mathbf{H}_{\nu-1}(lz) - \mathbf{H}_\nu(lz)\, \mathrm{J}_{\nu-1}(lz)]. \quad . \quad . \quad . \quad (9)$$

$$\int^z (lz)^\nu \mathrm{Y}_\nu(lz)\, dz \quad \text{and} \quad \int^z (lz)^\nu \mathrm{H}_\nu^{(1)(2)}(lz)\, dz$$

are found from (7), (8), and (9) by replacing the J functions by the Y and $\mathrm{H}^{(1)(2)}$ functions respectively.

The results for the modified Bessel functions are

$$\int^z (lz)^\nu \mathrm{I}_\nu(lz)\, dz = 2^{\nu-1}\sqrt{\pi}\Gamma(\nu+\tfrac{1}{2})z\,[\mathrm{I}_\nu(lz)\, \mathbf{L}_\nu'(lz) - \mathbf{L}_\nu(lz)\, \mathrm{I}_\nu'(lz)], \quad . \quad . \quad . \quad (10)$$

$$= 2^{\nu-1}\sqrt{\pi}\Gamma(\nu+\tfrac{1}{2})z[\mathrm{I}_\nu(lz)\, \mathbf{L}_{\nu+1}(lz) - \mathbf{L}_\nu(lz) \times \mathrm{I}_{\nu+1}(lz)] + (lz)^{\nu+1}\, \mathrm{I}_\nu(lz)/l(2\nu+1), \quad (11)$$

* The case $\nu=0$ is given by Watson, p. 752.

$$=2^{\nu-1}\sqrt{\pi}\Gamma(\nu+\tfrac{1}{2})z[\mathrm{I}_\nu(lz)\,\mathbf{L}_{\nu-1}(lz) -\mathbf{L}_\nu(lz)\,\mathrm{I}_{\nu-1}(lz)], \quad . \quad . \quad . \quad (12)$$

these being obtained by writing li for l in (7), (8), and (9). $\mathbf{L}_\nu(z)=i^{-(\nu+1)}\,\mathbf{H}_\nu(zi)$, this being the modified Struve function.

$$\int^z (lz)^\nu \mathrm{K}_\nu(lz)\,dz=2^{\nu-1}\sqrt{\pi}\Gamma(\nu+\tfrac{1}{2})z\,[\mathrm{K}_\nu(lz)\,\mathbf{L}_\nu'(lz) -\mathbf{L}_\nu(lz)\,\mathrm{K}_\nu'(lz)],. \quad . \quad . \quad (13)$$

$$=2^{\nu-1}\sqrt{\pi}\Gamma(\nu+\tfrac{1}{2})z\,[\mathrm{K}_\nu(lz)\,\mathbf{L}_{\nu+1}(lz)+\mathbf{L}_\nu(lz) \times\mathrm{K}_{\nu+1}(lz)]+(lz)^{\nu+1}\mathrm{K}_\nu(lz)/l(2\nu+1), \quad . \quad . \quad . \quad (14)$$

$$=2^{\nu-1}\sqrt{\pi}\Gamma(\nu+\tfrac{1}{2})z\,[\mathrm{K}_\nu(lz)\mathbf{L}_{\nu-1}(lz) +\mathbf{L}_\nu(lz)\,\mathrm{K}_{\nu-1}(lz)]. \quad . \quad (15)$$

Using (13), (14), or (15) and the asymptotic formulæ for the K and **L** functions at the upper limit, it can be shown that

$$\int_0^\infty z^\nu \mathrm{K}_\nu(z)\,dz=2^{\nu-1}\sqrt{\pi}\Gamma(\nu+\tfrac{1}{2}). \quad . \quad . \quad (16)$$

When $\nu=0$, we get the well-known result $\int_0^\infty \mathrm{K}_0(z)\,dz=\frac{1}{2}\pi$.

Writing $i^{1/2}$ for l in (13), we obtain

$$i^{\nu/2}\int^z z^\nu \mathrm{K}_\nu(zi^{1/2})\,dz=2^{\nu-1}\sqrt{\pi}\Gamma(\nu+\tfrac{1}{2})z\,[\mathrm{K}_\nu(zi^{1/2})\,\mathbf{L}_\nu'(zi^{1/2}) -\mathbf{L}_\nu(zi^{1/2})\,\mathrm{K}_\nu'(zi^{1/2})]. \quad (17)$$

The right-hand side of (17) can be expressed in terms of ker, kei, ster, and stei functions. To get a compact result it is preferable to use the polar forms of the functions. From ' Bessel Functions for Engineers,' and a former paper * on the ster and stei functions, we have

$$\mathrm{K}_\nu(zi^{1/2})=\mathrm{N}_\nu(z)e^{i(\phi_\nu+\nu\pi/2)}\,; \quad \mathbf{L}_\nu(zi^{1/2})=\mathrm{S}_\nu(z)e^{i[\psi_\nu-(\nu+1)\pi/2]}. \quad . \quad . \quad . \quad (18, 19)$$

* Phil. Mag. (7) xx. p: 435 (1936).

$$\mathrm{K}_\nu'(zi^{1/2}) = \frac{-\nu}{zi^{1/2}}\mathrm{K}_\nu(zi^{1/2}) - \mathrm{K}_{\nu-1}(zi^{1/2}) \text{ (recurrence formula)}$$

$$= \frac{-\nu}{z}\mathrm{N}_\nu(z)e^{i[\phi_\nu+(\nu/2-1/4)\pi]} - \mathrm{N}_{\nu-1}e^{i[\phi_{\nu-1}+(\nu-1)\pi/2]},$$

. . . (20)

$$\mathbf{L}_\nu'(zi^{1/2}) = \frac{-\nu}{zi^{1/2}}\mathbf{L}_\nu(zi^{1/2}) + \mathbf{L}_{\nu-1}(zi^{1/2})$$

$$= \frac{-\nu}{z}\mathrm{S}_\nu(z)\,e^{i[\psi_\nu-(\nu/2+3/4)\pi]} + \mathrm{S}_{\nu-1}(z)\,e^{i[\psi_{\nu-1}-\nu\pi/2]}. \quad (21)$$

The modulus $\mathrm{S}_\nu(z) = \sqrt{\mathrm{ster}_\nu{}^2 z + \mathrm{stei}_\nu{}^2 z}$ is of course quite distinct from the Lommel function $\mathrm{S}_{\mu,\nu}(z)$, which has *two* orders (or parameters) μ, ν.

Substituting from (18) to (21) in (17), and multiplying both sides by $i^{-3\nu/2}$, we find that

$$i^{-\nu}\int^z \mathrm{K}_\nu(zi^{1/2})z^\nu\,dz = \int^z (\mathrm{ker}_\nu z + i\,\mathrm{kei}_\nu z)z^\nu\,dz$$

$$= 2^{\nu-1}\sqrt{\pi}\Gamma(\nu+\tfrac{1}{2})z\,[\mathrm{N}_\nu\mathrm{S}_{\nu-1}e^{i[\phi_\nu+\psi_{\nu-1}-3\nu\pi/4]}$$

$$-\mathrm{S}_\nu\mathrm{N}_{\nu-1}e^{i[\psi_\nu+\phi_{\nu-1}-3\nu\pi/4]}]. \quad (22)$$

Hence, equating real and imaginary parts, we obtain

$$\int^z z^\nu\,\mathrm{ker}_\nu\,z\,dz = 2^{\nu-1}\sqrt{\pi}\Gamma(\nu+\tfrac{1}{2})z\,[\mathrm{N}_\nu\mathrm{S}_{\nu-1}\cos(\phi_\nu+\psi_{\nu-1}-\tfrac{3}{4}\nu\pi)$$

$$-\mathrm{S}_\nu\mathrm{N}_{\nu-1}\cos(\psi_\nu+\phi_{\nu-1}-\tfrac{3}{4}\nu\pi)], \quad (23)$$

and

$$\int^z z^\nu\,\mathrm{kei}_\nu\,z\,dz = 2^{\nu-1}\sqrt{\pi}\Gamma(\nu+\tfrac{1}{2})z\,[\mathrm{N}_\nu\mathrm{S}_{\nu-1}\sin(\phi_\nu+\psi_{\nu-1}-\tfrac{3}{4}\nu\pi)$$

$$-\mathrm{S}_\nu\mathrm{N}_{\nu-1}\sin(\psi_\nu+\phi_{\nu-1}-\tfrac{3}{4}\nu\pi)]. \quad (24)$$

In like manner it can be shown that

$$\int^z z^\nu\,\mathrm{ber}_\nu\,z\,dz = 2^{\nu-1}\sqrt{\pi}\Gamma(\nu+\tfrac{1}{2})\,z\,[\mathrm{M}_\nu\mathrm{S}_{\nu-1}\cos(\theta_\nu+\psi_{\nu-1}$$

$$-\tfrac{3}{4}\nu\pi) - \mathrm{S}_\nu\mathrm{M}_{\nu-1}\cos(\psi_\nu+\theta_{\nu-1}-\tfrac{3}{4}\nu\pi)], \quad (25)$$

and

$$\int^z z^\nu\,\mathrm{bei}_\nu\,z\,dz = 2^{\nu-1}\sqrt{\pi}\Gamma(\nu+\tfrac{1}{2})z\,[\mathrm{M}_\nu\mathrm{S}_{\nu-1}\sin(\theta_\nu+\psi_{\nu-1}-\tfrac{3}{4}\nu\pi)$$

$$-\mathrm{S}_\nu\mathrm{M}_{\nu-1}\sin(\psi_\nu+\theta_{\nu-1}-\tfrac{3}{4}\nu\pi)]. \quad (26)$$

If in (17) $\nu=0$, by aid of the relationships

$$\mathrm{K}_0'(zi^{1/2})=\mathrm{N}_1 e^{i(\phi_1-\pi/2)} \quad \text{and} \quad \mathbf{L}_0'(zi^{1/2})=\frac{2}{\pi}-\mathrm{S}_1 e^{i\psi_1},$$

we obtain

$$\int^z \ker z\,dz=\tfrac{1}{2}\pi z[\mathrm{N}_1\mathrm{S}_0\cos(\phi_1+\psi_0)-\mathrm{N}_0\mathrm{S}_1\cos(\psi_1+\phi_0)] + z\mathrm{N}_0\cos\phi_0, \quad . \quad (27)$$

$$\int^z \mathrm{kei}\, z\,dz=\tfrac{1}{2}\pi z[\mathrm{N}_1\mathrm{S}_0\sin(\phi_1+\psi_0)-\mathrm{N}_0\mathrm{S}_1\sin(\psi_1+\phi_0)] + z\mathrm{N}_0\sin\phi_0. \quad . \quad (28)$$

Also

$$\int^z \mathrm{ber}\, z\,dz=\tfrac{1}{2}\pi z[\mathrm{M}_1\mathrm{S}_0\cos(\theta_1+\psi_0)-\mathrm{M}_0\mathrm{S}_1\cos(\psi_1+\theta_0)] + z\mathrm{M}_0\cos\theta_0, \quad . \quad (29)$$

$$\int^z \mathrm{bei}\, z\,dz=\tfrac{1}{2}\pi z[\mathrm{M}_1\mathrm{S}_0\sin(\theta_1+\psi_0)-\mathrm{M}_0\mathrm{S}_1\sin(\psi_1+\theta_0)] + z\mathrm{M}_0\sin\theta_0. \quad . \quad (30)$$

2. *Additional Integrals.*

Hitherto we have confined our attention to the case where $f(z)$ in equation (1) is Az^ν, ν being the order of the Bessel function which satisfies equation (2). If we replace ν in the index by μ, and put $A=1$, equation (1) becomes

$$z\frac{d^2x}{dz^2}+\frac{dx}{dz}+(l^2z^2-\nu^2)\frac{x}{z}=z^\mu. \quad . \quad . \quad . \quad (31)$$

This case has been treated by Lommel, and is given in Watson, pp. 345, 347. The particular integral of (31) is a Lommel function, which Watson gives as $\frac{1}{l^{\mu+1}}\mathrm{S}_{\mu,\nu}(lz)$. $\mathrm{S}_{\mu,\nu}(z)$ takes various forms according to the values of μ, ν, and $\mu\pm\nu$. If $\mu=\nu$, the particular integral of (31) is, using Watson's notation *,

$$\frac{1}{l^{\nu+1}}s_{\nu,\nu}(lz)=2^{\nu-1}\sqrt{\pi}\Gamma(\nu+\tfrac{1}{2})\,\mathbf{H}_\nu(lz)/l^{\nu+1}, \quad . \quad . \quad (32)$$

thereby giving the relationship

$$s_{\nu,\nu}(z)=2^{\nu-1}\sqrt{\pi}\Gamma(\nu+\tfrac{1}{2})\,\mathbf{H}_\nu(z). \quad . \quad . \quad . \quad (33)$$

* It should be observed that there is a difference between the functions denoted by S and s: see Watson.

Using (4), and taking the particular integral of (31) to be $S_{\mu,\nu}(z)$ when $l=1$, we obtain

$$\int^z z^\mu J_\nu(z)\,dz = z\left[J_\nu(z)\frac{d}{dz}S_{\mu,\nu}(z) - S_{\mu,\nu}(z)\frac{d}{dz}J_\nu(z)\right]. \quad (34)$$

Watson (p. 350) gives this in the form

$$\int^z z^\mu J_\nu(z)\,dz = z[(\mu+\nu-1)\,J_\nu(z)\,S_{\mu-1,\nu-1}(z) - J_{\nu-1}(z)\,S_{\mu,\nu}(z)]. \quad . \quad . \quad . \quad (35)$$

If in (34) and (35) $\mu=\nu$, the forms in (7) and (9) are reproduced. A difficulty arises in connexion with (34) and (35), inasmuch that there are no tabular values of the Lommel functions. There are, however, several cases where the integral can be evaluated without introducing these functions. When $(\mu-\nu)$ is an odd positive integer or an even positive integer, the integral can be reduced to the forms

$$\int^z z^{\nu+1} J_\nu(z)\,dz \quad \text{or} \quad \int^z z^\nu J_\nu(z)\,dz$$

by the ordinary reduction formulæ. If μ and ν are both positive integers and $\mu<\nu$ the integral can be reduced to the form

$$\int^z J_{\mu+\nu}(z)\,dz = 2\sum_{r=0}^{\infty} J_{\mu+\nu+2r+1}(z).$$

When the integral is of the form $\int^z \frac{J_{\nu+1}(z)\,dz}{z^\nu}$ the result is well known.

Referring to equation (3), it is clear that since $\int^z yf(z)\,dz$ has been determined, we can now evaluate integrals of the form

$$(k^2-l^2)\int^z J_\nu(kz)x.z\,dz = z\left[J_\nu(kz)\frac{dx}{dz} - x\frac{d}{dz}J_\nu(kz)\right] - k(l/k)^{\mu+1}\int^z (kz)^\mu J_\nu(kz)\,dz,$$

$$= z\left[J_\nu(kz)\frac{dx}{dz} - x\frac{d}{dz}J_\nu(kz)\right] - k(l/k)^{\mu+1}z[(\mu+\nu-1)J_\nu(kz)S_{\mu-1,\nu-1}(kz) - J_{\nu-1}(kz)\,S_{\mu,\nu}(kz)], \quad . \quad . \quad . \quad . \quad . \quad (36)$$

where x is a Lommel function of argument lz, *i.e.* $S_{\mu,\nu}(lz)$.

If $\mu=\nu$ and $x=2^{\nu-1}\sqrt{\pi}\Gamma(\nu+\frac{1}{2})\,\mathbf{H}_\nu(lz)$, we obtain

$$(k^2-l^2)\int^z \mathrm{J}_\nu(kz)\mathbf{H}_\nu(lz)z\,dz=z\,[l\,\mathrm{J}_\nu(kz)\mathbf{H}_\nu'(lz)-k\mathbf{H}_\nu(lz)\,\mathrm{J}_\nu'(kz)]$$
$$-kz(l/k)^{\nu+1}[\mathrm{J}_\nu(kz)\,\mathbf{H}_\nu'(kz)$$
$$-\mathbf{H}_\nu(kz)\,\mathrm{J}_\nu'(kz)]. \quad . \quad (37)$$

If in equation (1), $f(z)=l^{\nu+1}z^\nu/2^{\nu-1}\sqrt{\pi}\Gamma(\nu+\frac{1}{2})$, and in (2) l is written for k and μ for ν, we get

$$(\nu^2-\mu^2)\int^z \frac{\mathbf{H}_\nu(lz)\,\mathrm{J}_\mu(lz)}{z}\,dz=lz\,[\mathrm{J}_\mu(lz)\,\mathbf{H}_\nu'(lz)-\mathbf{H}_\nu(lz)\,\mathrm{J}_\mu'(lz)]$$
$$-\frac{1}{2^{\nu-1}\sqrt{\pi}\Gamma(\nu+\frac{1}{2})}\int^z (lz)^\nu \mathrm{J}_\mu(lz)\,d(lz). \quad (38)$$

Using (35) we obtain

$$(\nu^2-\mu^2)\int^z \frac{\mathbf{H}_\nu(lz)\,\mathrm{J}_\mu(lz)}{z}\,dz$$
$$=lz[\mathrm{J}_\mu(lz)\,\mathbf{H}_\nu'(lz)-\mathbf{H}_\nu(lz)\,\mathrm{J}_\mu'(lz)]-\frac{lz}{2^{\nu-1}\sqrt{\pi}\Gamma(\nu+\frac{1}{2})}$$
$$\times[(\mu+\nu-1)\,\mathrm{J}_\mu(lz)\,\mathrm{S}_{\nu-1,\,\mu-1}(lz)-\mathrm{J}_{\nu-1}(lz)\,\mathrm{S}_{\nu,\,\mu}(lz)].$$
$$. \quad . \quad . \quad (39)$$

In (37) and (39) $\mathrm{J}_\mu(lz)$ can be replaced by $\mathrm{Y}_\mu(lz)$, $\mathrm{H}^{(1)}_\mu(lz)$, or $\mathrm{H}^{(2)}_\mu(lz)$. By changing k to ki, and making the necessary alterations, (37) and (39) can be used to evaluate the integrals :

$$\int^z \mathrm{I}_\nu(kz)\,\mathbf{H}_\nu(lz)z\,dz, \quad . \quad . \quad . \quad . \quad . \quad (40)$$

$$\int^z \mathrm{K}_\nu(kz)\,\mathbf{H}_\nu(lz)z\,dz, \quad . \quad . \quad . \quad . \quad (41)$$

$$\int^z \frac{\mathrm{I}_\mu(lz)\,\mathbf{H}_\nu(lz)}{z}\,dz, \quad . \quad . \quad . \quad . \quad . \quad (42)$$

$$\int^z \frac{\mathrm{K}_\mu(lz)\,\mathbf{H}_\nu(lz)}{z}\,dz. \quad . \quad . \quad . \quad . \quad . \quad (43)$$

In the first two cases, *i. e.*, (40) and (41), and also in (37), if $k=l$ the integral can be evaluated in the well-known manner by writing $k=l+\epsilon$, using Taylor's theorem, and making $\epsilon\to 0$.

3. *Integrals involving Bessel and Circular Functions.*

In equations (1) and (2) put $\nu=0$, $l=k=1$, and $f(z)=ie^{iz}$, then the particular integral of (1) is e^{iz}. Hence from (4) we obtain

$$i\int_0^z e^{iz}\mathrm{J}_0(z)\,dz=ze^{iz}[i\mathrm{J}_0(z)+\mathrm{J}_1(z)]. \quad . \quad . \quad (44)$$

Equating real and imaginary parts, we get

$$\int_0^z \cos z\mathrm{J}_0(z)\,dz=z\,[\cos z\mathrm{J}_0(z)+\sin z\mathrm{J}_1(z)]. \quad . \quad (45)$$

and

$$\int_0^z \sin z\mathrm{J}_0(z)\,dz=z\,[\sin z\mathrm{J}_0(z)-\cos z\mathrm{J}_1(z)] \quad . \quad (46)$$

These results can also be obtained from (6) by putting $\mathrm{B}(z)=e^{iz}$ and $\nu=0$. From (45) and (46)

$$\int_0^{\pi/2} \cos z\mathrm{J}_0(z)\,dz=\tfrac{1}{2}\pi\mathrm{J}_1(\tfrac{1}{2}\pi), \quad . \quad . \quad . \quad (47)$$

$$\int_0^{\pi/2} \sin z\mathrm{J}_0(z)\,dz=\tfrac{1}{2}\pi\mathrm{J}_0(\tfrac{1}{2}\pi). \quad . \quad . \quad . \quad (48)$$

By writing $\pm zi$ for z in (44) we get

$$\int_0^z e^{-z}\mathrm{I}_0(z)\,dz=ze^{-z}[\mathrm{I}_0(z)+\mathrm{I}_1(z)], \quad . \quad . \quad (49)$$

$$\int_0^z e^{z}\mathrm{I}_0(z)\,dz=ze^{z}[\mathrm{I}_0(z)-\mathrm{I}_1(z)]. \quad . \quad . \quad . \quad (50)$$

These two results can be used to evaluate

$$\int_0^z \cosh z\mathrm{I}_0(z)\,dz \quad \text{and} \quad \int_0^z \sinh z\mathrm{I}_0(z)\,dz.$$

If in (1) $\nu=0$, $l=1$, $f(z)=ize^{iz}$, and in (2) $\nu=0$, $k=1$, the particular integral of (1) is $\frac{1}{3}e^{iz}(z+i)$. This yields the integrals

$$\int_0^z z\cos z\mathrm{J}_0(z)\,dz=\tfrac{1}{3}z\,[z\cos z\mathrm{J}_0(z)+\mathrm{J}_1(z)\{z\sin z+\cos z\}],$$

$$. \quad . \quad . \quad (51)$$

$$\int_0^z z \sin z J_0(z)\, dz = \tfrac{1}{3}z[z \sin z J_0(z) - J_1(z)\{z \cos z - \sin z\}]. \quad . \quad . \quad . \quad (52)$$

These two results can be obtained from (6) by putting $\nu = 0$ and $B(z) = (i+z)e^{iz}$. They can be used to evaluate

$$\int_0^z z \cosh z\, I_0(z)\, dz \quad \text{and} \quad \int_0^z z \sinh z I_0(z)\, dz.$$

By putting $B(z) = e^{iz}$ in (6), we obtain

$$\int^z z^\nu e^{iz} J_\nu(z)\, dz = \frac{z^{\nu+1}e^{iz}}{(2\nu+1)}[J_\nu(z) - iJ_{\nu+1}(z)], \quad . \quad (53)$$

from which the integrals

$$\int^z z^\nu \left\{ \begin{matrix} \cos z \\ \sin z \end{matrix} \right\} J_\nu(z)\, dz$$

can be evaluated.

4. *Solution of a Differential Equation using Lommel Functions.*

Consider the equation

$$\frac{d^2x}{dz^2} + k^2 z x = a z^\mu. \quad . \quad . \quad . \quad . \quad . \quad (54)$$

Substituting $x = yv^{1/3}$ and $v = z^{3/2}$, we obtain

$$v\frac{d^2y}{dv^2} + \frac{dy}{dv} + \left(\frac{4k^2}{9}v^2 - \frac{1}{9}\right)\frac{y}{v} = \frac{4}{9}a.v^{2\mu/3}. \quad . \quad (55)$$

The complementary function is

$$y = A_1 J_{1/3}(\tfrac{2}{3}kv) + B_1 J_{-1/3}(\tfrac{2}{3}kv),$$

whilst the particular integral is Lommel's function

$$\frac{4}{9}a S_{2\mu/3,\,1/3}(\tfrac{2}{3}kv)/(\tfrac{2}{3}k)^{1+2\mu/3}.$$

Hence the complete solution of (54) is

$$x = z^{1/2}[A_1 J_{1/3}(\tfrac{2}{3}kz^{3/2}) + B_1 J_{-1/3}(\tfrac{2}{3}kz^{3/2})] + \frac{2a}{3k} z^{1/2} S_{2\mu/3,\,1/3}(\tfrac{2}{3}kz^{3/2})/(\tfrac{2}{3}k)^{2\mu/3}. \quad . \quad (56)$$

Appendix, giving Miscellaneous Formulæ.

Multiplying both sides of the recurrence formula $2J_\nu'(z)=J_{\nu-1}(z)-J_{\nu+1}(z)$ by $J_\nu(z)$, and integrating, we get

$$2\int^z J_\nu(z)dJ_\nu(z)=\int^z J_\nu(z)(J_{\nu-1}(z)-J_{\nu+1}(z))\,dz,$$

so
$$J_\nu^2(z)=\int^z J_\nu(z)\{J_{\nu-1}(z)-J_{\nu+1}(z)\}dz. \quad . \quad (1)$$

Writing $(\nu+n)$ for ν, giving n successively the values 1, 2, etc., and adding, we have

$$\int^z J_\nu(z)J_{\nu-1}(z)\,dz=\sum_{n=0}^{\infty} J_{\nu+n}^2(z). \quad . \quad . \quad . \quad (2)$$

In particular

$$\int_0^z J_1(z)J_0(z)\,dz=\tfrac{1}{2}[1-J_0^2(z)]. \quad . \quad . \quad . \quad (3)$$

Putting $n=-1$, -2, etc. in (1) above, we find that when $\nu=m$ is integral >0

$$\int^z [J_1(z)J_0(z)-J_m(z)J_{m+1}(z)]\,dz=\sum_{r=1}^{m} J_r^2(z). \quad . \quad (4)$$

Using (3), (4) becomes $(m\geqslant 0)$,

$$\int_0^z J_m(z)J_{m+1}(z)\,dz=\tfrac{1}{2}[1-J_0^2(z)]-\sum_{r=1}^{m} J_r^2(z). \quad . \quad (5)$$

From the recurrence formula $2I_\nu'(z)=I_{\nu-1}(z)-I_{\nu+1}(z)$ we have

$$2I_{\nu+1}(z)=\int^z [I_\nu(z)+I_{\nu+2}(z)]\,dz,$$

$$-2I_{\nu+3}(z)=-\int^z [I_{\nu+2}(z)+I_{\nu+4}(z)]\,dz,$$

$$2I_{\nu+5}(z)=\int^z [I_{\nu+4}(z)+I_{\nu+6}(z)]\,dz,$$

and so on.

By addition we obtain

$$\int_0^z I_\nu(z)\,dz=2\sum_{n=0}^{\infty}(-1)^{n-1}I_{\nu+2n+1}(z) \quad . \quad . \quad (6)$$

$$R(\nu)>-1.$$

In like manner we get

$$\int_{z_2}^{z_1} \mathrm{Y}_\nu(z)\,dz = 2\sum_{n=0}^{\infty} [\mathrm{Y}_{\nu+2n+1}(z_1) - \mathrm{Y}_{\nu+2n+1}(z_2)], \quad . \quad . \quad . \quad (7)$$

$$\int_{z_2}^{z_1} \mathrm{K}_\nu(z)\,dz = 2\sum_{n=0}^{\infty} (-1)^{n+1}[\mathrm{K}_{\nu+2n+1}(z_1) - \mathrm{K}_{\nu+2n+1}(z_2)], \quad (8)$$

$$\int_0^z \mathrm{ber}_\nu z\,dz = -\sqrt{2}\sum_{n=0}^{\infty} [\mathrm{ber}_{\nu+2n+1}(z) - \mathrm{bei}_{\nu+2n+1}(z)], \quad . \quad (9)$$

$$\mathrm{R}(\nu) > -1.$$

$$\int_0^z \mathrm{bei}_\nu z\,dz = -\sqrt{2}\sum_{n=0}^{\infty} [\mathrm{ber}_{\nu+2n+1}(z) + \mathrm{bei}_{\nu+2n+1} z]. \quad . \quad (10)$$

$$\mathrm{R}(\nu) > -1.$$

From recurrence formulæ we obtain

$$\mathbf{H}_{\nu-1}^2(z) - \mathbf{H}_{\nu+1}^2(z) = \frac{4\nu \mathbf{H}_\nu(z)\mathbf{H}_\nu'(z)}{z} - \frac{2(\frac{1}{2}z)^\nu \mathbf{H}_{\nu+1}(z)}{\sqrt{\pi}\Gamma(\nu+\frac{3}{2})} + \frac{(\frac{1}{2}z)^{2\nu}}{\pi[\Gamma(\nu+\frac{3}{2})]^2}. \quad . \quad (11)$$

In connexion with the functions $\mathrm{M}_\nu(z)e^{i\theta_\nu(z)}$ and $\mathrm{N}_\nu(z)e^{i\phi_\nu(z)}$, introduced in ' Bessel Functions for Engineers,' we have

$$\frac{d}{dz}\mathrm{M}_\nu(z) = \mathrm{M}_{\nu+1}(z)\cos(\theta_{\nu+1} - \theta_\nu - \tfrac{1}{4}\pi) + \frac{\nu}{z}\mathrm{M}_\nu(z), \quad . \quad . \quad (12)$$

$$\frac{d}{dz}\theta_\nu(z) = -\frac{\mathrm{M}_{\nu+1}(z)}{\mathrm{M}_\nu(z)}\cos(\theta_{\nu+1} - \theta_\nu + \tfrac{1}{4}\pi), \quad . \quad . \quad . \quad . \quad (13)$$

$$\frac{d^2}{dz^2}\mathrm{M}_\nu(z) = \frac{\mathrm{M}_{\nu-1}^2}{\mathrm{M}_\nu}\cos^2(\theta_\nu - \theta_{\nu-1} - \tfrac{1}{4}\pi) - \frac{\mathrm{M}_{\nu-1}}{z}\sin(\theta_\nu - \theta_{\nu-1} - \tfrac{1}{4}\pi) + \frac{\mathrm{M}_\nu}{z^2}(\nu+\nu^2), \quad (14)$$

$$= \frac{\mathrm{M}_{\nu+1}^2}{\mathrm{M}_\nu}\cos^2(\theta_{\nu+1} - \theta_\nu + \tfrac{1}{4}\pi) - \frac{\mathrm{M}_{\nu+1}}{z}\sin(\theta_{\nu+1} - \theta_\nu + \tfrac{1}{4}\pi) + \frac{\mathrm{M}_\nu}{z^2}(\nu^2 - \nu), \quad (15)$$

$$\frac{d^2}{dz^2}\theta_\nu(z) = \frac{\mathrm{M}_{\nu-1}^2}{\mathrm{M}_\nu^2}\sin 2(\theta_\nu - \theta_{\nu-1} + \tfrac{1}{4}\pi) + \left(\frac{2\nu-1}{z}\right)\frac{\mathrm{M}_{\nu-1}}{\mathrm{M}_\nu}\sin(\theta_\nu - \theta_{\nu-1} + \tfrac{1}{4}\pi) + 1, \quad (16)$$

$$= -\frac{M_{\nu+1}^2}{M_\nu^2} \sin 2(\theta_{\nu+1} - \theta_\nu + \tfrac{1}{4}\pi)$$

$$+ \left(\frac{2\nu+1}{z}\right) \frac{M_{\nu+1}}{M_\nu} \cos(\theta_{\nu+1} - \theta_\nu + \tfrac{1}{4}\pi) + 1. \quad (17)$$

These formulæ hold for the $N_\nu(z)e^{i\Phi_\nu(z)}$ function, provided M is changed to N and θ to ϕ.

XXXVII. *Photo-elastic Study of Stresses due to Impact* *. *By* Zirô Tuzi, *Dr.Engg., and* Masataka Nisida †.

[Plates III.–IX.]

Introduction.

FOR a long time one of us has been commending the so-called fringe method for photo-elastic study. This photographic method, using a monochromatic light source, is not only accurate by averting personal error, but the measurement of numerical data involved in it is very simple. In previous reports ‡ the author described the method in detail, showing that the exposure was shortened down to about 1/32–1/64 second, so that an ordinary motion picture could be taken. Even so, however, the exposure is not short enough to catch quickly varying dynamic stresses involved in a transient phenomenon such as oscillation or impact. Attempts in this direction have been made by Mr. Sekiguchi, who tried to catch the phenomena on a falling plate §, and by Dr. M. M. Frocht ‖, who used motion-picture apparatus of normal speed. But it seems that in these methods the analysing power is not enough for studying such quickly varying stresses.

The object of the present paper is to catch some transient stresses on a photographic film by means of the photo-elastic method. Some of the phenomena—for

* From the Bulletin of the Inst. Phys. Chem. Researches, Tokyo (in Japanese), xii. p. 57 (1933); xii. p. 909 (1933); xiii. p. 150 (1934).

† Communicated by Prof. R. V. Southwell, M.A., F.R.S.

‡ Z. Tuzi, Phil. Mag. ix. p. 210 (1930); 'Engineering,' cxxxi. pp. 116, 193 (1931).

§ J. Obata, Proc. World Engineering Congress, v. p. 87 (1929).

‖ M. M. Frocht, Trans. A.S.M.E. APM-54-9, p. 83 (1932).

instance, the impact of a short beam or that of a ring—finish within a few thousandths of a second, and the time of exposure should be at least a few ten-thousandths of a second. In the photo-elastic experiment the light beam should be polarized and essentially monochromatic. Both conditions greatly reduce the intensity of the light, and naturally make short exposures very difficult. To overcome this difficulty the present authors tried to limit the region to a certain linear section instead of studying the whole feature of the fringes at one time. The section in question was illuminated as brightly as possible, and it was projected through a very fine slit on to the film, which runs at a high speed in a direction perpendicular to the section.

If we denote the stress by σ (that is, the difference of the two principal stresses p–q) and the time by t, $\frac{\partial \sigma}{\partial t}$ is one of the quantities which can be studied by this principle. In the case of the quickly changing phenomenon $\frac{\partial \sigma}{\partial t}$ becomes large, and to analyse it exactly a considerable film speed is required. Denoting by y the direction perpendicular to the section in question, for a large value of $\frac{\partial \sigma}{\partial y}$ the thinner the slit the better is the result.

When both conditions are satisfied—of a high running speed of the film on the one hand and of a fine slit on the other—the exposure must naturally be shortened. In the experiment to be described an exposure of about 1/48,000 second could be realized, and stress variations due to shock in certain sections of beams or in rings were studied by this means.

Apparatus and Method of Experiment.

The apparatus used in our experiment is shown in fig. 1. In this experiment the most important problem is to pour a sufficiently brilliant illumination on a section of the specimen. As the light source (L.S.) a U-tube mercury arc lamp was tried first: it was nearly all right till the exposure of about 1/5000 second was reached, but for a far shorter exposure the intensity was found to be quite insufficient. A standard carbon

arc lamp with a deep red filter was tried : passing a heavy current at the instant of the experiment, satisfactory results were obtained up to the exposure of about 1/50,000 second. It is almost impossible to get a red filter strictly monochromatic, and our filter passed a band of the breadth of about 100 $\mu\mu$; but for our purpose it served sufficiently well, as will be shown later.

Two condenser lenses (C) are used in the arrangement to make as much use of the light beam as possible ; in addition, a cylindrical lens (Cy.L) is used to converge the parallel beam to a sharp line on a section of the specimen.

A photographic lens (Ph.L_1) having a focal length of 300 mm., F. 4·5, is placed very near to the specimen. This is used as a condenser lens for the light beam and

Fig. 1.

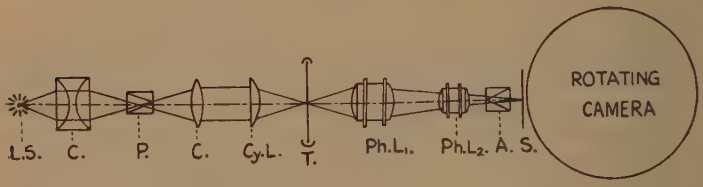

Light source : Carbon arc 10 amp.
Camera : Dia. 30 cm. ; periphery 100 cm. ; rev. p. m. 1700 ; film-speed 23 m./sec.–24·4 m./sec. ; slit 0·5 mm. ; time of exposure 1/46,000 sec.
Filter : Red.
Film : Super-sensitive panchromatic.

at the same time as the projection lens combined with the other photographic lens (Ph.L_2), which has the focal length of 210 mm., F. 4·5.

The rotating camera is of a special design. The rotor is an aluminium wheel having a diameter of about 30 cm. ; on the periphery of the wheel a standard motion picture film of effective length 1 metre can be fastened. Since the rotor can be rotated up to a speed of 1400 revolutions per minute, a peripheral film-speed of 23 metres per second can be obtained. A fine slit of various openings is mounted on the front of the camera casing ; with a slit of the breadth of $\frac{1}{2}$ mm., for instance, the time of exposure of 1/46,000 second can be obtained. Both vertical and horizontal types of camera were prepared, fig. 2 (Pl. III.) showing the vertical one.

As the time-mark the image of a small point-lamp lighted by D.C. current is focussed sharply on the film side by side with the phenomenon. The light beam is cut by a toothed disk mounted on a synchronous motor which serves to print a broken line of the interval of time up to 1/1200 second.

For nearly all experiments supersensitive panchromatic film was found sensitive enough with red monochromatic light up to an exposure of about 1/50,000 sec., and using the best possible arrangement of the optical system for getting a sharp and brilliant line illumination.

In some of the present experiments a slow film-speed of 1–3·5 m./sec. was used with an exposure of 1/2000–

Fig. 3.

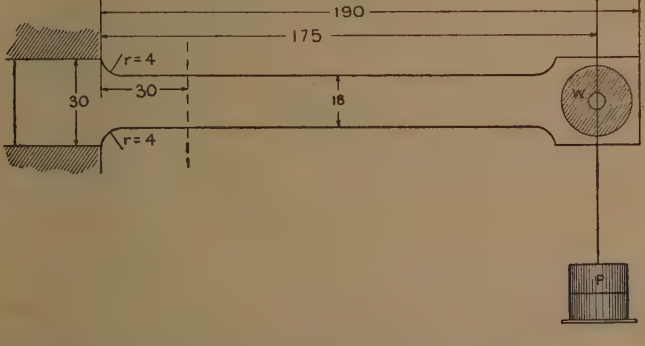

1/10,000 second, for which the green line 5461 Å. of the mercury arc lamp served just enough. For a very quickly varying phenomenon a film-speed of 12·5–23 m./sec. was used, with an exposure of 1/25,000–1/48,800 sec. under red illumination.

Preliminary Experiments on a Vibrating Beam.

Some experiments were done, as a preliminary test of the method, with a comparatively slow film-speed and long exposure. A few examples are described below.

Example 1.

The phenolite test-piece is shown on fig. 3. It is a cantilever clamped at one end, and was thrown into

vibration by releasing the weight P, carrying the weight W, at the other end.

Two experiments were done on the same specimen, having the dimensions as shown (in mm.) in fig. 3 with a uniform thickness of 6 mm., with various values of W and P. The section indicated by a broken line in fig. 3 was studied.

(*a*) W=0·417 kg.
P=2·735 kg.
Film-speed 938 mm./sec.
Width of slit 0·5 mm.
Corresponding time of exposure 1/1876 sec.

Fig. 5.

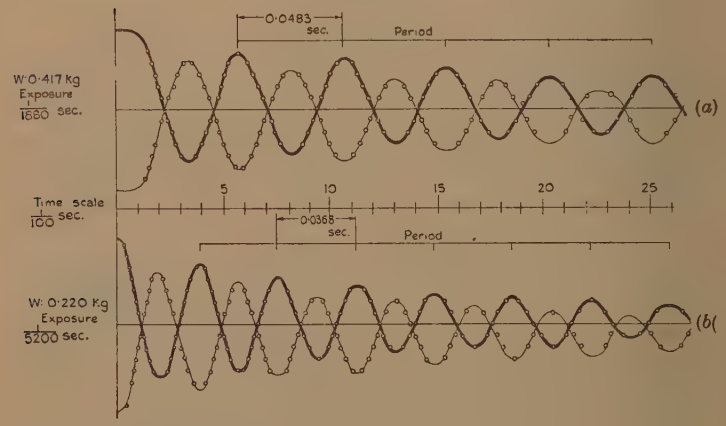

(*a*) W=0·220 kg.
P=3·234 kg.
Film speed 938 mm./sec.
Width of slit 0·18 mm.
Corresponding time of exposure 1/5200 sec.

The photographs on the running film are shown in fig. 4 (*a*) & (*b*) (Pl. IV.), in which the dotted lines are time-marks of 1/600 sec. The stresses on both free boundaries are plotted in fig. 5 (*a*) & (*b*), in which the abscissæ show the time in 1/100 sec. unit, while the ordinates show the extreme fibre stresses in fringe order (the thick line being the initially compressive side and the thin line

that of the tension). Both curves are asymmetrical with respect to the time axis, showing clearly that there have been some initial stresses.

From the results the period T can be observed as follows :—

For (*a*) T=0·0483 sec. ; for (*b*) T=0·0368 sec.

The period may be calculated theoretically from the following formula :

$$T=2\pi\sqrt{\frac{l^3W}{3EIg}}, \quad \ldots \quad (1)$$

where l is the length of span, 17·5 cm. ; E is the Young's modulus, 41100 kg./cm.^{2} ; I is the moment of inertia, 0·292 cm.^{4} ; W is the weight attached at the free end—for (*a*) 0·417 kg. ; for (*b*) 0·220 kg.

With this formula the theoretical values of T are calculated as follows :—

For (*a*) T=0·0498 sec. ; for (*b*) T=0·0363 sec.

These values seem to coincide rather well with the experimental values mentioned above. For such a slow phenomenon the film-speed of about 1 m./sec. and the exposure of 1/2000∼1/5000 seems sufficient for analysing the stress variation.

Example 2.

The period of the vibration of a cantilever becomes shorter without the top load, W. The same specimen as the first example (fig. 3) was used, with the top weight removed, and three photographs, as shown in fig. 6 (*a*), (*b*), (*c*) (Pl. III.), were taken under the following conditions :—

(*a*) Film-speed 938 mm./sec.
Slit 1 mm.
Time of exposure 1/938.
The specimen was thrown into vibration by cutting off the initial load P.

(*b*) Film-speed 938 mm./sec.
Slit 0·1 mm.
Time of exposure 1/9380 sec.
The vibration was caused in the same way as (*a*).

(*c*) Film-speed 938 mm./sec.
Slit 0·1 mm.
Time of exposure 1/9380 sec.

The vibration was caused by a falling weight dropped on to a dish hung at the free end, but in this case the string which was supporting the dish was broken at the instant of fall.

As is clear in the photographs, in (*a*) the resolving power seems to be insufficient to catch the variation of fringes, but an exposure of about 1/10,000 sec. is short enough, as shown on the photographs (*b*) and (*c*). In fig. 7 (*b*) & (*c*) the stresses on both the free boundaries are plotted from the photographs. In fig. 7 the thick

Fig. 7.

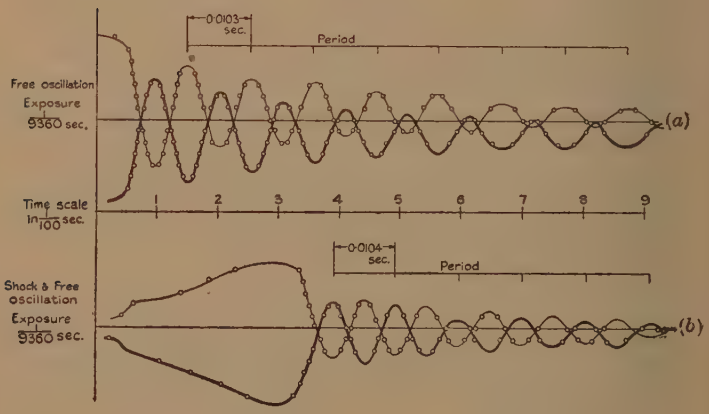

line shows the stress on the side which was initially in tension, and the thin line that of the side in compression. Both lines are asymmetrical with respect to the datum line, which seems to be clearly the effect of the remaining stress. In these cases the periods of the oscillation were found from the results to be

(*b*) 0·0103 sec. ; (*c*) 0·0104 sec.

The theoretical expression of the period of oscillation of a cantilever, one end fixed and the other end free, is

$$n = \frac{m^2}{2\pi l^2}\sqrt{\frac{EIg}{A\rho}}, \quad \ldots\ldots \quad (2)$$

in which l is the length of the beam, A the sectional area, ρ the density, E the modulus of elasticity, I the moment of inertia, while m is as follows :—

$m=1{\cdot}875$ for fundamental tone;
$m=4{\cdot}694$ for second harmonics ;
$m=7{\cdot}855$ for third harmonics.

With the value of $m=1{\cdot}875$ the following values are obtained with our specimen :—

$n=143$; $T=0{\cdot}0070$ sec.

Fig. 8.

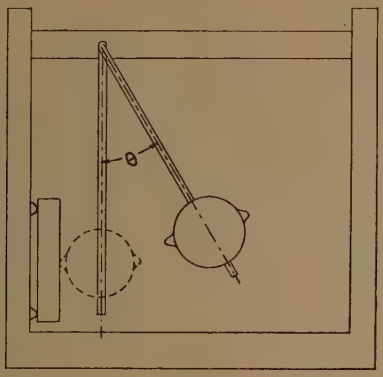

Fig. 9.

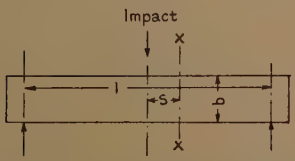

The period is about 30 per cent. shorter than the experimental ones, and the authors consider that the deviation is caused by the fact that the top of the test-piece is a little large and irregular in form.

Impact Stresses in a Beam.

A phenolite beam was supported at both ends and struck at the centre on a pendulum apparatus as shown in figs. 8 and 9. The study of the central section is the

most interesting, but as the fringes at the contact point are rather complicated, the section XX in fig. 9 was studied.

The specimens were as follows :—

Material : phenolite.
Modulus of elasticity : 58,200 kg./cm.^{2}
Length of span : l
Breadth : b.
Thickness : t.
Distance of the section XX from central section :

$$s = \frac{l}{8}.$$

For light source a carbon arc lamp with a red filter was used, fig. 10 (Pl. V.) being the statical photograph of the specimen under the same red illumination. The fringes are not as sharp as that of the mercury green line, but they are sufficiently so to permit numerical study. From such photographs the optical sensibility for red light was found to be $\alpha = 0{\cdot}609$ fringe order per kg./mm.^{2} stress per mm. thickness.

The dimensions of the test-pieces were as follows :—

Table I.

Test-piece.	Span (mm.).	Breadth b (mm.).	Thickness t (mm.).	$s = \frac{l}{8}$ mm.
No. 1	160	23	6	20
No. 2	120	23	6	15
No. 3	100	23	6	12·5

The impact was applied by a pendulum of equivalent top weight of 1·631 kg., and each specimen was struck by three different impulsive forces, as given in the following table, in which

θ is the angle of the starting position of the pendulum ;
h the height of the free fall of the pendulum ;
V the velocity of the pendulum.

TABLE II.

Experiment No.	θ deg.	h (cm.).	V (cm./sec.).
A	29·2	5·08	99·9
B	24·2	3·52	83·0
C	19·2	2·23	66·0

Fig. 12.—No. 1.

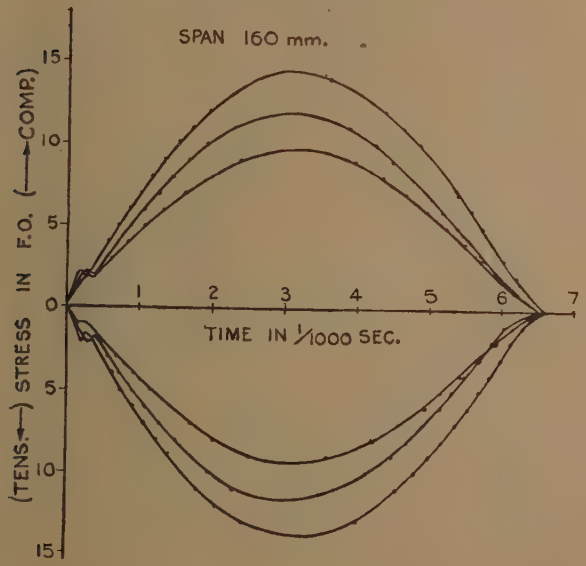

The film-speed was 22·25–22·56 m./sec., and the time of exposure 1/44,500–1/45,120 sec. The results are shown in the photographs, fig. 11 (Pl. V.) No. 1 (A), (B), (C), fig. 11 (Pl. VI.) No. 2 (A), (B), (C) and No. 3 (A), (B), (C). In the photographs the broken line shows the time-mark of 1/1200 sec. The stresses at the free boundary are plotted from the photographs as fig. 12, Nos. 1, 2, and 3, and the manner of the stress variation can be studied in detail. As is clear from the photographs, there is a remarkable oscillating disturbance until the maximum stress is

reached, and after the impact phenomenon is over some oscillating stress follows.

With the aid of the customary theory some of the results can be verified : for example, the maximum stress due to impact, the period of vibration, etc. If we denote by

y_s, the statical deflexion due to a weight W at the point of impact ;

Fig. 12.—No. 2.

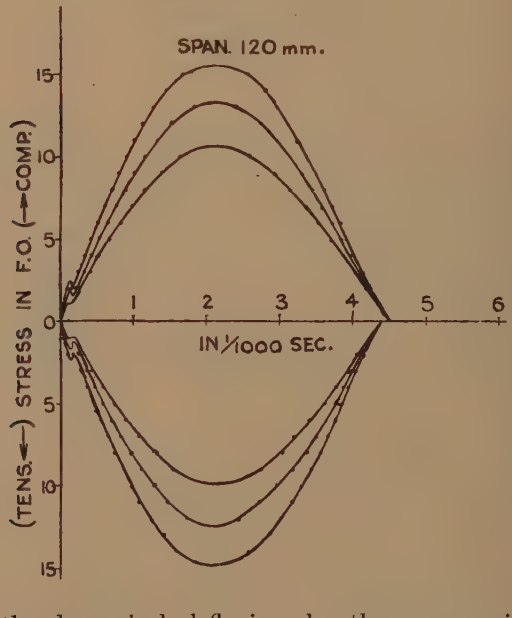

y_d, the dynamical deflexion by the same weight W dropped from a height h ; and

S_s and S_d, the stresses due to statical and dynamical load respectively,

the following expressions are known between these quantities * :—

$$y_d = y_s \left\{ 1 + \sqrt{1 + \frac{2h}{y_s}} \right\} . \quad . \quad . \quad . \quad . \quad (3)$$

* Timoshenko, ' Vibration Problems in Engineering,' p. 280 (1929) ; Marks, ' Mechanical Engineers' Handbook,' first ed., p. 390.

$$S_d = S_s \left\{ 1 + \sqrt{1 + \frac{2h}{y_s}} \right\} . \quad . \quad . \quad . \quad . \quad (4)$$

In our case the deflexion at centre may be expressed as

$$y_s = \frac{1}{48} \cdot \frac{Wl^3}{EI} \quad . \quad . \quad . \quad . \quad . \quad . \quad . \quad (5)$$

Fig. 12.—No. 3.

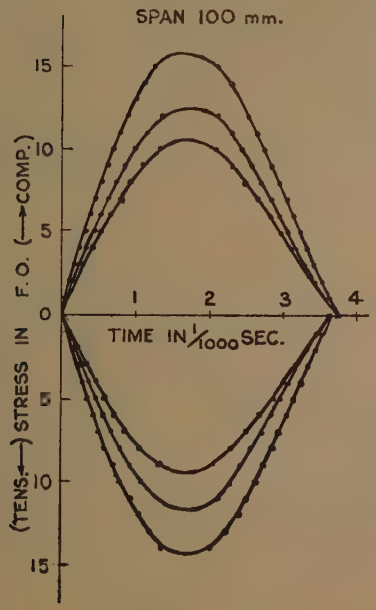

From equations (4) and (5) the dynamical stress S_d can be calculated with the measured value of the elastic constant E=58200 kg/cm.^{2} The statical deflexion at the centre $y_{s,c}$ for the equivalent load W=1·631 kg. is calculated as follows :—

No. 1.....	l=160 mm. ;	$y_{s,c}$=0·00393 cm.
No. 2.....	l=120 mm. ;	$y_{s,c}$=0·00166 cm.
No. 3.....	l=100 mm. ;	$y_{s,c}$=0·00096 cm.

With these values the experimental results are verified for the maximum stress as shown in Table III. In the table the value of the stress σ is expressed in fringe order of the red monochromatic.

From the results thus obtained the experimental values of the maximum dynamical stress were found about 70–80 per cent. those of the calculated, and some 20–30 per cent. of the energy can be considered to be absorbed from some other cause. The results indicate that the value approaches unity with the larger value of l/b, that is to say, in a slender beam. Any way it seems true that the theoretical value is on the safe side.

The time of duration of the impact can be given as follows *. Let m denote the mass of the falling weight, l the span of the beam, E the modulus of elasticity of the beam, and I the moment of inertia of the section : then the time of duration τ is as follows in the case of a beam struck at its centre :—

$$\tau=\pi\sqrt{\frac{ml^3}{48\mathrm{EI}}}.$$

This expression involves l, m, E, and I, but is independent of the height of fall, h. This fact is verified in the results of fig. 12, and the values, both experimental and calculated, are compared in Table IV.

After the impact phenomenon is finished there follow some oscillating stresses which are clearly reproduced in the photographs on fig. 11 (Pls. V. & VI.). These oscillations can be compared with the free oscillation of a free bar whose frequency, n_2, is expressed as follows :

$$n_2=\frac{k_r^2}{2\pi l'}\sqrt{\frac{\mathrm{EI}}{\rho\mathrm{A}}},$$

in which l' is the total length of the bar, A the sectional area, ρ the density of the specimen, and k_r the constant, which can be taken in our case as $k_r=4{\cdot}730$. The measured and calculated values of n_2 are also given in Table IV.

As is clear from the table, the experimental values of τ coincide fairly well with the theoretical ones, while the

* L. Jannin, ' Des chocs dans les calculs pratiques de résistance des matériaux,' p. 171 (1925).

TABLE III.

Test-piece.	Span and l/b.	h (cm.).	$1+\sqrt{1+\frac{2h}{y_{s,c}}}$.	σ_s.	$\sigma_{d,t}$ calc.	$\sigma_{d,e}$ Exper. Tension side.	$\sigma_{d,e}$ Exper. Compres. side.	$\sigma_{d,e}$ Exper. Mean.	$r=\frac{\sigma_{d,e}}{\sigma_{d,t}}$.	
No. 1 ..	160 mm.	5·08	51·8	0·338	17·5	14·5	13·8	14·15	0·812	0·810
	$l/b=6·96$	3·52	43·4	..	14·8	12·0	11·7	11·8	0·798	
		2·23	34·6	..	11·7	9·7	9·5	9·6	0·821	
No. 2 ..	120 mm.	5·08	79·2	0·254	20·0	15·6	14·6	15·1	0·756	0·789
	$l/b=5·22$	3·52	66·1	..	16·8	13·5	12·5	13·0	0·774	
		2·23	48·2	..	12·2	10·6	9·8	10·2	0·837	
No. 3 ..	100 mm.	5·08	103·8	0·211	21·5	15·6	14·5	15·15	0·707	0·693
	$l/b=4·35$	3·52	86·8	..	18·4	12·7	11·8	12·3	0·668	
		2·23	69·1	..	14·5	10·8	9·5	10·15	0·704	

measured values of n_2 also coincide with the theoretical values within the range of 93–97 per cent.

Impact of a Circular Ring.

The Specimen and Method.

Nearly the same method was followed with a circular ring, struck as shown in fig. 13, by dropping a weight W of 500 grammes from a height h on to phenolite rings having mean diameter (Dm) 100 mm., width 6 mm., and radial thickness (b) 26 mm., 22 mm., and 18 mm. respectively. The central section XX was photographed. In this case

TABLE IV.

Test-piece.	Span (mm.).	h (cm.).	Time of duration 10^{-3} sec. Exper.	Time of duration 10^{-3} sec. Calc.	Frequency n_2. Exper.	Frequency n_2. Calc.
No. 1 ..	160	5·08	6·31	6·59	1670	1712
		3·52	6·12		1650	
		2·23	6·26		1655	
			6·23		1658	
No. 2 ..	120	5·08	4·36	4·43	2850	2925
		3·52	4·40		2835	
		2·23	4·42		2850	
			4·39		2845	
No. 3 ..	100	5·08	3·54	3·59	3820	4090
		3·52	3·63		3820	
		2·23	3·59		3820	
			3·59		3820	

a plate-shutter S, having an opening H, was dropped simultaneously with the weight W to give a proper exposure during one rotation of the camera rotor. The film-speed was 24·4 m./sec., and with a 0·5 mm. slit, which was placed just in front of the rotor, the time of exposure was 1/48,800 sec.

A simple test-beam was taken from the same phenolite plate and the modulus of elasticity E and the optical constant α were measured. Fig. 14 shows the results as the mean of six observations. Since E is clearly a function of time, the value at $t=0$ must be taken for our purpose, and the following value was obtained :

$$E = 441 \frac{\text{kg}}{\text{mm.}^2}.$$

The optical sensibility α for the red illumination was

$$\alpha = 0{\cdot}731 \frac{\text{f.o.mm.}}{\text{kg.}}.$$

Fig. 13.

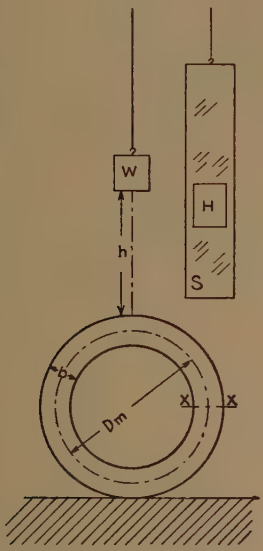

Flg. 14.

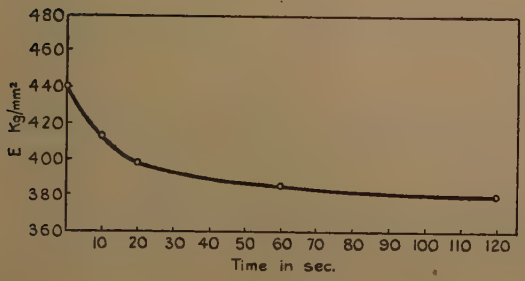

The Statical Experiment.

Statical compression was tried first. Fig. 15 (Pl. VII.) is a photograph of the specimen in which b had the value

26 mm. The load P was 92·38 kg. For each specimen four kinds of loads were applied, as shown in Table V. :—

TABLE V.

Breadth b.		26 mm.	22 mm.	18 mm.
Pl. No.	1	17·38	17·38	12·38
	2	32·38	32·38	22·38
	3	62·38	57·38	42·38
	4	92·38	77·38	52·38

In fig. 16 let the mean radius be R, let σ_i and σ_0 be the extreme fibre stresses inside and outside of the central section, and let y be the radial distance from the mean central line. Further, let σ be the tangential stress, t the

Fig. 16.

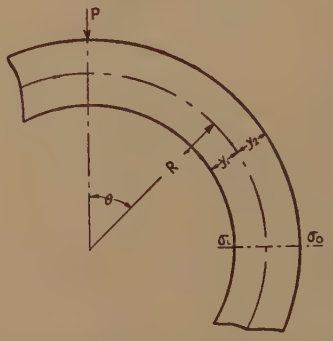

thickness of the ring, and M the bending moment ; then theoretical deduction gives the following expressions * :

$$\sigma = \frac{M}{R(A'-A)}\left\{\frac{A'}{A} - \frac{R}{R+y}\right\},$$

where

$$A' = Rt\int_{y_1}^{y_2}\frac{dy}{R+y} = Rt\log_e\frac{2R+b}{2R-b}.$$

* Morley, ' Strength of Material,' p. 379 (1926).

At the horizontal section, where $\theta = \frac{\pi}{2}$,

$$\sigma_i = \frac{P\left(\frac{1}{2} - \frac{1}{\pi}\right)}{A' - A}\left(\frac{R}{R - y_1} - \frac{A'}{A}\right) + \frac{P}{2A},$$

$$\sigma_0 = \frac{P\left(\frac{1}{2} - \frac{1}{\pi}\right)}{A' - A}\left(\frac{A'}{A} - \frac{R}{y_2 + R}\right) - \frac{P}{2A}.$$

The experimental values for σ_i and σ_0 obtained from the photographs were plotted as shown in fig. 17, and from

Fig. 17.

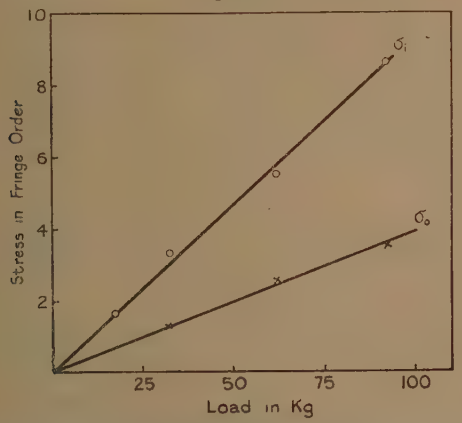

the results the stress for the load P=50 kg. was measured and compared with the calculated values as given in Table VI. :—

TABLE VI.

Test-piece.	Extreme fibre stress in f.o. Experiment. σ_i.	Experiment. σ_0.	Calculation. σ_i.	Calculation. σ_0.	$r = \frac{\text{Exper.}}{\text{Calc.}}$ r_i.	r_0.	Mean.
B_1 $b=26$ mm.	3·93	1·59	4·75	2·00	1·21	1·26	1·23
B_2 $b=22$ mm.	5·58	2·58	6·05	2·90	1·08	1·12	1·10
B_3 $b=18$ mm.	7·68	4·32	7·90	4·70	1·03	1·09	1·06

The results show that the theoretical values are a little smaller than the experimental values, which are not on the safe side ; it seems clear that the value of r approaches the more closely to unity the more slender the ring.

The Dynamical Experiment.

Impact was applied to three specimens of the same mean radius, R=50 mm., but having various radial thicknesses, b being 26 mm., 22 mm., and 18 mm. Various heights of fall, h, were adopted with the weight of 500 g. as given on Table VII.

TABLE VII.

Test-piece.	2R/b.	No.	(h mm.).
B_1 b=26 mm.	3·85	(1)	100
		(2)	200
		(3)	300
B_2 b=22 mm.	4·54	(1)	70
		(2)	150
		(3)	210
		(4)	250
B_3 b=18 mm.	5·56	(1)	45
		(2)	100
		(3)	150

The fringe photographs with the exposure of 1/48,800 sec. are shown on fig. 18 (Pl.VIII.), B_1 (1), (2), (3), fig. 19 (Pl. VIII.), B_2 (1), (2), (3), (4), and fig. 20 (Pl. IX.), B_3 (1), (2), (3), and in the photographs a time-mark of 1/1200 sec. is shown by broken lines.

From the photographs the extreme fibre stresses are plotted on fig. 21 (B_1), (B_2), and (B_3).

As is clear in figs. 18, 19, and 20 (Pls. VIII. & IX.) the impact is followed by a vibrating stress. This can be attributed to free oscillations of the ring, whose natural frequency f_i is given * as

$$f_i = \frac{1}{2\pi}\sqrt{\frac{EIi^2(1-i^2)^2}{mAR^4(1+i^2)}},$$

where $i=1, 2, 3, \ldots$.

* Timoshenko, ' Vibration Problems in Engineering,' p. 296 (1928).

Fig. 21.

(B_1)

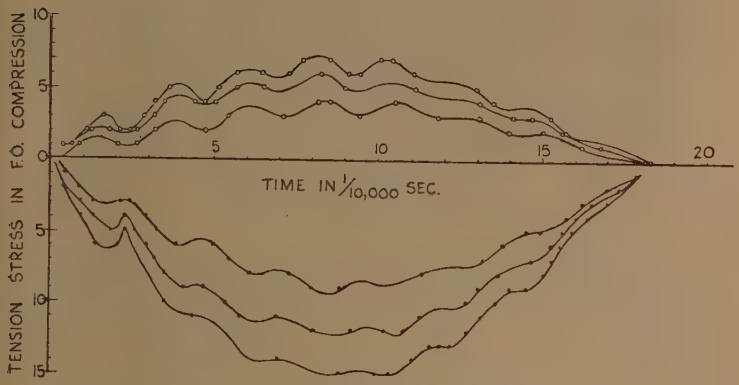

(B_2)

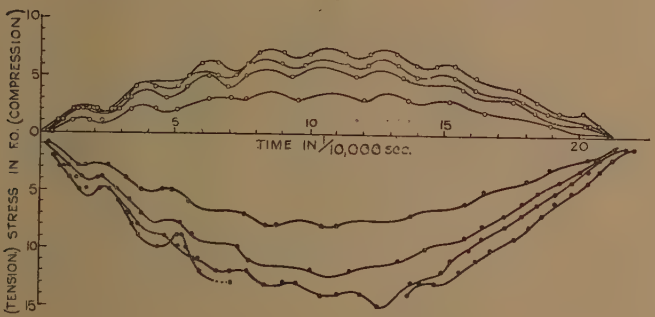

B_3)

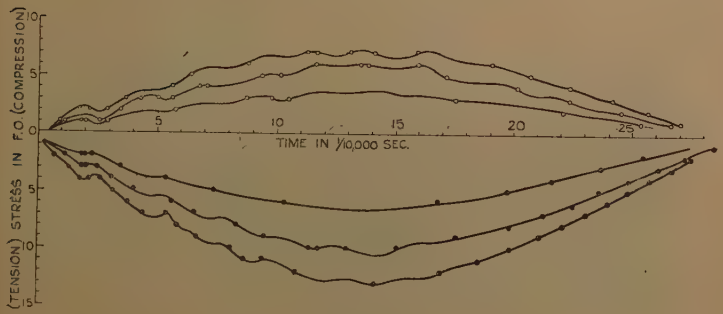

In this expression m is the density of the material of the specimen (for phenolite $m=1{\cdot}27$ g./cm.^{3}) ; A the sectional area of the ring in cm.^{2} ; I the moment of inertia in cm.^{4} ; R the mean radius (R$=$5 cm.) ; E the elastic constant in dyne/cm.^{2} ; i a positive integer.

When $i=2$, $\sqrt{\frac{i^2(1-i^2)^2}{1+i^2}}=2{\cdot}68$,

„ $i=3$, $\sqrt{\frac{i^2(1-i^2)^2}{1+i^2}}=7{\cdot}58$.

The mode of vibration for $i=2$ is as shown on fig. 22, and the value measured on the photograph coincides rather well in the case $i=2$, as shown in the following table :—

TABLE VIII.

Test-piece.	f_2. Calc.	f_2. Exper.
B_1	2348	2370
B_2	1987	2062
B_3	1625	1725

Fig. 22.

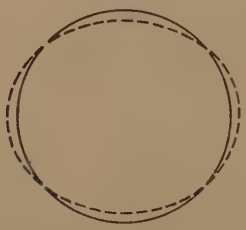

It is clear at a glance that after the impact the ring may be said to oscillate as shown in fig. 22.

The existence of the remarkable oscillation during the impact is one of the important results. As it is clear from fig. 21, the phase of the oscillation wave coincides for various heights of fall, and it seems that they are dependent on the dimension of the ring.

On the assumption that the energy of the falling weight is totally transferred into work of deformation (of the ring), and that the mass of the specimen is negligibly small compared with that of the falling weight, the maximum stress during the impact can be calculated theoretically.

Let λ_d be the dynamical deflexion, λ_{st} the statical deflexion, h the height of fall,

$$\frac{\lambda_d}{\lambda_{st}} = 1 + \sqrt{1 + \frac{2h}{\lambda_{st}}}.$$

In the case of a circular ring loaded at the top, the vertical deflexion λ_{st} is *

$$\lambda_{st} = \left(\frac{\pi}{4} - \frac{2}{\pi}\right)\frac{PR^3}{EI} = 0{\cdot}149\frac{PR^3}{EI},$$

and the deformation on the horizontal diameter λ'_{st} is

$$\lambda'_{st} = \left(\frac{2}{\pi} - \frac{1}{2}\right)\frac{PR^3}{EI} = 0{\cdot}137\frac{PR^3}{EI}.$$

In general, the bending moment M is as follows:—

$$M = \frac{PR}{2}\left(\sin\theta - \frac{2}{\pi}\right),$$

and at the horizontal section, where $\theta = \frac{\pi}{2}$,

$$M = \left(\frac{1}{2} - \frac{1}{\pi}\right)PR = 0{\cdot}1817PR.$$

On the assumption that the deflexion is proportional to the external force, the bending moment M for dynamical force is given as

$$M = \left(\frac{1}{2} - \frac{1}{\pi}\right)\frac{\lambda_d}{\lambda_{st}}PR,$$

$$= 0{\cdot}1817\frac{\lambda_d}{\lambda_{st}}PR.$$

* Timoshenco and Lessells, 'Applied Elasticity,' p 234 (1925).

Therefore the extreme fibre stresses σ_i and σ_0 are as follows:

$$\sigma_i = \frac{\lambda_d}{\lambda_{st}}\left\{\frac{0{\cdot}1817P}{A'-A}\left(\frac{R}{R-y_1}-\frac{A'}{A}\right)+\frac{P}{2A}\right\},$$

$$\sigma_0 = \frac{\lambda_d}{\lambda_{st}}\left\{\frac{0{\cdot}1817P}{A'-A}\left(\frac{A'}{A}-\frac{R}{R+y_2}\right)-\frac{P}{2A}\right\}.$$

A comparison of the experimental results with these deductions is made in the following tables:—

TABLE IX. (*a*).

Test-piece.	b (mm.).	I (mm.)^4.	λ_{st} calc. (mm.). (vertical).	λ_{st} calc. (mm.). (horizontal).
B_1	26	8788	0·00242	0·00222
B_2	22	5324	0·00398	0·00365
B_3	18	2916	0·00728	0·00667

In the table r_i indicates the ratio $\frac{\text{Experimental } \sigma_i}{\text{Theoretical } \sigma_i}$ and r_0 that of the σ_0. All the values of r fall nearly on 0·8 (more precisely, the mean of six ratios is 0·820); that is to say, the experimental maximum stage is about 80 per cent. of that calculated theoretically. In the case of the ring, also, some 20 per cent. of the energy of the falling weight may be spent otherwise than in work of deformation.

To ascertain the results from another fact, an experiment to measure the deflexion only was tried. With the ring for which $b=18$ mm. the variation of the horizontal diameter was measured. As shown in fig. 23, thin rods of metallic magnesium were bridged on the diameter having a slit at centre and fixed to the sample on both sides of the ring. The horizontal deflexion of the ring can be reproduced at the centre as the variation of the opening of the slit, and its image was projected on the rotating film by means of an objective of 26 mm. focal length with the magnification of fifteen times. The ring was struck with the falling weight of 500 g. from the heights of $h=100$ mm. and 200 mm., the photographs are shown in fig. 24 (Pl. IX.).

TABLE IX. (*b*).

Test-piece.	Film No.	λ_{st} $t=0$ calc. (mm.).	h (mm.).	$\frac{\lambda_d}{\lambda_{st}}$.	Stresses in f.o. Calc. σ_i.	Calc. σ_0.	Exper. σ_i.	Exper. σ_0.	Ratio $r=\frac{\text{Exper.}}{\text{Calc.}}$ r_i.		r_0.	
B_1 $b=26$ mm.	(1)	0·00242	100	287	11·30	4·54	9·4	4·1	0·832	0·789	0·897	0·907
	(2)	,,	200	407	15·98	6·46	**12·3**	5·9	0·770		0·913	
	(3)	,,	300	499	19·60	7·92	**15·0**	7·2	0·766		0·910	
B_2 $b=22$ mm.	(1)	0·00398	70	188	10·50	4·85	8·2	3·5	0·780	0·801	0·722	0·787
	(2)	,,	150	275	15·38	7·08	12·5	5·9	0·812		0·833	
	(3)	,,	210	325	18·18	8·38	14·5	6·6	0·798		0·787	
	(4)	,,	250	355	19·85	9·17	16·2	7·4	0·814		0·807	
B_3 $b=18$ mm.	(1)	0·00728	45	112	8·62	4·84	6·7	3·8	0·778	0·814	0·788	0·824
	(2)	,,	100	166	12·76	7·17	10·5	6·1	0·823		0·852	
	(3)	,,	150	204	15·65	8·80	13·2	7·3	0·843		0·831	

In this case let the statical contraction of the vertical diameter by the weight of 0·5 kg. be $\lambda_{st}=0{\cdot}00726$ mm., and the dilatation of the horizontal diameter $\lambda'_{st}=0{\cdot}00667$ mm. and λ_d be the vertical deflexion due to dynamical load, and λ'_d that of the horizontal.

Fig. 23.

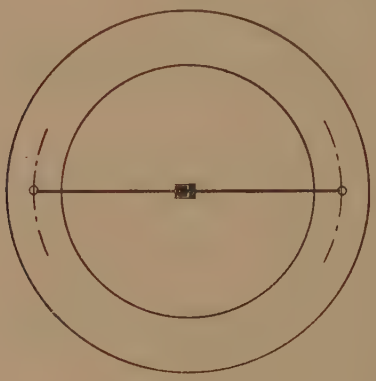

The following table gives the comparison of the experimental and theoretical values :—

TABLE X.

Test-piece.	Film no.	h (mm.).	λ'_d exper. (mm.).	$\frac{\lambda_d}{\lambda_{st}}$	λ'_d calc. (mm.).	$r=\frac{\text{Exp.}}{\text{Calc.}}$
B_3	(1)	100	0·966	166	1·106	0·873
	(2)	100	0·964	166	1·106	0·872
	(3)	200	1·402	235	1·566	0·895

Here also the experimental values are about 80–90 per cent. of the theoretical ones, and this seems to coincide with the results of the stress.

Time of Duration of the Impact.

The time of duration of the impact can be measured on the photographs, and it was compared with calculated

values. The theoretical expression for the time is as follows :

$$\tau = \pi \sqrt{\frac{\overline{\lambda_d} m}{P}} = \pi \sqrt{\frac{0{\cdot}149 R^3 m}{E l}}.$$

This expression is independent of the height of fall, and the conclusion is verified by fig. 21. The experimental results and a comparison with theory are given in the following table :—

TABLE XI.

Test-piece.	Time of duration 10^{-4} sec.	
	Calc.	Exper.
B_1	15·63	18·4
B_2	20·20	22·0
B_3	27·24	28·5

The authors are of the opinion that the results coincide rather well with the calculated values.

Résumé.

To analyse quick variations of internal stresses—*e. g.*, in vibrating specimens or in impact phenomena—kinematography of photo-elastic fringes at very high speeds was devised. As the light source an ordinary carbon arc lamp has been used with heavy current and with a red filter, selecting a very narrow band.

The study was limited to a certain section, and an exposure of about 1/5000–1/50,000 sec. has been achieved.

As actual examples with specimens of phenolite the vibrations of a cantilever, impact of a beam, and impact of rings were tried. On the various results obtained a cross-check has been worked out with the known theory for shock phenomenon, and the range of coincidence of the theory with the experiment is discussed. As for the maximum stress produced by impact, it was ascertained that 80–90 per cent. of the calculated value is usual in the cases tested.

XXXVIII. *Subsidiary Whirling of Rotors due to Speed Oscillation.* *By* David Robertson, *D.Sc., M.I.E.E.**

Contents.

	Page
1. Introduction	474
2. Causes of Speed Oscillation	475
3. Speed-Oscillation Whirls	478
4. Examples of Speed-Oscillation Whirls	481
5. Large Angular Oscillations	485
6. Gravitational Speed Oscillations	487
7. Spontaneous Speed Oscillations with D.C. Motor	492
8. Historical Notes	495
9. Bibliography	500

1. *Introduction.*

WHIRLING of a shaft is most commonly caused by unbalance, but it may also be produced in a number of other ways. By itself speed oscillation is not a source of whirling, but it does induce additional subsidiary whirls in a rotor which already has an unbalance whirl. These subsidiary whirls are usually quite small.

In what follows we shall suppose that the main whirl is caused by unbalance; when the shaft is free from whirling strain the c.g. is at the "neutral point" A lying at a distance a from the axis of rotation. This original eccentricity, OA in the diagrams, is referred to as the "neutral radius," and it rotates along with the shaft which has a mean speed ω.

When the main whirl is of some other type speed oscillations of the rotor can only produce subsidiary whirls in those rare cases where they also affect the speed of the rotating force which induces the main whirl. In such a case the only modification required by the theory is to define the neutral radius as the deflexion which would be caused by the inducing force if it did not rotate, and to take ω as the mean rotation of the force instead of that of the shaft.

The following notation will be employed :—

a=eccentricity of c.g. due to unbalance=neutral radius.

f=extra elastic force, per unit mass of rotor, due to oscillation of neutral radius.

g=acceleration due to gravity.

* Communicated by the Author.

h=static deflexion due to weight of rotor.
k=radius of gyration of rotor.
n=speed oscillation cycles per revolution.
r=radius of main whirl, supposed due to unbalance.
ρ_f, ρ_b=radii of forward and backward components of subsidiary whirl.
τ=grav.tational torque per unit mass of rotor.
α=damping constant=frictional force per unit mass of ideal rotor divided by velocity of c.g.
ω_0=critical speed = {elastic ditto divided by deflexion of c.g.}$^{1/2}$
ω=mean rotation (angular velocity) of shaft.
ω_s=rotation of subsidiary whirl relative to mean neutral radius.
ϕ=angle of lag of radius of main whirl behind mean neutral radius.
ψ_f, ψ_b=angle of lag for subsidiary whirls.
θ=angular displacement of neutral radius ahead of position corresponding to uniform rotation.
Θ=maximum value of θ.

2. *Causes of Speed Oscillation.*

Oscillations of speed of the whole rotor may arise because of a periodic variation of the driving torque, of the load torque, or of both. Well-known examples are those due to the varying crank effort of reciprocating engines, pumps, etc., and those which occur during phase swinging of synchronous electrical machines.

With an unbalanced horizontal shaft the torque due to gravity produces a once-per-revolution fluctuation of the speed, but we shall see that it is usually negligible.

Flexible couplings between two lengths of shafting may cause much greater speed oscillations when the shafts are inclined to one another or are parallel but out of line, because of the variation of velocity ratio during the revolution.

Under these circumstances a single-pin-in-slot coupling gives a once-per-revolution oscillation. A Hooke's joint gives a twice-per-revolution variation, and if it be not itself perfectly symmetrical it will at the same time give a once-per-revolution one as well.

In the general case of n pins the oscillation will be repeated n times per revolution, and if it be not

absolutely symmetrical there will also be impulses corresponding to all the integral factors of n down to once per revolution.

In addition the couplings may induce whirls directly because of the bending actions of the forces they exert. The bending moments are small when the coupling is close to a bearing, but increase with the amount of overhang. With the shafts not properly aligned rigid couplings may produce very large bending moments which may have rotating components able to induce whirling.

With the single-pin coupling the whole driving force is effective for bending. As this force rotates along with the shaft it modifies the effective unbalance both in amount and direction, and causes a perfectly balanced shaft to act as if its c.g. were slightly eccentric.

With the shafts inclined or out of line the variation of the driving force with the speed oscillation would give rise to additional rotating force components, one at rest in space and one rotating at twice the shaft speed. The latter would have a resonance when the shaft runs at half its critical speed.

With perfect symmetry and the shafts accurately aligned the resultant force would be zero, and the bending actions would disappear when there are more pins than one; but usually, owing to lack of symmetry and to misalignment, there will be some residual bending actions of which one component is similar to that with a single pin and the others give resonance at the same speeds as the subsidiary whirls caused by the speed variations.

In many cases the rotor as a whole is capable of angular oscillation under the control exerted on it by the motor or load. Should agreement exist between the frequency of such natural vibration and that of the variation of some external torque, resonance will occur and the angular vibration from the mean speed may be large.

The frequency of free angular vibration depends upon the rotary inertia of the whole mass which partakes of it and upon the restoring torque acting when the position differs from that corresponding to uniform rotation; these in turn depend upon the characteristics of the motor and load. No calculation is complete which does not allow for all these factors.

When away from the phase at which the motor torque

balances the mechanical load a synchronous electric motor exerts an additional controlling torque, pulling the rotor back towards that phase. The result is a vibratory system arising from the tendency of the motor to keep in step with the electrical supply.

When the set is hunting in this way, the angular displacement from mean rotation is equal to the angle of phase swing on the electrical side divided by the number of pairs of poles. With a small number of poles, the angular oscillations of the rotor might exceed the limits to which the theory given below applies, but with a large number of poles this is not likely to be the case.

The same sort of thing occurs with a belt drive, but in this case it is the elasticity of the belt which permits angular oscillations between the driving and driven pulleys and which determines their frequency. Even a geared drive has some spring and so can permit vibrations ; these would usually be of high frequency and small amplitude.

Most types of electric motor give a torque which diminishes as the speed rises. With fixed conditions on the electrical side the motor torque balances a given load torque at some particular speed. Should the speed differ from that equilibrium value the motor gives an additional torque opposing the deviation of the speed. Since this excess torque opposes the velocity of the angular oscillations, it acts as a damper. In the extreme case of a level speed torque characteristic for the motor it would effectively prevent any angular oscillations.

But even when one end of the rotor is driven at a perfectly constant speed there may be variations of speed at other places along its length because of torsional oscillations in the shaft. Their frequency depends upon the torsional stiffness of the shaft and upon the amount and distribution of the rotary inertia. With pulleys at irregular intervals there may be several such natural frequencies, and the motion becomes somewhat complicated.

The neutral radius is drawn in a plane through the c.g. at right angles to the axis of rotation, and has the same rotation as that plane of the shaft. At the driven end of the shaft, attached to the material of the shaft there, draw a second radius, called the index radius, parallel to the neutral radius when the shaft is free from torsion.

If the shaft be transmitting a constant torque the two radii will have a constant angle between them proportional to that torque. So long as there are no torsional oscillations the neutral and index radii will retain the same relative positions, and the rotation of one must continually be an exact replica of that of the other ; but when torsional oscillations occur the angular velocities of these two radii will not be identical at every instant, although they must be equal on the average.

Unless the distance between the index and neutral radii be greater than about 100 times the diameter of the shaft the angular displacement of the neutral radius because of torsional oscillations alone cannot exceed the limits assumed in our theory without endangering the shaft.

3. *Speed-Oscillation Whirls.*

If the shaft be running continuously at the constant speed ω the neutral radius at a particular instant would be OA in fig. 1, and the c.g. would be at G, the point of equilibrium for the main whirl ; but when the speed oscillates about a mean value ω the neutral point at this instant is at A′ instead of A and the c.g. at G′ instead of G. The neutral radius lies ahead of the position corresponding to uniform rotation by the angle $AOA' = \theta$, whose maximum value is Θ.

Now, assume that the speed oscillations are harmonic, so that

$$\theta = \Theta \sin \omega_s t, \quad . \quad . \quad . \quad . \quad . \quad (3{\cdot}01)$$

and also that Θ is sufficiently small, say not more than 0·1 to 0·2 radian, to permit us to write $\sin \theta \doteqdot \theta$ and $\cos \theta \doteqdot 1$ for all the values which θ may have.

The main whirl running at the mean speed takes account of the elastic force due to the deflexion AG, but does not allow for the additional deflexion AA′ caused by the angular oscillations of the neutral radius. There is consequently a discrepancy force whose amount per unit mass is

$$f = \omega_0^2 \times AA' \doteqdot \omega_0^2 a\theta = \omega_0^2 a\, \Theta \sin \omega_s t, \quad . \quad . \quad (3.02)$$

and this force induces the subsidiary whirl GG′.

With our restrictions as to the magnitude of Θ we may assume that the direction of the discrepancy

force is always at right angles to the mean neutral radius OA ; hence it rotates at the mean speed of the shaft at the same time as it varies harmonically in magnitude.

When the speed oscillations are first started there will also be a transient whirl, but after a time the transient will disappear, and no further account need be taken of it.

The harmonic force f in the straight line AA′ can be replaced by two constant rotating forces, each equal to $\frac{1}{2}\omega_0^2 a\,\Theta$, which have rotations of $+\omega_s$ and $-\omega_s$ relatively to the mean neutral radius. They must be so placed that at every instant their resultant is equal to f.

Fig. 1.

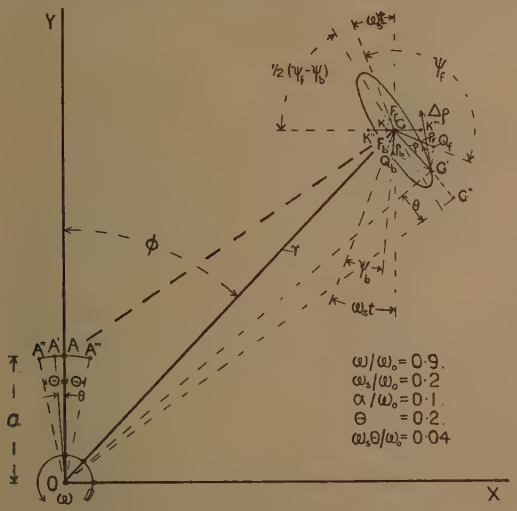

Effect of rapid oscillations of speed.

When the neutral point is at A the harmonic force is zero ; its rotating components then stand opposite to one another parallel to OA. They lie in the same direction, at right angles to OA, when the neutral radius is at either extreme of its swing relatively to the uniformly rotating line OA.

The forward component of the harmonic force is shown as GF_f in fig. 2 and the backward one as GF_b in figs. 2 and 3. The former gives rise to the forward subsidiary whirl $GQ_f = \rho_f$ and the latter to the backward whirl

$GQ_b = \rho_b$. These whirls have rotations of $\pm\omega_s$ relatively to OA and absolute rotations of $(\omega+\omega_s)$ and $(\omega-\omega_s)$ respectively.

Applying the general whirling equations * we have :—

$$\rho_f = \tfrac{1}{2}\omega_0^2 a\,\Theta \div [\{\omega_0^2-(\omega+\omega_s)^2\}^2+4\alpha^2(\omega+\omega_s)^2]^{\frac{1}{2}} \quad . \quad . \quad (3.03)$$

$$\rho_b = \tfrac{1}{2}\omega_0^2 a\,\Theta \div [\{\omega_0^2-(\omega-\omega_s)^2\}^2+4\alpha^2(\omega-\omega_s)^2]^{\frac{1}{2}} \quad . \quad . \quad (3.04)$$

$$\tan\psi_f = 2\alpha(\omega+\omega_s) \div \{\omega_0^2-(\omega+\omega)^2\} \quad . \quad . \quad . \quad . \quad . \quad (3.05)$$

$$\tan\psi_b = 2\alpha(\omega-\omega_s) \div \{\omega_0^2-(\omega-\omega_s)^2\} \quad . \quad . \quad . \quad . \quad . \quad (3.06)$$

The ψ's are the angles by which the radii lag behind their respective inducing forces and are to be measured against the rotation of the shaft when positive. When ω_s exceeds ω, ψ_b is negative ; ρ_b has then a backward

Fig. 2.

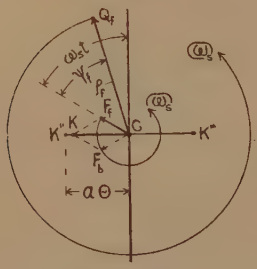

Fig. 3.

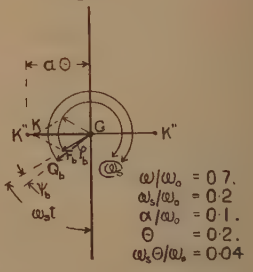

Vector components of subsidiary whirl due to harmonic oscillations of speed.

absolute rotation, and it lies ahead (in the direction of the shaft's rotation) of the backward component of the force.

Resonance occurs for either whirl when its absolute rotation is equal to the critical speed—that is, when $(\omega+\omega_s)=\omega_0$ for the forward whirl and when $(\omega-\omega_s)=\omega_0$ for the backward one.

If $\omega_s=n\omega$, so that n is the number of speed-oscillation cycles during one revolution, then the resonant speeds are

$$\omega=\omega_0/(n\pm1) \quad . \quad . \quad . \quad . \quad . \quad (3.07)$$

In either case the radius of the resonant whirl is $\frac{1}{2}\,\Theta(\omega_0/2\alpha)a$, whereas the radius of the main whirl at the critical speed is $(\omega_0/2\alpha)a$. Since the ratio of these

* See equations (6.06) to (6.12) of no. 13 in Bibliography.

is $\frac{1}{2}\Theta$, the maximum whirl due to speed oscillation will only be a fraction of the maximum unbalance whirl so long as the amplitude of the oscillation is kept within the limits for which our theory is reasonably accurate. This does not exclude the possibility of whirling trouble from angular oscillations beyond these limits.

Since the two subsidiary whirls have equal and opposite rotations with respect to the mean neutral radius, the resultant motion relative to axes revolving at the mean speed of the shaft is one round an ellipse.

The axes of the ellipse lie along the bisectors of the angle between the two component radii, and are equal to the sum and difference of these radii. The way of the rotation round the ellipse is that of the longer radius. The ellipse becomes a straight line when the radii are equal and a circle when one of them is zero.

When the neutral point is at its left extreme the two rotating forces point to the left and are perpendicular to OA; ρ_f and ρ_b lie behind that direction by the angles ψ_f and ψ_b. Consequently the major axis of the ellipse lies behind AA′ by the angle $\frac{1}{2}(\psi_f+\psi_b)$. With given constants these angles and the two radii are known; the axes of the ellipse can therefore be drawn in and the ellipse constructed in the usual way.

If we require the motion relative to axes rotating with the shaft itself, instead of to axes revolving at the mean speed, we must allow for the oscillations by turning OG′ through the same angle θ as is required to bring OA′ to OA.

Thus, if G″ be the position of the c.g. referred to axes OX, OY (fig. 1) which rotate along with the shaft OG″=OG′ and G′OG″=θ. The path of G″ is quite different from that of G′; both are shown in the following examples.

4. *Examples of Speed-Oscillation Whirls.*

Figs. 4–12 give examples of these whirls with $\omega_s/\omega_0=0{\cdot}4$, $\alpha/\omega_0=0{\cdot}1$, and $\Theta=0{\cdot}2$ radians$=11{\cdot}5°$. The amplitude of the speed oscillation, being $\omega_s\Theta$, is then $\pm 0{\cdot}08\omega_0$. The ellipses, whose major axes are shown by the chain-dotted lines, are the paths of the c.g. relative to axes revolving at the mean speed of the shaft, and the other loops, corresponding to G″ of fig. 1, show that relative to axes rotating at its actual speed.

In addition, that portion of the locus of G which corresponds to the speed range $(\omega \pm 0{\cdot}08\omega_0)$ has been drawn on each diagram to show the relative motion of the c.g. when the speed changes are very slow *.

In figs. 4–7 the rotation round the ellipse is positive and in figs. 9–12 it is negative. In each case the greater

Fig. 4.

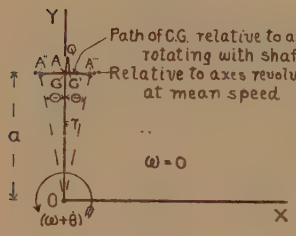

Fig. 5.

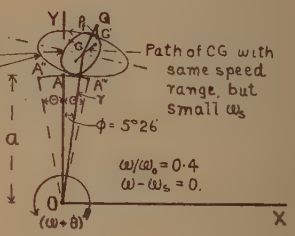

Fig. 6.

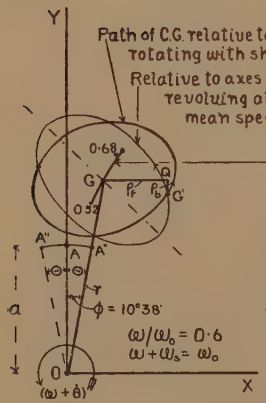

Fig. 7.

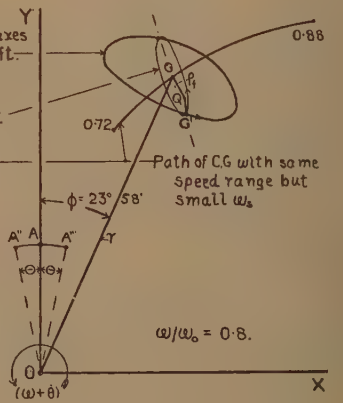

Common data:- $\omega_s/\omega_0 = 0{\cdot}4$, $\alpha/\omega_0 = 0{\cdot}1$, $\Theta = 0{\cdot}2$, $\omega_s\Theta/\omega_0 = 0{\cdot}08$.

Subsidiary whirls due to harmonic oscillations of speed with shaft running below its critical speed.

radius—that is, the forward one for the first group and the backward one for the second group—has been drawn as GQ and the smaller one as QG'.

* See fig. 5 of no. 13 in Bibliography.

These radii are shown in positions correct for the instant at which the neutral radius is passing its mean position and is moving to the left. The rotating forces are then vertical, the forward one being upward and the backward one downward.

Fig. 4 corresponds to oscillations of speed about zero. The two component radii are equal, and the c.g. moves approximately in the line A″A‴ to an extent depending upon ω_s. For the particular value chosen the extent of the motion is just a little greater than A″A‴, but it

Fig. 8.

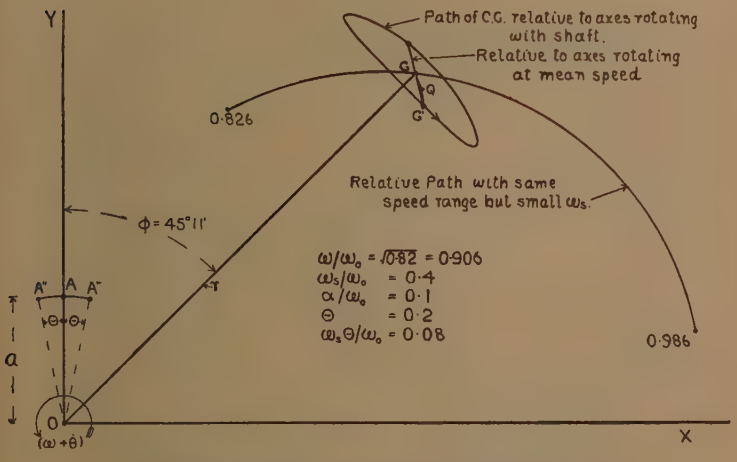

Subsidiary whirl due to harmonic oscillations of speed with $\omega^2 = \omega_0^2 - \omega_s^3 - 2\alpha^2$, when $\rho_f = \rho_b$.

may have any value up to a maximum of $\omega_0/2\alpha$ times A″A‴ at resonance with $\omega_s = \omega_0$.

The next diagram is for the case where $(\omega - \omega_s) = 0$, which means that the backward radius has a constant direction in space and gives the c.g. a constant deflexion QG′ in a fixed direction.

In fig. 6 the forward radius revolves at the critical speed and has a considerable length.

Up to this point the forward radius has been growing rapidly with increase of mean speed and the backward one only slowly. Further increases of speed cause the

former to decay until the two become equal again in fig. 8. The path relative to axes rotating at the mean speed is once more a straight line, but this time it has a considerable inclination. The speed of fig. 8 is almost exactly equal to the quadrantal speed, but this is a mere accident arising from the particular choice of ω_s and α.

At still higher speeds the backward radius is the greater and the rotation round the ellipse is negative.

Fig. 9.

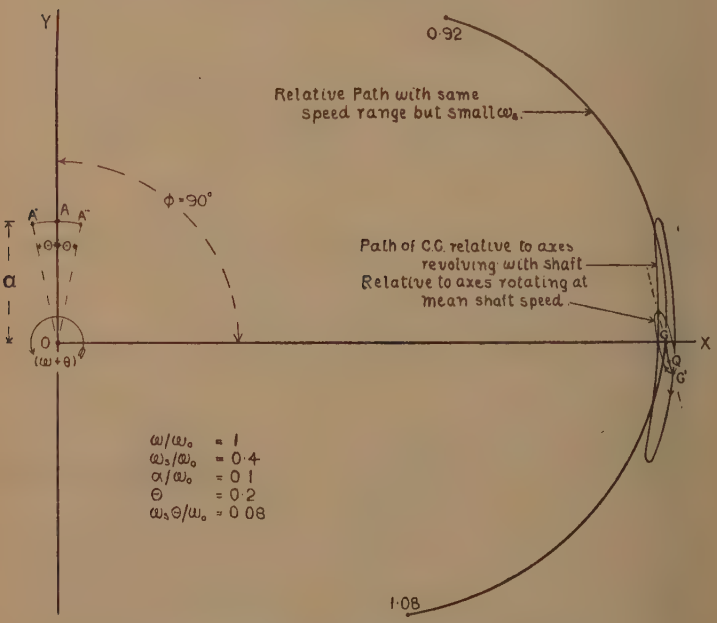

Subsidiary whirl due to harmonic oscillations of speed about the critical speed.

Fig. 9 applies when the mean speed of the shaft is equal to its critical speed. The ellipse is a fairly small one because both subsidiary whirls are remote from resonance; but, on account of the large radius of the main whirl, there is a considerable amount of drawing out when we convert to axes rotating with the shaft.

Up to now the major axis of the ellipse has been getting more and more inclined ; as the speed is pushed up further it continues to do so for a little, but it soon moves back, and ultimately returns to the horizontal.

The last set of diagrams, figs. 10–12, apply to shaft speeds above the critical. The backward radius continues to increase until it reaches the resonant point with $(\omega - \omega_s) = \omega_0$, as in fig. 11. Beyond that both radii decrease and they both vanish at infinite speed.

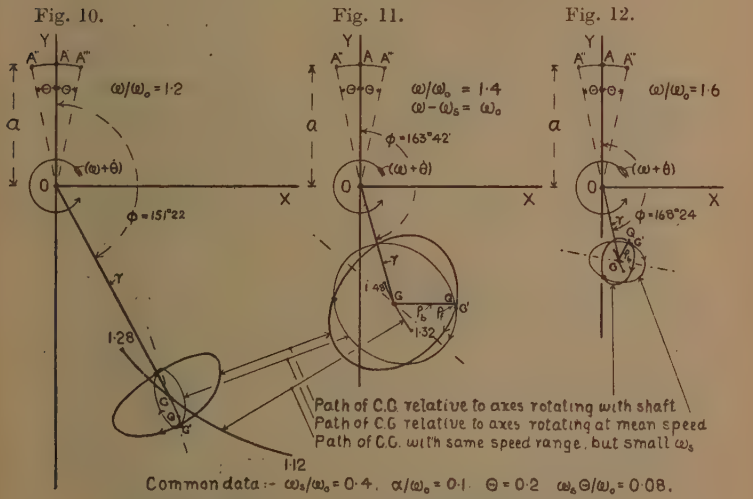
Fig. 10.
Fig. 11.
Fig. 12.
ω/ω₀ = 1·2
ω/ω₀ = 1·4
ω−ωs = ω₀
ω/ω₀ = 1·6
φ = 151°22
φ = 163°42'
φ = 168°24
1·28
1·32
1·12
Path of C.G relative to axes rotating with shaft
Path of C.G relative to axes rotating at mean speed
Path of C.G. with same speed range, but small ω₀
Common data :- ωs/ω₀ = 0·4. α/ω₀ = 0·1. Θ = 0·2 ω₀Θ/ω₀ = 0·08.

Subsidiary whirls due to harmonic oscillations of speed with shaft running above its critical speed.

5. *Large Angular Oscillations.*

The theory given above applies only when the relation between the speed range and the frequency of its variation is such that the maximum angular displacement of the neutral radius from the mean is small.

At the other extreme we have the case of a speed variation so slow that the c.g. traces out, relatively to the neutral radius, a portion of the locus of the point of equilibrium for the steady whirl.

When neither of these conditions is fulfilled the loop traced by the c.g. relative to the neutral radius will have some intermediate form.

As Θ gets bigger the first discrepancy to be noticeable is that the neutral point has a motion parallel to OA as well as one at right angles to it. We have a displacement of a versin θ in the AO direction as well a one of $a \sin \theta$ in the AA′ direction. From a diagram it can easily be seen that the former consists of a constant part plus an oscillating part of double frequency.

As a second approximation we may write

$$a \text{ versin } \theta \doteq \tfrac{1}{2}a\theta^2 = \tfrac{1}{2}a\,\Theta^2 \sin^2 \omega_s t \quad . \quad . \quad (5.01)$$

$$= \tfrac{1}{4}a\,\Theta^2(1-\cos 2\omega_s t). \quad . \quad . \quad (5.02)$$

The constant term has a direction opposite to the mean neutral radius and causes a small reduction of the effective unbalance. The double frequency term, and the corresponding elastic force, can be split up into a pair of revolving vectors having rotations of $\pm 2\omega_s$, relative to the mean neutral radius, and absolute rotations of $(\omega \pm 2\omega_s)$.

Each of these rotating forces induces a subsidiary whirl of the corresponding frequency, which may be calculated from the equations already given if $2\omega_s$ be inserted in place of ω_s and $\frac{1}{4}a\,\Theta^2$ instead of $a\,\Theta$. Because of the factor $\frac{1}{4}\,\Theta$ these additional whirls must be small with the values of Θ to which this approximation may be applied.

In a similar manner further terms in the expansion of $\sin \theta$ and versin θ will give rise to whirls having relative rotations of $\pm 3\omega_s$, $\pm 4\omega_s$, and so on, corresponding to the terms of a Fourier's series.

By following this idea out a numerical solution could be obtained for the whirls produced by any given periodic variation of the speed.

If the relation between the speed and time be specified by a graph or equation a second graph can be derived from it to show the variation of θ; from that we can get a pair showing $a \sin \theta$ and a versin θ. Each of the last pair can be analysed into harmonic components by one of the well-known methods. These harmonic components can be split into rotating vector components and dealt with as above.

We thus obtain a solution for the position of the c.g., relative to the mean revolving axes, in terms of a series of whirls of ascending frequency.

Whether the process is practical as well as possible will depend upon the number of terms required to make the harmonic series represent the given conditions with sufficient accuracy.

6. *Gravitational Speed Oscillations.*

When the shaft is horizontal the weight of the rotor bows the shaft downward and produces a downward deflexion of the c.g., whose amount is $h=g/\omega_0^2$. The axis of rotation is depressed below the centre line of the bearings by the same amount.

The bow produced by the unbalance whirl rotates along with the shaft and causes a fixed strain at each point in the material ; but that due to gravity, being fixed in space, rotates relatively to the shaft and causes an alternating strain. Alternating strain brings elastic hysteresis into play, and that deflects the gravitational bow to a very small extent in the direction of rotation ; we shall neglect this.

When an unbalanced shaft is rotating, the weight of the rotor no longer acts through the centre line of the bearings but lies alternately on one side and the other. It thus produces a fluctuating torque, which in turn induces oscillations of speed.

The frequency of these oscillations is the same as that of the rotation of the shaft—that is, $\omega_s=\omega$; but the amplitude of the torque oscillation is not Mgr, as might be expected, because the leverage of the other forces is modified by the static deflexion of the c.g.

We shall see later that the oscillations due to gravity are exceedingly small ; in estimating the torque we shall therefore neglect them and their subsidiary whirls, and suppose the neutral point to remain at A and the c.g. at G.

In fig. 13 OA is the mean neutral radius and G the point of equilibrium for the main whirl. H is on the centre line of the bearings and O on the axis of rotation ; with a vertical shaft H and O would coincide, but with a horizontal shaft O lies below H by the distance h.

In order to balance the weight and the inertia and frictional forces external forces must be applied to the rotor through the bearings, and they are transmitted elastically by the shaft. We shall asume that these external forces act through the centres of the bearings

and that the frictional forces act through the c.g. like the weight and inertia forces—in other words, the bearing forces act through H and the weight and inertia and frictional forces through G.

In the absence of gravity the axis of rotation would be at H and the neutral point at A_v. Thus when the weight is acting A_vG is the total deflexion of the shaft, and gives the direction of the elastic pull of the shaft on the bearings.

But A_vG is the vector sum of A_vH and HG; since the latter component passes through both H and G,

Fig. 13.

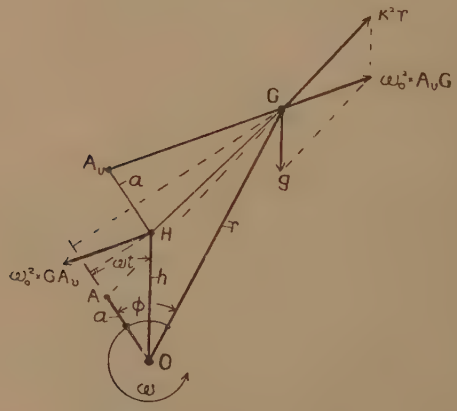

Forces on a horizontal rotor.

the corresponding component of the bearing force produces no torque on the rotor. The torque is entirely due to the other component of the bearing force, whose magnitude is $\omega_0^2 \times HA_v = \omega_0^2 a$.

Reckoning time from the instant when A passes its highest point the leverage of the torque-component of the force is $(r \sin \phi - h \sin \omega t)$, and the torque it exerts, per unit mass of rotor, is

$$\tau = \omega_0^2 ah \sin \omega t - \omega_0^2 ar \sin \phi, \quad . \quad . \quad . \quad (6.01)$$

the torque being taken as positive when it accelerates the rotor.

The second term of this expression is constant and must be balanced by the driving motor if the mean speed is not to change—it is, in fact, the torque due to the friction of the main whirl.

The first term is the oscillating gravitational torque, and it should be noted that its amount is exactly the same as if the rotation were very slow, in which case the c.g. would remain at A.

In order to calculate the extent of the angular oscillations brought about by this torque it is necessary to take account not only of the inertia of the rotor itself but also of that of the drive and load (if any) of their torque-speed and torque-phase characteristics, of the torsional stiffness of the shaft, of the distribution of inertia along it, and of the friction opposing such angular oscillations.

A complete solution is thus a rather complicated affair, and cannot even be attempted without data on all these points. So far as the author is aware no one has tackled this problem, but several writers have dealt with the academic one of a rotor running at a constant mean speed without friction of any kind and without connexion to any motor or load. Apparently, none of them realize the restricted nature of the problem they have attacked, for their solutions are put forward as if they were of general application.

Since the above-mentioned solutions take no account of friction, they fail entirely near the resonant condition of the shaft running at half its critical speed. Friction must not be neglected near resonance, although it may be of little importance elsewhere.

In this academic problem of a self-contained frictionless system there are other considerations which these writers have left out of account and which invalidate their assumption of a constant mean speed.

The energy content of the system is constant and finite ; it is therefore quite impossible for the whirl to reach an infinite size, involving infinite energy.

The energy consists of five parts, the gravitational energy, the strain energy of the deflexion, and the kinetic energy of the rotation about the c.g., of the whirling motion, and of the growth motion of the whirl ; any increase of one of these parts must take place at the expense of the others.

We shall deal with a modified problem, only slightly less academic, by supposing that the shaft is driven by a motor which somehow keeps the mean speed constant but does not otherwise influence the motion. The latter part of this condition could not be fulfilled by any actual motor.

With this restricted problem we have no inertia but that of the rotor itself; since there is no angular control the natural frequency of angular oscillation or size, and hence always small compared with that of any forced oscillation. It therefore follows that the amplitude of the forced angular oscillation is not appreciably affected by any reasonable amount of friction, and that its phase is opposite to that of the torque producing it.

Taking k as the radius of gyration of the rotor, the amplitude of the angular oscillation induced by the gravitational torque of amplitude $\omega_0{}^2ah=ga$ is

$$\Theta=(ga/k^2)\div\omega_s{}^2=ga/\omega^2k^2 \quad . \quad . \quad . \quad . \quad (6.02)$$

Inserting the above value of Θ in equations (3.03) to (3.06), and remembering that $\omega_s=\omega$, we get

$$\rho_f=\tfrac{1}{2}(ga^2/\omega^2k^2)\omega_0{}^2\div\{(\omega_0{}^2-4\omega^2)^2+16\alpha^2\omega^2\}^{\frac{1}{2}}. \quad (6.03)$$

$$\doteq\tfrac{1}{2}(ga^2/\omega^2k^2)\times\omega_0{}^2/(\omega_0{}^2-4\omega^2), \quad . \quad . \quad . \quad . \quad (6.04)$$

provided that α be small and that ω is not nearly equal to $\frac{1}{2}\omega_0$.

Also,

$$\rho_b=\tfrac{1}{2}a\,\Theta=\tfrac{1}{2}ga^2/\omega^2k^2 \quad . \quad . \quad . \quad (6.05)$$

$$\tan\psi_f=4\alpha\omega/(\omega_0{}^2-4\omega^2) \quad . \quad . \quad . \quad (6.06)$$

$$\tan\psi_b=0. \quad . \quad . \quad . \quad . \quad . \quad . \quad . \quad . \quad (6.07)$$

The backward whirl is stationary in space because $\omega_s=\omega$.

At the chosen zero of time OA lies vertically upwards, OG is ϕ behind it, and the alternating torque is zero but about to become positive or forward. Because of the antiphase of θ and τ, θ and AA′ are also zero, but about to become negative.

Thus the rotating components of AA′ and of the corresponding elastic forces lie along OA, the forward one being directed downward and the backward one upward. Thus at zero time ρ_f lies ψ_f behind the downward vertical and ρ_b is parallel to OA or vertically

upward. Since the backward radius retains this vertical direction, it represents a reduction of the static deflexion of the c.g.

There is resonance for the forward radius when $\omega=\frac{1}{2}\omega_0$, and at this speed the radii become

$$\rho_{fr}=ga^2/\alpha\omega_0 k^2 \quad . \quad . \quad . \quad . \quad . \quad . \quad . \quad (6.08)$$

$$\rho_{br}=2ga^2/\omega_0{}^2k^2. \quad . \quad . \quad . \quad . \quad . \quad . \quad . \quad (6.09)$$

To get some idea of the magnitude to be expected for the gravitational speed-oscillation whirls let us assume the following values, which are all reasonable :—

$g\doteqdot 400$ inches/second^2.

$a=2{\cdot}5$ mils.

$k=5$ inches, corresponding to a rotor diameter of about 15″.

$\omega_0=100$ radians/second$\doteqdot 1000$ r.p.m.

$\alpha=0{\cdot}01\omega_0=1$ radian/second.

Then, when $\omega=\frac{1}{2}\omega_0=50$ radians/second,

$\Theta=16\times10^{-6}$ radians.

$a\,\Theta=40\times10^{-6}$ mils.

$\rho_f=1\times10^{-3}$ mils.

$\rho_b=20\times10^{-6}$ mils.

$r_0=125$ mils.

These figures show very definitely that the speed oscillations induced by the gravitational torque, and the subsidiary whirls which they in turn produce, are entirely negligible.

With a real rotor resonance might occur between ω and one of the natural frequencies of angular oscillation already noted. This would make Θ considerably greater than our formula gives it, but there is a big enough margin to warrant the conclusion that these subsidiary whirls will never be of importance.

Moreover, unless the condition were purposely brought about it is extremely unlikely that the speed which is resonant for the angular oscillations would agree with the $\frac{1}{2}\omega_0$ required for a resonant forward radius.

The gravitational torque due to the transient and other subsidiary whirls will also cause speed oscillations ; but these whirls are usually smaller than the unbalance

whirl, and so their speed fluctuations can be safely neglected.

7. Spontaneous Speed Oscillations with D.C. Motor.

In his first experiments on the whirling of shafts the author's model was driven by a fractional H.P shunt-wound D.C. motor with a regulating rheostat in the armature circuit. That method had to be abandoned because the variation of the load with the growth and decay of the whirl produced large changes of speed. But one interesting phenomenon was observed when running close to the critical speed. The amplitude of the whirl would grow and decay with a period of about two seconds, and at the same time the speed would

Fig. 14.

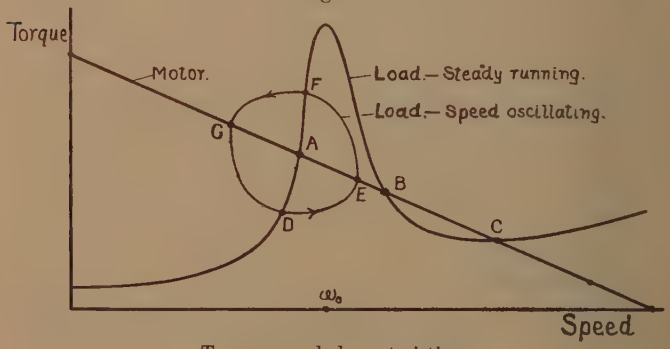

Torque-speed characteristics.

fluctuate to a considerable extent. So long as the regulator was left in a suitable position this action would continue, apparently indefinitely.

Fig. 14 gives a sketch of the torque-speed characteristics of the motor and of the load due to the model. The motor characteristic is a straight line joining the standstill torque point to the no-load speed point.

With a constant supply voltage the no-load point does not vary very much with a moderate resistance in the armature circuit, and it would not vary at all if the motor did not use up some torque in its own friction, eddy currents, and hysteresis. The standstill torque is approximately inversely proportional to the total resistance of the armature circuit.

With a constant resistance and a constant field current the standstill torque and the no-load speed are each nearly proportional to the voltage across the armature circuit.

The steeper the motor line—that is, the lower the resistance in the armature circuit—the more effectively does the motor tend to damp out any speed oscillations.

In the absence of whirling the load characteristic would be a line, probably somewhat curved, which rises as the speed goes up. Because of the whirling there is a large hump on the steady-running load line in the neighbourhood of the critical speed where the unbalance whirl is large. This extra resisting torque is partly due to the whirl friction, but a large portion of it is caused by the extra friction in the bearings which arises from the inclination of the shaft ends when the centre is bowed out.

Because of the time taken for the growth and decay of the whirl the load line with varying speed may differ greatly from that for steady running. When the transient condition is represented by a point below the steady-running load line the whirl is less than its equilibrium value for that speed, and it is growing ; above the steady-running line it is decaying.

Similarly with a transient condition below the motor line the driving torque exceeds the resisting torque and the speed is rising, whereas the speed is falling if the point lies above the motor line.

With the regulator set within certain limits the motor line cuts the steady-running load line in three points, A, B, C, of which A and C represent stable equilibrium and B unstable.

Now suppose that the speed is reduced to D by an additional external torque which is removed after the whirl has become steady. The speed then rises, and, as it is approaching the critical value, the whirl grows. But the whirl growth lags behind the speed change and the transient conditions are represented by the line DE lying below the steady-running line.

At E, where the transient line cuts the motor line, there is a balance of torques, but only for a moment ; if E lies below the steady-running line the whirl continues to grow and thus raises the load torque above the driving torque. The speed now falls, but the whirl continues

to grow until F, where the transient line cuts the steady-running line, after which it also decays.

At G there is again a momentary balance of torques, which is soon upset by the continued decay of the whirl. The motor then speeds up, and if a cyclic condition has been established the conditions will return to the starting point D; the whole cycle thus commences afresh.

If the conditions be such that E lies above the steady-running line, the motor will speed up to C and there will be no speed oscillations.

This explanation is quite satisfactory up to a point, but it fails to account for the oscillations being maintained instead of dying away as might be expected.

With the cyclic condition the kinetic energy given to the rotor during the path GDE must be the same as that abstracted during EFG. In order that the cyclic condition may be stable the shape of the loop must change when the amplitude of the oscillation varies from that for the cyclic loop in such a way that with bigger loops more energy is taken away than given, or with smaller loops more energy is given than taken away.

The experimental facts show that this must be true, but the author is unable to give any convincing explanation of why that is so.

Recently in the author's laboratory Mr. D. J. Pearce made some measurements to determine the exact conditions under which these spontaneous speed oscillations occur; he found that the lower limit of speed must be less than the critical speed, but the upper limit may lie either above or below it. The frequency of the oscillations seems to reach a minimum when the maximum speed is about the same as the critical speed, and it rises fairly rapidly when the mean speed is pushed up towards the limit at which the oscillations cease.

Stroboscopic observation showed a very definite pause in the speed change at the two limits.

The model was the same as that already described elsewhere * with some modifications. The shaft was a round one $\frac{1}{4}$ in. in diameter, with $35\frac{1}{2}$ in. clear between the bearings. A self-aligning ball bearing was used at the driven end and a short brass bearing (0·1 in. long) with 6 mils. diametral clearance at the other. The

* See fig. 11, p. 213, of no. 12 in Bibliography.

drive was through a pin-and-slot coupling with anti-chatter spring, as formerly described.

For speed measurement and stroboscopic examination a vibrator was used whose tuning could be adjusted to agree with either limit of speed or approximately with the critical speed.

Since the sustained transient * could be obtained when the model was run above its critical range the critical speed could be obtained with great accuracy by measuring the difference between the rotation of that transient and that set by the vibrator. The critical speed was found to be 767·5 r.p.m., and the no-load speed of the motor with the conditions of test no. 3 in the table 887 r.p.m.

Spontaneous Speed Oscillations with D.C. Motor.

Test no.	Mean speed, r.p.m.	Estimated speed limits, r.p.m.	Limits of whirl amplitude, ins.	Oscilln. freq. cycles/min.
1 ...	744	Varn. very small.	0–0·1	29·2
2 ...	756	750–760	0–0·25	21·7
3 ...	756·7	738·5–776·5 †	0–0·25	19·5
4 ...	759	c. 745–770	0–0·3	22·1
5 ...	761	?–780	0·1–0·3	22·8
6 ...	763	?–780	0·2–0·4	33·2
7 ...	764	?–780	0·4–0·45	48·0
ω_0	767·5			
N.L. ..	887			

† Measured.

For test no. 3, which was taken before the others, the speed limits were measured by adjusting the vibrator to agree with them and then calibrating the vibrator. For the other tests these limits were estimated against a constant vibrator frequency of 775·6 cycles per minute.

8. *Historical Notes.*

The study of the effects of speed oscillations on the whirling of a shaft seems to have originated as a side issue in the discussion following an article by Kerr [8] ‡ in 1916.

With an experimental steam turbine rated at 250 kW, 3000 r.p.m., Kerr found strongly resonant conditions

* See section 1 of no. 15 in Bibliography.
‡ These numbers refer to the Bibliography.

at 2450 r.p.m., which he thought to be $\omega_0/\sqrt{2}$. He produced a theory to account for resonance at that speed, but his theory was founded on an earlier one of Chree's [2], which was itself based on the erroneous assumption that the plane of vibration of a shaft would revolve along with the shaft, thus omitting consideration of the tangential Coriolis forces required to make it do so.

Actually Kerr did not measure the critical speed of this rotor, but had to calculate it from known dimensions and weights. Such a calculation involves some definite assumption as to the extent to which each bearing constrains the direction of the shaft, and there is considerable uncertainty as to the correct assumption to make.

Thus Kerr himself, in his calculations for a small Laval turbine rated at 30,000 r.p.m., found that the critical speed on one assumption was 10,500 and 3800 on another, a range of uncertainty of nearly 3 : 1. On test this machine gave resonance at 7600 r.p.m., but it is not stated whether any other critical speeds occurred below the running speed.

Instead of the calculated 3300 r.p.m. it is therefore quite possible that the critical speed of the larger turbine was about 4900, which would make the resonant speed found correspond to $\frac{1}{2}\omega_0$, in which case it was probably due to skew stiffness in the shaft (see [12]) or to speed oscillations due to some impulse repeated once per revolution. It is most unlikely that the gravitational-speed-oscillation whirl would be large enough to be perceptible.

The first reference to the latter whirl occurs in a letter from Carter [1], who found that an approximate solution of the polar equations of motion gave resonance at $\frac{1}{2}\omega_0$ as well as at ω_0. He showed that with the constants likely to occur in practice the gravitational speed oscillations are exceedingly small, and that at $\frac{1}{2}\omega_0$ the subsidiary whirl they cause, even without friction, would grow so very slowly that it can never be of any practical importance.

A minor correction is required in Carter's statement; his ω should be defined as the constant *mean* speed of the shaft instead of the actual shaft speed.

A week before Carter's there appeared a letter from Stodola [18]. He also found resonance at $\frac{1}{2}\omega_0$, but *without* speed oscillations. He proceeded to show that

this critical speed is "fallacious" by calculating the deflexion at that speed. His mathematics actually shows that the deflexion is the same for all shaft speeds, and that it is nothing but the static deflexion due to the weight expressed in terms of his rotating coordinates.

A few months afterwards Stodola [19] put forward two "new critical speeds" due to gravity at $\frac{1}{2}\omega_0(1 \mp 2a^2/k^2)^{\frac{1}{2}}$ and $\omega_0(1-a^2/k^2)^{\frac{1}{2}}$ *.

The factors within brackets are irrelevant excrescences arising from his approximations, which are valid only when the subsidiary whirl is very small; it is not to be expected that equations based upon these assumptions will give exactly the speeds at which the whirl would become infinite in the absence of friction.

But we can apply a very simple test. Since Stodola's mathematics includes the effects of unbalance, the ordinary critical speed ought to be one of its solutions. As that is not the case it is obvious that his approximations are not sufficiently accurate for the exact calculation of the resonant speeds.

In this connexion it is worth noting that Prandtl [11] (p. 181) shows that when there is no steady rotation the shaft has a higher frequency of transverse vibration in a direction at right angles to the eccentricity than along the eccentricity, in the ratio $(1+a^2/k^2)^{\frac{1}{2}} : 1$, because of the angular oscillations which accompany the former.

At first sight it might appear that the angular oscillation would reduce the elastic forces and so diminish the frequency, but, because the frequency of these forced angular oscillations is necessarily higher than the zero frequency of the natural angular vibration, the angular oscillation is always opposite to the torque producing it, and so the net deflexion for a given displacement of the c.g. is increased by it instead of reduced.

This effect, however, cannot influence the critical speed for the unbalance whirl, because there the forces are constant in amount and lie in a fixed direction relatively to the shaft; consequently they cannot produce speed oscillations.

The results of experiments carried out with models having excessive eccentricity, up to 80 per cent. of the radius of the disk, are quoted by Stodola [20] in support

* Equations (10) of this article contain a numerical slip; these are the corrected values given in equations (10) to (11) on p. 2 of no. 21.

of the correctness of his formula, but of the seven results given in his table [20] (p. 230) three show resonance *below* $\frac{1}{2}\omega_0$ and only four at speeds above that value as his formula requires.

Moreover, as his models could not be run at the critical speed, the value of ω_0 with which his resonant speeds were compared had to be calculated, and the uncertainty of these calculations is far too great to enable any definite conclusion to be drawn from the results as to the correctness or otherwise of the factor under discussion.

On the other hand, these experiments do show very definitely that resonance occurs round about $\frac{1}{2}\omega_0$. As Stodola ran his models both horizontally and vertically, and took special pains to eliminate fluctuations caused by the coupling, there is no doubt that he was dealing with the gravitational-speed-oscillation whirl. Seeing that the value of his a^2/k^2 was about a million times greater than is likely to be permissible in any ordinary machine, one would expect this whirl to show up in his tests.

It is rather uncertain whether Stodola regards his "new" critical condition as a consequence of the speed oscillations produced by gravity, or as being caused by the weight in some other way. In his mathematics it clearly does arise from the speed oscillations, and is therefore the same as that previously found by Carter.

In several places he definitely states that the speed oscillations are the cause, and in one [20] (p. 231) he quotes from the notes of his co-worker Meissner a very clear explanation of the way in which these oscillations do affect the whirling; but on the first page of a later article [21], just a few lines after mentioning the speed oscillations, he gives an entirely different explanation of the whirl in which these oscillations play no part. This explanation is quite wrong, for it would apply equally well if the shaft were at rest and the axes of coordinates alone rotated.

Stodola's first article led to a lengthy discussion, in which Gümbel [5], [6], [7], O. Föppl [3], [4], Prandtl [11] and Lorenz [9] took part, and in which Stodala [20], [21], [22], [23] restated his theory several times, employing rectangular coordinates rotating at the mean speed of the shaft instead of his original polar ones.

Gümbel insisted that the resonance at $\frac{1}{2}\omega_0$ was due

to speed oscillations, and refused to admit that the critical speed could be other than an integral fraction of the ordinary critical speed.

Prandtl considered that the resonances observed in practice at $\frac{1}{2}\omega_0$ were more likely to be caused by skew stiffness in the shaft than by gravitational speed oscillations [11] (p. 181), also [12].

In his 1918 article [3] (p. 170) O. Föppl seems to have been the first to discuss the effects of speed oscillations due to causes other than gravity, and in 1919 [1] (p. 867) he gave the lower of the two resonant speeds of equation (3.07) and also experimental results showing resonance at $\frac{1}{2}\omega_0$ and $\omega_0/3$ due to the irregularities introduced by a Hooke's joint between two shafts making an angle with one another. Both Stodola [22] (p. 868) and Lorenz in his reply [9] (p. 889) completed the theory by adding the second resonant speed.

At a later date Rodgers [16] (p. 134) gave a simpler mathematical treatment of the theory of the gravitational-speed-oscillation whirl, using fixed rectangular coordinates; but his theory contains a most elusive error, in that he starts from two earlier equations (numbered 20 and 21), derived for the case of constant speed, which no longer apply when the speed is variable.

After correcting for this slip, and inserting "g" in two places where the printers have omitted it, Rodgers' equations 34 and 35 will be found to agree with the author's no-friction result.

Quite recently, in 1931, Soderberg [17] (App. 1), using polar coordinates, attacked the problem afresh by a somewhat complicated analytical method. His result agrees with the author's, omitting friction, except for minor discrepancies arising from his approximations.

As these approximations are not admissible at resonance he gives a special solution for $\omega=\frac{1}{2}\omega_0$. This solution, however, is only the very special transient which supposes the c.g. to start out from the axis of rotation with a particular velocity in a particular direction (see equation (6.10) of no. 14).

Carter's calculation of the rate of growth of the whirl is based on the same transient.

Except Lorenz none of these writers include friction in their calculations. Nominally Lorenz takes the friction as proportional to the square of the velocity

of the c.g., but a later approximation required to make his equations manageable is equivalent to assuming that the friction is directly proportional to that velocity within the range concerned.

The spontaneous speed oscillations of section 7 seem to be identical with the "unexplained phenomenon" mentioned by Orr [10] (p. 712) in 1923.

No other reference to this oscillation has been found, although in 1918 Prandtl [11] (p. 180) gives torque characteristics resembling fig. 14 above, but without the oscillation loop.

9. *Bibliography.*

(1) F. W. Carter, "On the Whirling Speeds of Loaded Shafts," 'Engineering,' ci. p. 410 (April 28, 1916). (Disc. on no. 8.)
(2) C. Chree, "The Whirling and Transverse Vibrations of Rotating Shafts," Proc. Phys. Soc. xix. 1903–5, pp. 114–156 (Mar. 11, 1904); Phil. Mag. (6) vii. pp. 504–542 (May 1904).
(3) O. Föppl, "Kritische Schwingungen von schnellumlaufenden Rotoren," *Zeits. f. d. ges. Turbinenwesen*, xv. pp. 157–160 (June 30, 1918) and pp. 168–171 (July 10, 1918).
(4) O. Föppl, "Kritische Drehzahlen rasch umlaufender Wellen," *Zeits. d. Vereines deutscher Ingenieure*, lxiii. pp. 866–867 (Sept. 6, 1919). (Disc. on no. 9.)
(5) L. Gümbel, "Ueber mit Biegung verbundene Schwingungen von Wellen," Dingler's *Polyt. Journ.* cccxxxii. pp. 235–239 (July 28, 1917) and pp. 251–257 (Aug. 11, 1917).
(6) L. Gümbel, "Eine neue kritische Wellengeschwindigkeit bei mit Biegung verbunden Schwingungen?" Dingler's *Polyt. Journ.* cccxxxiii. pp. 71–75 (May 4, 1918). (Criticism of no. 21.)
(7) L. Gümbel, "Kritische Drehzahlen rasch umlaufender Wellen," *Zeits. d. Vereines deutscher Ingenieure*, lxiii. pp. 869–870 (Sept. 6, 1919). (Disc. on no. 9).
(8) W. Kerr, "On the Whirling Speeds of Loaded Shafts," 'Engineering,' ci. pp. 150–152 (Feb. 18, 1916), pp. 197–199 (Mar. 3, 1916), pp. 224–226 (Mar. 10, 1916), and pp. 245–248 (Mar. 17, 1916). Also p. 320 (April 7, 1916), p. 420 (May 5, 1916), and p. 536 (June 2, 1916).
(9) H. Lorenz, "Kritische Drehzahlen rasch umlaufender Wellen," *Zeits. d. Vereines deutscher Ingenieure*, lxiii. pp. 240–245 (Mar. 15, 1919), and Supplement, pp. 888–892 (Sept. 13, 1919).
(10) W. M'F. Orr, "Note on Mr. Lee's paper on the Whirling of an Overhung Shaft," Phil. Mag. (6) xlv. pp. 708–714 (April 1923).
(11) L. Prandtl, "Beiträge zur Frage der Kritischen Drehzahlen," Dingler's *Polyt. Journ.* cccxxxiii. pp. 179–182 (Oct. 5, 1918). (Disc. on no. 9.)
(12) D. Robertson, "Whirling of a Shaft with Skew Stiffness," 'The Engineer,' clvi. pp. 152–153 (Aug. 18, 1933), pp. 179–181 (Aug. 25, 1933), and pp. 213–214 (Sept. 1, 1933).
(13) D. Robertson, "The Whirling of Shafts," 'The Engineer,' clviii. pp. 216–217 (Aug. 31, 1934), and pp. 228, 229, 231 (Sept. 7, 1934).
(14) D. Robertson, "Transient Whirling of a Rotor," Phil. Mag. (7) xx. pp. 793–825 (Nov. 1935).
(15) D. Robertson, "Hysteric Influences on the Whirling of Rotors," Inst. Mech. Eng. Proc. cxxxi. (1935).

(16) C. Rodgers, "On the Vibrations and Critical Speeds of Rotors," Phil. Mag. (6) xliv. pp. 122–156 (July 1922).
(17) C. R. Soderberg, "On the Subcritical Speeds of the Rotating Shaft," Trans. Am. Soc. Mech. Engrs. liv. APM-54-4, pp. 45–50, disc. 50–52, 1932. (Paper read to the Purdue meeting of the Mechanics Division, June 1931.)
(18) A. Stodola, "On the Whirling Speeds of Loaded Shafts," 'Engineering,' ci. p. 386 (Apr. 21, 1916). (Disc. on no. 8.)
(19) A. Stodola, "Neuere Beobachtungen über die kritischen Umlaufzahlen von Wellen," *Schweiz. Bauzeitung*, lxviii. pp. 197–199 (Oct. 28, 1916) and pp. 209–210 (Nov. 4, 1916).
(20) A. Stodola, "Neuere Beobachtungen über die kritische Winkelgeschwindigkeit von Wellen," *Schweiz. Bauzeitung*, lxix. pp. 93–94 (Mar. 3, 1917), and lxx. pp. 229–232 (Nov. 17, 1917).
(21) A. Stodola, "Eine neue kritische Wellengeschwindigkeit," Dingler's *Polyt. Journ.* cccxxxiii. pp. 1–3 (Jan. 12, 1918), pp. 17–19 (Feb. 9, 1918), and pp. 117–120 (July 13, 1918). Also correction on p. 135.
(22) A. Stodola, "Kritische Drehzahlen rasch umlaufender Wellen," *Zeits. d. Vereines deutscher Ingenieure*, lxiii. pp. 867–869 and 870–872 (Sept. 6, 1919). (Disc. on no. 9.)
(23) A. Stodola, "Zur Theorie der kritische Drehzahlen," *Zeits. f. d. ges. Turbinenwesen*, xvii. pp. 1–5 (Jan. 10 1920) and pp. 18–22 (Jan. 20, 1920).

University of Bristol.
31st August, 1934.

XXXIX. *Wave-length Measurements in the* K-*Series of Aluminium, Sulphur, and Chlorine, and in the* L-*Series of Zinc. By* J. Shearer, *B.A., M.Sc., Lecturer in Physics, University of Western Australia* *.

IN the course of an investigation † on the nickel L-spectrum with a concave cylindrical crystal of mica, lines in the K-series of chlorine, sulphur and aluminium appeared (arising from impurities), and also a line in the L-series of zinc. The crystal was used as a concave reflexion grating (radius 500 mm.) and mounted in a vacuum spectrograph. The film was mounted on the Rowland circle of the crystal. For details of the experimental method reference may be made to the report referred to.

As some interest attaches to precise measurement of the wave-length of these lines, a comparison of their wave-lengths with the wave-lengths of the reference lines used in the previous investigation has been made.

* Communicated by the Author.
† Shearer, Phil. Mag. ser. 7, vol. xx. p. 504 (1935).

Only in the case of the sulphur lines was it possible to use the method of interpolation between reference lines on either side of the line of unknown wave-length. For chlorine, aluminium, and zinc the only method available was one of extrapolation. It was necessary to apply this method also to some of the films on which the sulphur lines appeared.

In this method of extrapolation the linear distance on the film between the " unknown " line and the nearest

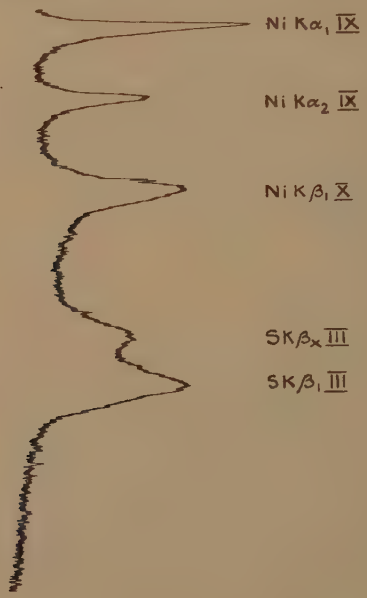

reference line on the same film was measured. From the effective radius of curvature of the crystal (see below) this distance was converted into angular measure. By adding this angle (algebraically) to the grazing angle calculated for the reference line, the grazing angle for the " unknown " line, and therefore its wave-length, was calculated.

The wave-length of the reference lines and the grating space of mica were obtained from Siegbahn's ' Spektroskopie der Röntgenstrahlen,' 1931, Table 46 (p. 183), and Table 17 (p. 48). The effective radius of curvature

of the crystal (which for various reasons will differ from the radius of curvature of the crystal holder) was obtained as follows.

From the calculated grazing angles of any pair of reference lines (on one and the same film) whose linear distance apart on the film is measured, a value of the effective radius of the crystal may be calculated for a grazing angle that is a mean of the grazing angles of the two reference lines. This calculation was carried out for the pairs of reference lines listed in Table I. In every case the α_1 and α_2 lines were used separately.

The three mean values of the radius so obtained and the corresponding mean grazing angles were plotted. From this graph was read off the effective radius required to convert into angular measure the linear separation of an " unknown " line from its reference line.

TABLE I.

Pairs of reference lines.	Approx. mean grazing angle.
NiKα VIII and CoKα VII	40°
NiKα IX and CoKα VIII	47°
NiKα X and CoKα IX	55°

In the case of the element sulphur, those films for which two reference lines are supplied permitted a calculation of wave-length by the method of interpolation between reference lines on either side of the line of unknown wave-length. The sulphur Kα lines calculated in this way are of particular interest, in that they appeared beautifully situated between the two components of the Cobalt KαIX doublet.

Where a line appeared on more than one film a value of the wave-length was calculated for each film and a mean obtained When more than one film was used in this way in the calculation of a wave-length the range covered by the individual values is shown against the wave-length recorded in the table.

The column headed $d\lambda$ contains the wave-length error calculated on the basis of an error in the effective crystal radius of $\pm 0{\cdot}4$ mm. in the case of chlorine and of

TABLE II.

Contains all the calculated Wave-lengths.

Element.	Line.	Order.	Wave-length X.U.	Number of films.	Reference line.	$d\lambda$.
Al 13	$K\alpha_1$	II	$8319{\cdot}88 \pm 0{\cdot}07$	2	$NiK\alpha_1$ X	$\pm 0{\cdot}21$
	$K\alpha_2$	II	$8322{\cdot}35 \pm 0{\cdot}25$	2	$NiK\alpha_1$ X	$\pm 0{\cdot}21$
S 16	$K\alpha_1$	III	$5361{\cdot}14 \pm 0{\cdot}03$	2	$NiK\alpha_1$ X	$\pm 0{\cdot}19$
			$5361{\cdot}12$	1	$CoK\alpha_1$ IX, $CoK\alpha_2$ IX	$\pm 0{\cdot}13$
	$K\alpha_2$	III	$5363{\cdot}88 \pm 0{\cdot}10$	2	$NiK\alpha_1$ X	$\pm 0{\cdot}19$
			$5363{\cdot}87$	1	$CoK\alpha_1$ IX, $CoK\alpha_2$ IX	$\pm 0{\cdot}13$
	$K\beta_x$	III	$5012{\cdot}78$	1	$NiK\alpha_1$ IX	$\pm 0{\cdot}19$
			$5012{\cdot}74$	1	$NiK\alpha_1$ IX, $CuK\alpha_1$ X	$\pm 0{\cdot}13$
	$K\beta_1$	III	$5021{\cdot}60$	1	$NiK\alpha_1$ IX	$\pm 0{\cdot}19$
			$5021{\cdot}51$	1	$NiK\alpha_1$ IX, $CuK\alpha_1$ X	$\pm 0{\cdot}13$
Cl 17	$K\alpha_1$	III	$4718{\cdot}07 \pm 0{\cdot}11$	4	$CoK\alpha_1$ VIII, $CoK\alpha_2$ VIII	$\pm 0{\cdot}19$
	$K\alpha_2$	III	$4720{\cdot}96 \pm 0{\cdot}17$	4	$CoK\alpha_1$ VIII, $CoK\alpha_2$ VIII	$\pm 0{\cdot}19$
Zn 30	$L\alpha_{1,2}$	I	$12227{\cdot}73$	1	$NiK\alpha_2$ VIII	$\pm 1{\cdot}3$
			$12227{\cdot}92$	1	$CuK\alpha_1$ VIII	$\pm 1{\cdot}3$

$\pm 0{\cdot}2$ mm. in the case of aluminium and sulphur, and of an error of $\pm 0{\cdot}02$ mm. in the linear distance on the film between the "unknown" line and the reference line. In view of the diffuseness of the Zinc $L\alpha_{1,2}$ line, $d\lambda$ in the case of this line was calculated on the basis of an error of $\pm 0{\cdot}04$ mm. in measuring its separation from the reference line. Where the method of interpolation was used the effective radius (and therefore any error arising from it) does not enter into the calculation.

The relative intensity of the sulphur $K\beta_x$ and sulphur $K\beta_1$ lines is of interest. Lindh and Lundquist * have observed the relative intensity to vary with the material of the anticathode. It may be seen from the microphotometer record that the $K\beta_1$ line is of greater intensity than the $K\beta_x$ line. The material of the anticathode used in this work was copper. On the assumption that the sulphur was an impurity on the surface of the anticathode, this result is in accord with the observations of Lindh and Lundquist.

Perth, Western Australia.
August 1, 1935.

XL. *Variations in Colour Vision and Colour Measurement.*

By R. A. Houstoun, *M.A.*, *D.Sc.*, *F.Inst.P.* †

IN this Journal there appears an article by Mr. Alex. J. Younger and myself entitled "The Personal Error in Colorimetry" ‡, and it is attacked by Mr. T. Smith in another article entitled "Variations in Colour Vision and Colour Measurement" §. I consider Mr. Smith's attack quite unjustified, but do not propose to go over the ground again. Our article is there to speak for itself. I have also difficulty in following Mr. Smith's argument in places, and do not think his readers will gain anything except the impression that the matter is highly technical and that he is much upset by our results. I am content to leave it at this. But as he seems to think my views on the C.I.E. system of colori-

* Siegbahn, 'Spektroskopie der Rontgenstrahlen,' 1931, p. 161.
† Communicated by the Author.
‡ Phil. Mag. xix. p. 1107 (1935).
§ Phil. Mag. xx. p. 1055 (1935).

metry of importance, and as he has misrepresented them very thoroughly, I shall state them briefly here :—

(1) Previously to 1932 there was no authoritative method of measuring colour, but in that year the committee presided over by Mr. Smith established the C.I.E. system. It was necessary to base it on three primary colours and a white. Now there are a large number of people interested in colour measurement, physicists generally, amateur photographers, colour printers, and to some extent physiologists and psychologists. For all these people red, green, and blue are the primary colours. With the exception of a few physicists no one is interested in the mathematical aspect of the subject. The obvious course would have been to accept the popular idea and refine upon it, and to use, for example, the working primaries of the Guild trichomatic colorimeter, which are provided by colour filters. The committee instead of this adopted as two of the three primaries stimuli which possess imaginary colour but no luminosity, a conception which can be understood only by specialists, but is mathematically elegant and saves a little time in calculations. It is consequently almost impossible to popularise the result of their labours. I have attempted to do so, but the difficulty come up against is that the audience invariably think of the mixing of colours as the superposition of coloured lights on a screen. The question is put " How can you affect the colours already there by the superposition of another colour which of itself has no luminosity ? " and the questioner refuses to argue the question from any standpoint but his own.

There is no difficulty in explaining the meaning of primary colours to audiences such as schoolboys and classes of the Workers' Educational Association. They can understand the use of negative components and imaginary colours more saturated than the colours occurring in nature. But a stimulus which has colour but no luminosity is quite beyond their grasp, and the wisest course of action is to say nothing whatever about the matter.

But it may be argued that the basis of the system of measurement is a matter which concerns only the professional colorimeterist. I differ. It is necessary to " sell colorimetry." In the course of the past three

years I have lent my copy of the article * explaining the system to industrial chemists and others interested. The verdict is unanimous, that a system that cannot be understood in half an hour, and which is so much involved in mathematical reasoning as this one is, has little chance of widespread adoption, and in one particular case the perusal of the article led to the purchase of a Lovibond Tintometer.

I consequently regard the system with mixed feelings. I am grateful for the tables provided, and recognise that from the scientific standpoint it is all that can be desired. But I am sorry that after waiting so many years for a scientific system we are now in possession of one that is so devoid of popular appeal.

(2) There are two different ways of putting the system into operation, direct and indirect colorimetry. In the indirect method the transmission coefficient or "reflectance" of the specimen is measured throughout the spectrum by a spectrophotometer, and the colour co-ordinates are thereafter only a matter of calculation. The result is independent of the colour vision of the observer and will be accepted everywhere without question. The one sentence in our paper referring to this method means simply that there is nothing in the nature of a concealed trap or hidden pitfall connected with it. There is no danger of the observer being tripped up by an unsuspected peculiarity of his own colour vision. It is nowhere stated in our paper that the indirect method is in any way unreliable, so the second sentence in Mr. Smith's paper and the paragraph at the top of p. 1057 are, to put it mildly, extremely misleading.

There are three direct methods, the trichomatic colorimeter, the vector method, and the monochromatic plus white method. The two latter, though potentially important, are not fully developed yet. If we consider only the first method, observers fall into four groups :—

(*a*) Those in good agreement with the C.I.E. observer.

(*b*) The five per cent. or so definitely colour blind.

* "The C.I.E. Colorimetric Standards and their Use." Trans. Opt. Soc. xxxiii. p. 73 (1932).

(*c*) Observers differing from the C.I.E. observer who when forced into agreement with the C.I.E. observer at the white point agree with him elsewhere.

(*d*) Observers differing from the C.I.E. observer who when forced into agreement with him at the white point do not agree with him elsewhere and who pass the usual tests for colour blindness.

It is with reference to group (*d*) that Mr. Smith and I differ. Where there are several observers who can check one another, or where there is the indirect method to fall back on, there is no danger, but I was thinking of isolated workers equipped with only a trichomatic colorimeter. I consider that in such circumstances observers of group (*d*) might go far wrong and at the same time honestly think they were doing good work. Mr. Smith thinks the danger negligible, although he has no definite statistics to offer. I am certain that class (*d*) will be a large class, and that members of this class are quite unsuitable for direct colorimetry of legal or commercial importance.

There is one simple step which might be taken to prevent error, and that is the provision of suitable substandards of colour. If x, y, z were determined for solutions of common salts such as copper sulphate, potassium dichromate, nickel sulphate, etc., when illuminated by source A—the reddest of the three sources authorised by the committee—together with the mean error permissible in accurate work, it would enable observers to test themselves and their equipment. I assume that Mr. Smith will be a member of the next committee that deals with these matters, and I commit the suggestion to his care.

XLI. *The Thermal Conductivity of Carbon Dioxide.*

To the Editors of the Philosophical Magazine.

Gentlemen,—

MR. ARCHER * has recently made experiments on the variation of the thermal conductivity of carbon dioxide with temperature using Gregory's

* C. T. Archer, Phil. Mag. vol. xix. p. 901 (1935).

method. This method, which was first used by Dr. Gregory * for hydrogen, provides a powerful means of attacking this difficult problem. Mr. Archer concludes that his results give no indication of any effect which would be due to a change in the nature of the inter-molecular field of carbon dioxide at about 140° C. The effect of such a change has been found in thermal diffusion †, and this has received consistent support from the evidence of viscosity measurements.

An examination of Mr. Archer's log K–log T graph for carbon dioxide shows that the eight consecutive points extending from 36·7° C. to 254·7° C. can be surprisingly well represented by two intersecting straight lines meeting at a point corresponding to about 140° C. The bending effect is in the right direction, and it can be shown that its amount is at least as great as could be expected if it followed from the change in viscosity. The increased accuracy of representation thus obtained appears to correspond with that given by the straight line portion of a similar graph obtained from Dr. Gregory's measurements on hydrogen. A further examination of Dr. Gregory's results suggests that Mr. Archer's three remaining points, two in the neighbourhood of 300° C. and possibly the point at the lowest temperature, may be experimentally less reliable than the rest of the observations.

As the question of the influence of a change in the nature of the molecular field on thermal conductivity is of considerable importance, it is hoped that Mr. Archer will give this matter further consideration. The method employed in his interesting experiments appears to be sufficiently accurate for the purpose, over a considerable temperature range.

Physics Department,
The University, Birmingham.
December 10th, 1935.

Yours faithfully,
T. L. Ibbs.

* H. S. Gregory, Proc. Roy. Soc. A, vol. cxlix. p. 35 (1935).

† T. L. Ibbs and A. C. R. Wakeman, Proc. Roy. Soc. A, vol. cxxxiv. p. 613 (1932).

XLII. *Notices respecting New Books.*

A Table of Eisenstein-reduced Positive Ternary Quadratic Forms of Determinant $\leqslant 200$. By BURTON W. JONES. (National Research Council Bulletin, no. 97, Washington, D.C., 1935. Price $1.00.)

THESE tables represent the valuable results of a computation begun by their author while a National Research Fellow. They are prefaced by three pages of explanatory introduction which help to make their meaning clear.

Two quadratic forms

$$f=ax^2+by^2+cz^2+2ryz+2szx+2txy,$$
$$F=AX^2+BY^2+CZ^2+2RYZ+2SXZ+2TXY$$

with integer coefficients are said to be equivalent if there exists a transformation

$$\begin{aligned} T: \quad x&=a_{11}X+a_{12}Y+a_{13}Z,\\ y&=a_{21}X+a_{22}Y+a_{23}Z,\\ z&=a_{31}X+a_{32}Y+a_{33}Z, \end{aligned}$$

with integer coefficients and determinant 1, which sends f into F.

The determinant of f is

$$d=\begin{vmatrix} a & t & s\\ t & b & r\\ s & r & c \end{vmatrix}$$

and a form f is called positive if $f\geqslant 0$ for all real x, y, z and $f=0$ only for $x=y=z=0$. A necessary and sufficient condition for this is

$$a>0, \quad ab-t^2>0, \quad d>0.$$

A primitive form is one in which a, b, c, r, s, t have the highest common division 1, a primitive form is properly primitive when one of a, b, c is odd, otherwise it is improperly primitive.

For each set x_1, y_1, z_1 of integer values of x, y, z there is defined by T a unique set X_1, Y_1, Z_1 of integer values of X, Y, Z such that

$$f(x_1, y_1, z_1)=F(X_1, Y_1, Z_1),$$

and conversely. It follows that if there are n_k distinct sets of integers x, y, z for which

$$f(x, y, z)=k$$

(i. e., n_k representations of the given integer k by the form f), then there are n_k distinct sets of integers X, Y, Z, for which

$$F(X, Y, Z)=k.$$

Thus equivalent forms represent the same integers k and with the same multiplicities n_k; any question concerning the totality of values of a form for integer values of the variables has the same answer for f and for any form F equivalent to f. The totality of forms equivalent to f constitute a *class* of forms. Eisenstein gave what is probably the most satisfactory method of selecting, by means of inequality-conditions on the coefficients, a single representative from each class of equivalent forms; such a representative is called a reduced form.

It is a fundamental theorem in the subject that the number of classes of equivalent forms of given determinant is finite. Thus the number of reduced positive forms of given determinant d is finite, and they can be tabulated. Eisenstein constructed a table of reduced forms of determinant $d \leqslant 100$; the present pamphlet carries on the computation as far as $d \leqslant 200$. The tables are excellently clear and well arranged; the class-number for each determinant and the number of automorphs of each reduced form are listed, while the improperly primitive forms are given in a separate table.

E. H. L.

Organic Solvents: Physical Constants and Methods of Purification. By A. Weissberger and E. Proskauer. Translated from the German manuscript by R. G. New. (Humphrey Milford, Oxford University Press, 1935. Price 15*s.* net.)

In the last twenty years numerous advances have been made in the methods available for organic synthesis. There has arisen almost simultaneously a considerable interest in the chemistry and physics of non-aqueous solutions. The rapid development of the use of cellulose esters in the lacquer industry has called into technical prominence a large number of organic liquids which but a short time ago were regarded purely as chemical curiosities.

For these reasons the authors decided to make a collection in tabular form of the physical constants of the various solvents now in use, both for technical and for research purposes.

This forms the first main section of the book (83 pages), and is, of course, in the nature of a dictionary. The next section is of the same length, and deals with the impurities likely to be present, their effect on the physical constants, and the methods for their removal. The physical chemist will find that special attention is given to the methods employed in the purification of solvents for electrical and optical measurements. The research worker in organic chemistry will turn with much interest to the second part of the book, and will not be disappointed.

Many of the processes outlined are, of course, well-known, but the reader will frequently encounter records of methods or observations which are new to him and which, with the aid of the bibliography of over 1400 references, he can study at leisure. The use of the boric ester in the purification of *iso*butyl alcohol may be cited, also that of boron triacetate in the removal of water from acetic acid, and the presence of aminothiophen in dimethylaniline. As would be expected from the recent increase in our knowledge of constant boiling mixtures the addition of a third substance (C) to form such a mixture with an impurity (B) in a solvent (A) is very frequently mentioned. Alcohol may apparently be used in the separation by distillation of the *cis-* and *trans-* dibromoethylenes. References are also given to the corresponding isomeric dichloroethylenes which are now manufactured and separated by an English firm.

In view of the occasional incidence of industrial poisoning in the case of new commercial products this question also receives some attention. The cases of carbon bisulphide, nitrobenzene, and chlorinated aliphatic hydrocarbons (in general, though not in particular) are mentioned. The poisonous properties of aniline, dimethylaniline, pyridine, and amyl alcohol are perhaps regarded as too well known to be recorded. Some interest attaches to the toxic action of glycol chlorhydrin, since this compound is somewhat akin to dioxan, a solvent which has come into rather wide use and was recently responsible for several deaths at a large factory in the Midlands. From statements published at the time it would appear that this oxide is converted in the body into oxalic acid. Reference to the poisonous action of dioxan might be incorporated in a later edition.

The authors have produced a work of reference which contains a fund of most useful information and, to the frequent user, will in many instances suggest further investigations in pure chemistry.

[*The Editors do not hold themselves responsible for the views expressed by their correspondents.*]

Fig. 2 (*a*).

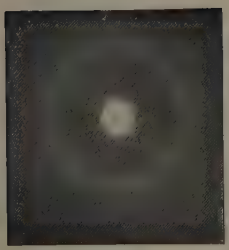

Fig. 2 (*b*).

β-ray photographs: (*a*) with carbon tube, (*b*) with brass tube in smaller camera.

Fig. 2.

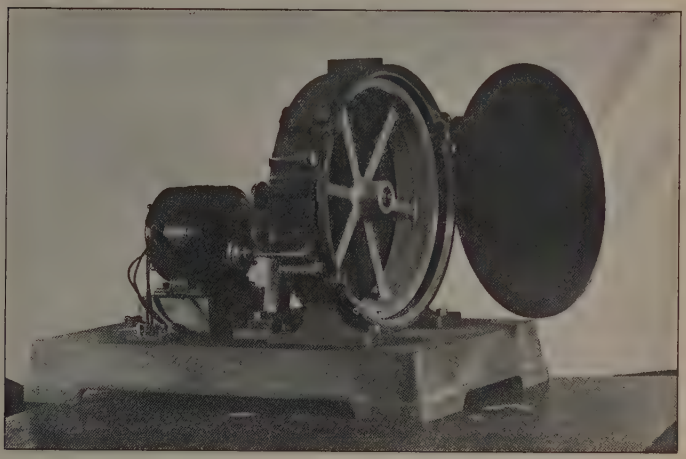

Fig. 6.

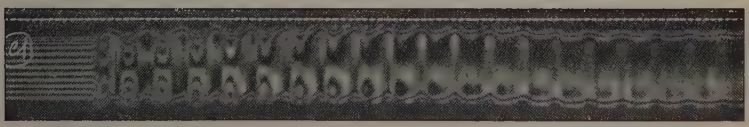

(*a*) Time of exposure 1/938 sec.

(*b*) Time of exposure 1 9380 sec.

(*c*) Time of exposure 1/9380 sec,

Fig. 4.

(*a*) W=0·417 kg. Time of exposure 1/1876 sec.

(*b*) W=0·220 kg. Time of exposure 1/5200 sec.

Fig. 10.

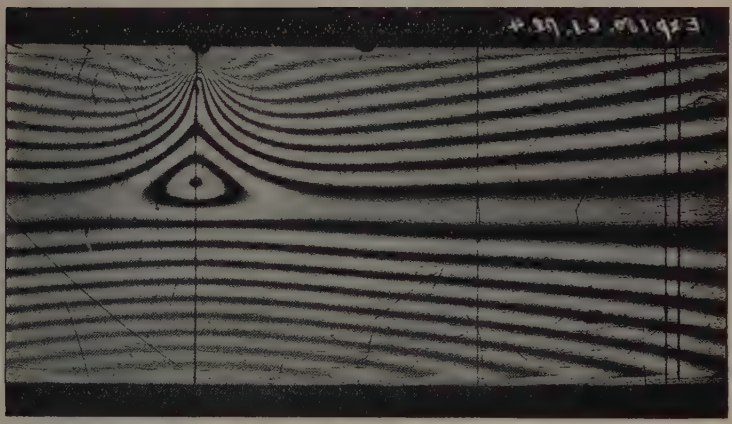

Fig. 11.—No. 1.

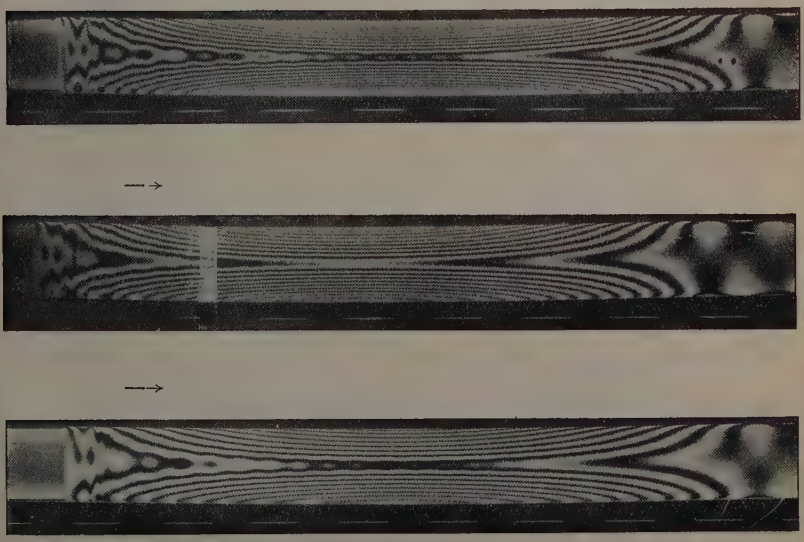

Time of exposure 1/44,500 sec.

Fig. 11.—No. 2.

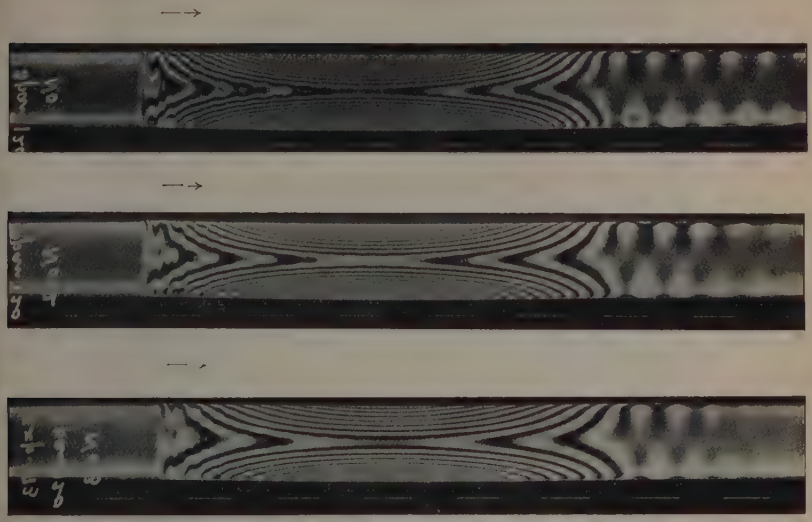

Time of exposure 1/45,000 secs.

Fig. 11.—No. 3.

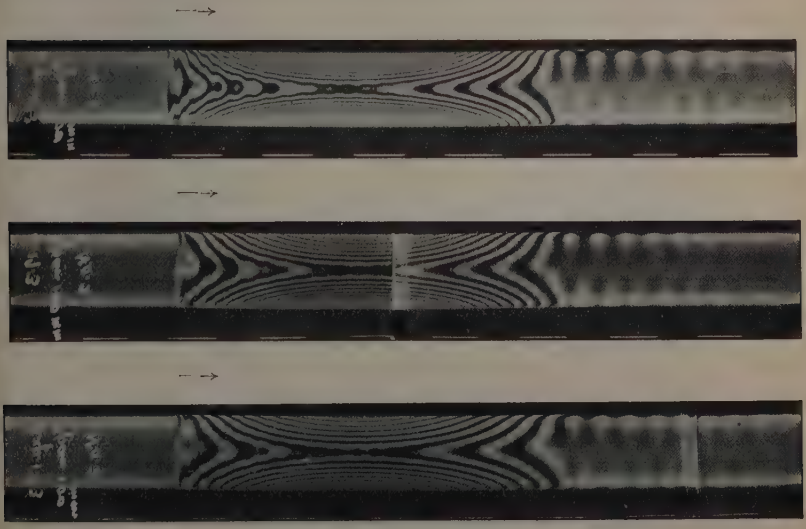

Time of exposure 1/44,500 sec.

Fig. 15.

Fig. 18.—B_1.

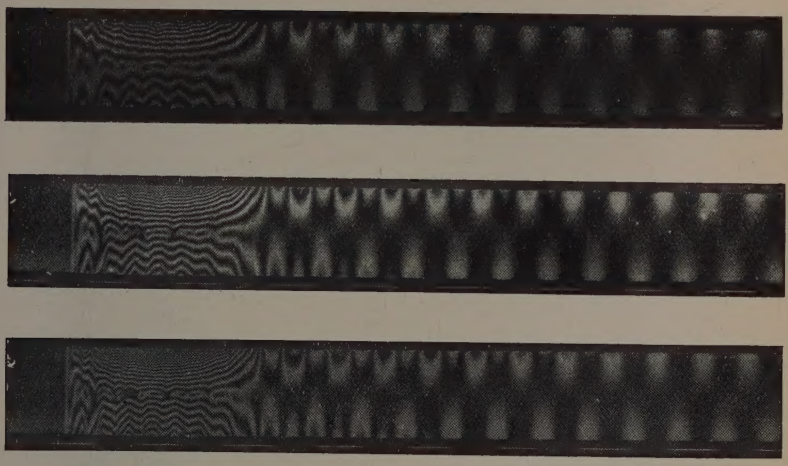

Fig. 19.—B_2.

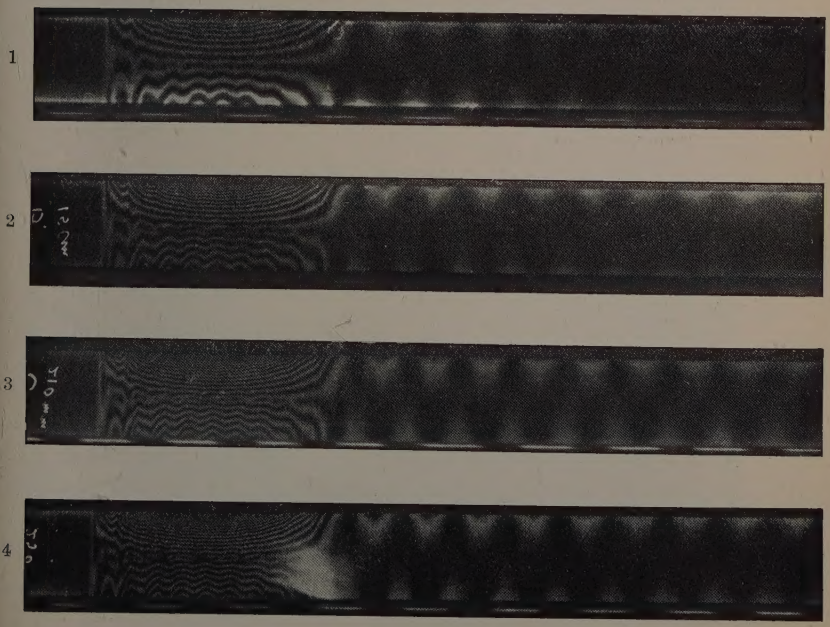

Fig. 20.—B_3.

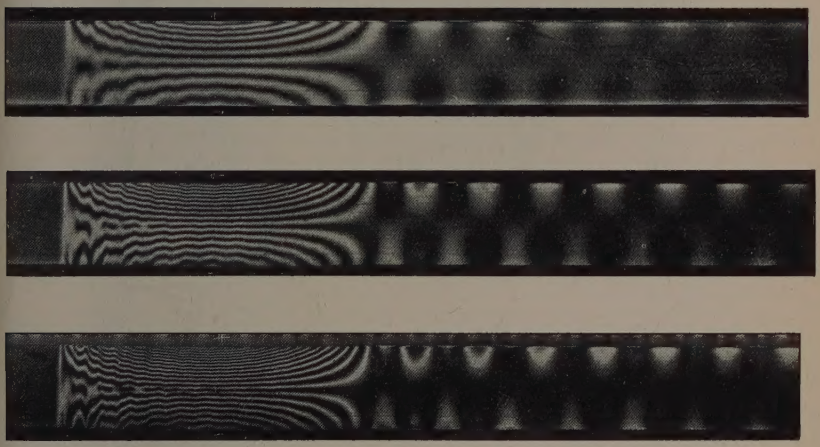

Fig. 24.